2011

PARTIALLY HALOGENATED ACENES AND HETEROACENES FOR ORGANIC ELECTRONICS

Balaji Purushothaman
University of Kentucky, balagepk@gmail.com

ABSTRACT OF DISSERTATION

Balaji Purushothaman

The Graduate School

University of Kentucky

2011

PARTIALLY HALOGENATED ACENES AND HETEROACENES FOR ORGANIC ELECTRONICS

ABSTRACT OF DISSERTATION

A dissertation submitted in partial fulfillment of the
requirements for the degree of Doctor of Philosophy in the
College of Arts and Sciences
at the University of Kentucky

By
Balaji Purushothaman
Lexington, Kentucky
Director: Dr. John E. Anthony, Professor of Chemistry
Lexington, Kentucky

2011

ABSTRACT OF DISSERTATION

PARTIALLY HALOGENATED ACENES AND HETEROACENES FOR ORGANIC ELECTRONICS

Inorganic materials have dominated electronic applications such as photovoltaic cells, thin film transistors (TFTs) and light emitting diodes (LEDs). However developments in the field of organic electronics over the past three decades have enabled the use of organic materials in these devices. While significant improvements have been made to improve their electronic properties there are several road blocks towards commercial application. One of the significant obstacles is the poor charge carrier mobility associated with organic semiconductors processed by well established printing methods. The goal of my research project is to improve the charge carrier mobility of solution cast films of acene semiconductors by partial halogenation and heteroatom substitution. Spin coated films of triisopropylsilylethynylated difluoropentacene exhibited higher hole mobility compared to TIPS pentacene due to contact induced nucleation of pentacene on perfluorobenzenethiol treated gold electrodes. The success of this project allowed me to further investigate the effect of degree of fluorination on the electronic properties of pentacene. A series of trialkylsilylethynylated tetrafluoro and octafluoropentacenes were synthesized and their performances in thin film transistors and solar cells were explored. Solar cells made from these materials using poly(3-hexylthiophene) as donor exhibited poor open circuit voltages (V_{oc}) resulting in low power conversion efficiency (PCE). Better device performances were achieved using pentacenes having single halogen substituent.

In order to improve the charge carrier mobility in TFTs soluble trialkylsilylethynylated hexacenes were explored. However these molecules exhibited a greater tendency to photo-dimerize in solution and solid state. Partial halogenation was used as a tool to improve the solution stability of reactive hexacene. The improved solution stability of partially halogenated hexacenes allowed me to successfully extend this approach to heptacene and nonacene.

Finally a series of new trialkylsilylethynylated anthradiselenophenes were synthesized to improve molecular ordering in the solid state by increasing non-bonding Se – Se interaction. However single crystal x-ray diffraction studies revealed no such interaction between the acene chromophore resulting in poor device performance.

Keywords: *Organic Thin Film Transistors, Organic Photovoltaics, Acene Semiconductors, Partially Halogenated acenes, Larger acenes, Anthradiselenophenes.*

Balaji Purushothaman

01/31/2011

PARTIALLY HALOGENATED ACENES AND HETEROACENES

FOR

ORGANIC ELECTRONICS

By

Balaji Purushothaman

Dr. John E. Anthony

Director of Dissertation

Dr. John E. Anthony

Director of Graduate Studies

01/31/2011

Date

RULES FOR USE OF DISSERTATIONS

Unpublished dissertations submitted for the Doctor's degree and deposited in the University of Kentucky Library are as a rule open for inspection, but are to be used only with due regard to the rights of the authors. Bibliographical references may be noted, but quotations or summaries of parts may be published only with the permission of the author, and with the usual scholarly acknowledgements.

Extensive copying or publication of the dissertation in whole or in part also requires the consent of the Dean of Graduate School of the University of Kentucky.

A library that borrows this dissertation for use by its patrons is expected to secure the signature of each user.

Name Date

_____

_____

_____

_____

_____

_____

_____

_____

_____

_____

DISSERTATION

Balaji Purushothaman

Graduate School

University of Kentucky

2011

ACKNOWLEDGEMENTS

First and foremost I would like to thank my graduate advisor Prof. John Anthony for his guidance and support during the course of my graduate career. His creative and logical thinking has greatly influenced my approach towards solving problems. I thank him for sharing his wisdom and knowledge in the field of organic electronics as I hope to shape my future in this exciting field of work.

I am greatly honored to have Prof. Mark Watson, Prof. Folami Ladipo and Prof. Bruce Hinds as my committee members and would like to thank them for their constructive criticism on my research. I would like to thank my collaborators Prof. Thomas Jackson (Pennsylvania State University) for his thin film transistor device studies on anthradiselenophenes. I would like thank Mr. Yee-Fun Lim from the Malliaras group at Cornell University for his solar cell device studies on partially halogenated pentacene acceptors and hexacene. I would also like to thank my former colleague and collaborator Ms. Jes Sherman (University of California, Santa Barbara) for her solar cell device studies on octafluoropentacenes. I would like thank Prof. Oana Jurchescu (Wake Forest University) for her thin film transistor device studies on partially fluorinated pentacenes. I would like to thank Office of Naval Research (ONR) and National Science Foundation (NSF) for their financial support.

I am greatly indebted to all the departmental staff for their administrative help and support during my PhD career. I would like to thank past members of the Anthony Aromatic Research Group (AARG) for their help and support during the formative years of my graduate life. I would also like to thank the present members of AARG for establishing a cordial working atmosphere and for the good times both inside and outside the lab. I would like to thank all my friends at University of Kentucky for their love and support and for making me feel at home.

I am grateful for the unconditional love and support from my parents Purushothaman and Kasthuri. I would also like thank my two brothers Madan and Dayalan for their support and encouragement towards my quest for a better future. I am greatly indebted to my friends at University of Madras (UM) for encouraging me to pursue my dreams.

TABLE OF CONTENTS

LIST OF FIGURES

LIST OF SCHEMES

LIST OF TABLES

LIST OF SYMBOLS AND ABBREVIATIONS

Å	Angstrom
α-6T	α-Sexithiophene
ADS	Anthradiselenophene
ADT	Anthradithiophene
AFM	Atomic Force Microscopy
AIBN	2,2'-Azobis-(*2*-methylpropionitrile)
$AlCl_3$	Aluminum chloride
BCP	2,9-Dimethyl-4,7-diphenyl-1,10-phenanthroline
BHJ	Bulk Heterojunction
Bu_4NPF_6	Tetrabutylammonium Hexafluorophosphate
˚C	Degree Celsius
C_i	Capacitance of dielectric layer
C_{Ar}	Aromatic sp^2 hybridized carbon
C_{sp}	sp hybridized carbon
CH_3COOH	Acetic acid
C_6D_6	Deuterated benzene
$CDCl_3$	Deuterated chloroform
cm	Centimeter
Conc.	Concentrated
$(COCl)_2$	oxalyl chloride
CsF	Cesium Fluoride
CuCN	Copper(I)cyanide
d (for NMR)	Doublet
DCE	1,2-dichloroethane
DCM or CH_2Cl_2	Dichloromethane
DIBALH	Diisobutyl aluminum hydride
DiEt-α-6T	α,α′-diethylsexithiophene
DMA	Dimethylacetamide
DMSO	Dimethyl sulfoxide
DMF	Dimethyl formamide
DMSO-d_6	Deuterated dimethyl sulfoxide
DMAD	Dimethyl acetylene dicarboxylate
DPV	Differential pulse voltammetry
e	Charge of electron
E_g	Energy gap
E_{ox}	Oxidation Potential
EI	Electron ionization
EQE	External quantum efficiency
EtOH	Ethanol
eV	electronvolt
Fc/Fc^+	Ferrocene/Ferrocenium Couple
FF	Fill factor
g	Grams

GC	Gas Chromatography
GXID	Grazing incidence x-ray diffraction
hν	Photon
h or hr.	Hour(s)
HBr	Hydrobromic acid
HCl	Hydrochloric acid
HI	Hydroiodic acid
HMDS	Hexamethyldisilazane
HOMO	Highest Occupied Molecular Orbital
H_2SO_4	sulfuric acid
ITO	Indium tin oxide
J (for NMR)	Coupling constant
J_{sc}	Short circuit current density
K	Kelvin
KI	Potassium iodide
LEDs	Light Emitting Diodes
LUMO	Lowest Occupied Molecular Orbital
m (for NMR)	Multiplet
M	Moles per liter
M^+	Molecular Ion
MALDI	Matrix Assisted Laser Desorption Ionization
MeOH	Methanol
$MgSO_4$	Magnesium sulfate
mg	Milligrams
MHz	Mega Hertz
min	Minute
mL	Milliliter
mmol	Millimole
mm	Millimeter
μm	Micrometer
mol	Mole
MP	Melting Point
MS	Mass Spectrometry
mV	Millivolts
m/z	Mass to charge ratio
μ	Charge carrier mobility
n-BuLi	n-Butyllithium
$NaBH_4$	Sodium borohydride
NaCl	Sodium chloride
NaOH	Sodium hydroxide
NBS	N-bromosuccinimide
NEt_3	Triethylamine
NH_4Cl	Ammonium chloride
NIR	Near Infra Red
nm	Nanometer
NMR	Nuclear Magnetic Resonance

NODIPS	n-octyldiisopropylsilylethynyl
o	ortho
OFETs	Organic Field Effect Transistors
OSC	Organic Semiconductor
OTFTs	Organic Thin Film Transistors
OTS	Octadecyltrichlorosilane
P	Power
P3HS	Poly(3-hexylselenophene)
P3HT	Poly(3-hexylthiophene)
PCC	Pyridinum chlorochromate
PCE orη	Power conversion efficiency
PDI	Polydispersity Index
PEDOT:PSS	Poly(3,4-ethylenedioxythiophene) doped with polystyrenesulphonic acid
PFBT	Perfluorobenzenethiol
PαMS	Poly-α-methylstyrene
PMMA	Polymethylmethacrylate
PTSA	*p*-toluene sulfonic acid
PV	Photovoltaic
PVA	Polyvinylalcohol
PVP	Poly-4-vinylphenol
RB	Round bottom
RFID	Radio Frequency Identification
rpm	Rotations per minute
RT	Room temperature
s or sec	Second(s)
s (for NMR)	Singlet
SiO_2	Silicon dioxide
$SnCl_2$	Stannous chloride
$t_{1/2}$	Half-life
TCHS	Tricyclohexylsilylethynyl
TCPS	Tricyclopentylsilylethynyl
TES	Triethylsilylethynyl
TFTs	Thin Film Transistors
THF	Tetrahydrofuran
TIBS	Triisobutylsilylethynyl
TIPS	Triisopropylsilylethynyl
TLC	Thin Layer Chromatography
TNBS	Tri-n-butylsilylethynyl
TNPS	Tri-n-propylsilylethynyl
TTBS	Tri-*t*-butylsilylethynyl
TTMSS	Tris(trimethylsilyl)silylethynyl
UV	Ultra Violet
V	Voltage
V_{oc}	Open circuit voltage
W	Watt
Wt	Weight

Chapter 1: Introduction

1.1 Organic Semiconductors

Inorganic materials have dominated electronic applications such as photovoltaic cells, thin film transistors (TFTs) and light emitting diodes (LEDs). However developments in the field of organic electronics over the past three decades have enabled the use of organic materials in these devices.[1-4] Two different classes of organic molecules, namely polymers and small molecules have been extensively studied for application in these devices.[3] Compared to inorganic semiconductors both polymers[2,6] and small molecules[1,6-8] can be solution processed allowing the use of low cost processing techniques such as inkjet printing and spin coating. While small molecules have well defined molecular weight, polymers on the other hand do not have well defined molecular weight and are usually expressed as average molecular weight. The distribution in molecular weight is measured in terms of polydispersity index (PDI), the ratio of weight average molecular weight and number average molecular weight of the polymer. Polymers with very high molecular weight and PDI close to one are a key requirement for better device performance.[9,10]

The variations in molecular weights which arise due to synthetic methods used can have pronounced effect on the electronic properties of materials, which gives small molecules a unique advantage over polymers. In comparison to polymers, which are semicrystalline and disordered, small molecule semiconductors are highly crystalline and exhibit very high charge carrier mobility (the ease with which charge carriers travel under the influence of electric field). Most conjugated polymers are usually synthesized using transition metal reagents and the presence of metallic impurities in the final polymer is known to significantly affect the electronic

properties of polymers.[11] Also the presence of reactive end groups in the polymers needs to be capped to improve the long time stability of these molecules.[12]

One of the greatest advantages of polymers over small molecules is that they form uniform films on solution processing and the inherent solution viscosity associated with these molecules allows them to be formulated into inks. In spite of all the challenges both polymers and small molecules have found application in TFTs, solar cells and LEDs.

1.2 Organic Thin Film Transistor (OTFT)

Transistors are the basic building blocks for modern day electronic devices. They are used in logic circuits[13], sensors[14], radio frequency identification (RFID) tags[15] and in backplanes for flat-panel displays.[16] Organic thin film transistors (OTFTs) are also known as organic field effect transistors (OFETs) as the conductivity of the semiconductor channel is controlled by an applied electric field. There are three major components to OTFT device, namely dielectric, semiconductor and electrodes (source, drain and gate). The source and drain electrodes are usually Au, however other metals such as Ag, Pd, Pt, Al, Ca, Ni, Cr, Ti, W, Zn and polymers PEDOT:PSS, poly(aniline) have also been used. The gate is often heavily doped silicon; however metal and polymers electrodes have also been used. Both inorganic insulators (SiO_2[17,18], Al_2O_3[19], hafnium oxide[20]) and polymer insulator (Figure 1.1) (PMMA[21-23], PVP[17,23], PVA[23,24], BCB[25], PαMS[23], Cytop[26-28]) have been used as dielectric layer. The semiconducting layer is either vacuum deposited or solution processed by techniques such as spin coating, drop casting, inkjet printing, gravure and flexo printing.

Depending on how these components are deposited relative to one another, four different device configurations are possible, namely bottom contact bottom gate (a), top contact bottom gate (b) bottom contact top gate (c) and top contact top gate (d) as shown in Figure 1.2.

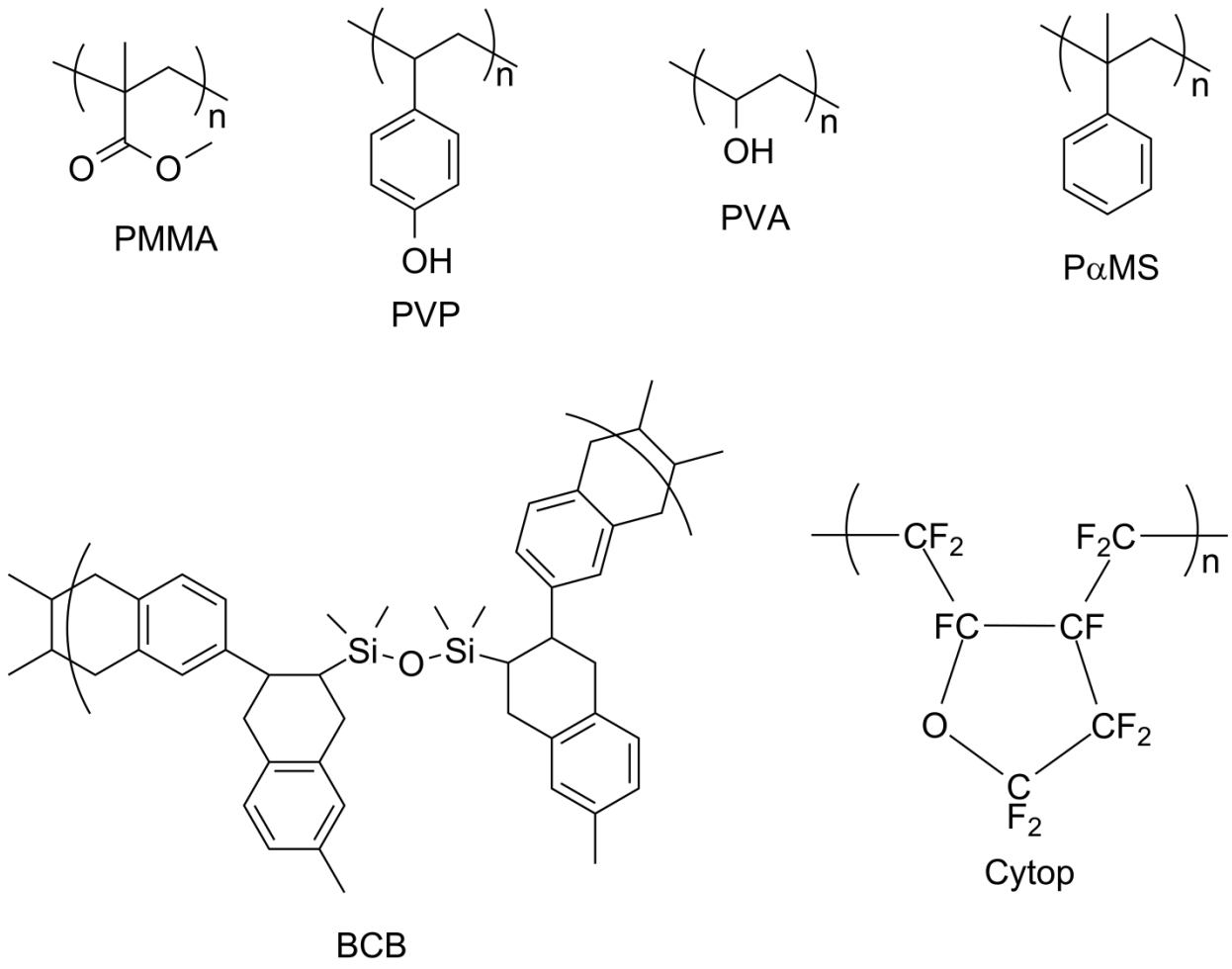

Figure 1.1 Common polymer insulators for OTFTs

Although the working principle for each device configuration is the same, there are certain unique advantages in using one configuration over the other. Better device performance is achieved using top contact bottom gate configuration (Figure 1.2(b)), which has a low contact resistance due to the larger area for charge injection from the electrode to the semiconductor.[29] However patterning of metal electrodes could damage the underlying organic semiconducting layer and as a result bottom contact bottom gate configuration is often preferred. In recent years

top gate devices have also been studied because the polymer gate insulator can also act as a protective encapsulating agent for the active layer, especially for air-sensitive n-type materials.[28,30]

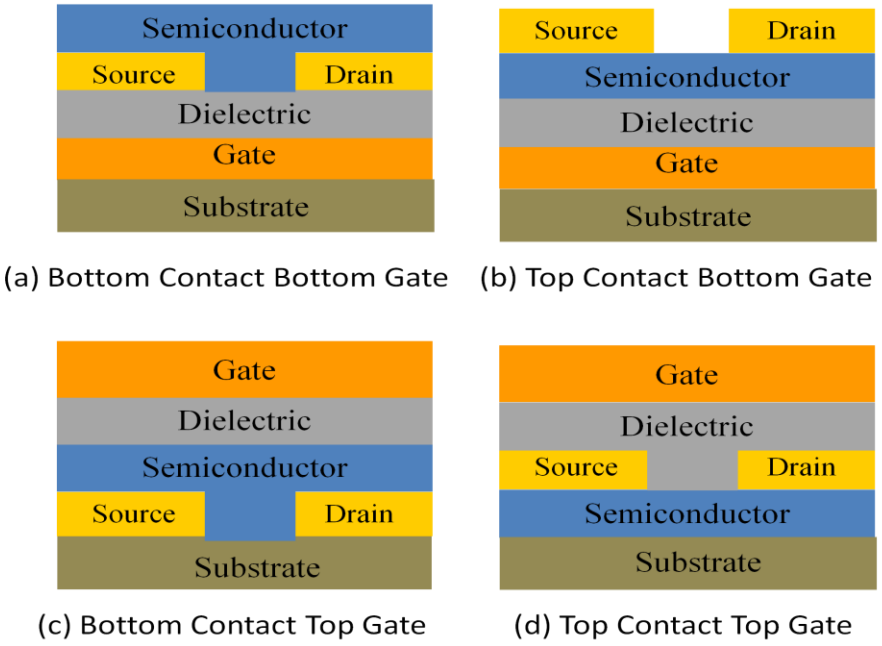

Figure 1.2 Common OTFT configurations

Since OTFTs consist of layers of different materials, the interfaces between the different layers play a key role in the device performance.[4] For example, silicon dioxide, the most commonly used dielectric layer in OTFTs, contains many hydroxyl groups on the surface and as a result hydrophobic organic molecules do not form a uniform layer over the surface of the dielectric. In order to overcome this, the dielectric layer is often treated with octadecyltrichlorosilane (OTS)[17,31,32] or hexamethyldisilazane (HMDS)[33,34] to react with the surface hydroxyl groups. This results in a layer of alkyl chains which influences the growth of crystalline domains of organic semiconductor on the dielectric.[17,31-34] Similarly for bottom contact devices treatment of gold electrodes with benzenethiol helps improve morphology of the semiconducting layer and charge injection from the electrode to the semiconductor.[35,36]

1.2.1 Working Principle of OTFTs

Application of a potential (V_G) between the source and gate electrode polarizes the semiconductor - insulator interface resulting in the accumulation of charge carriers between the source and drain electrode (Figure 1.3). Application of potential (V_D) between the source and drain electrodes results in the conduction of charge carriers in the *accumulation layer* and this is known as the "*on*" state of the device. In "*off*" state no gate potential is applied and hence no current or very little current flows between the electrodes.

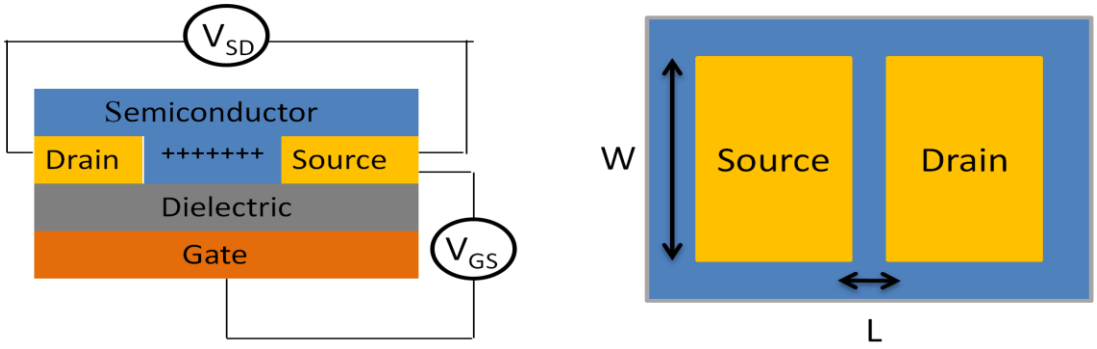

Figure 1.3 Formation of conducting channel in OTFT

The output characteristics of OTFTs can be obtained by plotting drain current *versus* drain voltage at various gate voltages (Figure 1.4(a)). At low drain voltages the current flowing through the device is proportional to the applied voltage and is known as the linear regime (Figure 1.4(a)). The current (I_d) flowing through the device is given by equation (1).

$$I_D = (W/L)C_i\mu_{lin}(V_G - V_{TH})V_D \ldots\ldots\ldots\ldots\ldots(1)$$

Where W = channel width, L = channel length, C_i = capacitance of the insulator, μ = charge carrier mobility, V_G = gate voltage, V_{TH} = threshold voltage, V_D = drain voltage.

As the applied potential is increased the device deviates from Ohmic behavior and with further increase in potential the current flowing through the device reaches a constant value. This is the saturation regime of the device (Figure 1.4(a)).

$$I_D = (W/2L)C_i\mu_{sat}(V_G - V_{TH})^2 \quad \ldots\ldots\ldots\ldots(2)$$

$$\sqrt{I_D} = \sqrt{\{(W/2L)C_i\mu_{sat}\}}(V_G - V_{TH}) \quad \ldots\ldots\ldots\ldots(3)$$

The charge carrier mobility in the linear and saturation regime can be estimated from equations (1) and (2) respectively. The μ_{sat} and μ_{lin} values calculated from both equations are different because the device exhibits gate dependent mobility.

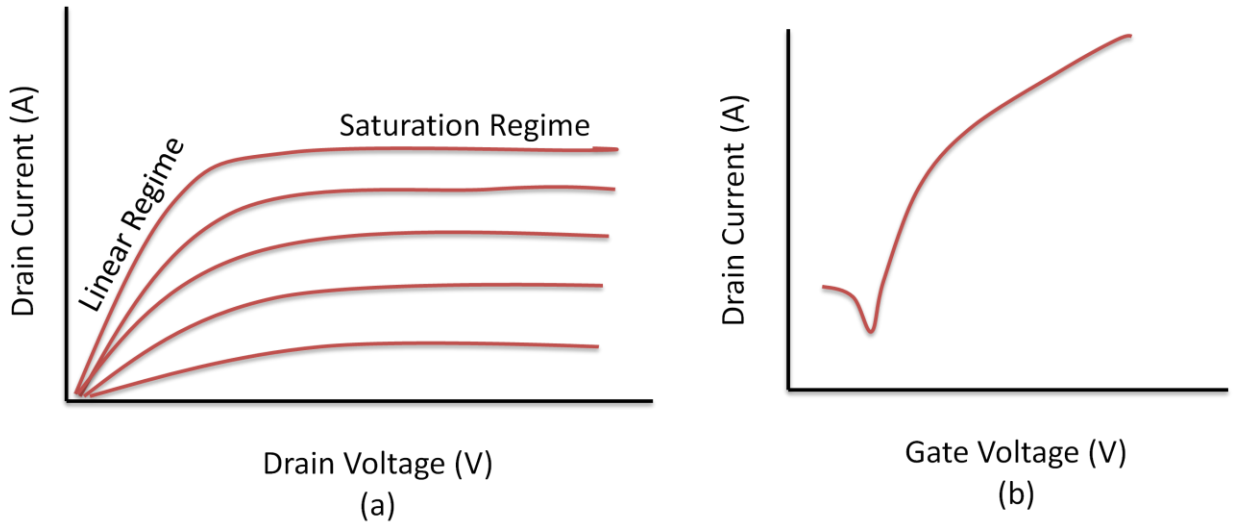

Figure 1.4 Output and transfer plot of OTFT

Another way of characterizing transistor performance is to plot drain current as a function of gate voltage under constant drain voltage (Figure 1.4(b)). A more commonly seen plot, which is of practical use, is to plot both the square root drain current ($\sqrt{I_D}$) and log (I_D) *versus* gate voltage (V_G) (Figure 1.5).

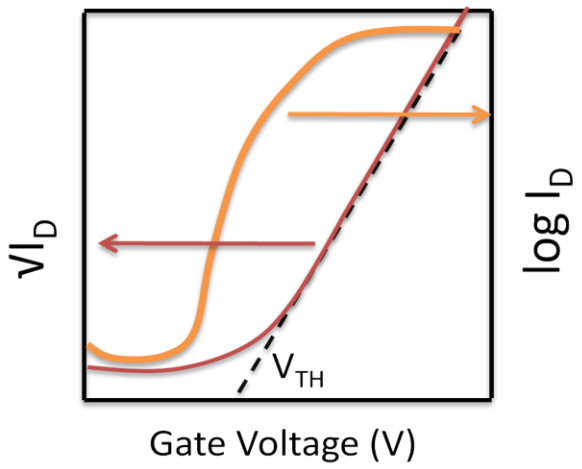

Figure 1.5 $\sqrt{I_D}$ and log (I_D) *vs.* V_G

From equation (3) it is evident that the charge carrier mobility of device in the saturation regime can be obtained from slope of the plot of square root of drain current ($\sqrt{I_D}$) *versus* gate voltage (V_G) and the intercept of the x-axis gives the threshold voltage (V_{TH}) of the device. The plot of log (I_D) *versus* gate voltage (V_G) gives the on/off ratio and the ease with which the device switches from the "*on*" state to the "*off*" state.

1.2.2 Parameters that determine performance of OTFTs

The performance of thin film transistors is determined by the following parameters:

Charge carrier mobility (μ): Charge carrier mobility is a measure of the ease with which charge carriers move under the influence of applied electric field. For practical application this value should be greater than 0.5 cm^2/Vs.

On/off current ratio ($I_{on/off}$): On/off current ratio is the ratio of the current flowing between source and drain electrode in the "*on*" sate to that of the "*off*" state. An on/off ratio of greater than 10^5 is required for any potential application.

Threshold voltage (V_{TH}): Threshold voltage is the voltage at which a conducting channel is formed between the source and drain electrodes in the semiconductor layer. Low turn *"on"* voltages are preferred for practical applications.

Sub-threshold swing or slope (S): The Sub-threshold slope of a transistor is expressed by equation (4).

$$S = d(V_G) / d(\log I_D) \quad \ldots\ldots..(4)$$

It is defined as the change in gate voltage (V_G) required for a 10 fold increase in drain current in the sub-threshold region ($V_G<V_{TH}$) and is expressed in V/decade. A smaller sub-threshold swing (S) is indicative of how easy it is to turn the device on and off.

1.2.3 Classification of Organic Semiconductors

Based on the charge carriers formed in the conducting channel, organic semiconductors are classified into two types, namely p-type and n-type (Figure 1.6). In OTFTs where the semiconducting layer is p- type, the transistors are turned on using negative gate voltages, while for n-types, positive gate voltages are required to turn on the device. In some organic semiconductors both holes and electrons are formed in the channel depending on the sign of the gate bias. These materials are classified as ambipolar materials (Figure 1.6).

The ability of organic molecules to transport electrons or holes can be best explained by looking at relative ease with which they can accept or lose an electron and the inherent stability of the radical anion or cation species. Most organic semiconductors are π electron rich species and have greater tendency to lose an electron to form the more stable radical cation rather than accept an electron to form the radical anion. As a result most organic semiconductors reported in

the literature are hole-transporting materials. However by adding electron withdrawing functional groups the stability of the radical anion can be improved. For example, pentacene **(1)**, a p-type material can be converted into n-type by perfluorination of the pentacene chromophore.[37] Nevertheless the stability of radical anion towards air and moisture seems to be the main problem plaguing the development of air stable electron transport materials.[38] In recent years air stable n-type semiconductors have reported for molecules whose LUMO energy levels are lower than – 4.3 eV.[39] However molecules with LUMO energy levels above – 4 eV have also shown reasonable stability due to the closely packed molecules that prevent any diffusion of air or water molecules through the thin film.[40,41]

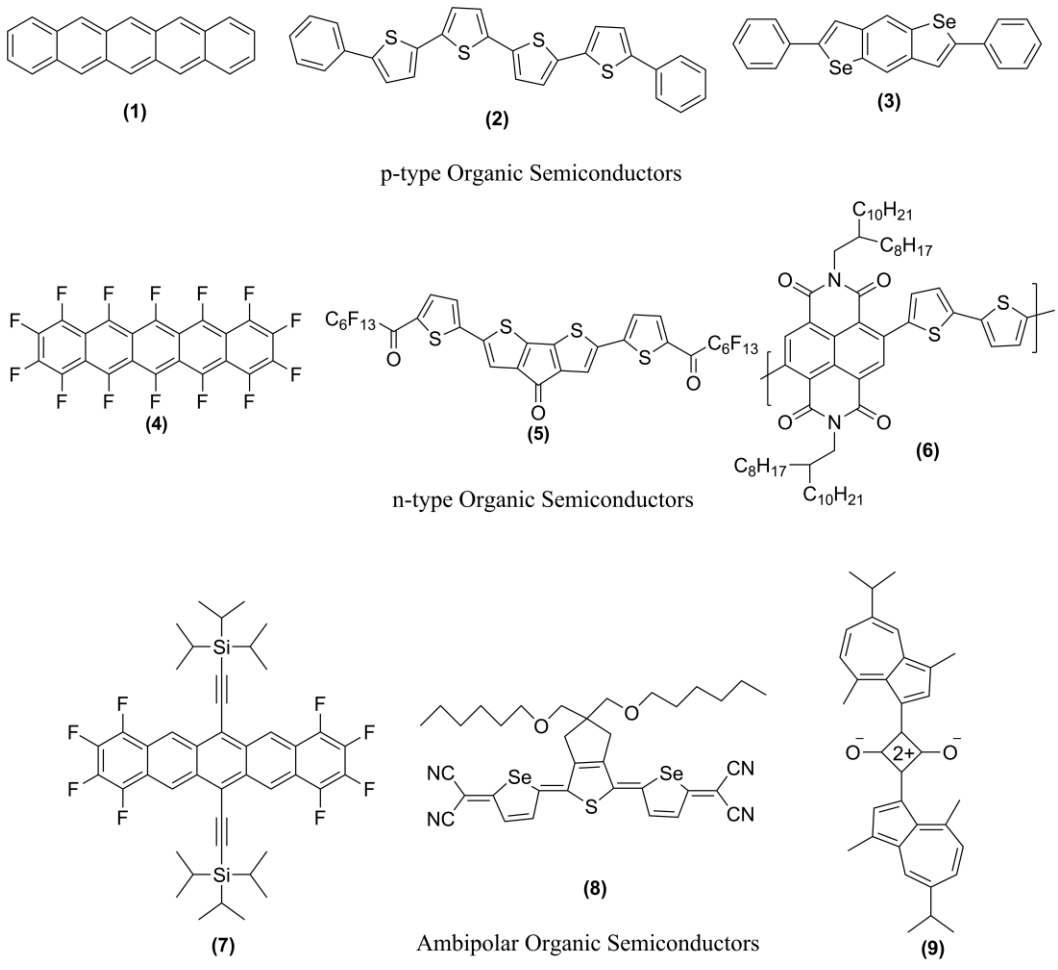

Figure 1.6 Examples of p-type, n-type and ambipolar semiconductors

The n-type behavior of organic semiconductors is also affected by the traps present at the dielectric – semiconductor interface. In the case of inorganic oxide dielectrics (SiO_2) and in some polymer dielectrics (PVA, PVP), the presence of surface hydroxyl groups can act as traps resulting in lower mobilities and higher operating voltages in these devices.[42-46] Devices using polymer dielectric, Cytop,[27,28] exhibit better device performance and stability with lower operating voltages.

1.3. Acene Semiconductors

Among small molecule semiconductors, acene based semiconductors have been the most widely studied class of compounds because of their ability to form highly ordered crystalline films.[6-8] These molecules pack in a herringbone fashion with edge to face interactions (Figure 1.7(a)).[47] Vapor deposited thin films of pentacene (**1**), the largest sufficiently stable acene for device studies, have shown charge carrier mobility greater than 3 $cm^2\ V^{-1}\ s^{-1}$ in a field effect device.[17] However these molecules exhibit poor solubilty in common organic solvents like benzene (0.005 wt% at room temperature for pentacene).[48] The decomposition pathways for acenes are typically assumed to proceed through photo-induced endoperoxide formation (Figure 1.7(b)), with subsequent oxidation to the corresponding quinone,[49] or through a "butterfly" dimerization (Figure 1.7(c)) of the aromatic rings.[50] In pentacene, endoperoxide formation is assumed to dominate in the solid state, while dimerization is the main decomposition pathway in solution.[50]

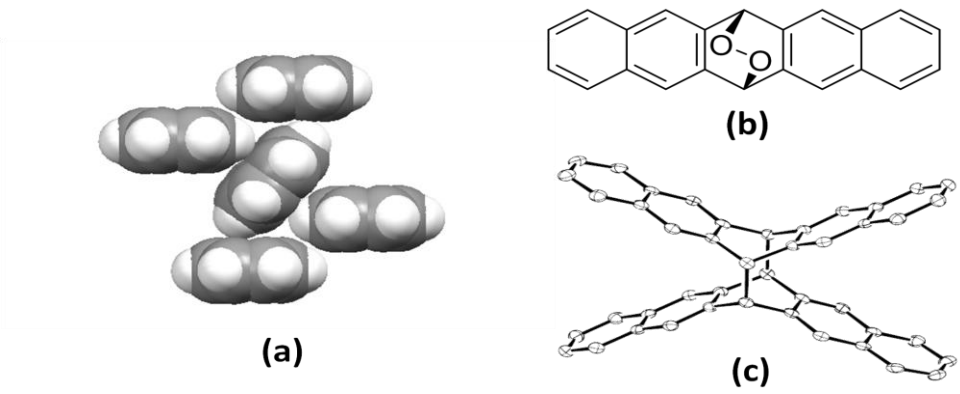

Figure 1.7 Crystal packing[47] and decomposition products of Pentacene[49,50]

1.3.1 Pentacene Thin Film Transistors

Due to their poor solubility, solution processed pentacene OTFTs have been scarce. Nevertheless pentacene thin film transistors made by drop casting hot solution of pentacene in halogenated aromatic hydrocarbons has been reported. Pentacene films exhibited mobility as high as 0.45 cm^2/Vs for devices made by drop casting from hot solution of trichlorobenzene.[51]

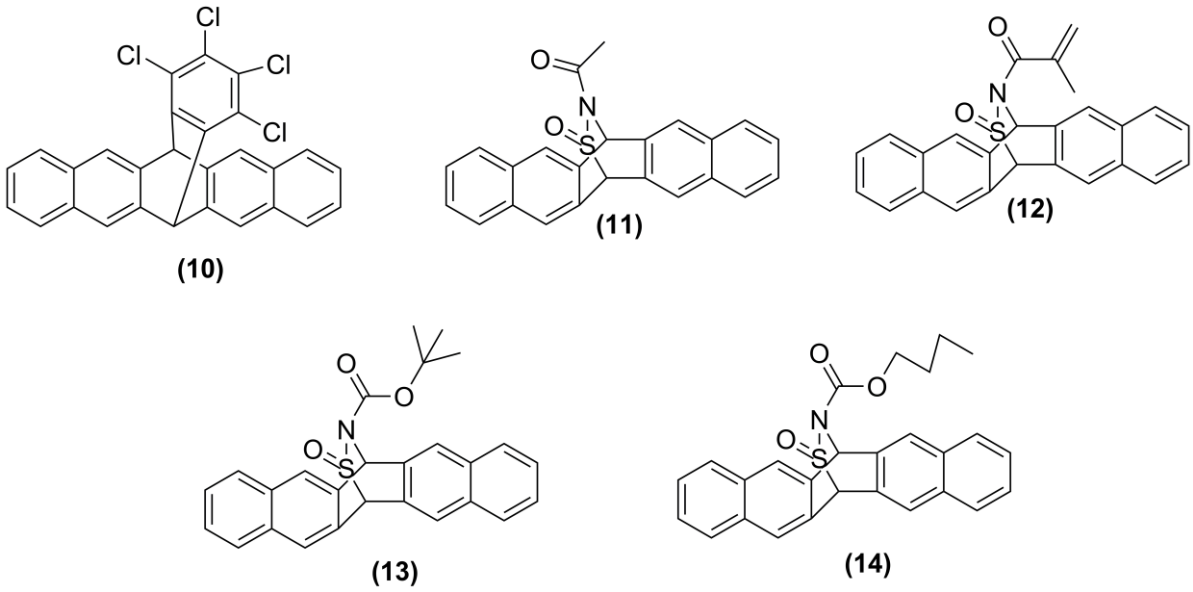

Figure 1.8 Soluble pentacene precursors for OTFT[52-57]

In order to circumvent solubility issues and take advantage of solution processing techniques, soluble pentacene precursors have been synthesized (Figure 1.8).[52-57] The

solubilizing groups enhance solubility in organic solvents allowing drop casting of thin films of the intermediate precursor which is then converted into the final pentacene by annealing the film in an inert atmosphere at high temperature. Thin films of pentacene made from precursor (**11**) gave a mobility of 0.89 cm^2/Vs for a bottom contact device configuration using HMDS treated SiO_2 gate dielectric.[54] Although reasonable mobilities can be achieved by this method the high temperature involved in this process is a significant drawback.[52-57]

1.3.2 Functionalized Pentacene

Another approach for improving solubility of acenes is to functionalize the pentacene core with solubilizing groups such as alkyl[58,59] or aryl[60] substituents. These substituted pentacene derivatives show improved solubility but suffer the same stability issues as the parent pentacene. Among the recent functionalization strategies employed for the synthesis of soluble and stable acene derivatives, the *peri* – functionalization approach utilizing trialkylsilylethynyl groups developed by the Anthony group[61] has been widely used to develop organic electronic materials.[62-64] The ethynyl group acts as spacer to separate the solubilizing groups from the pentacene core. The size of the trialkylsilyl groups not only determines the solubility and stability of these molecules but also influences the π – stacking between these molecules in the solid state. In the case of pentacene, the triisopropylsilyl derivative (**15**) (Figure 1.9) exhibited two dimensional π stacking with a interplanar spacing of 3.36 Å and good solubilty in common organic solvents .[65] The improved solubility and stability of these molecules has enabled the use of solution processing techniques for making thin films for electronic devices. Field effect transistors made from these molecules by drop casting have shown mobility as high as 1.8 cm^2/Vs and an on / off ratio of 10^7.[66]

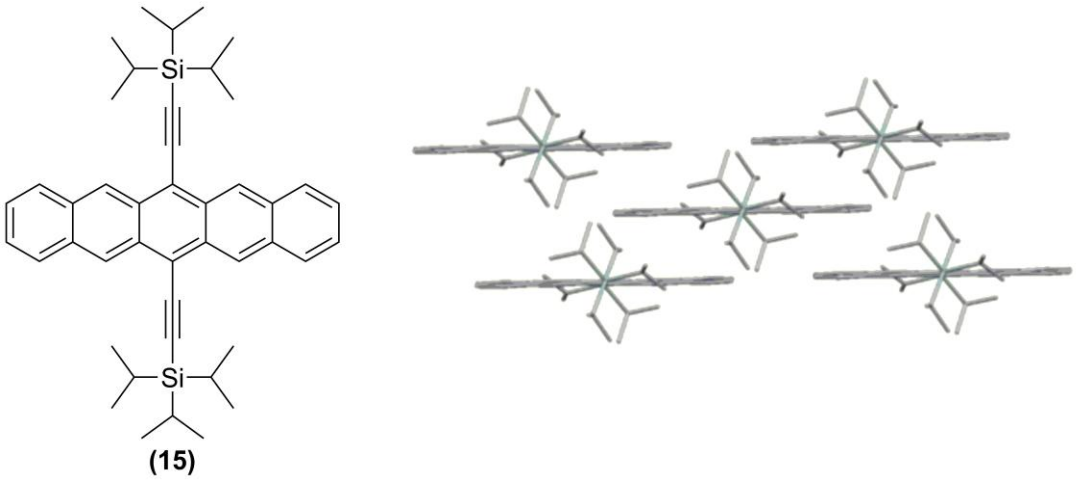

Figure 1.9 TIPS Pentacene structure and crystal packing[65]

1.3.3 Functionalized Anthradithiophenes

Another approach for improving the stability of acene molecules is by introducing heteroatoms to acene core. Anthradithiophene (**ADT, 16**), a heteropentacene, and its alkyl derivatives were synthesized by Katz and co-workers at Bell laboratories as an alternative to pentacene. [67] Field effect transistors made from the vapor deposited thin films of dihexyl derivative (**16**) exhibited mobility of 0.15 cm^2/Vs, while solution processed thin films yielded significantly lower mobility of 0.02 cm^2/Vs. [67]

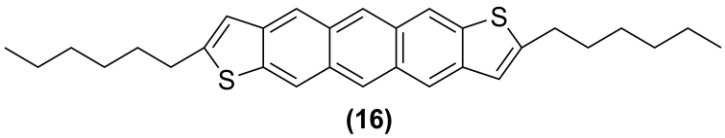

Figure 1.10 2,8-dihexylanthradithiophene[67]

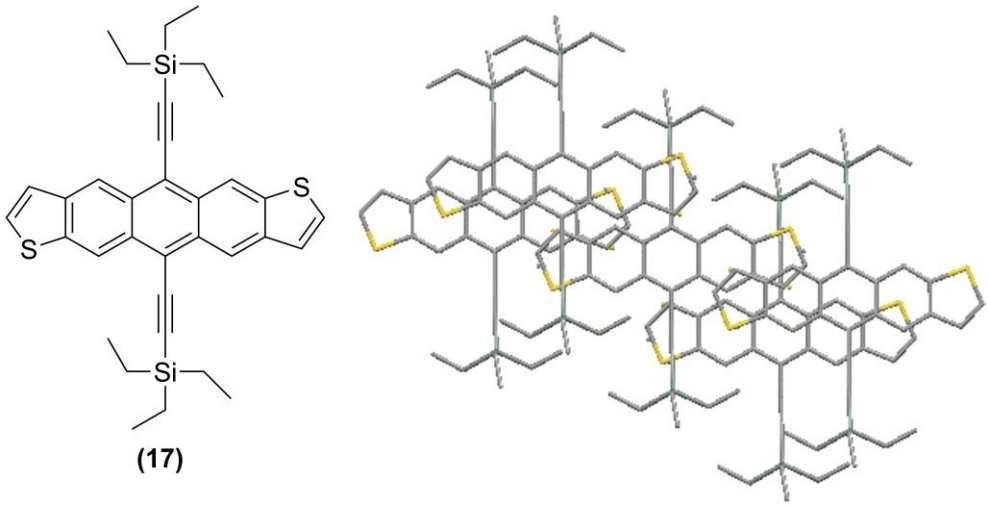

Figure 1.11 Structure and crystal packing of TES ADT[68]

Similar to the approach of improving solubility and π – stacking of pentacenes, the Anthony group used the *peri*-functionalization approach on anthradithiophenes.[68] In the case of anthradithiophenes, the shorter acene length requires a smaller triethylsilyl substituent to achieve 2D π – stacking. TES Anthradithiophene (**TES ADT, 17**) exhibits 2D π stacking with a reduced carbon – carbon distance of 3.23 Å compared to TIPS pentacene. Field effect transistor made from drop-cast thin film of these molecules yielded mobility of 1 cm^2/Vs. However spin coated thin films of TES ADT (**17**) were amorphous and exhibited poor device performance.[68]

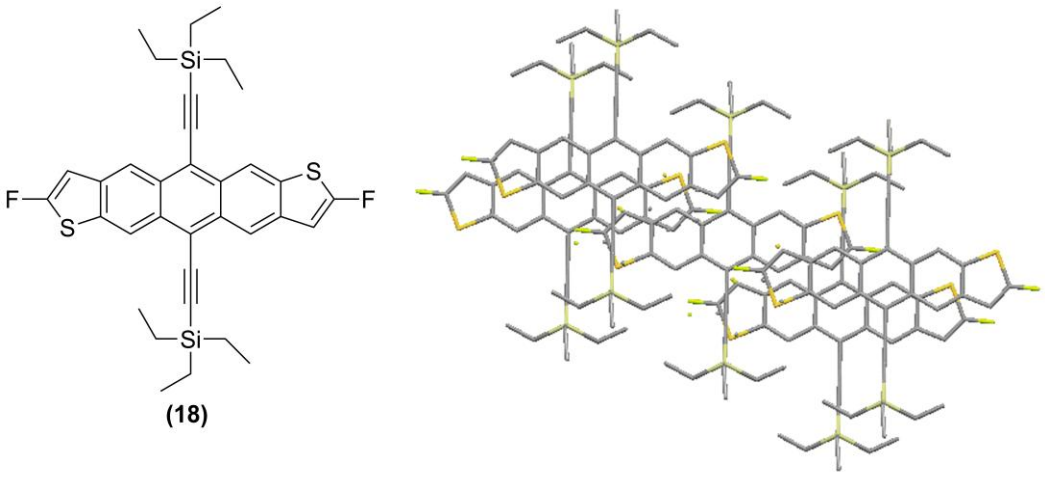

Figure 1.12 Structure and crystal packing of TES DifluoroADT[69]

In order improve the crystallinity of spin coated films of ADT the difluoro derivative was synthesized.[69] TES FADT (**18**) derivative packs in a 2D fashion with smaller carbon – carbon distance. Devices made by spin casting gave uniform, crystalline films with mobility as high as 1.5 cm^2/Vs. The extension of the above strategy to improve crystallinity and mobility of TIPS pentacene will be described in Chapter 2. The synthesis of partially halogenated pentacenes for application in OTFTs will be discussed in Chapter 3.

1.3.4 Higher Acenes

Acenes larger than pentacene have been of great interest due to their predicted lower reorganization energy[70], potential higher charge carrier mobility[71] and smaller band gap.[72] However, such an improvement in electronic properties is concomitant with decreasing stability and solubility in organic solvents, which in turn hampers the synthesis and application of these interesting molecules.[73] Unsubstituted higher acenes such as hexacene and heptacene (**20**) have only been synthesized successfully by photodecarbonylation of soluble diketone precursors (**19**) (Figure 1.13) in a polymer matrix, where such decomposition pathways can be retarded.[74,75] Recently the photodecarbonylation approach was successfully extended to octacene and nonacene by Bettinger et al.[76]

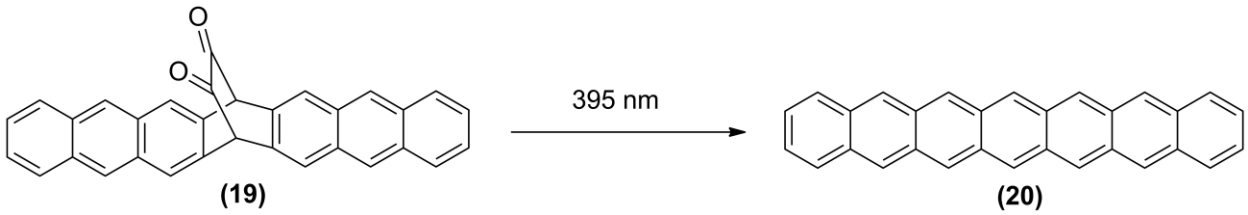

Figure 1.13 Photodecarbonylation of heptacenediketone precursor[75]

The improved solubility, stability and crystallinity of trialkylsilylethynyl pentacene have paved the way for the synthesis of stable and soluble higher acenes.[77,78] However, in order to stabilize these highly reactive materials, significantly bulkier substituents had to be used to

prevent Diels-Alder reaction between the alkyne substituent of one molecule and the reactive acene chromophore of another.[79] Hence bulky tri-*t*-butylsiliylethynyl (**TTBS, 21**) (Figure 1.14) groups were used to stabilize hexacene, while for heptacene, a larger tris(trimethylsilyl)silylethynyl (**TTMSS, 22**) (Figure 1.14) substituent had to be used.[77] In a recent report, Wudl and co-workers have reported the synthesis of a stable tetraphenyl heptacene derivative (**23**) using a tri-*iso*-propylsilylethynyl substituent (Figure 1.14).[78] The phenyl groups are effective in preventing the aromatic cores from reacting with each other or with the alkyne, and as a result the smaller alkyne substituent could be used. Photoxidation of the aromatic core was reported to be the major decomposition process for this heptacene derivative.

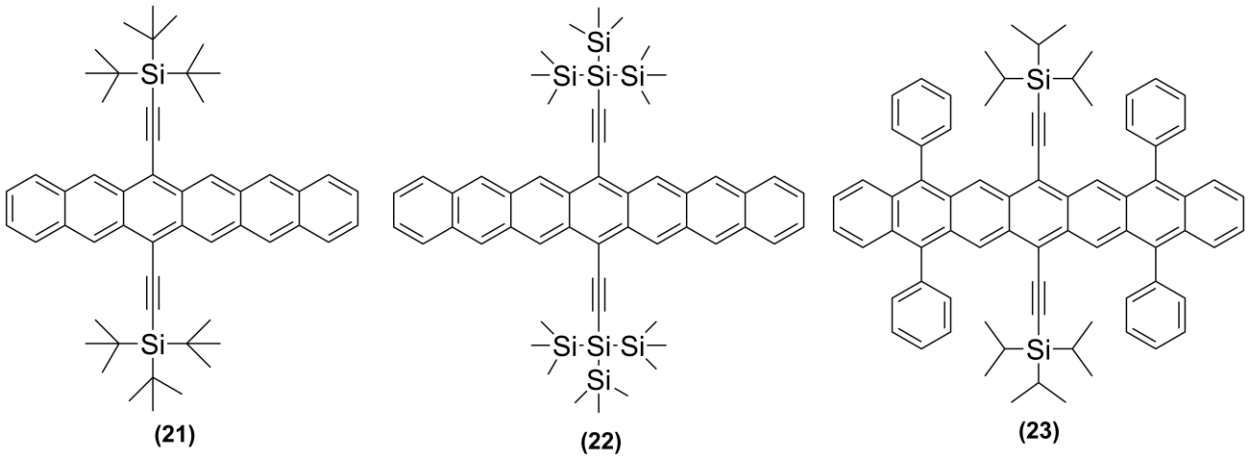

Figure 1.14 Trialkylsilylethynylated higher acenes[77,78]

Although TTBS Hexacene (**21**) exhibits reasonable stability in solution, the poor solubility in solvents such as toluene and chlorobenzene has prevented the measurement of its transport properties in organic thin film transistors (OTFTs). My approach to improve the solubility and crystal packing of these unique molecules for application in OTFT will be explained in Chapter 3. Chapter 4 will also deal with the stability and decomposition pathways for trialkylsilylethynylated hexacenes. Further improvement in stability of reactive higher acenes by partial halogenations will be explored in Chapter 5.

1.4 Solar Cells

Fossil fuels have shaped our global economy ever since the dawn of industrial revolution. However in recent decades our ever increasing dependence on them has had significant impact both economically and environmentally. In order to overcome the dependence on fossil fuels alternative energy sources such as wind, solar, geothermal, tidal wave energy have come under intense scrutiny. Among these renewable energy sources available to humankind, solar energy stands out as a viable alternative for our future energy needs.

There are two ways by which one can tap the energy of sun. (1) The first approach is to concentrate the solar energy and use it to generate steam which is then converted into electricity using a steam turbine. (2) The second approach is to take advantage of photovoltaic effect and use sunlight to generate photocurrent using a photovoltaic (PV) cell. While the first approach is suitable only for large scale energy production, the second approach can meet smaller energy requirements and can be tailored to individual needs.

Photovoltaic cells based on crystalline silicon have dominated photovoltaic technology for the last 50 years due to their high power conversion efficiency (monocrystalline Si $\eta \sim 25\%$, polycrystalline Si $\eta \sim 20\%$)[80] associated with these cells. However high production costs involved in making monocrystalline and polycrystalline silicon wafers have fueled the search for low cost photovoltaic cells. Solar cells based on inorganic semiconductors such as amorphous silicon, copper indium gallium diselenide (CIGS) and cadmium telluride (CdTe) have also been explored for cost effective solar cells. However the use of low cost solution processing techniques has allowed organic semiconductor to be explored for cheaper energy production using solar cells.

1.4.1 Organic solar cells

The general working operation of a solar cell is described below:

1. Exciton generation: Light absorption by the organic semiconductor to generate exciton, a bound electron – hole pair.
2. Exciton migration and dissociation: The exciton can either recombine or migrate to the donor – acceptor interface or semiconductor metal interface where it dissociates into electrons and holes.
3. Charge separation: The separated charge carriers then migrate to their respective electrodes.

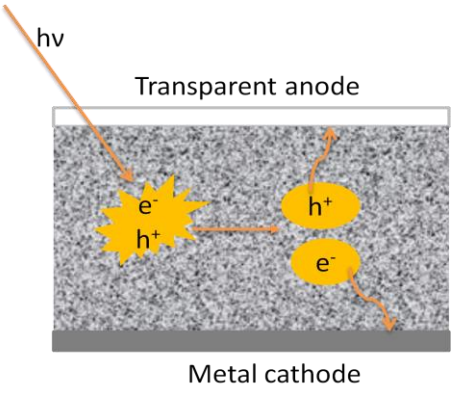

Figure 1.15 Schematic of power generation in an organic solar cell

1.4.1.1 Factors affecting Solar cell performance

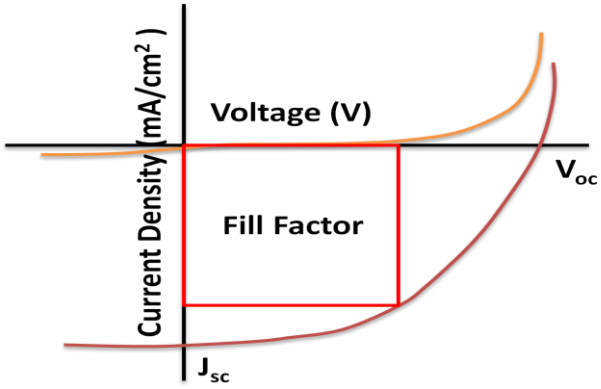

Figure 1.16 J – V curve of an organic solar cell

The performance of a solar cell is expressed in terms power conversion efficiency (PCE), which depends on following key factors and can be determined from the J-V curve shown in Figure 1.16

J_{sc}: Short circuit current (I_{sc}) is the current flowing through the device when the potential across the solar cell is zero. The amount of current produced is dependent on the area of the solar cell that is illuminated by the light. In order to remove the dependence of current on area, it is expressed in terms of short circuit current density (J_{sc}).

V_{oc}: Open circuit voltage is the voltage across the terminals of the cell when no current is flowing through the cell.

FF: Fill factor is the ratio of the maximum power produced by the cell to the product of V_{oc} and J_{sc}. Fill factor is also described as the squareness of the J – V curve.

$$FF = J_m \times V_m / J_{sc} \times V_{oc} \quad \ldots\ldots\ldots\ldots (5)$$

The efficiency of a solar cell also known as power conversion efficiency (PCE) is related to J_{sc}, V_{oc} and FF by the following equation (6).

$$\eta = J_{sc} \times V_{oc} \times FF / P \quad \ldots\ldots\ldots\ldots\ldots (6)$$

where P is the power of the incident light.

The performance of the solar cell depends on the conditions under which the values are measured. Standard Test Conditions (STC) for measuring solar cell performance is the Air Mass 1.5 spectrum, a light intensity of 1000 W/m^2 incident at an angle of 48.19˚ and at a temperature of 25˚C. It is also important to note that the area of the device affects solar cell efficiency;

smaller cells have higher efficiency than larger cells. One needs to take into account the active area of the device and test conditions before comparing device performance.

Another important term used to measure the performance of solar cells is external quantum efficiency (EQE). It is a measure of the number of charge carriers collected to the number of photons of a given energy incident on the device.

EQE (%) = Number of charge carrier generated / Number of incident photons

A lower EQE is indicative of losses due to recombination of charge carriers in the devices.

1.4.1.2 Single Layer Solar Cells

The first organic solar cells were made by sandwiching the organic layer between two metal electrodes of different work function resulting in the formation of a Schottky barrier between the organic semiconducting layer and the low work function metal.[81] In these devices the exciton dissociation takes place at semiconductor - metal interface, as a result only excitons generated closer to the metal electrodes contribute to overall photocurrent resulting in low power conversion efficiencies. The highest PCE (0.7%) reported for a single layer solar cell was achieved using merocyanine dye sandwiched between Ag and Al electrodes.[82]

1.4.1.3 Bilayer Solar Cells

In 1958, Kearns and Calvin reported photovoltaic effect in a bilayer heterojunction device using magnesium phthalocyanine and air oxidized tetramethyl *p*-phenylenediamine.[83] After nearly three decades, a breakthrough in device performance was achieved in 1986, when Tang reported solar cells made from two different organic semiconductors, copper phthalocyanine (**24**), a hole transporting layer and 3,4,9,10-perylene tetracarboxylic bis-

benzimidazole (**25**), as an electron transport layer sandwiched between the two electrodes.[84] Devices using this architecture gave a higher PCE (~1%) than single layer cells. The reason for this improved efficiency is due to the fact that in bilayer cells the excitons dissociate at the donor – acceptor interface rather than diffusing to semiconductor – metal interface which significantly reduces the loses due to recombination. Improvement in efficiency up to 4.2% was achieved for CuPc/C_{60} bilayer devices by placing an exciton blocking layer between C_{60} layer and Al electrode.[85] However PCE is limited by the planar interface and only excitons generated closer to the interface are effective in producing free charge carriers.

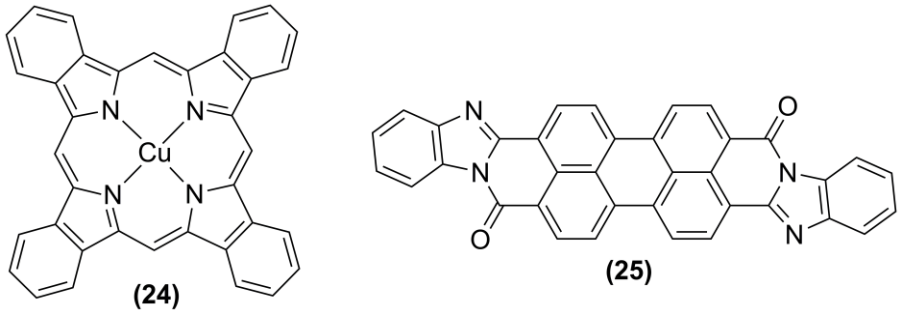

Figure 1.17 Structure of donor and acceptor molecules used by Tang[84]

1.4.1.4 Concept of Bulk Heterojunction (BHJ) Solar Cells

In order to increase the interface between the donor and acceptor material the bulk heterojunction concept was introduced, where both the donor and the acceptor were co-deposited either by vacuum deposition or solution processing. The first BHJ solar cells were reported by Yu et al.[86] and Halls et al.[87] using active layer made by spin casting (poly(2-methoxy-5-(2'-ethyl-hexyloxy)-1,4-phenylene vinylene, (MEH-PPV, **26**) as the donor and CN-PPV (**27**) as the acceptor yielding external quantum efficiency of 5-6%. Improvements in power conversion efficiency were not achieved until 2004, when Kietzke et al. reported power conversion efficiency of 1.7% for polymer devices made using M3EH-PPV (**28**)donor and CN ether-PPV (**29**) acceptor spin coated from chlorobenzene.[88] These devices exhibited very high open circuit

voltage (1.36 V), however the device performance was limited by low fill factor (35%). The poor conversion efficiency in polymer BHJ solar cells is due to low electron and hole mobilities and poor phase separation in these devices.

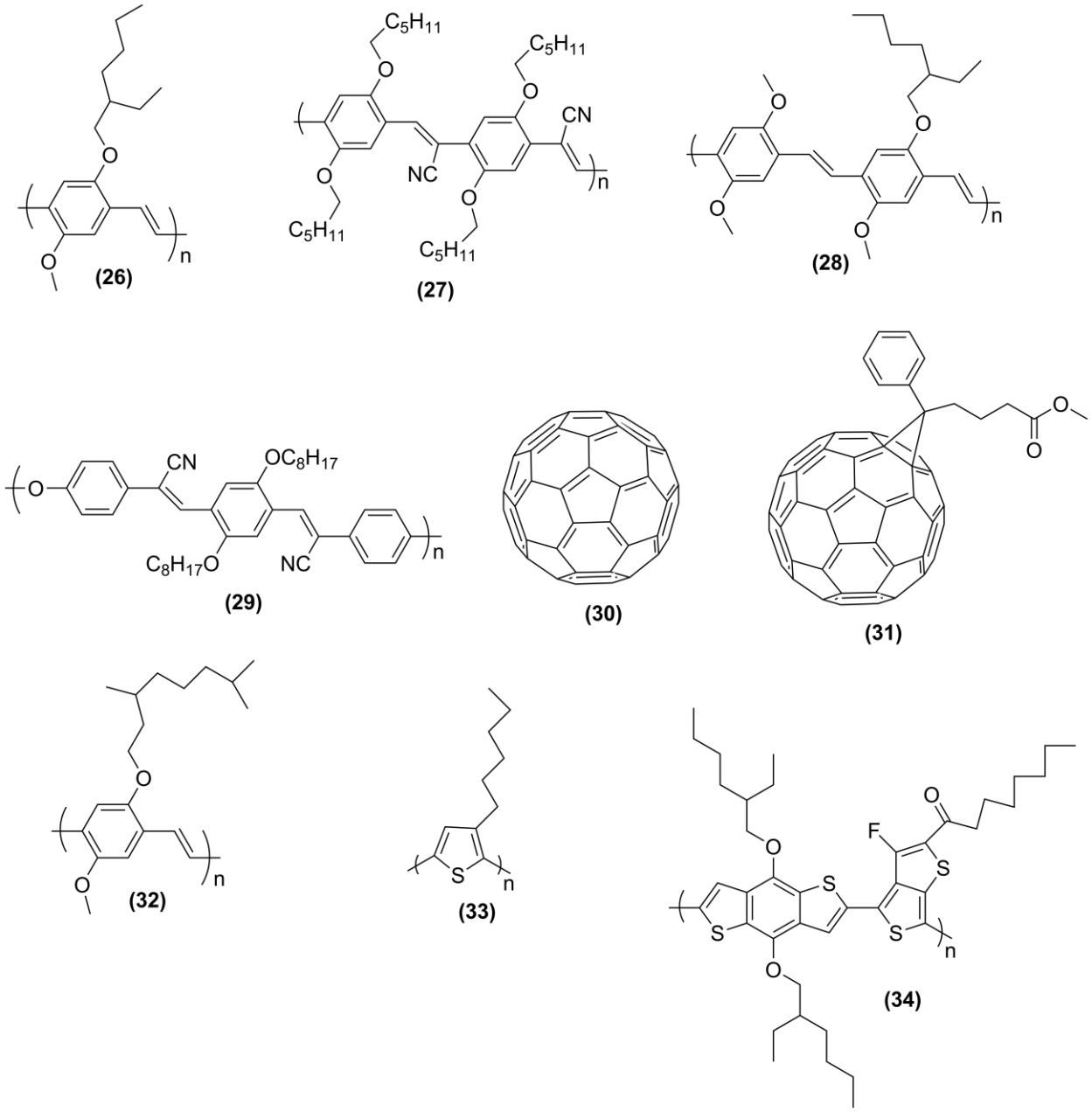

Figure 1.18 Structures of donor and acceptor materials used organic solar cells

After successfully applying the bulk heterojunction concept to polymer blend solar cells Yu et al. applied the same concept on polymer/small molecule solar cells using a blend of MEH-

PPV and soluble C_{60} fullerene derivative, (6,6)-phenyl C_{61}-butyric acid methyl ester, (PCBM, **31**).[89] These devices gave higher external quantum efficiency (EQE) of 45% compared to polymer blend solar cells. Improvements in efficiency were achieved by Shaheen et al. using poly(2-methoxy-5-(3',7'-dimethyl-octyloxy)-p-phenylene vinylene, (MDMO-PPV, **32**) as the donor polymer with PCBM acceptor spin coated from chlorobenzene.[90] The authors noted that the improvement in efficiency is due to the increased solubility of PCBM in chlorobenzene resulting in the formation of smaller crystallites thereby increasing interface between the PCBM and MDMO-PPV(**32**).

In recent years thiophene based polymers have been extensively studied as donors for fullerene based solar cells, due to their absorption in the longer wavelength region compared to PPV based donors.[91-95] Devices based on regioregular poly(3-hexylthiophene) (P3HT, **33**) have shown efficiencies as high as 5%.[91,92] The improvement in performance for P3HT/PCBM solar cells is attributed to the increased crystallinity of the P3HT phase and improved light absorption of the blend upon annealing at high temperature closer to the glass transition temperature of the polymer. Efficiency of P3HT/PCBM solar cells is also dependent on the degree of regioregularity,[93] polydispersity and molecular weight[94] of P3HT. Recently Caroll et al. reported P3HT/PCBM solar cells with record efficiency of 6%,[95] however these devices had smaller active area (5-10 mm^2) compared to 4.9% efficient devices (19 mm^2) reported by the same group.[92]

Since 2007 there haven't been any significant improvements in the efficiency of P3HT/PCBM solar cells. The reason for this upper limit on efficiency is the low V_{oc}. It has been shown that for PCBM based solar cell the maximum V_{oc} is related to the HOMO of the donor and the LUMO of the acceptor equation (7).[96]

$$V_{oc} = (1/e) (\left| E_{donor}\ HOMO \right| - \left| E_{PCBM}\ LUMO \right|) - 0.3V \text{ …….....(7)}$$

Based on the LUMO value of -4.3 eV for $PC_{61}BM$ and HOMO value of -5.1 eV for P3HT, the maximum V_{oc} for P3HT/PCBM solar cell is 0.5 V, which is lower than the V_{oc} (0.6 V) for best performing device. For efficient exciton dissociation the difference between the LUMO energies of the donor and acceptor should be ~ 0.4 eV, as a result for P3HT/PCBM solar cells a significant amount of energy is lost during the transfer of photoexcited electron from the LUMO of the donor to the LUMO of the acceptor. The efficiency is also affected by the low hole mobility of P3HT (10^{-5} – 10^{-6} cm^2/Vs) and the poor absorption of both P3HT and PCBM in the visible region of the spectrum.

In order to improve the efficiency of PCBM based solar cells low band gap polymers have been used in place of P3HT.[97-100] In recent years higher efficiencies up to 7.4% have been achieved by using poly[4,8-bis-substituted-benzo [1,2-b:4,5-b′]dithiophene-2,6-diyl-alt-4-substituted-thieno[3,4-b]thiophene-2,6-diyl] (PBDTTT, **34**)-derived polymers.[99,100]

1.4.2 Pentacene Solar cells

Pentacene with its high hole mobility in OTFT devices[17] and strong absorption in the visible region of the spectrum coupled with large excition diffusion length[103] makes it an ideal candidate as donor for solar cells. C_{60} fullerene has been the most commonly used acceptor for pentacene based solar cells.[103-105] Efficiency as high as 2.7% has been reported for pentacene /C_{60} bilayer solar cells using an exciton blocking BCP (2,9-Dimethyl-4,7-diphenyl-1,10-phenanthroline) layer.[103] These devices had an active layer of 10 mm^2 and the photocurrents were measured using a broadband light source (300-700nm). The authors estimated an efficiency of 1.5% for these devices under standard AM1.5G illumination. A slightly higher efficiency of 1.6% was reported

for devices using the same configuration deposited on flexible polyethylene terephthalate (PET) substrate under an AM1.5 simulated solar intensity of 80 mW/cm^2. However these devices had a smaller active cell area of 3 mm^2.[104]

While bilayer heterojunction solar cells with efficiencies >1% have been more commonly reported for pentacene/C_{60} solar cells, Koch et al. reported that bulk heterojunction devices exhibited significantly poor efficiencies.[106] The poor performance of co-deposited films of Pentacene/C_{60} was attributed to poor morphology and unfavorable interface energy. Another important factor is the high reactivity of pentacene with C_{60} molecules to form mono and bis adducts.[107]

1.4.2.1 Soluble Pentacene Solar Cells

The poor solubility of pentacene has prevented the use of solution processing techniques for device fabrication. In recent years soluble pentacene derivatives have been used to fabricate bilayer solar cells with C_{60} as acceptor. Bilayer solar cells made from thermally annealed TIPS pentacene and vacuum deposited C_{60} films gave an efficiency of 0.52% after incorporation of mobile ions in the donor layer.[108] Higher efficiency of 1.4% was achieved by Nuckolls et al. using spin coated 6,13-di(2-thienyl)pentacene (BTP, **35**) and vacuum deposited C_{60} in bilayer solar cells.[109]

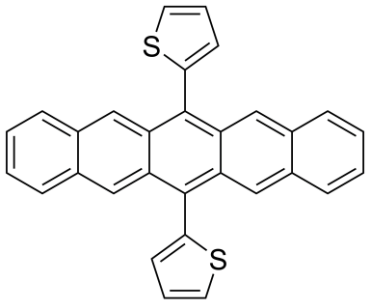

(35)

Figure 1.19 6,13-di(2-thienyl)pentacene (BTP)[109]

1.4.3 Small Molecule Acceptors

PCBM has been extensively used as an acceptor for P3HT BHJ solar cells due to its ability to form small crystallites and improved phase separation into donor/acceptor nanoscale domains on spin coating from solution. However PCBM exhibits very poor absorption in the visible region of the spectrum and generates highly reactive singlet oxygen resulting in poor device stability under ambient conditions.[110] Another important factor limiting the practical use of PCBM is the relatively high cost associated in synthesizing these molecules. While the cost of 100 mg of $PC_{61}BM$ is $85, the cost of the C_{70} analogue is threefold the price of $PC_{61}BM$ (100mg $PC_{71}BM$ - $250).[111] Even though large scale production of PCBM might lower the cost, the overall production cost of PV modules based on PCBM acceptors will still be higher.

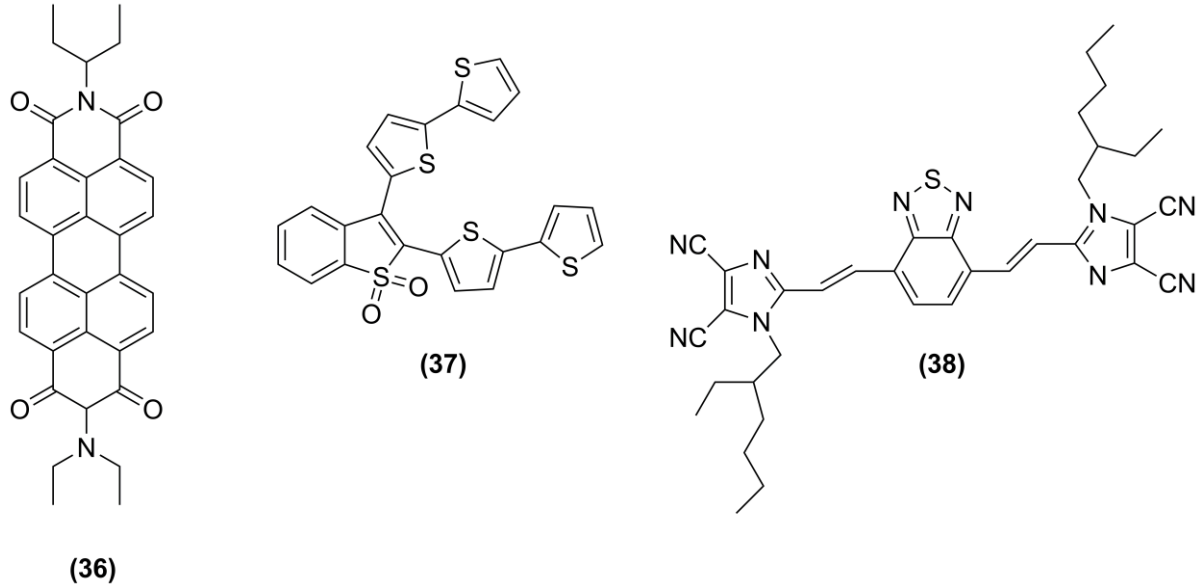

Figure 1.20 Small molecule acceptors for P3HT solar cells[113-115]

In order to overcome these problems associated with PCBM, other soluble acceptors have been explored for P3HT based solar cells.[112-117] Among the molecules that have been reported are the perylene tetracarboxylic diimide (PTCDI) derivatives,[112,113] benzo[b]thiophene dioxide oligomers[114] and vinazene derivatives.[115-117] While both PCTDI and branched benzo[b]thiophene

dioxide oligomers gave poor efficiencies the vinazene derivative, 4,7-bis(2-(1-(2-ethylhexyl)-4,5-dicyanoimidazol-2-yl)vinyl)-benzo[c][1,2,5]-thiadiazole (EV-BT, **38**), has recorded the highest efficiency of 1.1% for a non-fullerene based small molecule acceptor for P3HT solar cells.

1.4.3.1 Pentacene Acceptors

While electron deficient pentacenes have been extensively studied as n-type materials in OTFTs,[64,118] their application as acceptors in solar cells has not been reported until recently by Anthony et al.[119] The authors reported a series of cyano pentacenes and studied their performance in solar cells with P3HT as the donor. It was found that the V_{oc} was dependent on the number of nitrile substituents on pentacene chromophore and molecules that pack in a 1-D sandwich herringbone fashion exhibited higher efficiency within the series. Compared to P3HT/PCBM solar cells a higher V_{oc} of 0.84 V was reported for devices made from 6,13-bis(tricyclopentylsilyethynyl)-2-cyanopentacene (**39**), which packs in a 1D sandwich herringbone motif. Chapter 2 will extend the above approach by synthesizing monohalogenated pentacenes for application as acceptors for solar cells.

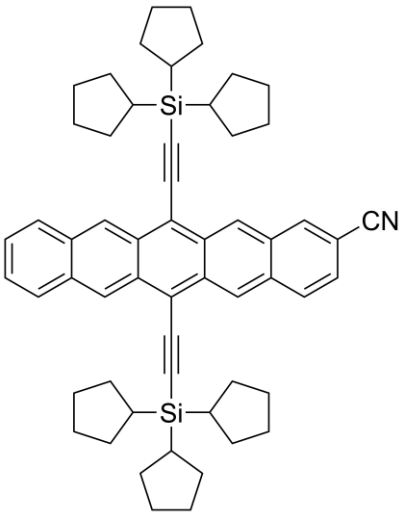

(39)

Figure 1.21 Pentacene acceptor for P3HT solar cells[119]

1.5 Overall objectives of the present work

The goal of the present work is to synthesize heteroacenes and partially halogenated acenes for application in both OTFTs and solar cells. Partial halogenation will be used as a tool to improve crystallinity of spin cast thin films (Chapter 2) and to develop new class of ambipolar materials (Chapter 3). Partial halogenation is also used to tune energy levels of pentacene for application as acceptors for solar cells (Chapter 2 and 3). Chapter 4 will describe my approach to improve solubility of hexacenes and study their stabilities both in solution and solid state. Partial halogenation is also used to improve stability of higher acenes such as hexacene, heptacene and nonacene (Chapter 5). Finally the synthesis and device properties of trialkylsilylethynylated anthradiselenophenes will be reported in chapter 6.

Chapter 2: Partially Halogenated Pentacenes for Organic electronics

2.1 Solution processed organic semiconductors

The greatest advantage of organic semiconductors is their ability to be solution processed using low cost techniques such as drop casting, spin coating and inkjet printing. However the success of these solution processing techniques depends on crystallinity[120], grain size[121] and orientation of the $\pi - \pi$ stacking direction[122-124] which influences the charge carrier mobility. The crystallinity of thin films depends on the drying rate of solvents and the solution processing technique used to make thin films[68]. For example, high boiling solvents tend to form highly crystalline films due to the slow evaporation of solvents compared to low boiling solvents. Crystallinity of thin films is also affected by the solution processing method used to make the films. Thin films made by drop casting, which has slower solvent evaporation rate, gives highly crystalline films compared to films made by spin casting, which has faster solvent evaporation rate, using the same solvent. While drop casting can be used to screen for high mobility organic semiconductor it is however not suitable for high-throughput production.

Several approaches have been explored to improve morphology and molecular ordering of solution processed thin films.[125-128] One approach is to post treat the films by thermally annealing at high temperatures[125,126] or annealing by exposing to solvent vapors for prolonged period of time.[127-130] While both thermal and solvent annealing enhance the thin film properties of solution processed organic semiconductors, they do cause dewetting of the organic semiconductor and are not compatible for high throughput production.[131] A more practical approach is to design molecules that can self assemble on solution processing to give highly crystalline well ordered thin films.[70,132,133]

2.2 Solution processed acene semiconductors

While solution processed pentacenes have been rare due to their poor solubility in organic solvents,[51] *peri*-functionalization with trialkylsilylethyne groups have enabled the use of solution processing techniques.[65] Drop cast TIPS pentacene (**15**) and TES ADT (**17**) have both shown high mobilities, however spin cast films of both acenes exhibit poor mobility due to poor crystallinity of the films.[68] In 2006 Loo et al. reported that the crystallinity of spin cast thin films of TES ADT (**17**) can be improved on solvent annealing.[130] Films exposed to 1,2-dichloroethane vapors for 2 min exhibited a mobility of ~ 0.1 cm^2/Vs. However these devices showed huge variation in threshold voltage (V_{TH}) due to the presence of solvent molecules at the interface and also due to untreated SiO_2 dielectric used in these devices. In 2007 Cho et al. reported a higher mobility of 0.43 cm^2/Vs for solvent annealed TES ADT films spin cast on octyltrichlorosilane treated SiO_2 dielectric.[131] This increase in mobility was attributed to the formation of continuous crystalline domain and to the increased π-stacking between the molecules along the high mobility direction. In a recent report Cho et al. have shown that spin cast film of TES ADT (**17**) molecules do have a tendency to slowly self assemble over a period of time to form crystalline films.[134] The authors attributed the tendency of TES ADT (**17**) to reorganize itself to its low glass transition temperature (T_G). Field effect mobility of ~ 0.1 cm^2/Vs was reported for spin cast films of TES ADT (**17**) after 7 days of aging.

In order to improve the crystallinity of spin cast thin films of TES ADT (**17**) Anthony et al. partially fluorinated the ADT core.[69] TES DifluoroADT (TES FADT**, 18**) molecules pack in a 2D fashion similar to TES ADT with a 0.3 Å long-axis shift between neighboring molecules in the π-stacks (Figure 2.1). Films spin cast from chlorobenzene gave a hole mobility as high as 1.5 cm^2/Vs. The high mobility was attributed to nucleation of TES FADT (**18**) on

perfluorobenzenethiol (PFBT) treated Au source and drain electrodes (Figure 2.1(a&b)). PFBT is usually used to treat the source and drain electrodes to improve charge injection from the electrodes to the semiconductor but in the case of TES FADT (**18**) the treatment of electrodes with PFBT induces crystallization on the electrodes which eventually grows into the transistor channel (Figure 2.1(c)).[135]

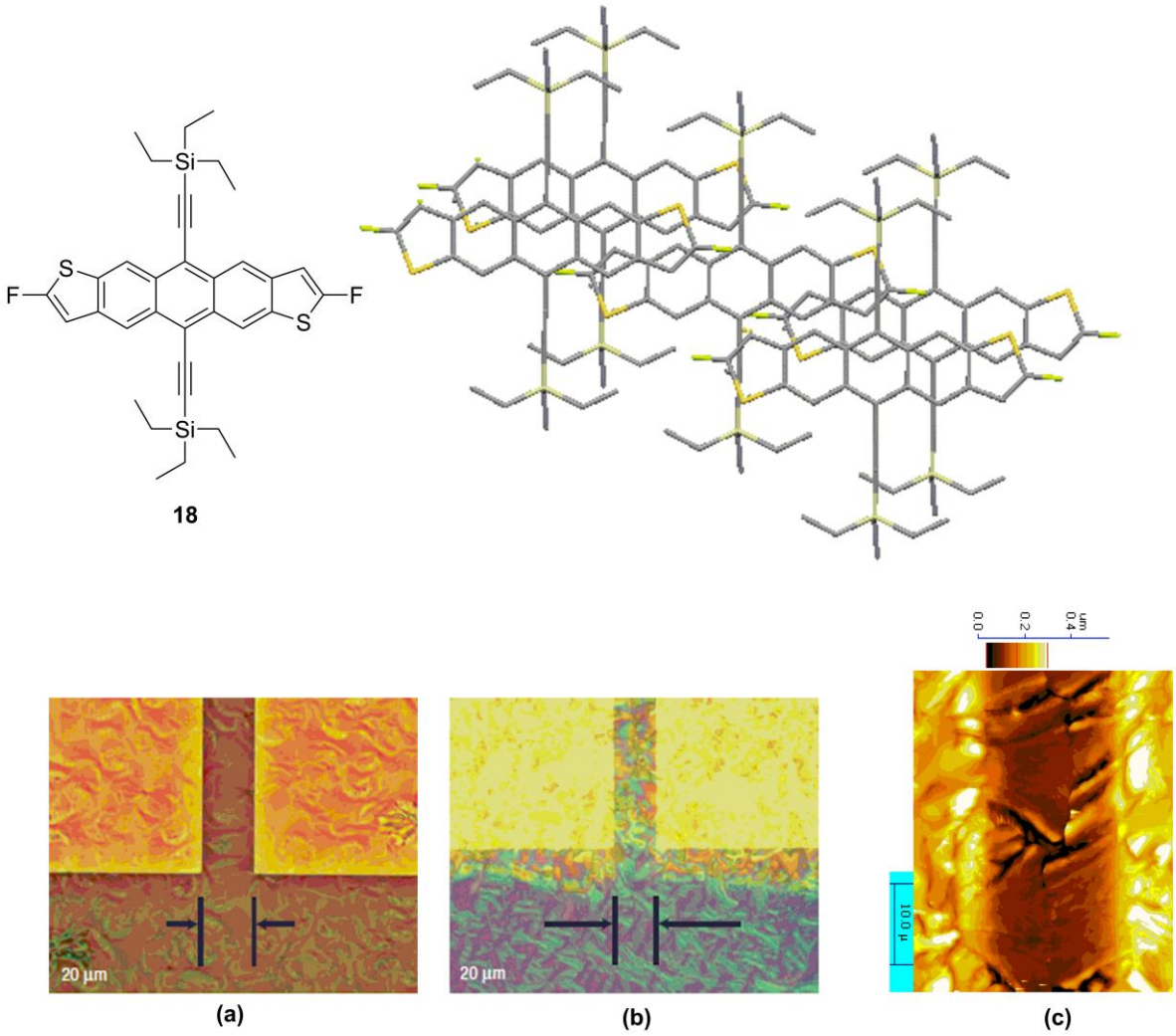

Figure 2.1. Structure and crystal packing of TES FADT(18) along with optical micrograph of spin cast TFTs. (a) Untreated device (b) PFBT treated device (Gundlach et al. Nature. Mater. 2008)[135] (c) AFM image of channel (Anthony et al. JACS 2008)[69]

While partial fluorination serves as valuable tool to improve morphology of spin cast films, the mobility of solution processed thin film can also be improved by blending small molecules that can improve crystallinity and molecular ordering.[136,137] Addition of small quantities of TES FADT (**18**) has been used to seed the nucleation of TES ADT on spin casting from solution. TES ADT (**17**) solution containing > 3 mol% of TES FADT formed crystalline thin films on spin coating yielding a mobility of 0.13 cm^2/Vs.

2.3 Partially fluorinated pentacenes

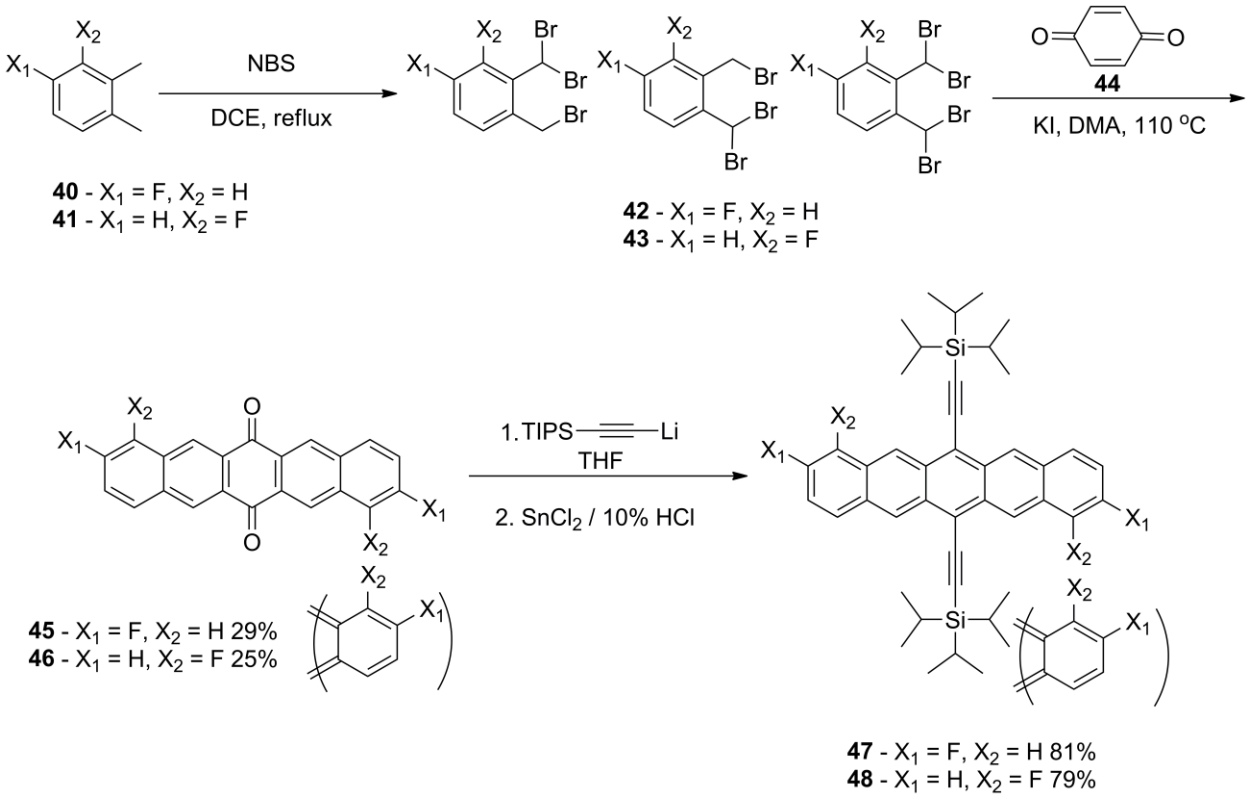

Scheme 2.1. Synthesis of TIPS Difluoropentacene

2.3.1 Difluoropentacene

In order to take advantage of contact induced nucleation in pentacene I decided to substitute fluorine atoms on the pentacene chromophore. Unlike the synthesis of FADT[69] the fluorinated *o*-xylenes are commercially available. The final pentacene was synthesized in three

steps starting from commercially available monofluoro-*o*-xylene as shown in scheme **2.1**. Benzylic bromination of *o*-xylene (**40 & 41**) gave a mixture of α, α, α′ - tribromo-*o*-xylene and α, α, α′, α′ - tetrabromo-*o*-xylene (**42 & 43**), which was then allowed to react with 1,4-benzoquinone (**44**) to give the corresponding difluoropentacene quinones (**45 & 46**) in 17-20% yield as mixture of isomers. Reaction with lithium triisopropylsilyl acetylide gave the intermediate diol which was converted to the final pentacene by treatment with $SnCl_2 \bullet 2H_2O$ and 10% HCl. Purification of the crude pentacenes by silica gel chromatography followed by recrystallization from acetone gave pure pentacene in 70% yield as a mixture of isomers. The dark blue crystals obtained from recrystallization were suitable for single crystal x-ray diffraction analysis.

Similar to TIPS pentacene (**15**) both TIPS *cata*-difluoropentacene (TIPS CFP, **47**) and TIPS *peri*-difluoropentacene (TIPS PFP, **48**) pack in a 2D fashion (Figure 2.2 & 2.3). Compared to TIPS pentacene (**15**) both TIPS CFP (**47**) and TIPS PFP (**48**) have closer contacts between the aromatic faces, with TIPS CFP (**47**) having the closest contact distance of 3.23 Å.

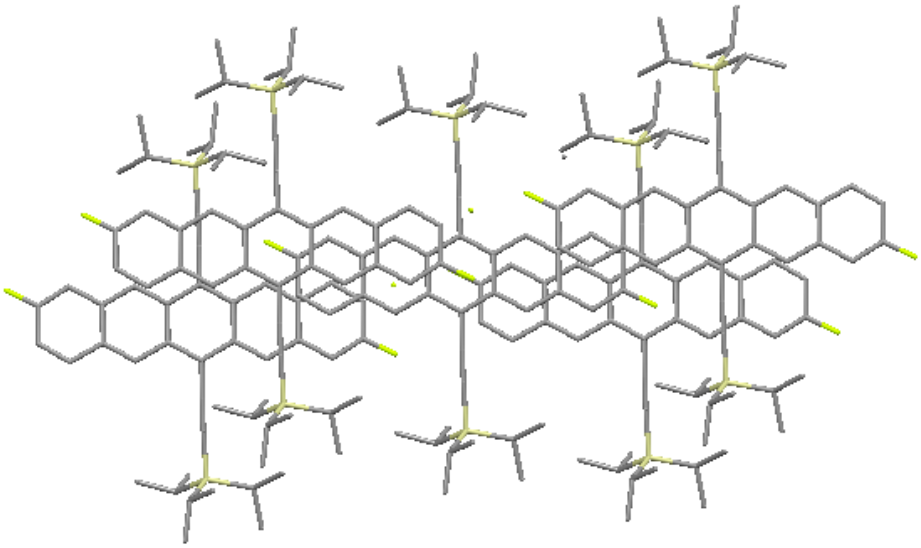

Figure 2.2 Crystal packing of TIPS CFP (47)

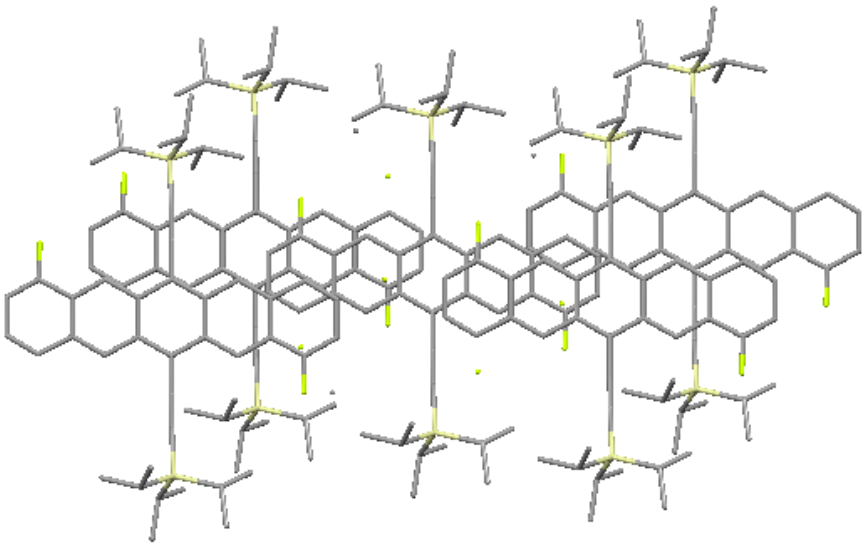

Figure 2.3 Crystal packing of TIPS PFP (48)

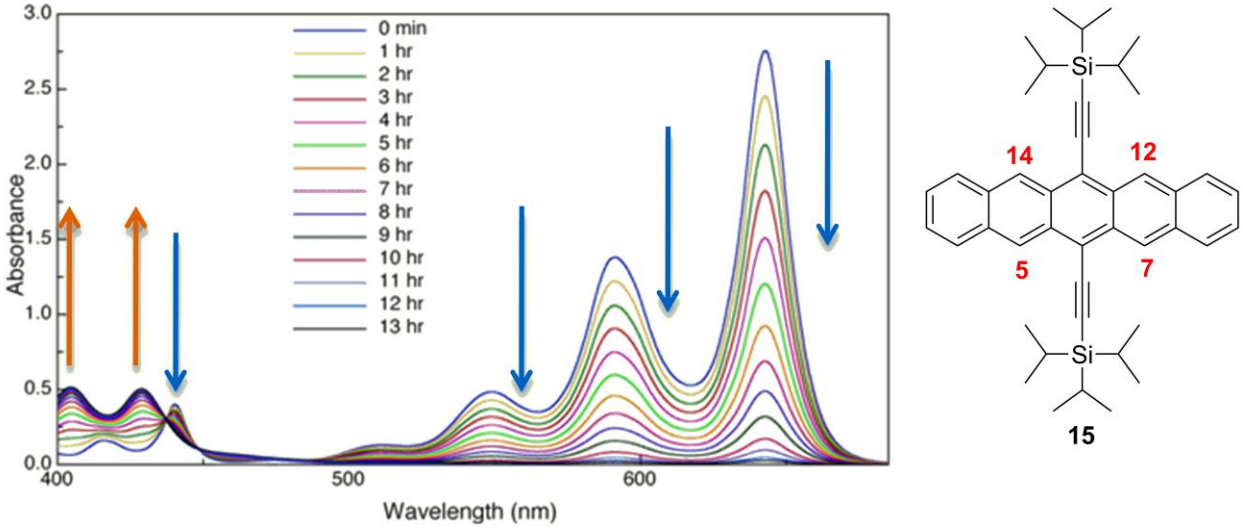

Figure 2.4 UV-vis stability study of TIPS pentacene (15)

Since I was interested in studying TFT performance of spin cast films I decided to study the relative stability of difluoropentacenes *versus* TIPS pentacene (**15**) molecules in solution using UV-visible spectroscopy. 10^{-4} M solution of pentacene were made in N_2 purged toluene and an initial spectrum of the pentacene was obtained. The solution was then exposed to a bright full-spectrum light source and the spectra were acquired at regular intervals until the absorption bands at longest wavelength disappeared. A plot of absorbance maximum at longest wavelength

versus time was used to calculate the solution half-life (time taken to reach half the initial absorbance) of each pentacene derivative. In comparison to TIPS pentacene (**15**) which has a solution half life of 296 min both TIPS CFP (**47**) ($t_{1/2}$ - 552 min) and TIPS PFP (**48**) ($t_{1/2}$ - 972 min) exhibited significantly higher stability in solution, similar to that seen in TES FADT (**18**) in comparison to TES ADT (**17**). This difference in solution stabilities can be better explained by understanding the decomposition pathways for TIPS pentacene (**15**).[138] The functionalization of the reactive 6 and 13 position of the pentacene core improves the stability of pentacene, however the 5&14 and 7&12 carbon atoms are still reactive enough to undergo dimerization. As a result in solution TIPS pentacene (**15**) undergoes decomposition by dimerization of the pentacene core at either 5&14 or 7&12 carbon atoms (Figure 2.4). The addition of electron withdrawing fluorine atoms to the pentacene chromophore reduces the electron density at those reactive positions thereby reducing the reactivity at these positions (Figure 2.5).

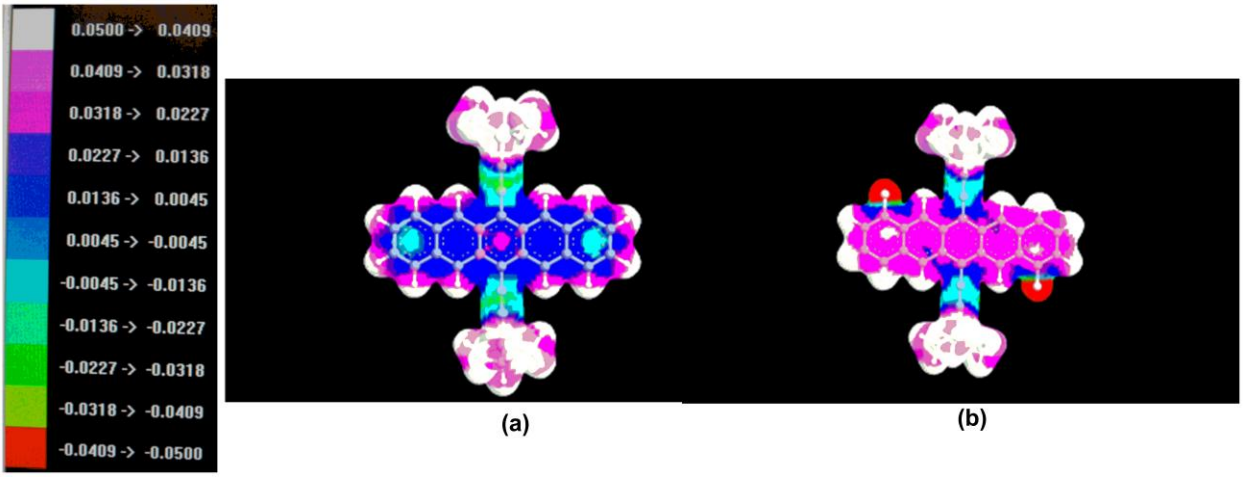

Figure 2.5 Electrostatic surface potentials (ESP) mapped on to a surface of total electron density for Pentacene (a) and PFP (b) (ESP were mapped using software ArgusLab4.0, www.arguslab.com)

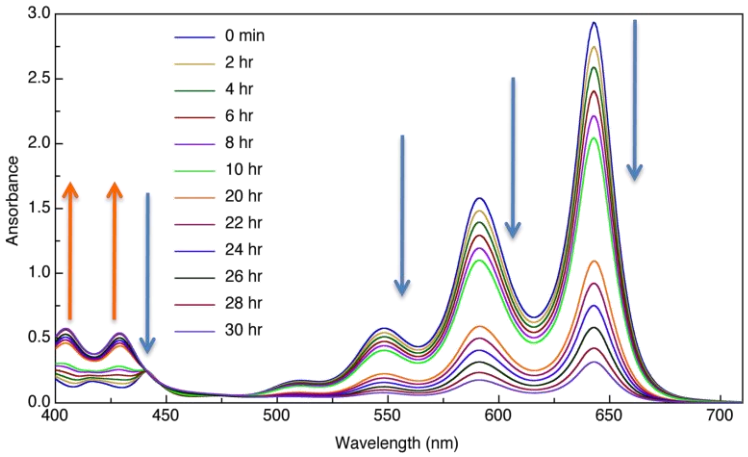

Figure 2.6 UV-vis stability study of TIPS PFP (48)

Both TIPS PFP (**48**) and TIPS CFP (**47**) exhibit higher stability due the presence of electron withdrawing fluorine substituents. However the position of the fluorine substituent on the pentacene chromophore plays a crucial role in the stability of the pentacene. Substitution of electron withdrawing fluorine atoms closer to the reactive carbon atoms has greater effect in reducing electron density at those reactive positions in the pentacene chromophore, as a result TIPS PFP (**48**) exhibits higher solution half life than TIPS CFP (**47**) (Figure 2.6).

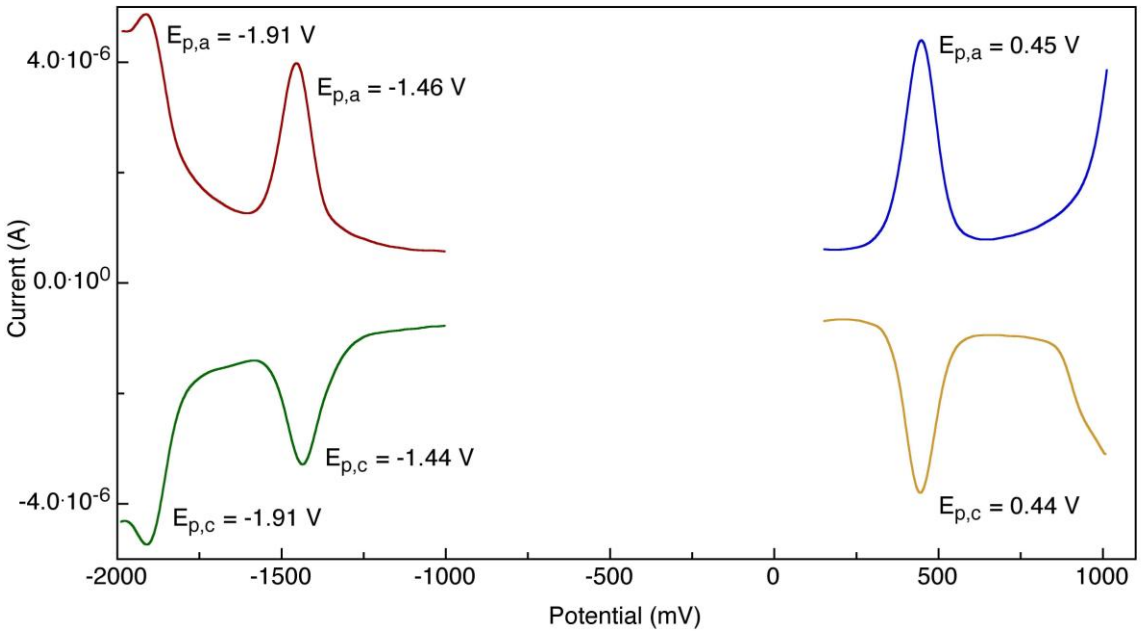

Figure 2.7 DPV of TIPS CFP (47)

Table 2.1 Energy levels of difluoropentacene and TIPS Pentacene (15)

Acene	E_{ox} (mV)	E_{red} (mV)	HOMO (eV)	LUMO (eV)	E_{gap} (eV)	$t_{1/2}$ min
TIPS pentacene (**15**)	**366**	**-1472**	**-5.16**	**-3.33**	**1.83**	**296**
TIPS CFP (**47**)	**446**	**-1445**	**-5.24**	**-3.41**	**1.89**	**552**
TIPS PFP (**48**)	**479**	**-1391**	**-5.28**	**-3.35**	**1.87**	**972**

Since both TIPS CFP (**47**) and TIPS PFP (**48**) exhibit 2D π-stacking we decided to study their thin film transistor properties from spin-cast from solution and compare the mobilities with TIPS pentacene. The OTFT device measurements were done by Marina Feric under the guidance of Dr. Oana Jurchescu and Dr. David Gundlach at the National Institute of Standards and Technology (NIST). The devices were fabricated in a bottom contact configuration using heavily doped Si as the gate electrode and thermally grown SiO_2 as the gate dielectric. Au source and drain electrodes were deposited on to the SiO_2 dielectric. The channel length for these devices varied from 5, 10, 20, 25, 50, 80 and 100 μm. The Au source and drain electrodes were treated with PFBT prior to spin casting the active layer. Finally the SiO_2 gate dielectric was treated with HMDS. 2 wt% solutions of the pentacene in toluene and chlorobenzene were then spin cast on to these devices at 1000 rpm. Devices fabricated from chlorobenzene gave relatively higher mobilities compared to films spin cast from toluene. This is due to the difference in the rate of evaporation between the two solvents. The use of higher boiling chlorobenzene allows the pentacene molecules to form crystalline films with larger grain size. PFBT treatment of the electrodes results in the formation of crystalline film on the electrodes (Figure 2.8) resulting in higher mobilities compared to untreated devices.

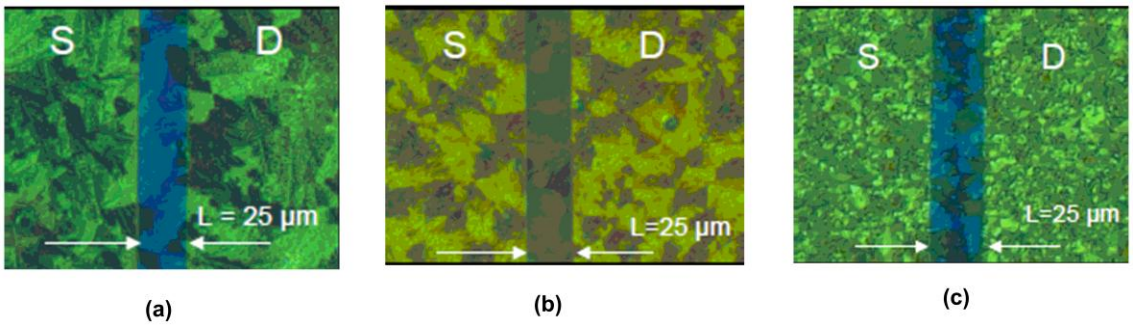

Figure 2.8 Optical micrographs of TIPS PFP (48) (b) and TIPS CFP (47) (c) TFT devices in comparison with TIPS Pentacene (15) (a) (Optical micrographs taken by Dr. Oana Jurchescu, NIST)

Compared to TIPS pentacene (**15**) (0.007 cm^2/Vs) both TIPS CFP (**47**) (0.06 cm^2/Vs) and TIPS PFP (**48**) (0.02 cm^2/Vs) exhibit higher mobility in PFBT treated devices, with TIPS CFP (**47**) exhibiting the highest mobility due to closer packing between the molecules. In order to better understand the difference in mobility between TIPS pentacene (**15**) and difluoropentacene, the thin films were analyzed using Grazing Incidence X-ray Diffraction (GXID) by Dr. Joseph Kline at NIST. In the case of TIPS pentacene (**15**), two different orientations were observed on the PFBT treated electrodes, the high mobility 001 orientation and the low mobility 100 orientation (Figure 2.9 & 2.10). For both TIPS CFP (**47**) and TIPS PFP (**48**), only the high mobility 001 orientation was observed on the electrodes. The difference in orientation of the molecules in crystalline films explains the higher mobility observed in difluoropentacenes.

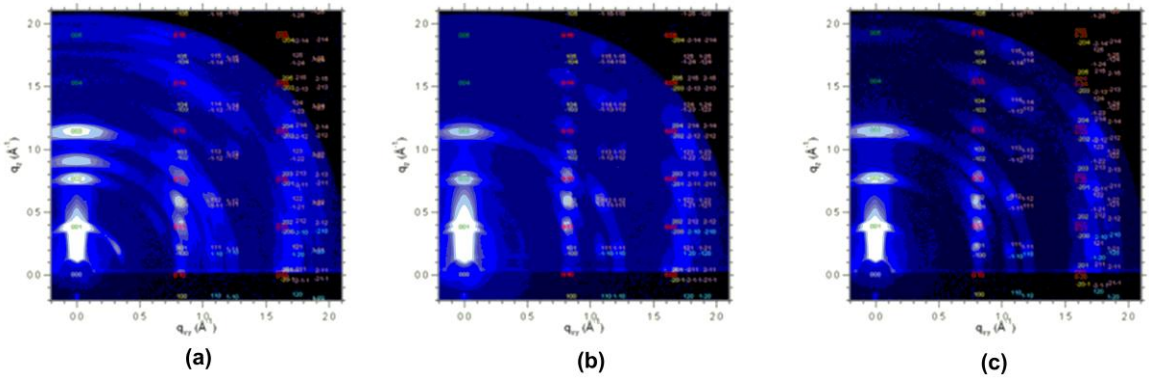

Figure 2.9 GIXD pattern of pentacene thin films on PFBT treated Au electrodes. (a) TIPS Pentacene (b) TIPS PFP (48) (c) TIPS CFP (47) (Dr. Joseph Kline, NIST)

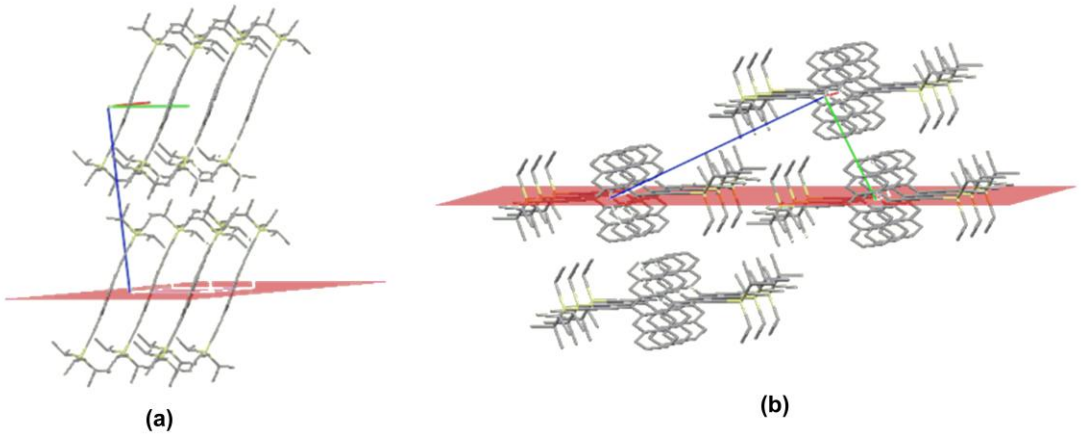

Figure 2.10 Orientation of TIPS pentacene (15) molecules on PFBT treated Au. (a) 001 (b) 011

2.3.2 Tetrafluoro and octafluoropentacenes

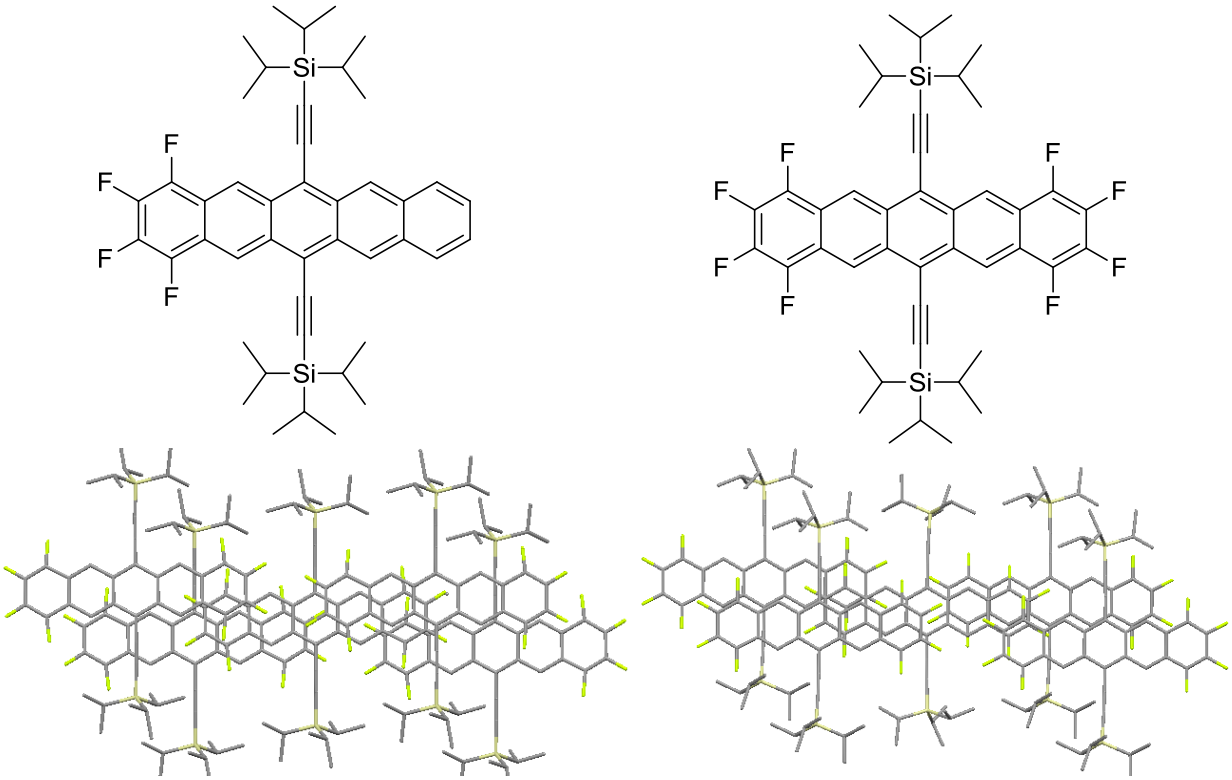

Figure 2.11 Crystal packing of TIPS F_4 (49) & F_8 pentacene (7)[139]

Due to the improved mobility of spin cast difluoropentacene I wanted to study the effect of degree of fluorination on the mobility of solution cast pentacene films. As a result I wanted to synthesize trialkylsilylethynylated terafluoro (F_4) and octafluoro (F_8) pentacenes. TIPS F_4

pentacene (**49**) & TIPS F_8 pentacene (**7**) were previously synthesized by Anthony et al. for OTFTs.[139] Vapor deposited films of both TIPS F_4 (**49**)and TIPS F_8 (**7**) pentacene exhibited hole mobility of 0.014 cm^2/Vs and 0.045 cm^2/Vs respectively. Recently Bao et al. reported ambipolar behavior for vapor deposited films of both TIPS F_4 (**49**) and TIPS F_8 (**7**) pentacene exhibiting electron mobilities of 0.072 cm^2/Vs and 0.33 cm^2/Vs respectively.[140] The lower solubility of TIPS derivative has prevented solution processed OTFT studies on these derivatives. In order to improve the solubility of F_4 and F_8 pentacene I decided to explore different trialkylsilyl substituents.

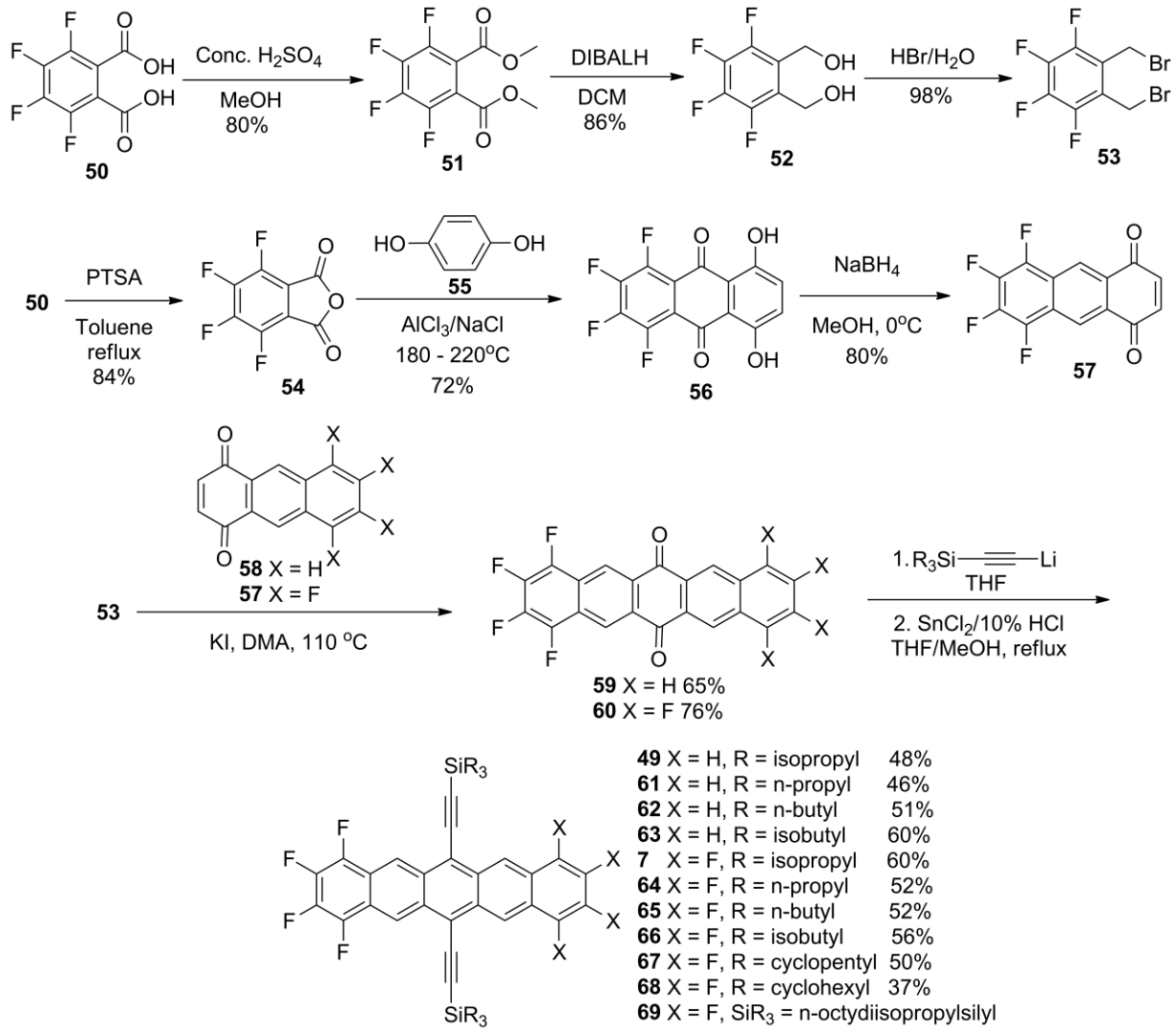

Scheme 2.2 Synthesis of tetrafluoro(F_4) & octafluoro(F_8) pentacene

The pentacene quinones were made from commercially available 3,4,5,6-tetrafluorophthalic acid (**50**) as shown in scheme 2.2. The phthalic acid was converted to dimethanol (**52**) by Fisher esterification followed by reduction using DIBALH. The dimethanol was refluxed in 48% HBr in water to give the 1,2-bis(bromomethyl)-3,4,5,6-tetrafluorobenzene (**53**) as an oil. 3,4,5,6-tetrafluorophthalic acid (**50**) was converted in to 3,4,5,6-tetrafluorophthalic anhydride (**54**) by refluxing in toluene with *p*-toluene sulfonic acid. Friedel-Crafts acylation of 1,4-dihydroxybenzene (**55**) with anhydride (**54**) gave tetrafluoroquinizarin (**56**) which on sodium borohydride reduction in methanol gave 5,6,7,8-tetrafluoro-1,4-anthraquinone (**57**) as a yellow solid. Cava reaction between 1,2-bis(bromomethyl)-3,4,5,6-tetrafluorobenzene (**53**) and 1,4-anthraquinone (**58**) or tetrafluoroanthraquinone (**57**) gave F_4 and F_8 pentacene quinones respectively. The pentacene quinones were treated with lithiated trialkylsilyl acetylenes and the intermediate diol was converted to final pentacenes by treating with saturated solution of $SnCl_2 \bullet 2H_2O$ in 10% HCl. Purification of the crude acene by silica gel chromatography followed by recrystallization gave pure pentacenes.

Single crystal x-ray diffraction analysis was performed to determine the packing motif for different derivatives except triisobutylsilyl (TIBS) and tricyclohexylsilyl (TCHS) derivative. Similar to TIPS F_4 and F_8 pentacenes, the straight chain n-propyl (TNPS) and n-butyl (TNBS) derivatives exhibit 2D π-stacking (Figure 2.12, 2.13 & 2.14), however changes in the alkyl substituent results in slippage along the long and short axis of the pentacene core. It has been reported small changes in solid state ordering can significantly affect band gap and charge transport properties in organic semiconductors.[141-144] With increasing size of alkyl substituent the packing arrangement changes from 2D to 1D sandwich herringbone in the case of cyclopentyl substituent (Figure 2.14). Interestingly the bulky n-octyl disopropylsilyl (NODIPS) derivative

exhibited a 2D packing motif with a close contact of between the aromatic faces (Figure 2.15). It should be noted that nonfluorinated NODIPS pentacene (**70**) exhibited *no* π-stacking between the aromatic faces (Figure 2.16).[145] This clearly indicates the efficacy of fluorination to induce π-stacking in molecules by aryl-perfluoroaryl interaction between the molecules.

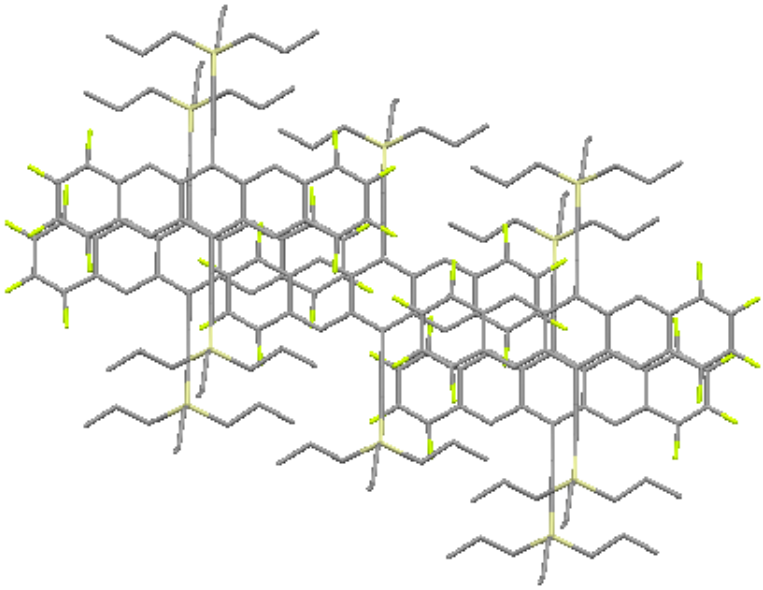

61

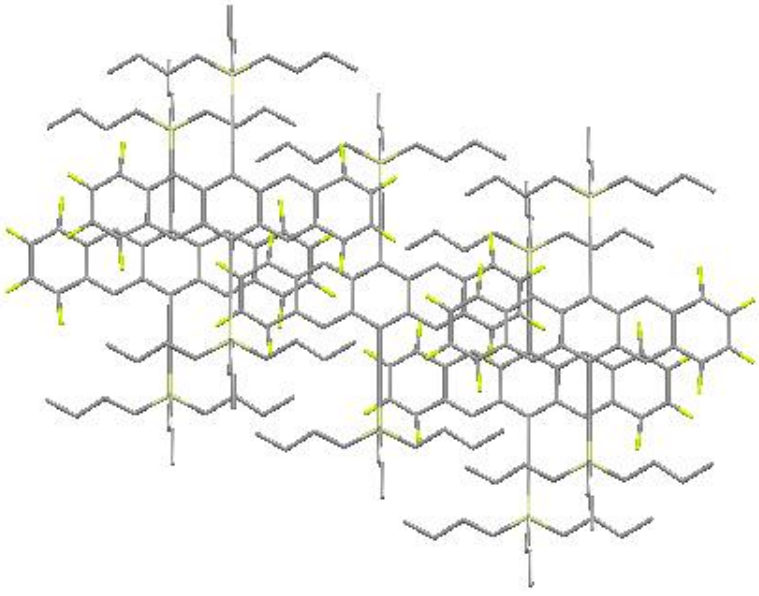

62

Figure 2.12 Crystal packing of TNPS F_4 pentacene (61) and TNBS F_4 pentacene (62)

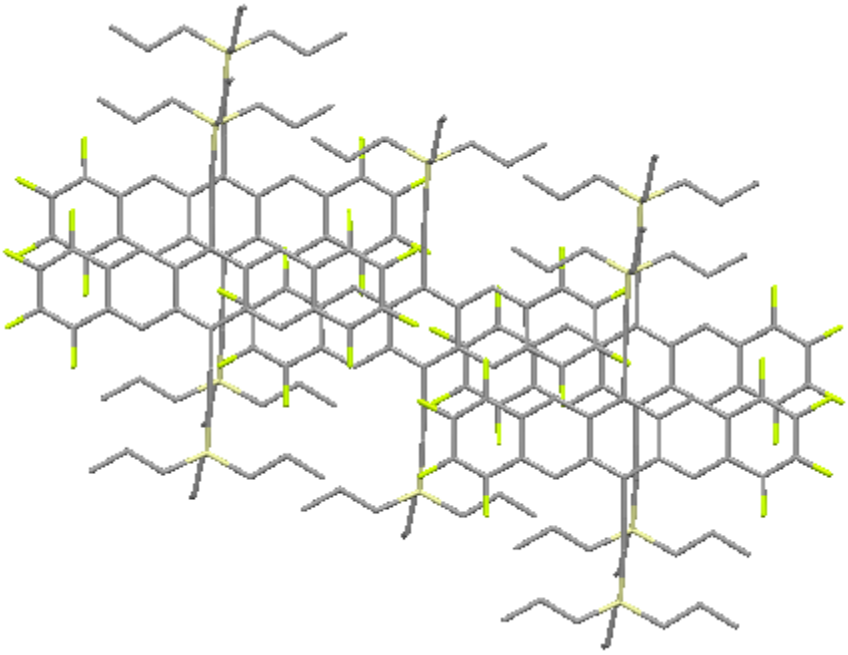

64

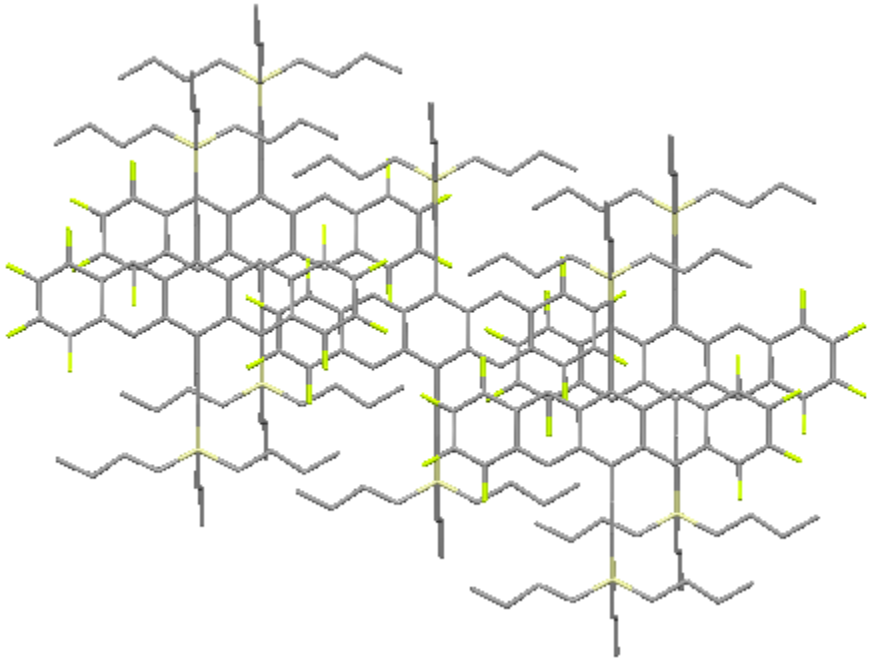

65

Figure 2.13 Crystal packing of TNPS F_8 pentacene (64) & TNBS F_8 pentacene (65)

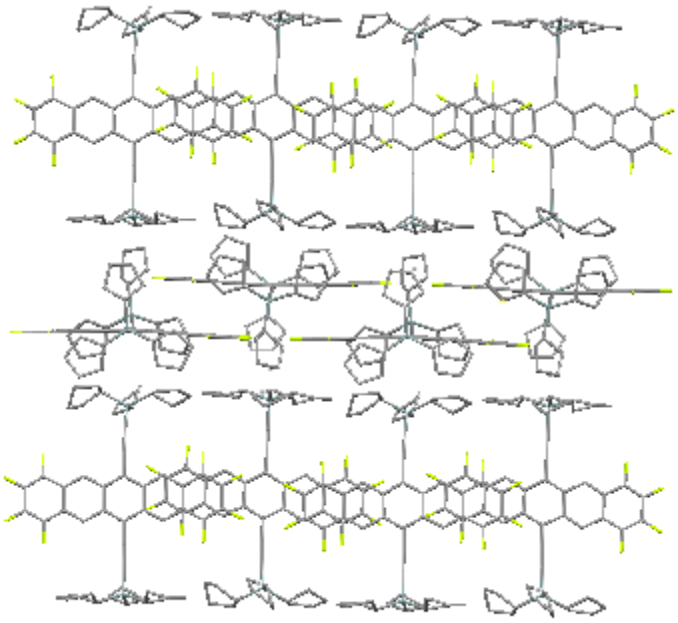

67

Figure 2.14 Crystal packing of TCPS F_8 pentacene (67)

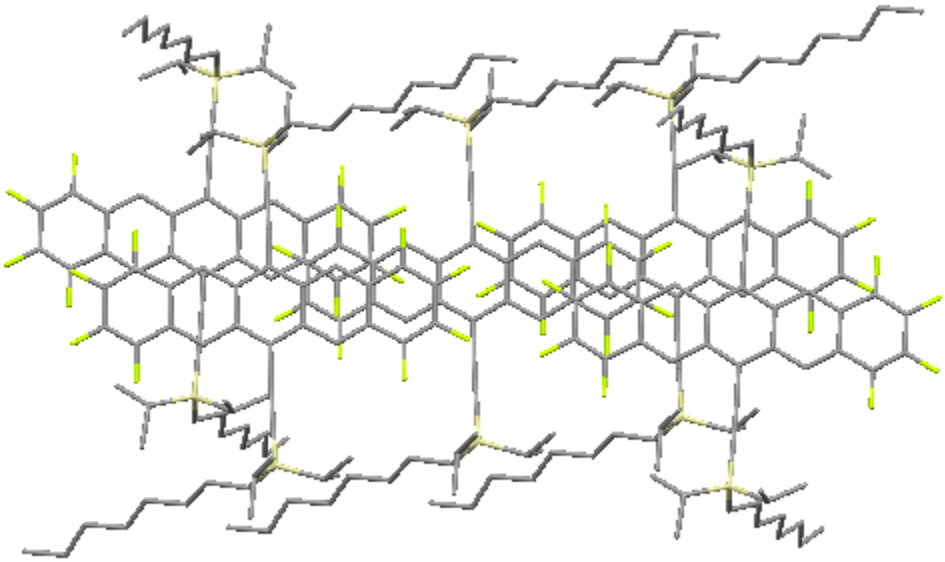

69

Figure 2.15 Crystal packing of NODIPS F_8 pentacene (69)

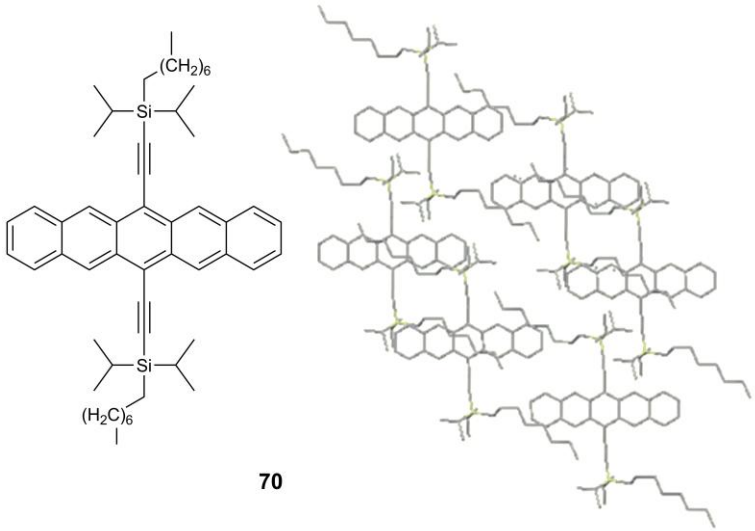

70

Figure 2.16 Structure and crystal packing of NODIPS Pentacene (70)[145]

Table 2.2 Energy levels of F_4 & F_8 Pentacene

Pentacene	E_{ox} (mV)	E_{red} (mV)	HOMO (eV)	LUMO (eV)	E_{gap} (eV)
TIPS F_4 (49)	548	-1342	-5.34	-3.45	1.89
TNPS F_4 (61)	528	-1341	-5.33	-3.46	1.87
TNBS F_4 (62)	535	-1346	-5.33	-3.45	1.88
TIBS F_4 (63)	544	-1347	-5.34	-3.45	1.89
TIPS F_8 (7)	752	-1202	-5.55	-3.60	1.95
TNPS F_8 (64)	740	-1226	-5.54	-3.57	1.97
TNBS F_8 (65)	740	-1215	-5.54	-3.58	1.96
TIBS F_8 (66)	741	-1263	-5.54	-3.56	1.98
TCPS F_8 (67)	742	-1240	-5.54	-3.54	2.00
TCHS F_8 (68)	739	-1214	-5.54	-3.59	1.95
NODIPS F_8 (69)	772	-1222	-5.57	-3.58	1.99

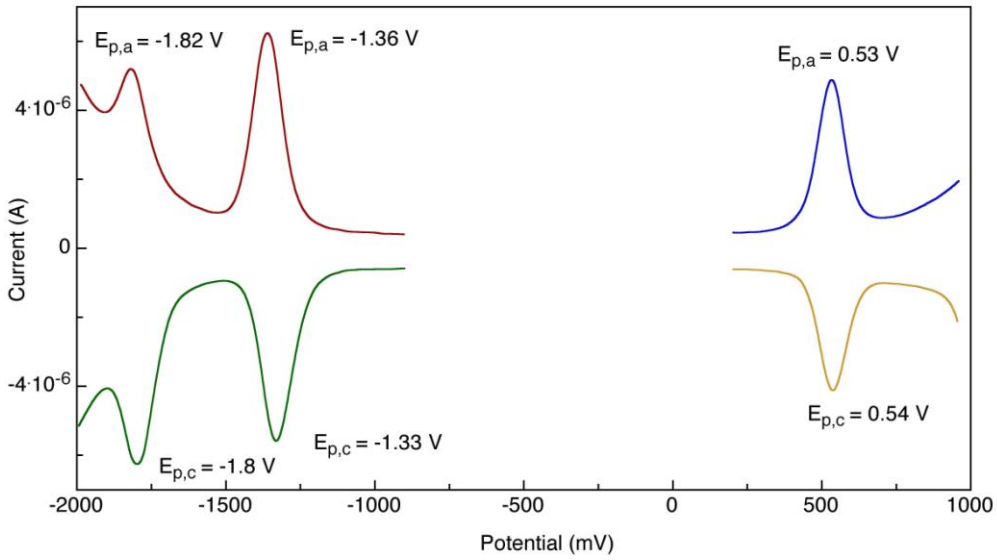

Figure 2.17 DPV of TNBS F_4 Pentacene (62)

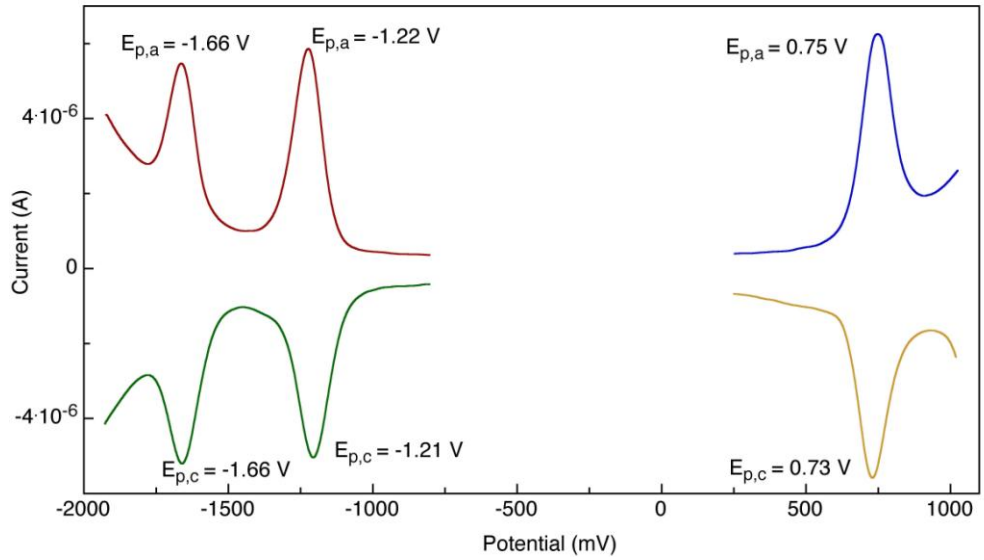

Figure 2.18 DPV of TNBS F_8 Pentacene (65)

Based on our experience with difluoropentacene we decided to study the electronic properties of our F_4 and F_8 pentacene derivatives which exhibited 2D π-stacking. Solution processed OTFT studies were performed by our collaborator Dr. Oana Jurshescu at Wake Forest University. The devices were fabricated in a bottom contact configuration using highly doped Si as the gate electrode and 200 nm of thermally grown SiO_2 as the gate dielectric. Au Source and drain electrodes were deposited on to the SiO_2 dielectric. The Au electrodes were treated with

PFBT solution prior to deposition of the active layer. TIPS F_4 Pentacene (**49**) films drop cast from chlorobenzene exhibited hole mobilities of 0.12 cm^2/Vs for a 50 μm channel length device (Figure 2.19), the highest ever mobility values reported for solution processed TIPS F_4 pentacene (**49**). The calculated mobility was higher than previously reported values using vapor deposited thin film.[139,140] Interestingly yellow-orange crystals were observed from long standing solutions in chlorobenzene on drop casting. The decomposition product was formed as a result of dimerization of the pentacene chromophore. The pentacene decomposition product exhibited hole mobility of 0.012 cm^2/Vs in a 5 μm channel length device.

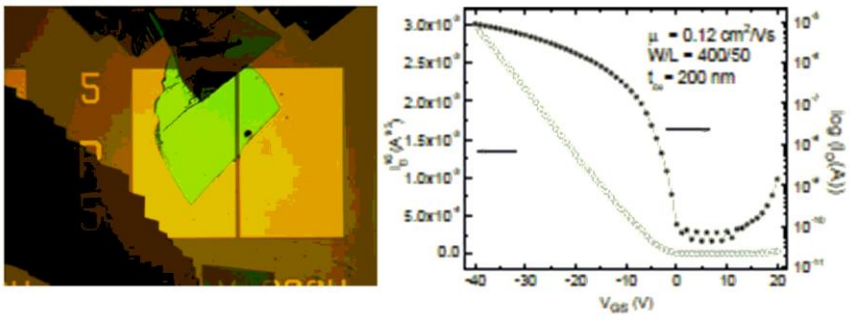

Figure 2.19 I-V curve of transistors TIPS F_4 Pentacene (49) (Prof. Oana Jurchescu, Wake Forest University)

As expected the change in π-stacking arrangement had significant effect on the device properties. The TNPS derivative (**61**) which exhibited 2D π-stacking with slippage between the stacks exhibited a threefold increase in mobility (0.3 cm^2/Vs) compared to TIPS F_4 pentacene (**49**). However further increase in slippage along the long and short axis of the pentacene core in the case of the TNBS derivative (**62**) lead to a tenfold drop in hole mobility (0.01 cm^2/Vs) compared to TIPS F_4 pentacene (**49**). Changing the silyl substituent to TIBS group lead to a significant drop in mobility to 4 x 10^{-7} cm^2/Vs. Since no crystal packing information is available for TIBS derivative (**63**) the reason for the low mobility might be due to poor π-stacking between molecules and poor morphology of the as cast film (Figure 2.20 (a)).

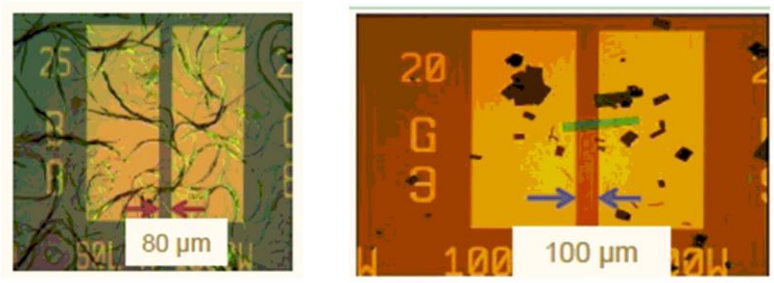

Figure 2.20 Images of drop cast thin films of (a) TIBS F_4 Pentacene (63) (b) TIPS F_8 Pentacene (7) (Prof. Oana Jurchescu, Wake Forest University)

TIPS F_8 pentacene (**7**) which exhibited 2D π-stacking similar to TIPS pentacene (**15**) exhibited a low hole mobility of 10^{-5} cm^2/Vs due to poor morphology of as cast thin film (Figure 2.20 (b)). Under similar conditions TIPS pentacene (**15**) gave a hole mobility of 0.45 cm^2/Vs while TIPS CFP (**47**) exhibited the highest hole mobility of 1.7 cm^2/Vs among partially fluorinated pentacene. TFT studies are currently underway on rest of the F_8 pentacene derivatives to better understand the influence of molecular packing and morphology on charge carrier mobility at Wake Forest University.

2.4. Partially chlorinated pentacenes

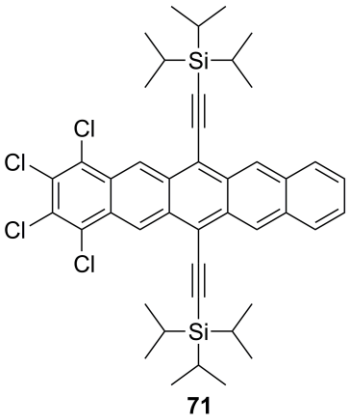

71

Figure 2.21 TIPS Cl_4 pentacene (71)[140]

Recently Bao et al. reported chlorination as an effective tool to synthesize ambipolar acene semiconductors.[140] Chlorine substitution was shown to effectively reduce the LUMO energy level due to the presence of vacant *3d* orbitals in chlorine. Vapor deposited thin films of

TIPS Cl_4 pentacene (**71**) exhibited ambipolar behavior with electron and hole mobilities of 0.054 cm^2/Vs and 0.111 cm^2/Vs respectively. However the authors were unable to convert the octachloro (Cl_8) pentacene quinone to the final pentacene. Based on my experience with fluorinated pentacene I decided to tackle the synthesis of Cl_8 pentacene.

The Cl_8 pentacene quinone was synthesized in an analogous manner to F_8 pentacene according to the scheme 2.3. Commercially available 3,4,5,6-tetrachlorophthalic anhydride (**72**) was converted to dimethyl ester (**73**) by Fisher esterification. DIBALH reduction of the resulting ester gave the dimethanol (**74**) which was heated at reflux in 48% HBr in water to give 1,2-bis(bromomethyl)-3,4,5,6-tetrachlorobenzene (**75**). Freidel-Craft acylation of 1,4-dihydroxybenzene (**55**) with anhydride (**72**) gave tetrachloroquinizarin (**76**) which on reduction by sodium borohydride in methanol gave 5,6,7,8-tetrachlro-1,4-anthraquinone (**77**). Cava reaction between 5,6,7,8-tetrachlro-1,4-anthraquinone (**77**) and 1,2-bis(bromomethyl)-3,4,5,6-

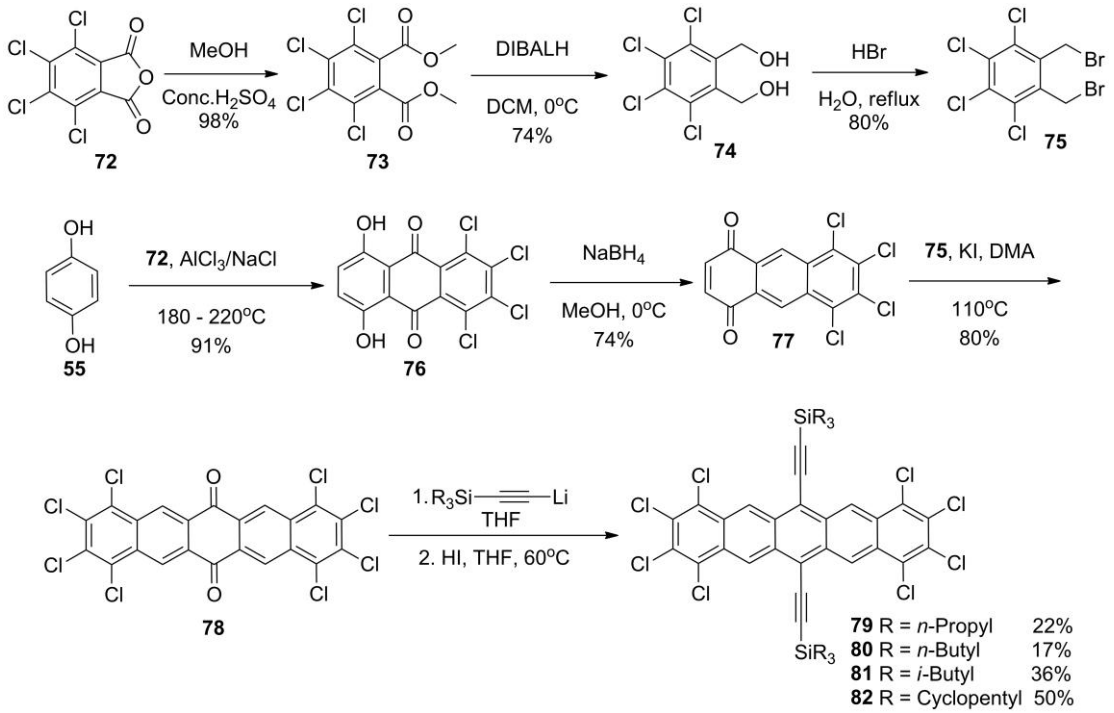

Scheme 2.3 Synthesis of octachloro(Cl_8)pentacene

tetrachlorobenzene (**75**) gave 1,2,3,4,,8,9,10,11-octachloropentacene-6,13-dione (**78**). Since the triisopropylsilyl substituent had lower solubility in the case of F_8 pentacenes, I decided to tune the solubility of Cl_8 pentacene by changing the alkyl substituent. Linear, branched and cycloalkyl substituted silyl acetylenes were used to improve the solubility of Cl_8 pentacene. The quinones were allowed to react with lithiated trialkylsilylacetylene to the intermediate diols which when treated with usual the deoxygenation agent $SnCl_2$/10%HCl either gave the final acene in <5% yield or no product. However treatment of the intermediate diol with HI gave the desired acene in 20-30% yield.

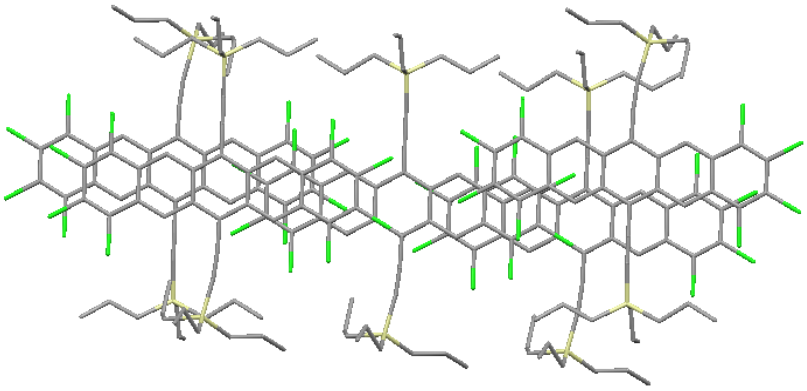

79

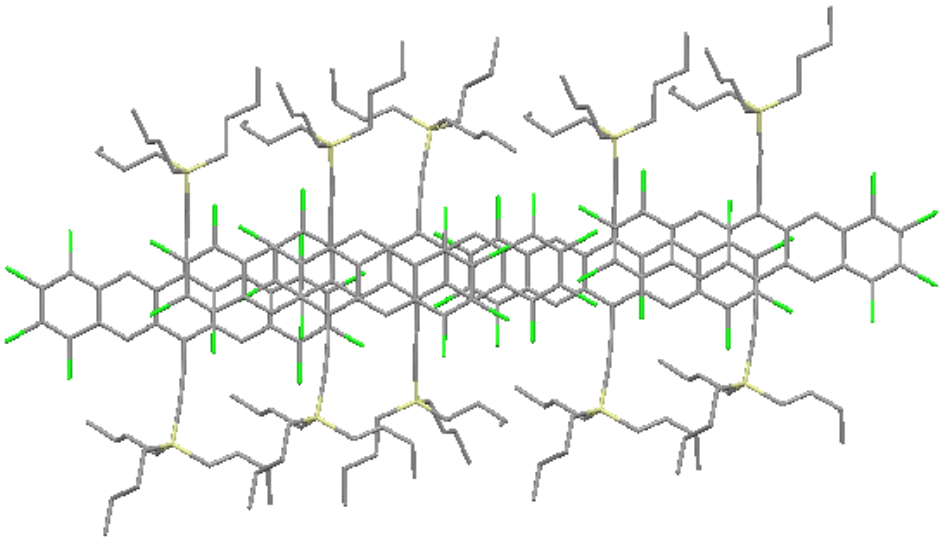

80

Figure 2.22 Crystal structures of TNPS (79) and TNBS Cl_8 pentacene (80).

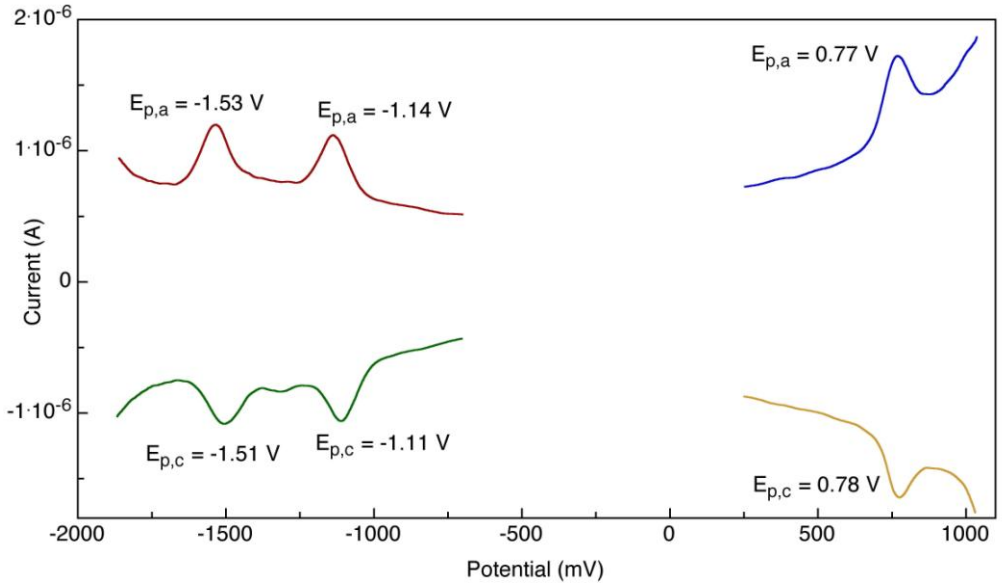

Figure 2.23 DPV of TIBS Cl_8 pentacene (81)

Differential pulse voltammetry was performed on the soluble Cl_8 pentacenes in DCM (Figure 2.23). As expected chlorine substitution has a more pronounced effect on the LUMO energy levels (Table 2.3) compared to fluorine substitution (Table 2.2). Thin film device studies are currently underway at Imperial College, London to explore ambipolar behavior of both F_8 and Cl_8 pentacene.

Table 2.3 Energy levels of Cl_8 pentacene

Cl_8 Pentacene	**E_{ox} (mV)**	**E_{red} (mV)**	**HOMO (eV)**	**LUMO (eV)**	**E_{gap} (eV)**
TNBS (80)	**773**	**-1123**	**-5.57**	**-3.68**	**1.89**
TIBS (81)	**774**	**-1113**	**-5.57**	**-3.69**	**1.88**

2.5 Partially halogenated pentacene acceptors

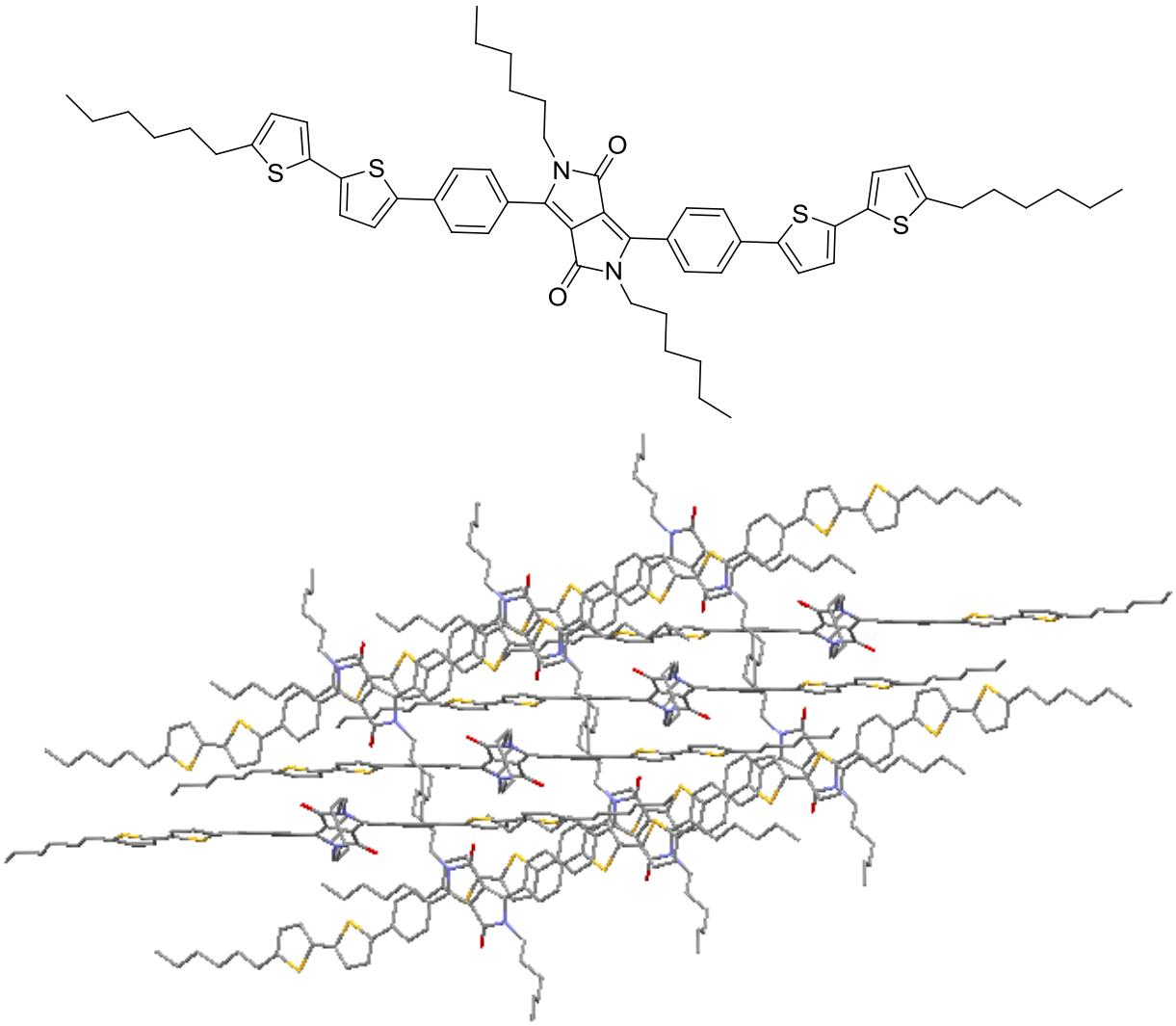

Figure 2.24 DPP(C6)PT2(C6) (83) structure and packing (Prof. Thuc-Quyen Nguyen, University of California, Santa Barbara)

Fullerene based OSCs have been well researched as acceptors for both small molecule and polymer BHJ solar cells.[90-95] However the poor absorption in the visible region of the spectrum coupled with low V_{oc} has stymied improvements in PCE in these donor/acceptor systems. In recent years small molecule based semiconductors have been explored as an alternative to fullerene based acceptors.[112-117]

The reasonable electron mobilities reported for F_8 pentacenes in OTFTs along with better absorption in visible region of the spectrum makes them ideal candidates as acceptors for solar cell devices. BHJ solar cells studies using our F_8 pentacene acceptors along with diketopyrrolopyrrole based donor DPP(C6)PT2(C6), **(83,** Figure 2.24) were performed by Jessica Sherman at University of California, Santa Barbara. Devices were fabricated on pre-patterned ITO coated glass substrates spin coated with PEDOT:PSS. Blend solutions of donor and acceptor in chloroform were spin coated onto this treated ITO substrate at 2000 RPM for 60 seconds. Thermally evaporated aluminum was used as the cathode.

Table 2.4 Device parameters for 1:1 P3HT/F_8 pentacene blend

F_8 pentacene	**V_{oc} (V)**	**J_{sc} (mA/cm^2)**	**FF**	**PCE (%)**	**Annealing temperature (°C)**	**π-stacking**
TIPS (7)	**1.07**	**0.16**	**0.42**	**0.07**	**160**	**2D**
TIBS (66)	**1.07**	**0.08**	**0.39**	**0.03**	**100**	**n/a**
TCPS (67)	**1.00**	**0.69**	**0.57**	**0.39**	**100**	**1D Sandwich herringbone**
TCHS (68)	**1.03**	**0.48**	**0.53**	**0.26**	**120**	**n/a**
NODIPS (69)	**1.00**	**0.18**	**0.34**	**0.06**	**100**	**2D**

The device performance of various F_8 pentacene derivatives is summarized in Table 2.4. All derivatives showed improvements in device performance upon thermal annealing. AFM images of as-cast and thermally annealed TCPS F_8 pentacene/DPP films are shown in Figure 2.25. These images show that thermal annealing results in a more uniform film, which is evident from the reduced surface roughness. All derivatives exhibited a very high V_{oc} of 1V, higher than V_{oc} values reported for PCBM based solar cells. However the devices suffered from low J_{sc} resulting

in poor PCE. Similar to results published by Anthony et al. only molecules that exhibit 1D-sandwich herringbone packing exhibited better device performance. The best performing TCPS F_8 pentacene gave a high PCE of 0.39% for an all small molecule solar cell.

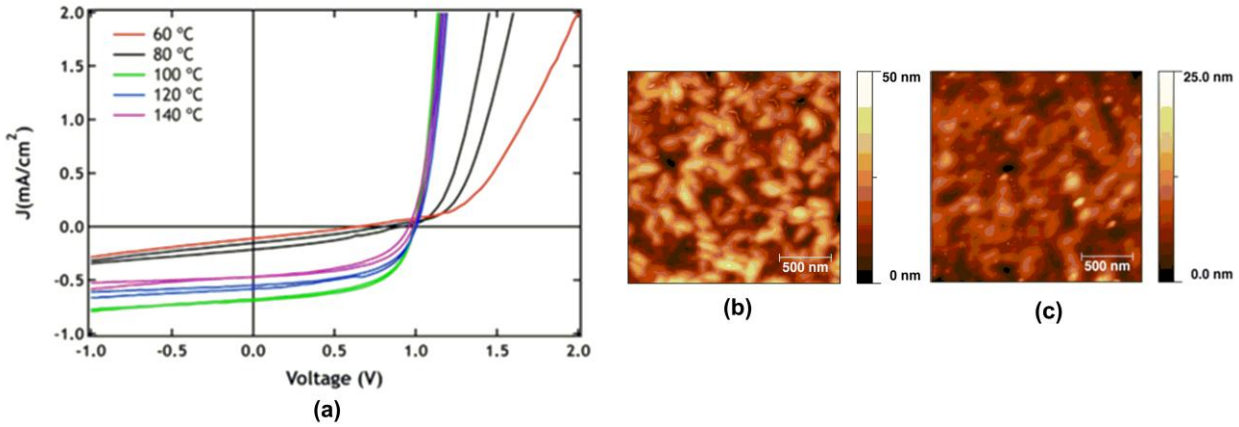

Figure 2.25 J-V curve and AFM height images of TCPS F_8 pentacene (67): DPP(C6)PT2(C6) (83) (50:50) spin-coated from chloroform (b) as cast, and (c) annealed at 100 °C for 20 min. RMS surface roughness values of the AFM images are (b) 8.24 nm, (c) 1.92 nm. (Devices fabricated by Jes Sherman, UCSB)

We also studied the solar performance of our best performing TCPS F_8 pentacene as acceptors in P3HT based solar cells. The devices were fabricated by Yee-Fun Lim at Cornell University. Compared to diketopyrrolopyrrole donors the P3HT based devices exhibited worse performance. The as cast films gave a performance with V_{oc}=0.66 V, J_{sc}=0.58 mA/cm^2, FF=0.35, PCE=0.14%. On thermally annealing the film at 160˚C the short circuit current density was almost doubled (1.1 mA/cm^2) however the V_{oc} dropped to 0.44 V resulting in a very small increase in PCE to 0.18%.

As shown in equation (7) the V_{oc} depends on the HOMO energy level of the donor and LUMO energy level of the acceptor.[96] The V_{oc} of P3HT (**33**) based solar cell can be maximized by tuning energy level of the pentacene acceptors. Anthony et al. reported that the V_{oc} of cyanopentacene acceptors for P3HT (**33**) based solar cells depended on the number of nitrile

substituents on the pentacene.[119] Better device performance was achieved with pentacene functionalized with single cyano group and molecules that packed in a 1D sandwich herringbone motif. I decided to tune the energy levels by functionalizing pentacene core with single halogen substituent. Our experience with Cl_8 pentacene showed that chlorine was more effective in reducing LUMO energy levels in pentacene and hence was our choice of substituent for pentacene based acceptors in P3HT (**33**) based solar cells.

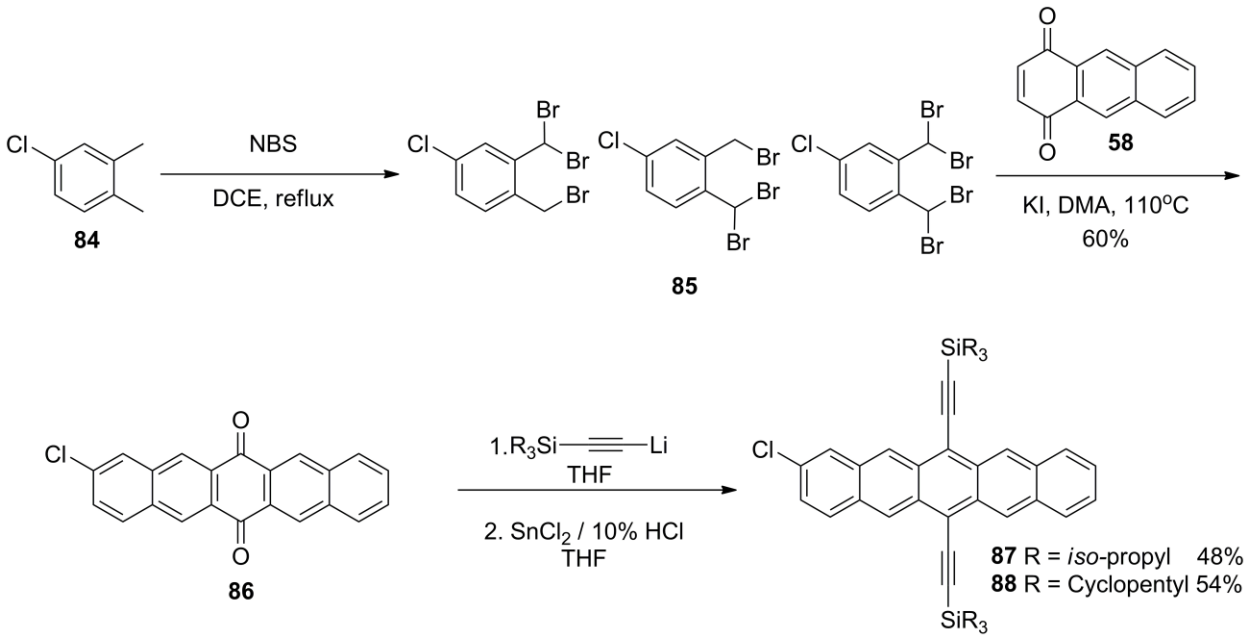

Scheme 2.4. Synthesis of 2-chloropentacene

Trialkylsilylethynyl 2-chloropentacenes were synthesized according to scheme 2.4. Benzylic bromination of commercially available 4-chloro-*o*-xylene (**84**) gave a mixture of α, α, α′-tribromo and α, α, α′, α′-tetrabromo-*o*-xylene (**85**). Cava reaction between 1,4-anthraquinone (**58**) and brominated *o*-xylenes gave the pentacene quinone in 70% yield. Treatment of 2-chloropentacene quinone (**86**) with lithiated acetylene followed by reaction of intermediate diol with $SnCl_2 \bullet 2H_2O$ in 10% HCl gave the final pentacene in moderate yield. Purification by silica gel chromatography followed by recrystallization from acetone gave the pure pentacene. Single

crystal x-ray diffraction analysis of crystals revealed that the smaller triisopropylsilyl substituent exhibited a 2D π-stacking arrangement while the larger tricyclopentylsilyl substituent resulted in a 1D sandwich herringbone motif (Figure 2.26).

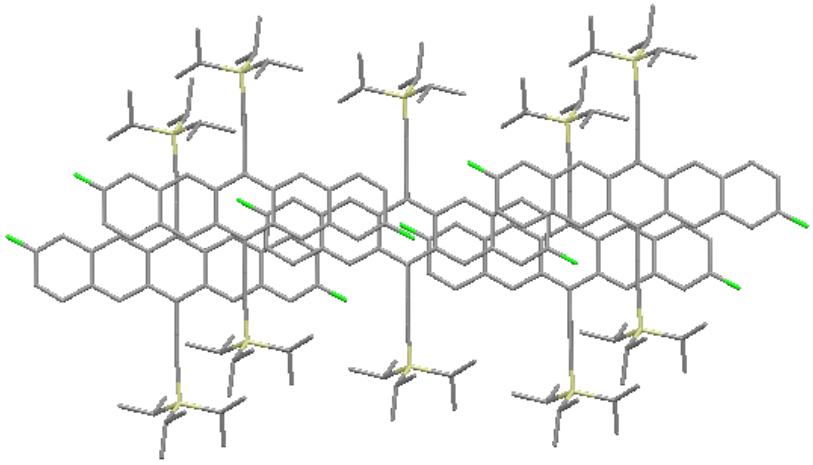

87

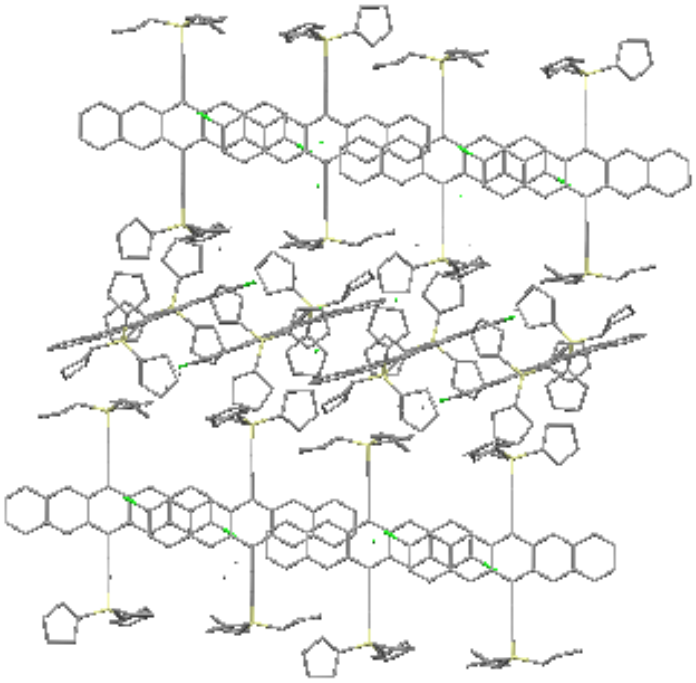

88

Figure 2.26 Crystal structures of TIPS 2-chloropentacene (87) and TCPS 2-chloropentacene (88)

Table 2.5 Energy levels of 2-chloropentacene

2-Cl Pentacene	E_{ox} (mV)	E_{red} (mV)	HOMO (eV)	LUMO (eV)	E_{gap} (eV)
TIPS (87)	**416**	**-1470**	**-5.17**	**-3.33**	**1.84**
TCPS (88)	**425**	**-1464**	**-5.23**	**-3.34**	**1.89**

TIPS and TCPS 2-chloropentacene were used as acceptors for P3HT donors in solar cells. The 2D π-stacking TIPS derivative gave a poor device performance with PCE of 0.24% due to the poor short circuit current. Devices using TCPS derivative showed significant improvement in device performance with a J_{sc} of 2.51 mA/cm^2, thereby resulting in a higher PCE of 1.03%.

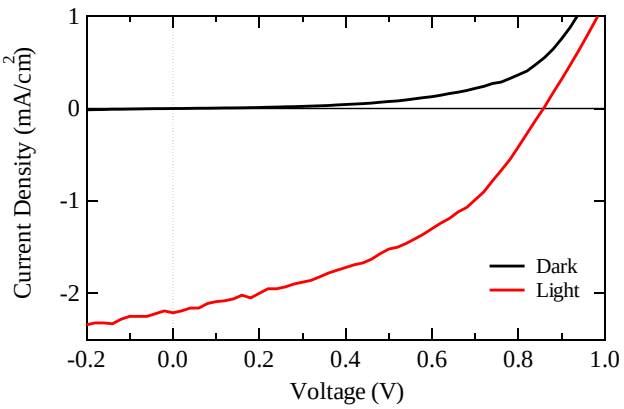

Figure 2.27 J-V curve for TCPS 2-chloropentacene (88)

2.6 Conclusion

The concept of contact induced nucleation was successfully extended to pentacene by partially fluorinating the pentacene chromophore. TIPS Difluoropentacenes exhibited significantly higher mobility than TIPS pentacene on spin coating on to PFBT treated electrodes. The higher mobility of difluoropentacenes is attributed to its ability to form crystalline ordered films as evidenced from GIXD studies. Partial fluorination of the pentacene core also has the added advantage of improving stability in solution. F_4 and F_8 pentacenes were also successfully synthesized for

application in OTFTs and OPVs. Solar cells made from TCPS F_8 pentacene acceptor and DPP donor exhibited high V_{oc} with a PCE of 0.39%. Devices made from the same acene acceptor with P3HT donor however gave a very low efficiency of 0.18% with a V_{oc} of 0.44V. The V_{oc} of P3HT solar cells was increased by tuning the LUMO energy of pentacene acceptors. Higher V_{oc} was achieved with pentacene acceptors with single halogen substituent. TCPS 2-Chloropentacene exhibited PCE > 1% with a V_{oc} of 0.96V.

2.7 Experimental details

All solvents were purchased from Pharmco Aaper except anhydrous tetrahydrofuran which was purchased from Aldrich. Chromatography was performed on silica gel (60 Å, 40-63 μm) purchased from Sorbent technology. Thin layer chromatography was performed using Silica Gel HL TLC plates (w/UV254) purchased from Sorbent Technologies. NMR spectra were recorded on Varian Inova 400MHz instrument. High resolution mass spectra were recorded in EI mode on JOEL JMS-700T MStation or in MALDI mode on Bruker Daltonics Autoflex MALDI-TOFMS. Electrochemical analysis was performed using BAS CV-50W voltammetric analyzer performed on 0.1M Bu_4NPF_6 solution in dichloromethane with ferrocene as internal standard. Tri-n-propylsilylacetylene, tri-n-butylsilylacetylene, and triisobutylsilyl acetylene were prepared from commercially available trialkylchlorosilane by reacting with ethynylmagnesium bromide. Tricyclopentylsilylacetylene and tricylohexylsilylacetylene were prepared in three steps from commercially available trichlorosilane. Halogenated *o*-xylenes were purchased from Alfa Aesar. Tetrafluorophthalic acid was purchased from AK scientific Inc. All other chemicals were purchased from Aldrich. The solvents were degassed by purging N_2 gas through them for 30 min. UV – Visible spectra were recorded using Shimadzu UV-visible Spectrophotometer model UV-2501PC. The spectra were recorded between the wavelength ranges of 400 – 700 nm using

quartz cells with 1cm path length. 10^{-4} M solutions of pentacenes in degassed toluene (UV Grade, Pharmco Aaper) were made in the dark and an initial spectrum of the acene was obtained. The solution was then exposed to a bright full-spectrum light source and the spectra were acquired at regular intervals until the absorption bands at longest wavelength disappeared. Electrostatic surface potential mapped electron density surfaces were generated using ArgusLab 4.0 software. The surface potentials were calculated using Zerner Intermediate Neglect of Diatomic Differential Overlap Hamiltonian (ZINDO).

General procedure for benzylic bromination of 3-fluoro-*o*-xylene (41) and 4-fluoro-*o*-xylene (40)

5 ml (5 g, 40.3 mmol) of fluoro-*o*-xylene was dissolved in 300 ml of 1,2-dichloroethane. 15.77 g (88.6 mmol) of NBS and 200 mg of AIBN were added and the reaction mixture was heated to 97 ˚C. 47.32 g of NBS was added in 3 portions at 6 h interval and the reaction mixture was heated at reflux overnight. The next day the reaction mixture was cooled to 0˚C and the precipitated succinimide was filtered and washed with chloroform. The filtrate was washed with sodium thiosulfate solution followed by water, dried over $MgSO_4$ and the solvent was removed under vacuum to give crude dark yellow solid. The crude product was purified further by running through a short plug using hexanes to give 13 g of product as an inseparable mixture.

General procedure for synthesis of difluoropentacene quinones

To a 100 ml RB flask equipped with a reflux condenser were added 5 g of mixture (**42**) or (**43**), 615 mg (5.68 mmol) of 1,4-benzoquinonev(**44**). 40 ml of degassed DMA was added and the reaction mixture was heated to 70˚C. 12.63 g (76.1 mmol) of KI was added and the temperature was raised to 110˚C. The reaction mixture was allowed to stir for 24 h. During the course of the

reaction a yellow precipitate crashes out from solution. The hot reaction mixture was poured into 800 ml of water and allowed to stir for 30 min. The precipitate was filtered and washed with plenty of water, followed by acetone and finally with 200 ml THF.

1,8-difluoropentacene-6,13-dione & 1,11-difluoropentacene-6,13-dione (46)

MS (EI 70 eV) *m/z* 344 (M^+, 100%)

2,9-difluoropentacene-6,13-dione & 2,10-difluoropentacene-6,13-dione (45)

557 mg (29% based on tetrabromo) of the quinone (**45**) was obtained as a beige colored solid.

MS (EI 70 eV) *m/z* 344 (M^+,100%)

General procedure for the synthesis of 6,13-Trialkylsilylethynylated difluoropentacenes (47 & 48):

To a flame dried 100 ml flask cooled under nitrogen was added 1.06 g (1.3 ml, 5.8 mmol) of triisopropylsilylacetylene, followed by 5 ml of THF. The reaction mixture was then placed in an ice bath. 2.1 ml of n-BuLi (5.23 mmol, 2.5 M solution in hexanes) was added dropwise and the reaction mixture stirred at 0 ºC for an hour. 15 ml of anhydrous THF was added followed by 500 mg (1.46 mmol) of difluoropentacene quinone. The reaction mixture was allowed to stir overnight at room temperature and was quenched with 2 ml of saturated NH_4Cl solution the next day. 2 ml of 10% HCl was added followed by 3.3 g of $SnCl_2 \bullet 2H_2O$. The reaction mixture was monitored by TLC by following the disappearance of intermediate diol. The reaction mixture was then poured on to thick pad of silica gel and the acene was eluted using 100% hexanes. The solvent was removed under vacuum to give the product which was further purified by recrystallization from acetone.

6,13-bis(tri(isopropyl)silylethynyl)-1,8-difluoropentacene & 6,13-bis(tri(isopropyl)silylethynyl)-1,11-difluoropentacene (48) – 774 mg (79%)

^{1}H NMR (400 MHz, $CDCl_3$) δ 9.59 (d, *J* = 4.8 Hz, 2H), 9.31 (d, *J* = 3.5 Hz, 2H), 7.79 – 7.72 (m, 2H), 7.31 (ddd, *J* = 8.6, 7.3, 5.4 Hz, 2H), 7.04 (dd, *J* = 10.7, 7.3 Hz, 2H), 1.41 – 1.31 (m, 42H). ^{13}C NMR (100 MHz, $CDCl_3$) δ 160.42, 157.87, 133.46, 133.43, 133.39, 133.36, 131.25, 131.06, 130.80, 130.61, 126.66, 126.62, 126.54, 126.50, 125.56, 125.50, 124.83, 124.55, 124.48, 124.36, 124.29, 120.59, 120.48, 119.48, 118.72, 108.75, 108.43, 108.23, 108.18, 108.08, 108.04, 107.99, 104.43, 104.29, 104.15, 19.15, 11.85, 11.83. MS (LDI) *m/z* 674 (M^+,100%). Decomposition temperature-282˚C

6,13-bis(tri(isopropyl)silylethynyl)-2,9-difluoropentacene & 6,13-bis(tri(isopropyl)silylethynyl)-2,10-difluoropentacene (47) – 795 mg (81%)

^{1}H NMR (400 MHz, $CDCl_3$) δ 9.30 (s, 2H), 9.21 (s, 2H), 7.98 (dd, *J* = 9.4, 5.8 Hz, 2H), 7.53 (dd, *J* = 9.9, 2.0 Hz, 2H), 7.30 – 7.21 (m, 2H), 1.45 – 1.30 (m, 42H). ^{13}C NMR (100 MHz, $CDCl_3$) 161.96, 161.90, 159.52, 159.40, 132.72, 132.68, 132.55, 132.48, 132.38, 132.30, 131.29, 131.28, 131.10, 130.97, 130.90, 130.57, 130.50, 130.24, 130.17, 130.06, 129.99, 128.02, 126.40, 124.79, 119.91, 119.86, 119.69, 119.62, 119.56, 118.34, 118.27, 117.99, 110.76, 110.55, 109.13, 110.76, 110.55, 109.13, 108.92, 107.9, 107.82, 107.73, 104.48, 104.42, 21.14, 21.08, 21.02, 19.93, 19.88, 19.83, 19.77, 18.67, 18.62, 18.57, 18.51, 17.42, 17.31, 12.411, 11.25. MS (LDI) *m/z* 674 (M^+,100%). Decomposition temperature-282˚C

Dimethyl-3,4,5,6-tetrafluorophthalate (51)

250 ml of methanol was added to 25 g of 3,4,5,6-tetrafluorophthalic acid(**50**) in a 500 ml RB flask. 20 ml of conc. sulfuric acid was added to the reaction mixture slowly and the resulting

solution was allowed to reflux for 24 h. The reaction mixture was cooled to room temperature the next day and poured into 500 ml water and extracted using ether. The combined ether layers were washed with water, dried over anhydrous $MgSO_4$. The solvent was evaporated to give white solid (22.44 g, 80%).

^{1}H NMR (400 MHz, $CDCl_3$) δ 3.93 (s, 6H). ^{19}F NMR (376 MHz, $CDCl_3$) δ 190.13 – 189.86 (m), 177.95 – 177.70 (m). MS (EI 70 eV) *m/z* 266 (M^+, 9%)

1,2-dimethanol-3,4,5,6-tetrafluorobenzene (52)

22.4 g (84.31 mmol) of the dimethyl ester (**51**) was added to a flame dried, N_2 cooled 1000 ml RB flask. 100 ml of DCM was added and the flask was cooled to 0˚C using ice water bath. 355 ml of 1M solution of DIBALH in hexanes was added drop wise and the reaction mixture was allowed stir overnight. The reaction mixture was quenched by adding a saturated solution of NH_4Cl with cooling. The precipitated aluminum salts are filtered off and the filtrate is concentrated to give the diol dissolved solution. The precipitates were refluxed with 500 ml ethyl acetate for an hour and the precipitates were filtered off, washed with ethyl acetate and the filtrate was saved. The process was repeated couple of times and the filtrate were combined together and solvent was removed to give off-white solid (15.18 g, 86%).

^{1}H NMR (400 MHz, DMSO) δ 4.95 (s, 2H), 4.63 (s, 4H). ^{19}F NMR (376 MHz, DMSO) δ -146.73 – -146.98 (m), -160.31 – -160.53 (m). MS (EI 70 eV) *m/z* 192 (M^+-18,100%)

1,2-bis(bromomethyl)-3,4,5,6-tetrafluorobenzene (53)

13.43 g of dimethanol (**52**) was added to 500 ml RB Flask followed by 350 ml 48 wt% HBr in water and the resulting mixture was heated to 120˚C and maintained at this temperature

overnight. Viscous oil is formed in the bottom the flask which was extracted into DCM. The organic layer was washed with water couple of times and dried over $MgSO_4$. Evaporation of solvents gave light brown oil which was purified by running through a silica gel plug using hexanes as solvent to give a clear liquid (21 g, 98%).

^{1}H NMR (400 MHz, $CDCl_3$) δ 4.62 (s, 4H). ^{19}F NMR (376 MHz, $CDCl_3$) δ -142.60 – -143.42 (m), -156.18 – -156.63 (m). MS (EI 70 eV) *m/z* 336 (M^+, 6%)

3,4,5,6-tetrafluorophthalic anhydride (54)

10 g of 3,4,5,6-tetrafluorophthalic acid (**50**) and 200 mg of *p*-toluenesulfonic acid monohydrate was dissolved in 50 ml toluene. The mixture was heated to reflux overnight and water was collected in a Dean Stark trap. The solvent was removed under reduced pressure to give a white solid (7.8 g, 84%). ^{19}F NMR (376 MHz, $CDCl_3$) δ -142.60 – -143.42 (m), -156.18 – -156.63 (m). MS (EI 70 eV) *m/z* 220 (M^+, 24%)

1,2,3,4-tetrafluoro-5,8-dihydroxyanthracene-9,10-dione (56)

A mixture of pulverized $AlCl_3$(35 g) and NaCl (7.7 g) was heated to 180˚ C under N_2 in a 500 ml flame dried RB flask. 7.7 g (35 mmol) 3,4,5,6-tetrafluorophthalic anhydride (**54**) and 4.2 g (38.14 mmol) of 1,4-dihydroxybenzene (**55**) were pulverized into homogeneous mixture. The above mixture was added to pulverized $AlCl_3$ in a flame dried 250 ml RB flask and mixed thoroughly to form intimate mixture. The mixture was then added to the $AlCl_3$/NaCl melt and the temperature was raised to 225˚C and held there for 2 hours. The reaction mixture was then cooled to room temperature; crushed ice was added to it and conc HCl was added slowly in portions until all the solids were dissolved. The resulting red slurry was stirred for an hour and

the solids were filtered using a Büchner funnel. The precipitates were then washed with plenty of water and air dried to give an orange solid (7.9 g, 72%).

^{1}H NMR (400 MHz, $CDCl_3$) δ 7.36 (s, 2H), 7.26 (s, 2H). ^{19}F NMR (376 MHz, $CDCl_3$) δ -137.69 – -137.93 (m), -145.76 – -146.01 (m). MS (EI 70 eV) *m/z* 312 (M^+, 100%)

5,6,7,8-tetrafluoroanthracene-1,4-dione (57)

To a stirred solution of 11.45 g (36.68 mmol) powdered 1,2,3,4-tetrafluoro-5,8-dihydroxyanthracene-9,10-dione (**56**) in 185 ml of methanol, maintained at 0˚C was added 5.55 g (146.71 mmol) sodium borohydride in small portions under N_2 atmosphere. The reaction was followed by working up an aliquot of the reaction mixture and checking for the disappearance of 1,2,3,4-tetrafluoro-5,8-dihydroxyanthracene-9,10-dione by TLC. The reaction mixture was then acidified with 100 ml of 6N HCl and the precipitates were filtered and washed with water to give a greenish brown solid. Purification by silica gel chromatography using 100% DCM as eluent gave 8.24 g (80%) of quinone as yellow solid.

^{1}H NMR (400 MHz, $CDCl_3$) δ 8.87 (t, *J* = 1.0 Hz, 2H), 7.15 (s, 2H). ^{19}F NMR (376 MHz, $CDCl_3$) δ -148.20 – -148.29 (m), -154.57 – -154.66 (m). MS (EI 70 eV) *m/z* 280 (M^+,100%)

1,2,3,4-tetrafluoropentacene-6,13-dione (59)

To a 100ml RB flask equipped with a reflux condenser were added 5 g of **53**, 3.87 g (18.6 mmol) of 1,4-anthraquinone (**58**). 50 ml of degassed DMA was added and the reaction mixture was heated to 70˚C. 16.56 g of KI was added to the reaction mixture and the temperature was raised to 110˚C. The reaction mixture was allowed to stir for 24 h. During the course of the reaction yellow precipitate crashes out from solution. The hot reaction mixture was poured into 800 ml of

water and allowed to stir for 30 min. The precipitate was filtered and washed with plenty of water, followed by acetone and finally with 200 ml THF. 3.68 g (65%) of the quinone was obtained as a greenish brown solid.

MS (EI 70 eV) *m/z* 380 (M^+, 100%)

1,2,3,4,8,9,10,11-octafluoropentacene-6,13-dione (60)

To a 100 ml RB flask equipped with a reflux condenser were added 5 g of **53**, 5.22 g (18.6 mmol) of **57**. 50 ml of degassed DMA was added and the reaction mixture was heated to 70˚C. 16.56 g of KI was added to the reaction mixture and the temperature was raised to 110˚C. The reaction mixture was allowed to stir for 24 h. During the course of the reaction yellow precipitate crashes out from solution. The hot reaction mixture was poured into 800 ml of water and allowed to stir for 30 min. The precipitate was filtered and washed with plenty of water, followed by acetone and finally with 200 ml THF. 5.16 g (77%) of the quinone was obtained as a light brown solid. MS (EI 70 eV) *m/z* 452 (M^+, 100%)

General procedure for synthesis of 6,13-bis(trialkylsilyleythynylated)-1,2,3,4-tetrafluoropentacene

To a flame dried 100 ml flask cooled under nitrogen was added 6.57 mmol of acetylene, followed by 5 ml of hexanes. The reaction mixture was then placed in an ice bath. 2.37 ml (5.92 mmol) of n-BuLi (2.5 M solution in hexanes) was added dropwise and the reaction mixture stirred at 0 ºC for an hour. 13 ml of hexanes and 4 ml of anhydrous THF were added followed by 500 mg (1.31 mmol) of tetrafluoropentacene quinone. The reaction mixture was allowed to stir overnight at room temperature and was quenched with 2 ml of saturated NH_4Cl solution the next day. The intermediate diol was extracted into ether and dried over anhydrous $MgSO_4$. The

solvent was evaporated under reduced pressure to give the crude diol which was dissolved in 75 ml methanol. 10 ml of HI was added and the reaction mixture was stirred at room temperature. The reaction was monitored by TLC by following the disappearance of intermediate diol. The precipitated solids were filtered washed with methanol. The crude pentacene was then purified by silica gel chromatography using 100% hexanes.

6,13-bis(tri(n-propyl)silylethynyl)-1,2,3,4-tetrafluoropentacene (61)- 46%

^{1}H NMR (400 MHz, $CDCl_3$) δ 9.41 (s, 2H), 9.21 (s, 2H), 8.00 (dd, *J* = 6.5, 3.2 Hz, 2H), 7.47 (dd, *J* = 6.7, 3.1 Hz, 2H), 1.81 – 1.68 (m, 12H), 1.18 (t, *J* = 7.3 Hz, 18H), 0.99 – 0.91 (m, 12H). ^{13}C NMR (100 MHz, $CDCl_3$) δ 141.91 (dm, *J* = 257.3 Hz), 137.31 (dm, *J* = 255 Hz), 132.98, 130.99, 130.19, 128.84, 126.80, 126.70, 120.41, 119.23, 110.57, 103.26, 18.56, 18.16, 16.47. MS (EI 70 eV) *m/z* 710 (M^+, 100%). Decomposition temperature-209˚C

6,13-bis(tri(n-butyl)silylethynyl)-1,2,3,4-tetrafluoropentacene (62)-51%

^{1}H NMR (400 MHz, $CDCl_3$) δ 9.47 (s, 2H), 9.26 (s, 1H), 8.02 (dd, *J* = 6.6, 3.2 Hz, 2H), 7.48 (dd, *J* = 6.7, 3.1 Hz, 2H), 1.75 – 1.63 (m, 12H), 1.61 – 1.49 (m, 12H), 1.06 – 0.92 (m, 30H). ^{13}C NMR (100 MHz, $CDCl_3$) δ 141.93 (dm, *J* = 257.4 Hz), 137.34 (dm, *J* = 255 Hz), 133.01, 131.06, 130.25, 128.82, 126.82, 126.76, 120.47, 119.60, 119.50, 119.40, 119.30, 119.16, 110.67, 103.21, 26.80, 14.10, 13.47. MS (LDI) *m/z* 794 (M^+, 100%). Decomposition temperature-178˚C

6,13-bis(tri(isobutyl)silylethynyl)-1,2,3,4-tetrafluoropentacene (63)-60%

^{1}H NMR (400 MHz, $CDCl_3$) δ 9.48 (s, 2H), 9.28 (s, 2H), 7.99 (dd, *J* = 6.5, 3.2 Hz, 2H), 7.47 (dd, *J* = 6.7, 3.1 Hz, 2H), 2.27 – 2.11 (m, 6H), 1.19 (d, *J* = 6.6 Hz, 36H), 0.97 (d, *J* = 7.2 Hz, 12H). ^{13}C NMR (100 MHz, $CDCl_3$) δ 141.96 (dm, *J* = 257.1 Hz), 137.33 (dm, *J* = 255.2 Hz), 133.01,

131.24, 130.37, 128.77, 126.83, 126.73, 120.48, 119.61, 119.50, 119.39, 111.65, 103.91, 26.69, 25.68, 25.52. MS (EI 70 eV) *m/z* 794 (M^+, 100%). Decomposition temperature-248˚C

General procedure for synthesis of 6,13-bis(trialkylsilyleythynylated)-1,2,3,4,8,9,10,11-octafluoropentacene

To a flame dried 100 ml flask cooled under nitrogen was added 5.53 mmol of acetylene, followed by 5 ml of hexanes. The reaction mixture was then placed in an ice bath. 2 ml (4.97 mmol) n-BuLi (2.5 M solution in hexanes) was added dropwise and the reaction mixture stirred at 0 ºC for an hour. 13 ml of hexanes and 4 ml of anhydrous THF were added followed by 500 mg (1.1 mmol) of octafluoropentacene quinone. The reaction mixture was allowed to stir overnight at room temperature and was quenched with 2ml of saturated NH_4Cl solution the next day. The intermediate diol was extracted into ether and dried over anhydrous $MgSO_4$. The solvent was evaporated under reduced pressure to give the crude diol which was dissolved in 75 ml methanol. 10 ml of HI was added and the reaction mixture was stirred at 50˚C. The reaction was monitored by TLC by following the disappearance of intermediate diol. The precipitated solids were filtered washed with methanol. The crude pentacene was then purified by silica gel chromatography using 100% hexanes.

6,13-bis(tri(n-propyl)silylethynyl)-1,2,3,4,8,9,10,11-octafluoropentacene (64)-52%

^{1}H NMR (400 MHz, $CDCl_3$) δ 9.41 (s, 4H), 1.78 – 1.66 (m, 12H), 1.15 (t, *J* = 7.3 Hz, 18H), 0.97 – 0.89 (m, 12H). ^{13}C NMR (100 MHz, $CDCl_3$) δ 141.86 (dm, *J* = 257.5 Hz), 137.67 (dm, *J* = 256.6 Hz), 130.56, 120.73, 120.15, 120.03, 119.95, 112.22, 102.30, 18.48, 18.14, 16.33. MS (LDI) *m/z* 782 (M^+, 100%). Decomposition temperature-214˚C

6,13-bis(tri(n-butyl)silylethynyl)-1,2,3,4,8,9,10,11-octafluoropentacene (65)-52%

^{1}H NMR (400 MHz, $CDCl_3$) δ 9.43 (s, 2H), 1.71 – 1.61 (m, 12H), 1.58 – 1.46 (m, 12H), 1.05 – 0.89 (m, 30H). ^{13}C NMR (100 MHz, $CDCl_3$) δ 141.88 (dm, *J* = 257.6 Hz), 137.69 (dm, *J* = 256.5 Hz), 130.59, 120.75, 120.16, 120.08, 119.97, 112.30, 102.25, 26.77, 26.71, 13.98, 13.33. MS (LDI) *m/z* 866 (M^+, 100%). Decomposition temperature-189˚C

6,13-bis(tri(isobutyl)silylethynyl)-1,2,3,4,8,9,10,11-octafluoropentacene (66)-56%

^{1}H NMR (400 MHz, $CDCl_3$) δ 9.49 (s, 4H), 2.23 – 2.10 (m, 6H), 1.17 (d, *J* = 6.6 Hz, 36H), 0.97, *J* = 6.8 Hz (m, 12H). ^{13}C NMR (100 MHz, $CDCl_3$) δ 141.93 (dm, *J* = 257.6 Hz), 138.98 (dm, *J* = 256.2 Hz), 136.41, 130.83, 120.83, 120.22, 120.11, 120.01, 113.37, 102.99, 26.61, 25.70, 25.44. MS (LDI) *m/z* 866 (M^+, 100%). Decomposition temperature-264˚C

6,13-bis(tri(cyclopentyl)silylethynyl)-1,2,3,4,8,9,10,11-octafluoropentacene (67)-50%

^{1}H NMR (400 MHz, $CDCl_3$) δ 9.50 (s, 4H), 2.15 – 1.95 (m, 12H), 1.86 – 1.69 (m, 24H), 1.69 – 1.56 (m, 12H), 1.42 – 1.24 (m, 6H). ^{13}C NMR (100 MHz, $CDCl_3$) δ 141.91 (dm, *J* = 257.6 Hz), 137.66 (dm, *J* = 256.1 Hz), 130.77, 120.87, 120.19, 120.11, 120.01, 111.20, 102.15, 29.61, 27.23, 24.00. MS (LDI) *m/z* 938 (M^+, 100%). Decomposition temperature-300˚C

6,13-bis(tri(cyclohexyl)silylethynyl)-1,2,3,4,8,9,10,11-octafluoropentacene (68)- 37%

^{1}H NMR (400 MHz, $CDCl_3$) δ 9.55 (s, 4H), 2.06 (d, *J* = 12.8 Hz, 12H), 1.97 – 1.70 (m, 18H), 1.68 – 1.48 (m, 12H), 1.45 – 1.26 (m, 18H), 1.26 – 1.13 (m, 6H). ^{13}C NMR (100 MHz, $CDCl_3$) δ 143.21, 140.64, 138.95, 136.39, 130.81, 120.93, 120.19 (t, *J* = 4.8 Hz), 120.04, 111.12, 103.38, 29.13, 28.60, 27.20, 23.53. MS (EI 70 eV) *m/z* 1022 (M^+, 100%). M.P-287˚C

6,13-bis(n-octyldiisopropylsilyl)ethynyl)-1,2,3,4,8,9,10,11-octafluoropentacene (69)- 80%

^{1}H NMR (400 MHz, $CDCl_3$) δ 9.50 (s, 4H), 1.77 – 1.64 (m, 4H), 1.53 – 1.42 (m, 4H), 1.40 – 1.16 (m, 44H), 0.99 – 0.88 (m, 4H), 0.86 – 0.79 (m, 6H). ^{13}C NMR (100 MHz, $CDCl_3$) δ 141.86 (dm, *J* = 257.6 Hz), 137.68 (dm, *J* = 256.6 Hz), 130.70, 120.79, 120.20, 120.13, 120.00, 110.87, 102.84, 34.11, 32.15, 29.52, 29.43, 25.00, 22.86, 18.74, 18.47, 14.26, 12.19, 10.42. MS (EI 70 eV) *m/z* 922 (M^+, 100%). M.P-127˚C

Dimethyl-3,4,5,6-tetrachlorophthalate(73)

250 ml of methanol was added to 25 g (87.45mmol) of 3,4,5,6-tetrachlorophthalic anhydride(**72**) in a 500 ml RB flask. 25 ml of conc. sulfuric acid was added to the reaction mixture slowly and the resulting solution was allowed to reflux 24 h. The reaction mixture was cooled to room temperature the next day and poured into 500 ml water and extracted using ether. The combined ether layers were washed with water, dried over anhydrous $MgSO_4$. The solvent was evaporated to give 28.46 g (98%) of white solid.

^{1}H NMR (400 MHz, $CDCl_3$) δ 3.89 (s, 6H). ^{13}C NMR (100 MHz, $CDCl_3$) δ 164.33, 136.16, 132.08, 130.66, 53.59. MS (EI 70 eV) *m/z* 332 (M^+, 18%)

1,2-dimethanol-3,4,5,6-tetrachlorobenzene(74)

28.46 g (85.73 mmol) of the dimethyl ester (**73**) was added to a flame dried, N_2 cooled 1000 ml RB flask. 170 ml of DCM was added followed by 2ml of THF and the flask was cooled to 0˚C using ice water bath. 360 ml of DIBALH (1M solution in hexanes) was added drop wise and the reaction mixture was allowed stir overnight. The reaction mixture was quenched by adding a saturated solution of NH_4Cl with cooling. The precipitated aluminum salts are filtered off and the

filtrate is concentrated to give the diol dissolved in DCM. The precipitates were refluxed with 500 ml ethyl acetate for an hour and the precipitates were filtered off, washed with ethyl acetate and the filtrate was saved. The process was repeated twice and the filtrates were combined together and solvent was removed to give 17.48 g (74%) of diol as a white solid.

^{1}H NMR (400 MHz, DMSO) δ 5.36 (s, 2H), 4.76 (s, 4H). ^{13}C NMR (100 MHz, DMSO) δ 139.68, 132.78, 131.21, 58.49. MS (EI 70 eV) *m/z* 257 (M^{+}-18, 100%)

1,2-bis(bromomethyl)-3,4,5,6-tetrachlorobenzene(75)

17.48 g of dimethanol (**74**) was added to 500 ml RB flask followed by 350 ml 48 wt% HBr in water and the resulting mixture was heated to 120˚C and maintained at this temperature overnight. The product was extracted into DCM (3x200 ml). The organic layer was washed twice with water and dried over $MgSO_4$. Evaporation of solvent gave the crude product which was purified by running through a silica plug using hexanes as solvent to give 20.4 g (80%) of light yellow solid.

^{1}H NMR (400 MHz, $CDCl_3$) δ 4.76 (s, 4H). ^{13}C NMR (100 MHz, $CDCl_3$) δ 135.54, 134.38, 133.82, 26.79. MS (EI 70 eV) *m/z* 402 (M^{+}, 13%)

1,2,3,4-tetrachloro-5,8-dihydroxyanthracene-9,10-dione(76)

A mixture of 35 g of pulverized $AlCl_3$ and 7.67 g of NaCl was heated to 180˚ C under N_2 in a 500 ml flame dried RB flask. 10 g (34.97 mmol) of 3,4,5,6-tetrachlorophthalic anhydride (**72**) and 4.24 g (38.47mmol) of 1,4-dihydroxybenzene (**55**) were pulverized into a homogeneous mixture. The above mixture was added to 18.66 g (140 mmol) of pulverized $AlCl_3$ in a flame dried 250 ml RB flask and mixed thoroughly to form intimate mixture. The mixture was then

added to the $AlCl_3$/NaCl melt and the temperature was raised to 225˚C and held there for 2 hours. The reaction mixture was then cooled to room temperature; crushed ice was added to it and conc HCl was added slowly in portions until all the solids were dissolved. The resulting red slurry was stirred for an hour and the solids were filtered using a Buchner funnel. The precipitates were then washed with water and air dried to give 12.12 g (91%) of reddish brown solid.

^{1}H NMR (400 MHz, $CDCl_3$) δ 12.5 (s, 2H), 7.35 (s, 2H). ^{13}C NMR (100 MHz, $CDCl_3$) 184.02, 157.63, 142.08, 134.37, 130.92, 129.94, 112.79. MS (EI 70 eV) *m/z* 378 (M^+, 100%)

5,6,7,8-tetrachloroanthracene-1,4-dione(77)

To a stirred solution of 11.36 g (30.05 mmol) of powdered 1,2,3,4-tetrachloro-5,8-dihydroxyanthracene-9,10-dione in 150 ml of methanol, maintained at 0˚C was added 4.55 g (120 mmol) of sodium borohydride in small portions under N_2 atmosphere. The reaction was followed by working up an aliquot of the reaction mixture and checking for the disappearance of 1,2,3,4-tetrachloro-5,8-dihydroxyanthracene-9,10-dione by TLC. The reaction mixture was then acidified with 100 ml of 6N HCl solution to precipitate out the product. The precipitates were filtered and washed with plenty of water and air dried to give the crude product. Purification by silica gel chromatography using 100% DCM as an eluent gave a yellow solid (7.68 g, 74%).

^{1}H NMR (400 MHz, $CDCl_3$) δ 8.59 (s, 2H), 6.8 (s, 2H). ^{13}C NMR (100 MHz, $CDCl_3$) 182.59, 139.38, 132.93, 131.54, 130.97, 129.52, 125.29. MS (EI 70 eV) *m/z* 346 (M^+, 100%)

1,2,3,4,8,9,10,11-octachloropentacene-6,13-dione (78)

To a 100 ml RB flask equipped with a reflux condenser were added 1.5g (3.73 mmol) of **75**, 1.55 g (4.48 mmol) of **77**. 30 ml of degassed DMA was added and the reaction mixture was heated to 70˚C. 4.15 g (25 mmol) of KI was added to the reaction mixture and the temperature was raised to 110˚C. The reaction mixture was allowed to stir for 24 h. During the course of the reaction yellow precipitate crashes out from solution. The hot reaction mixture was poured into 800 ml of water and allowed to stir for 30 min. The precipitate was filtered and washed with plenty of water, followed by acetone and finally with 200 ml THF. 1.8 g (80%) of the quinone was obtained as a dark brown solid. MS (EI 70 eV) *m/z* 584 (M^+, 100%)

General procedure for synthesis of 6,13-trialkylsilylethynylated-1,2,3,4,8,9,10,11-octachloropentacene

To a flame dried 100 ml flask cooled under nitrogen was added 3.43 mmol of acetylene, followed by 5 ml of anhydrous THF. The reaction mixture was then placed in an ice bath. 1.23 ml of n-BuLi (3.08 mmol, 2.5 M solution in hexanes) was added dropwise and the reaction mixture stirred at 0 ºC for an hour. 15 ml of anhydrous THF was added followed by 500 mg (0.86 mmol) of octachloropentacene quinone (**78**). The reaction mixture was allowed to stir overnight at room temperature the next day and was quenched with 2ml of saturated NH_4Cl solution followed by 5 ml of HI and reaction mixture was heated to reflux. The reaction mixture was monitored by TLC by following the disappearance of intermediate diol. The reaction mixture was then poured into methanol and the precipitated solids were filtered washed with methanol followed by hexanes to give the crude pentacene which was further purified by recrystallization.

6,13-bis(tri(n-propyl)silylethynyl)-1,2,3,4,8,9,10,11-octachloropentacene (79)-22%

^{1}H NMR (400 MHz, *o*-Dichlorobenzene-d_4) δ 9.89 (s, 4H), 2.08 (m, 12H), 1.44 (t, *J* = 7.2 Hz, 18H), 1.26 – 1.16 (m, 12H). MS (LDI) *m/z* 914 (M^+, 100%). Decomposition temperature-308˚C

6,13-bis(tri(n-butyl)silylethynyl)-1,2,3,4,8,9,10,11-octachloropentacene (80)-17%

^{1}H NMR (400 MHz, C_6D_6) δ 9.60 (s, 4H), 1.61-1.52 (m, 12H), 1.46-1.34 (m, 12H), 0.89-0.82 (m, 30H). ^{13}C NMR (100 MHz, Benzene-d_6) δ 131.62, 130.86, 130.10, 128.61, 126.41, 120.62, 112.34, 102.44, 26.85, 26.68, 14.07, 13.44. MS (LDI) *m/z* 998 (M^+, 100%). Decomposition temperature-283˚C

6,13-bis(tri(isobutylyl)silylethynyl)-1,2,3,4,8,9,10,11-octachloropentacene (81)-36%

^{1}H NMR (400 MHz, *o*-Dichlorobenzene-d_4) δ 9.62 (s, 4H), 2.17 (dp, *J* = 13.3, 6.6 Hz, 2H), 1.14 (d, *J* = 6.6 Hz, 12H), 1.0 (d, *J* = 6.8 Hz, 4H). ^{13}C NMR (100 MHz, *o*-Dichlorobenzene-d_4) δ 131.72, 130.86, 130.06, 128.54, 126.42, 120.72, 113.68, 103.15, 26.76, 25.63, 25.53. MS (LDI) *m/z* 998 (M^+, 100%). Decomposition temperature-264˚C

6,13-bis(tri(cyclopentyl)silylethynyl)-1,2,3,4,8,9,10,11-octachloropentacene (82)-50%

^{1}H NMR (400 MHz, *o*-Dichlorobenzene-d_4) δ 9.88 (s, 4H), 2.44 – 2.32 (m, 12H), 2.17 – 1.98 (m, 24H), 1.98 – 1.84 (m, 12H), 1.66 – 1.53 (m, 6H). MS (LDI) *m/z* 1070 (M^+, 100%)

Benzylic bromination of 4-chloro-*o*-xylene(84)

5 ml (5.235 g, 37.23 mmol) of 4-chloro-*o*-xylene(**84**) was dissolved in 300 ml of 1,2-dichloroethane. 14.6 g (81.9 mmol) of NBS and 200 mg of AIBN were added and the reaction mixture was heated to 97 ˚C. 29.2 g of NBS was added in 2 portions at 4 h interval and the

reaction mixture was refluxed overnight. The next day the reaction mixture was cooled to 0˚C and the precipitated succinimide was filtered and washed with chloroform. The filtrate was washed with sodium thiosulfate solution followed by water, dried over $MgSO_4$ and the solvent was removed under vacuum to give crude dark yellow solid. The crude product was purified further by pouring on to a thick pad of silica gel and eluting with hexanes to give 16 g of tribromo and tetrabromo(**85**) as an inseparable mixture.

2-chloropentacene-6,13-dione(86)

To a 100 ml RB flask equipped with a reflux condenser were added 4.4 g of mixture of brominated 4-chloro-*o*-xylene (**85**), 2.5 g (12 mmol) of 1,4-anthraquinone (**58**). 35 ml of degassed DMA was added and the reaction mixture was heated to 70˚C. 16.56 g (64.35 mmol) of KI was added and the temperature was raised to 110˚C. The reaction mixture was allowed to stir for 24 h. During the course of the reaction yellow precipitate crashes out from solution. The hot reaction mixture was poured into 800 ml of water and allowed to stir for 30 min. The precipitate was filtered and washed with plenty of water, followed by acetone and finally with 200 ml THF. 1.93 g (60% based on tetrabromo) was obtained as a light golden brown solid.

MS (EI 70 eV) *m/z* 342 (100%)

General procedure for the synthesis of 6,13-Trialkylsilylethynylated 2-chloropentacenes (87 & 88)

To a flame dried 100 ml flask cooled under nitrogen was added 4.38 mmol of acetylene, followed by 5 ml of THF. The reaction mixture was then placed in an ice bath. 1.6 ml of n-BuLi (4 mmol, 2.5 M solution in hexanes) was added dropwise and the reaction mixture stirred at 0 ºC for an hour. 15 ml of anhydrous THF was added followed by 500 mg (1.46 mmol) of 2-

chloropentacene quinone (**86**). The reaction mixture was allowed to stir overnight at room temperature the next day and was quenched with 2 ml of saturated NH_4Cl solution. 2 ml of 10% HCl was added followed by 5 g of $SnCl_2 \bullet 2H_2O$. The reaction mixture was monitored by TLC by following the disappearance of intermediate diol. The reaction mixture was then poured on to thick pad of silica gel and the acene was eluted using 100% hexanes. The solvent was removed under vacuum to give the final pentacene which was further purified by recrystallization using acetone.

6,13-bis(tri(isopropyl)silylethynyl)-2-chloropentacene (87) – 472 mg (48%)

^{1}H NMR (400 MHz, $CDCl_3$) δ 9.32 – 9.24 (m, 3H), 9.18 (s, 1H), 8.02 – 7.94 (m, 2H), 7.94 – 7.88 (m, 2H), 7.46 – 7.38 (m, 2H), 7.31 (dd, 9.2 Hz, 2 Hz, 1H), 1.37-1.34 (m, 42H).

^{13}C NMR (100 MHz, $CDCl_3$) δ 132.69, 132.59, 132.29, 131.97, 131.06, 130.87, 130.74, 130.71, 130.43, 128.88, 127.56, 127.02, 126.84, 126.61, 126.57, 126.43, 126.39, 125.7, 118.89, 118.61, 107.8, 107.74, 104.64,19.21, 11.86. MS (EI 70 eV) *m/z* 672(100%). Anal calc. C 78.46%, H 7.93% Found: C 78.54%, H 8.07%. Decomposition temperature - 255˚C

6,13-bis(tri(cyclopentyl)silylethynyl)- 2-chloropentacene (88) – 650 mg (54%)

^{1}H NMR (400 MHz, $CDCl_3$) δ 9.30 – 9.23 (m, 3H), 9.17 (s, 1H), 8.01 – 7.94 (m, 2H), 7.94 – 7.89 (m, 2H), 7.47 – 7.41 (m, 2H), 7.34 (dd, *J* = 9.1, 1.9 Hz, 1H), 2.17 – 1.99 (m, 12H), 1.92 – 1.57 (m, 36H), 1.45 – 1.25 (m, 6H).

^{13}C NMR (100 MHz, $CDCl_3$) δ 132.66, 132.57, 132.28, 131.92, 131.03, 131.00, 130.81, 130.70, 130.63, 130.42, 128.82, 127.57, 127.01, 126.81, 126.60, 126.55, 126.42, 126.38, 125.69, 118.88, 118.61, 108.40, 108.33, 103.66, 29.63, 27.32, 24.13. MS (EI 70 eV) *m/z* 828 (100%). Anal calc. C 81.06%, H 7.90% Found: C 80.88%, H 8.11%. Decomposition temperature - 263˚C

Chapter 3: Stabilizing Hexacenes for Device Applications

3.1 Hexacene

Electronic devices based on pentacene[17,103-105] and other smaller acenes such as tetracene[146,147] and anthracene[148] have been widely studied. However device studies on acenes larger than pentacene have not been reported. The lack of device studies on these higher acenes stems from their low solubility and poor stability both in solution and solid state. Similar to pentacene, higher acenes such as hexacene and heptacene are assumed to decompose either by "butterfly" dimerization or endoperoxide formation.[49] The reactivity of acene toward singlet oxygen and toward itself increases with higher members of the acene family.

Despite the stability issues associated with higher acenes, researchers in the past have attempted to synthesize these unstable molecules.[149-154] While the synthesis of hexacene has been sucessfully reported,[149-152] the synthesis of heptacene has been called into question due to lack of characterization and reproducibility of results.[149,153,154] Hexacene was sucessfully characterized by single crystal x-ray diffraction analysis.[155] Although the data was insufficient for detailed analysis of the structure, nevertheless it showed that these molecules pack similar to the lower analogs of the acene family.

While synthesis of higher acenes has been plagued by their poor stability, extensive theoretical studies have been performed to understand the reactivity[156,157] and electronic properties[158-162] of these synthetically elusive molecules. In recent years theoretical studies have predicted lower reorganization energy,[160] potential higher charge carrier mobility[161] and smaller band gap[162] for larger acenes. In order to take advantage of the interesting properties associated with these molecules, recent research has been focussed on synthesizing these reactive acenes.[74-78,163] In 2007 Neckers et al. successfully reported the synthesis of hexacene by

photodecarbonylation of soluble diketone precursors in a polymer matrix, where decompostion due to photooxidation or dimerization can be retarded.[74] The authors also reported synthesis of aryl substituted hexacene, however these compounds exhibited poor stability and were only characterized by mass spectrometry. In order to improve the stability and solubility of reactive hexacene Anthony et al. successfully extended their perifunctionalization approach to hexacene.[77] The higher reactivity of hexacene required a significantly bulkier TTBS substituent to prevent Diels-Alder reaction between the alkyne substituent of one molecule and the reactive hexacene chromophore of another.

3.2 Soluble Trialkylsilylethynyl Hexacene

Although TTBS Hexacene (**21**) exhibits reasonable stability in solution, the poor solubility in solvents such as toluene and chlorobenzene has prevented the measurement of its transport properties in organic thin film transistors (OTFTs). A major objective of this project is to improve the solubility and π-stacking of these *peri*-functionalized hexacenes by changing the alkyl substituents on silicon. I also decided to study the decomposition pathways of these molecules, both in solution and solid state, to gain a better understanding of reactivity for the design of effective functionalization strategies.

Similar to my approach to improve the solubility of F_8 and Cl_8 pentacenes by modifying the alkyl substituents I decided to use a variety of branched alkyl and cycloalkyl substituted silyl acetylene substituents, such as tri-isobutylsilylethynyl (TIBS), tricyclopentylsilylethynyl (TCPS), tricyclohexylsilyl-ethynyl (TCHS) and TTMSS to tune the solubility. Soluble trialkylsilylethynylated hexacenes were synthesized according to scheme 3.1. 6,15-hexacenequinone (**91**) was synthesized by Aldol condensation between 1,4-dihydroxyanthracene[164] and naphthalene-2,3-dicarbaldehyde.[165] The quinone was converted into

series of diethynyl diols by treatment with excess acetylide. Treatment of the resulting diols with a saturated solution of tin (II) chloride in 10% HCl gave the desired hexacenes. Purification of the crude hexacenes by silica gel chromatography followed by recrystallization gave dark green hexacene crystals in yields ranging from 8% to 36%, depending on the substituent. Compared to aryl-substituted hexacenes, these materials exhibit significant persistence both in solution and the solid state. These materials showed higher solubility than the TTBS derivative, and all of them could be prepared as 1 wt% solutions in toluene.

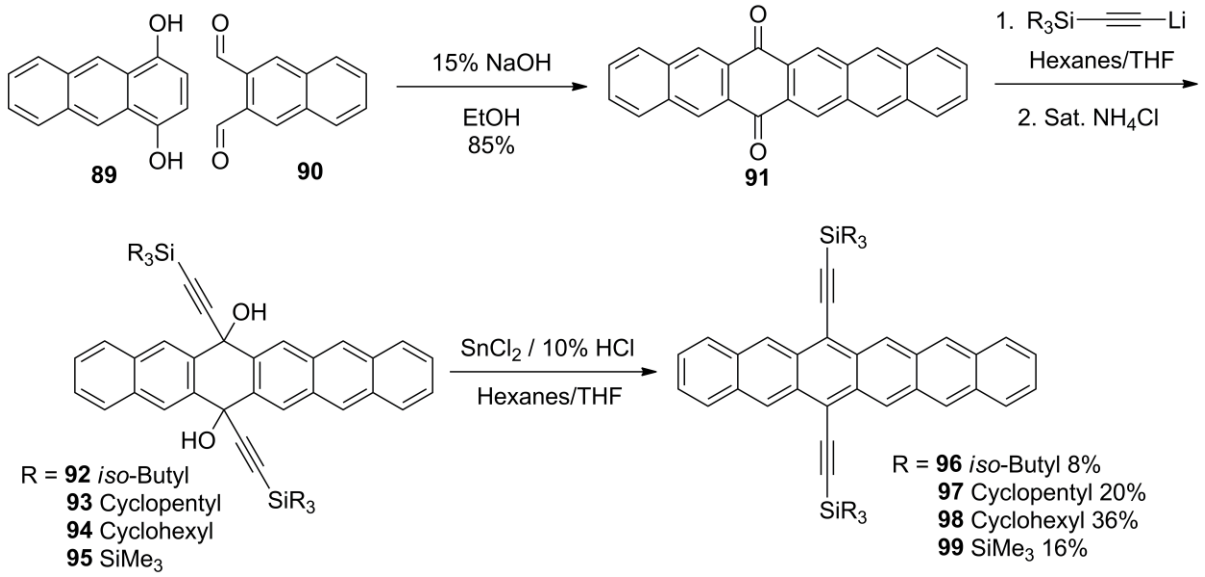

Scheme 3.1 Synthesis of new trialkylsilylethynyl hexacenes

The dark green crystals of these compounds obtained from recrystallization were suitable for single crystal X-ray diffraction analysis. Like TTBS hexacene, TCPS hexacene (**97**) exhibited a two-dimensional π-stacking motif with a close contact of 3.42 Å between the aromatic faces (Figure 3.1). By changing the substituent to the smaller TIBS group (**96)** the π-stacking motif changed to a one-dimensional sandwich herringbone packing, while larger TCHS or TTMSS substituents (**98**) or (**99)** led to one-dimensional π-stacked arrangements with close contacts of 3.30 Å and 3.36 Å respectively (Figure 3.1). The change in packing motif with the size of the trialkylsilyl substituent is in accordance with the functionalization model developed for

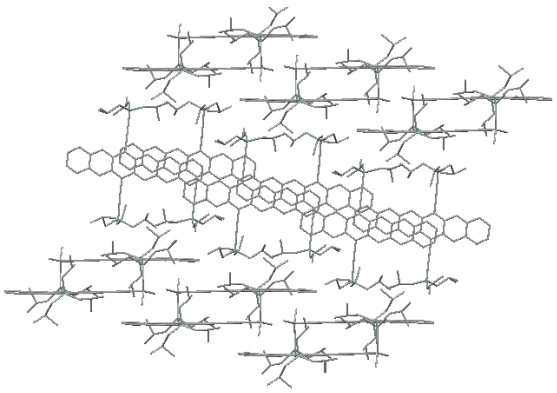

96

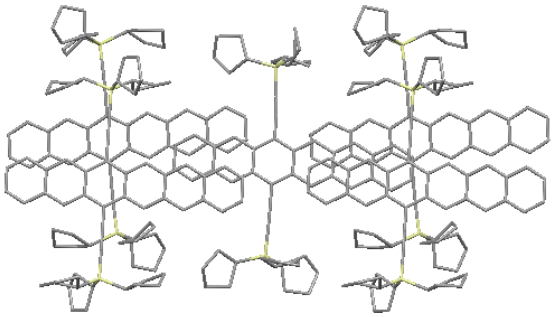

97

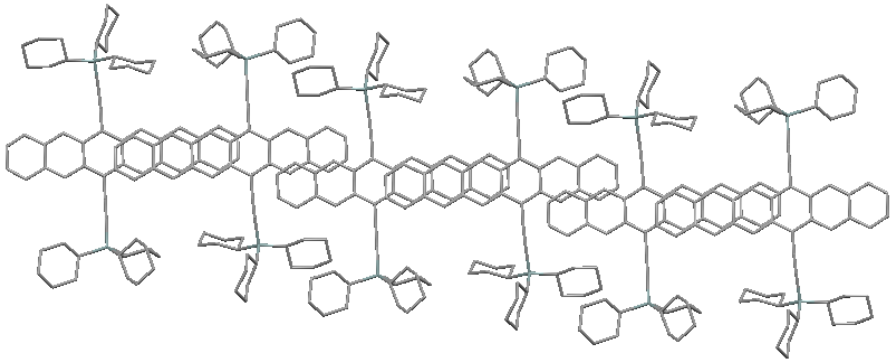

98

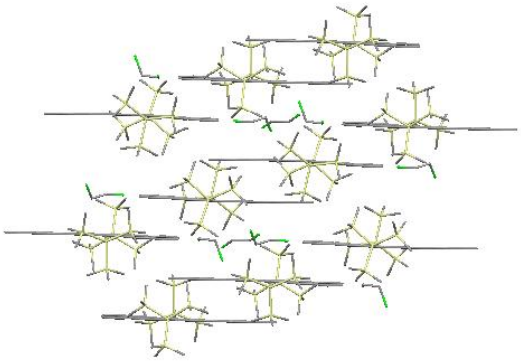

99

Figure 3.1 Crystal packing of new trialkylsilylethynyl hexacenes

controlling π-stacking in pentacene. All of these hexacene dervatives exhibit significant bending of the alkyne substituents ($C_{Ar} - C_{sp} - C_{sp}$ ~ 176˚ - 178˚ and $C_{sp} - C_{sp} - Si$ ~ 169˚ - 179˚) induced by crystal packing effects. However, the distortion is not as dramatic as seen with TTBS Hexacene (**21**) ($C_{Ar} - C_{sp} - C_{sp}$ ~ 176º & 173º and $C_{sp} - C_{sp} - Si$ = 169º & 174º) and is typical of alkynes having large substituents.[61,77,166] Another important observation is the twisting of the acene core (torsion angle 13.4º) of TCHS hexacene (**98**) compared with all other derivatives (< 5º), which likely arises to alleviate strain in crystal packing due to the bulky cyclohexyl substituents.

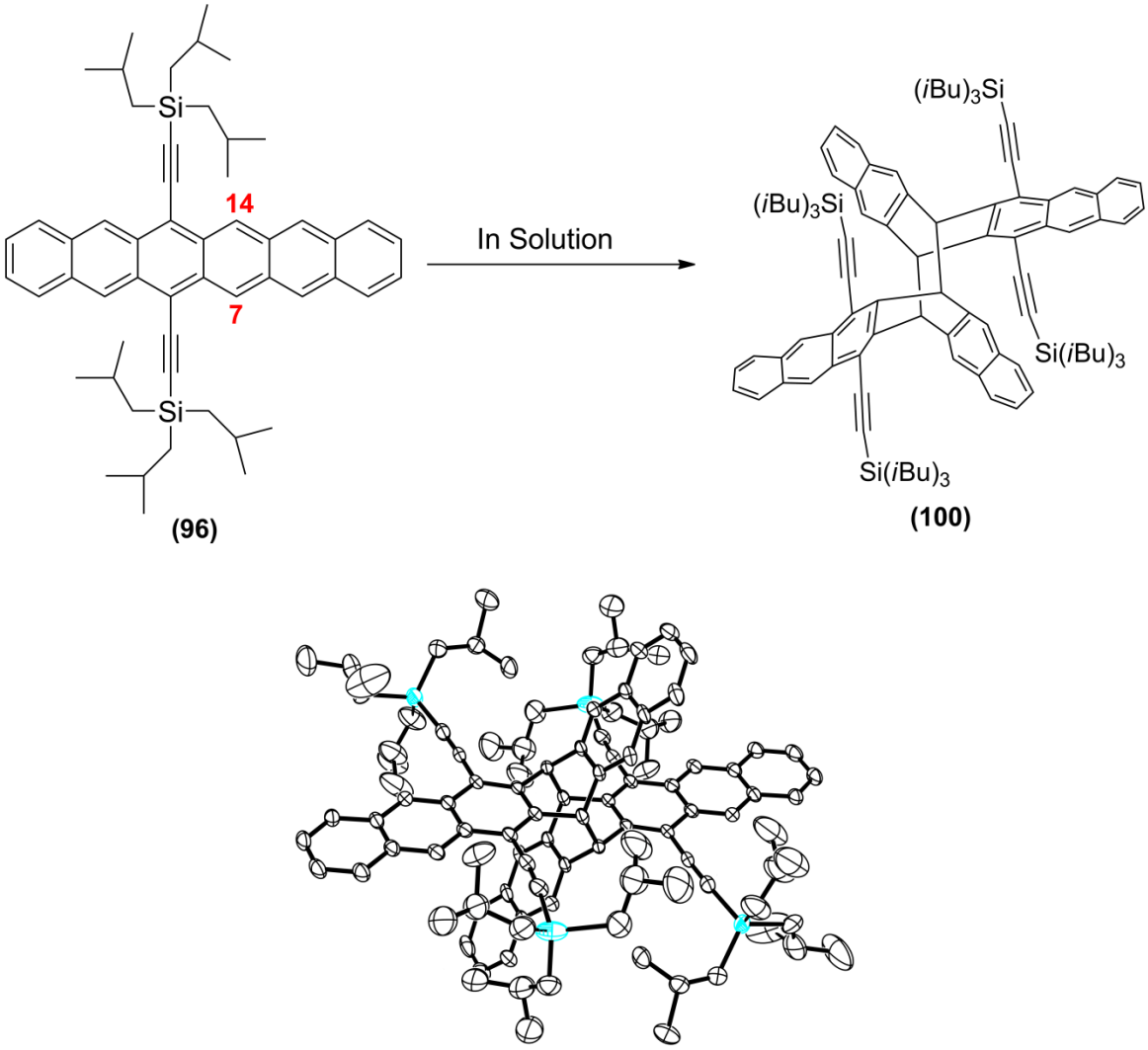

Figure 3.2 Decomposition product of TIBS Hexacene (96) in solution

The study of decomposition pathways for hexacenes began during the recrystallization of TIBS hexacene (**96**) under ambient laboratory lighting, where a small amount of yellow crystals formed along with the green hexacene. Single crystal X-ray diffraction analysis of this byproduct showed that this compound was a symmetrical dimer formed between the reactive C7 and C14 carbons of two hexacene molecules (**100**, Figure 3.2). Unlike the two dimer products proposed for TIPS pentacene (**15**) decomposition, only the centrosymmetric dimer product was observed, as the planosymmetric product is significantly more sterically hindered.[138]

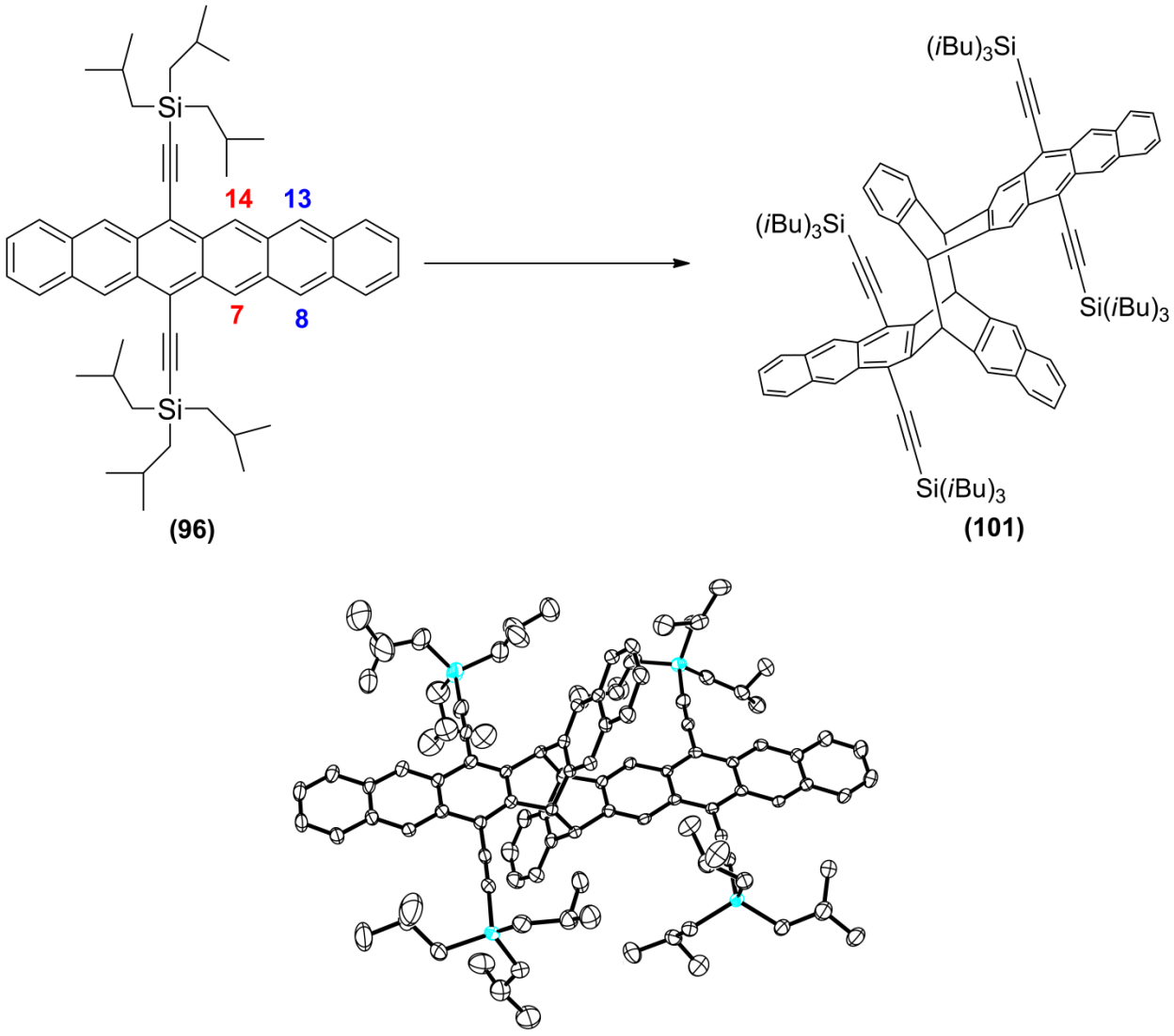

Figure 3.3 Decomposition product of TIBS Hexacene (96) in solid state

When pure crystals of TIBS hexacene were kept in air in the dark, they slowly (~ 1 month) turned from crystalline green needles into a reddish brown powder. Purification of this powder by silica gel chromatography to remove unreacted hexacene, followed by recrystallization and single crystal X-ray diffraction analysis showed that this material was another dimerization product formed between the C7 and C14 carbons of one hexacene molecule with the C8 and C13 carbons of another to give a dimer with tetracene and anthracene chromophores (**101**, Figure 3.3). The change in the regiochemistry of dimerization arises simply from the orientation of the chromophores in the solid state.

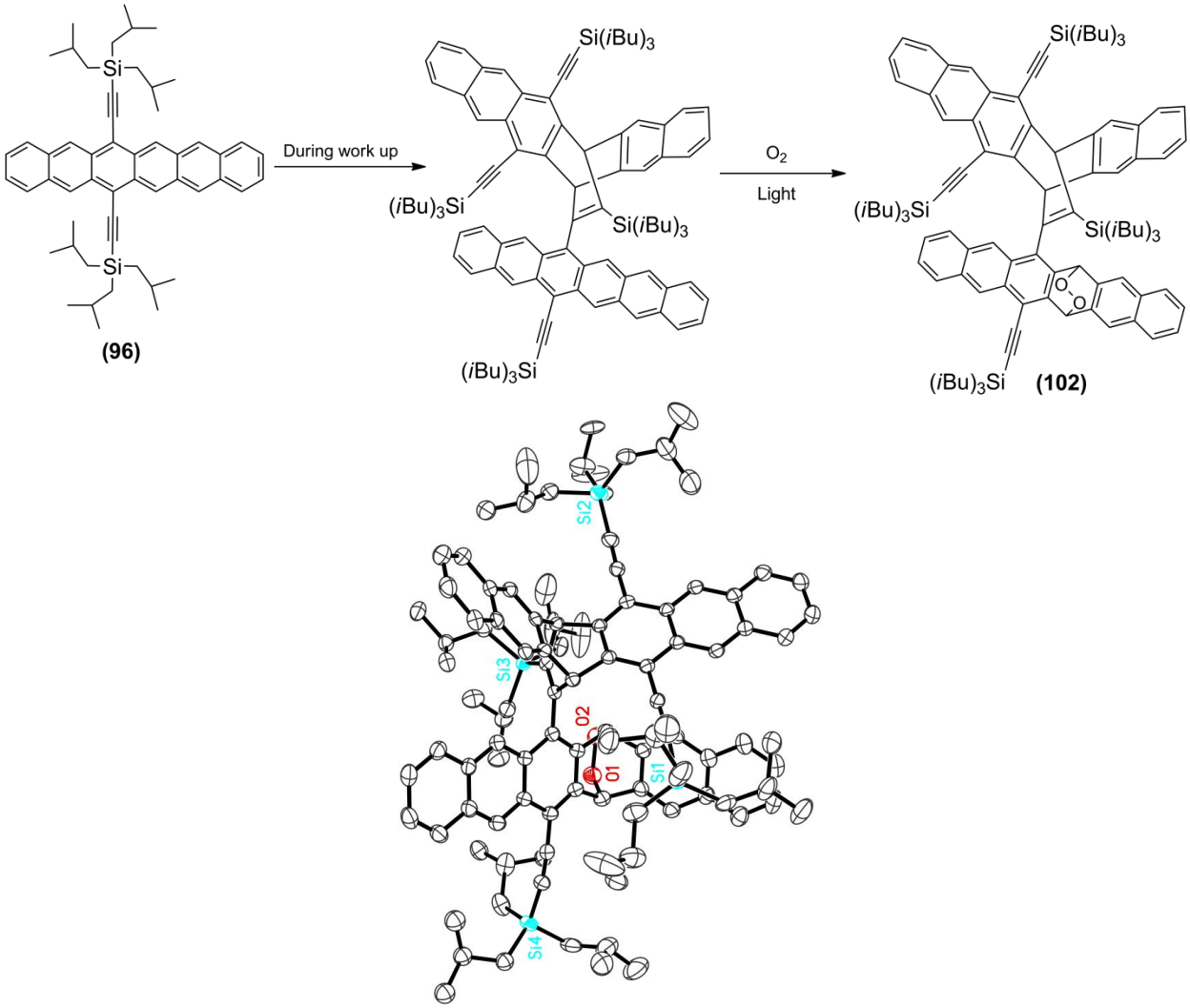

Figure 3.4 Decomposition of TIBS Hexacene (96) *via* endoperoxide formation during work up

Another byproduct observed during the synthesis of TIBS hexacene (**96**) was initially isolated as a deep green material which turned yellow-orange during chromatographic purification on silica gel. X-ray crystallographic analysis of this purified material showed that initial decomposition arose from a Diels – Alder reaction of the hexacene core with the alkyne substituent of another molecule, to yield the initially observed green species, followed by endoperoxide formation during chromatography (**102**, Figure 3.4), which bleached the remaining hexacene chromophore. Thus, the only photo-oxidation product observed in this series of hexacenes arose from reaction on a chromophore where one of the alkyne substituents had been compromized.

Differential pulse voltammetry was performed on all the hexacene derivatives to determine the oxidation and reduction potentials of these molecules (ferrocene used as internal standard – Table 3.1). TTMSS hexacene (**99**) has the lowest oxidation potential compared to the other derivatives due to the electropositive tris-(trimethylsilyl)silylethynyl group. The lower energy gap is also evident from a ~13 nm red shift in toluene compared to other derivatives.

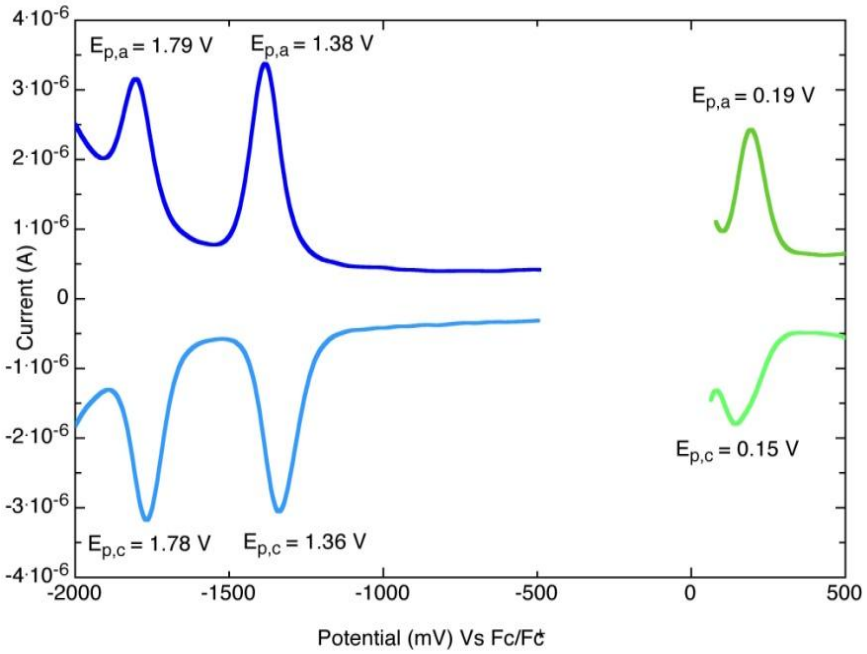

Figure 3.5 Differential pulse voltammetry of TCPS hexacene (97)

Table 3.1 Energy levels and solution half lives of trialkylsilylethynyl hexacene

Hexacene	Oxidation Potential (mV)	Reduction Potential (mV)	HOMO (eV)	LUMO (eV)	E_{gap} (eV)	Solution Half Life $t_{1/2}$ (min)
TIBS (96)	181	-1376	-4.98	-3.42	1.56	93
TCPS (97)	172	-1370	-4.97	-3.43	1.54	38
TCHS (98)	198	-1370	-5.0	-3.43	1.56	45
TTMSS (99)	123	-1421	-4.92	-3.38	1.54	19

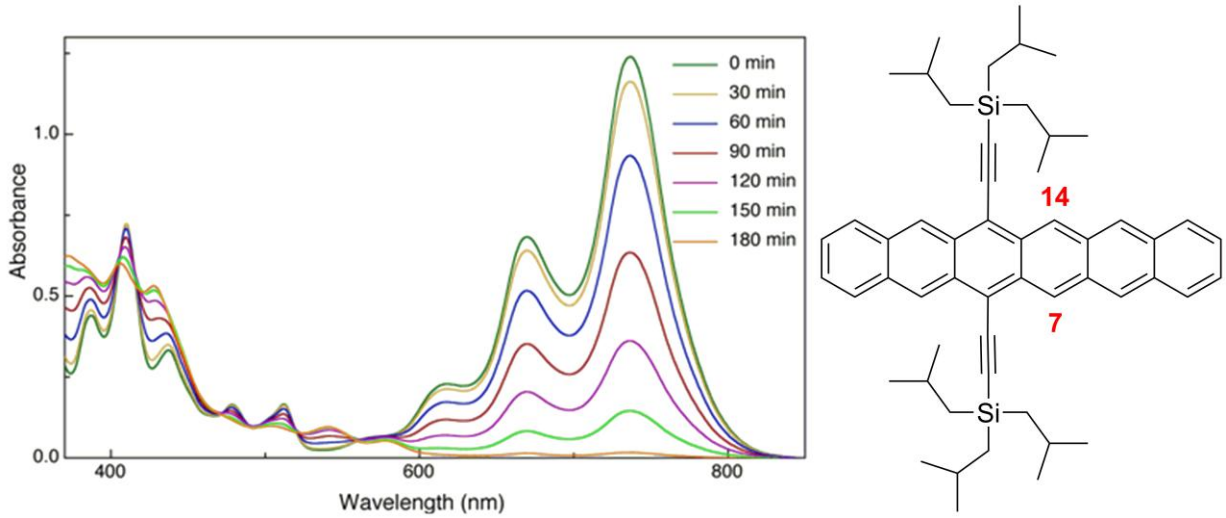

Figure 3.6 UV-vis solution stability of TIBS Hexacene (96)

In order to study their relative stabilities in solution, all of these hexacene derivatives were subjected to UV-Vis stability studies (Table 3.1). Disappearance of the long-wavelength hexacene absorptions is coupled with the appearance of a strong absorption at 430 nm, characteristic of an anthracene chromophore, and weak absorbance at ~550 nm, characteristic of tetracene (Figure 3.6). Comparison of the decomposition UV-vis spectrum with absorption spectra of **100** and **101** (Figure 3.7) suggests that these are indeed the major decomposition

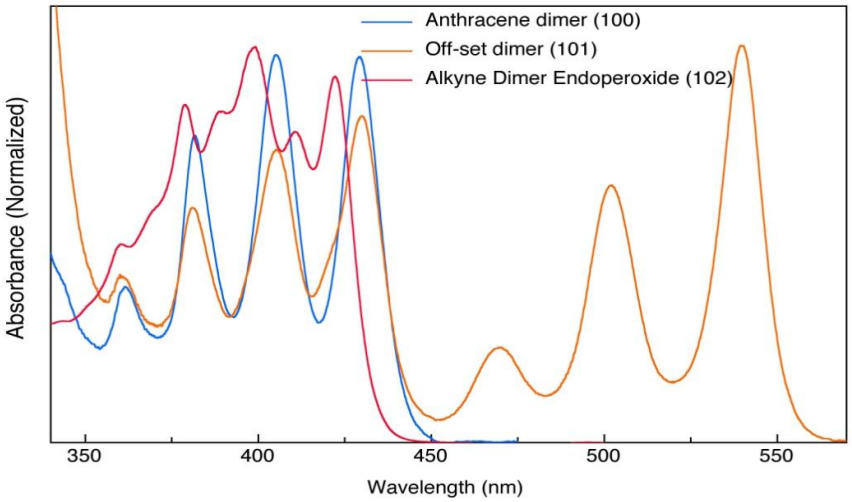

Figure 3.7 UV – visible spectra for decomposition products of TIBS Hexacene (96)

products in solutions illuminated in air. Similar decomposition products were observed for hexacene derivatives (**97-98**). It is noteworthy that TTMSS hexacene (**99**), which was expected to have higher stability due to the effectiveness of the bulky substituents in preventing dimerization, had a half life of only 19 min in solution (Table 3.1). This lower stability may be due to the photolysis of the silane into hexamethyldisilane and a radical byproduct, which effectively reduces the size of the silyl group and hence its efficacy in stabilizing the hexacene.[167] It is also interesting to note that smaller TIBS group has a higher solution half life in spite of its poor stability. This discrepancy in solution half life is due to fact that the TIBS group is not bulky enough to prevent reaction between the acene chromophore and the alkyne – this decomposition product retains a hexacene chromophore, resulting in a small drop in absorbance over time.

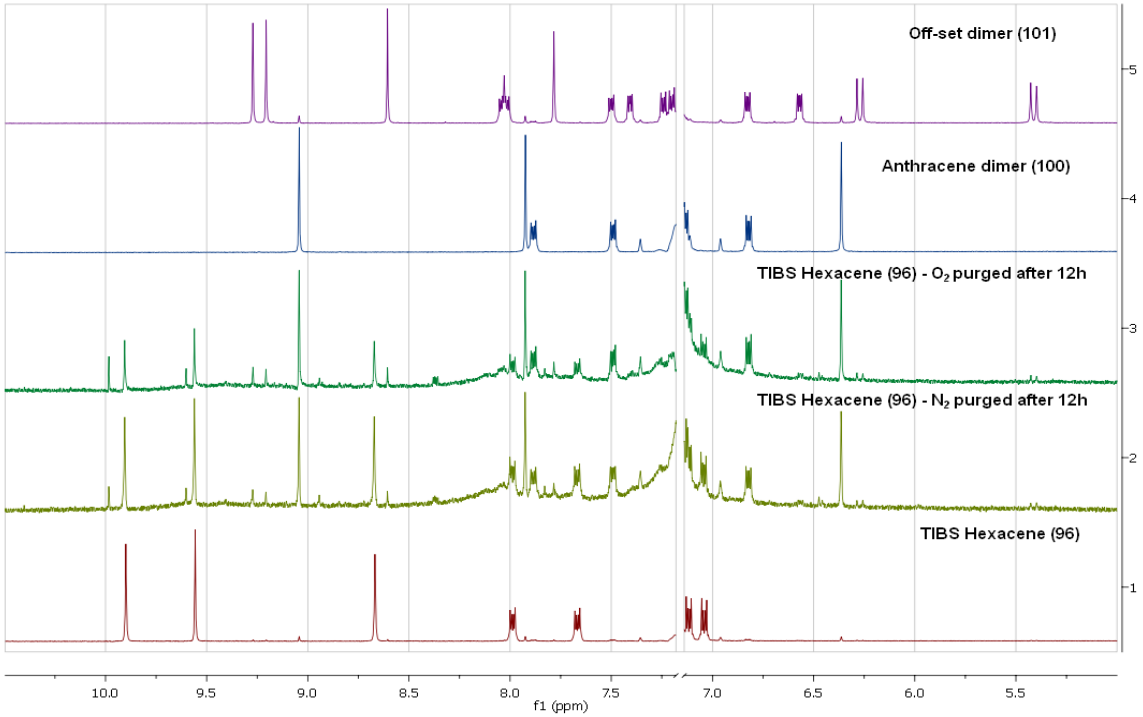

Figure 3.8 ^{1}H NMR spectra of 11a in benzene exposed to a bright light source in comparison with 12 and 13. N_2-purged and O_2-purged samples yielded nearly identical product mixtures

While UV-vis solution stability studies were helpful in determining the relative stabilities of different hexacene derivatives, it failed to provide meaningful information on the decomposition products being formed and their composition. In order to beter understand the decomposition pathways in solution a ^{1}H NMR stability study was performed on TIBS hexacene (**99**) in deuterated benzene at a concentration of 1wt% (Figure 3.8). The ^{1}H NMR spectra of both N_2 and O_2 purged solutions before and after exposure to bright light again showed that dimerization, rather than oxidation, was the dominant degradation pathway in these silylethyne-functionalized hexacenes. In both case the anthracene dimer (**100**) seems to be the major decomposition product in solution.

3.3 Stabilizing Hexacene by Partial Halogenation

Although the initial goal of improving the solubility of hexacene was achieved, the stability in solution needs to be improved for successful device applications. My experience with trialkylsilylethynylated pentacene showed that the solution stability can improved on partial fluorination. The position of the substituent also played a critical role in the stability of pentacene. In order to enhance the solution stability of trialkylsilylethynylated hexacenes I decided to partially fluorinate the hexacene chromophore. Since C7 and C14 are the most reactive positions of the hexacene chromophore I decided to fluorinate the end rings of the hexacene to enhance the stability. Due to the unsymmetrical nature of the trialkysilyethynylated hexacene chromophore I decided to synthesize both the isomers of tetrafluorohexacene along with octafluorohexacene and study their photostability in solution.

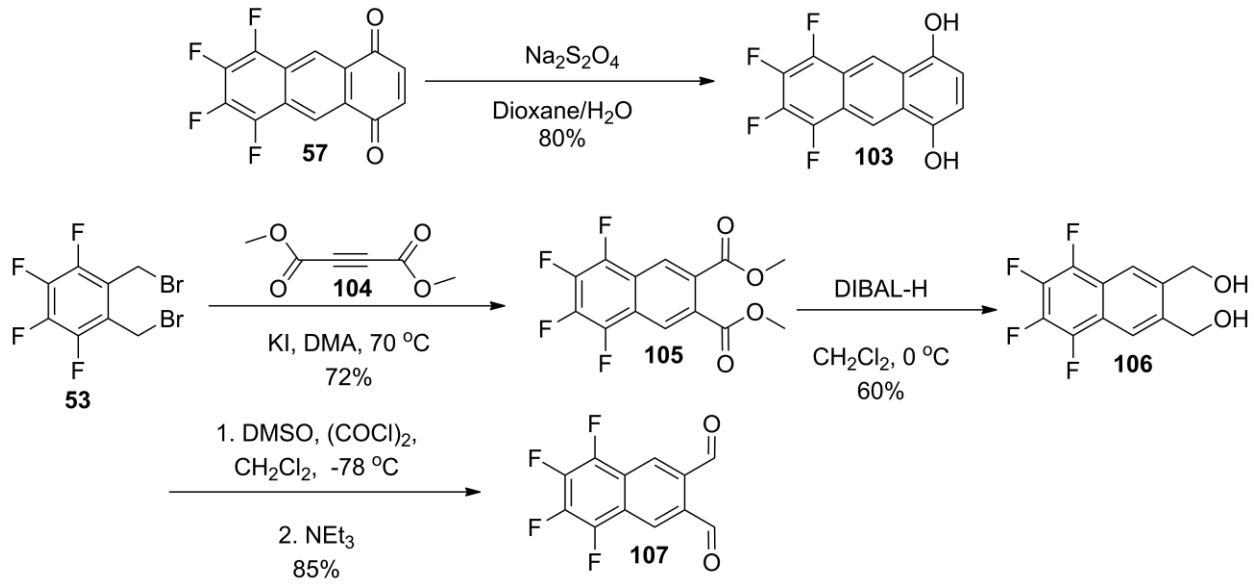

Scheme 3.2 Synthesis of tetrafluorodihydroxyanthracene and tetrafluoronaphthaldehyde

Similar to the synthesis of hexacenequinone all of the partially fluorinated hexacene quinones were made by Aldol condensation of respective dialdehyde with dihydroxyanthracene or dihydroxytetrafluoroanthracene (Scheme 3.3). The 5,6,7,8-tetrafluoro-1,4-dihydroxyanthracene (**103**) was synthesized by sodium dithionite reduction of

tetrafluoroanthraquinone (**57**) in a 1:1 mixture of 1,4-dioxane and water (Scheme 3.2). Tetrafluoronaphthaldehyde was synthesized in three steps from 1,2-bis(bromomethyl)-3,4,5,6-tetrafluorobenzene (**53**) (Scheme 3.2). Cava reaction between **53** and dimethyl acetylene dicarboxylate (DMAD) (**104**) gave the dimethyl ester (**105**) which was converted to the dimethanol (**106**) by DIBALH reduction. Swern oxidation of the dimethanol (**106**) gave 5,6,7,8-tetrafluoronaphthalene-2,3-dicarbaldehyde (**107**).

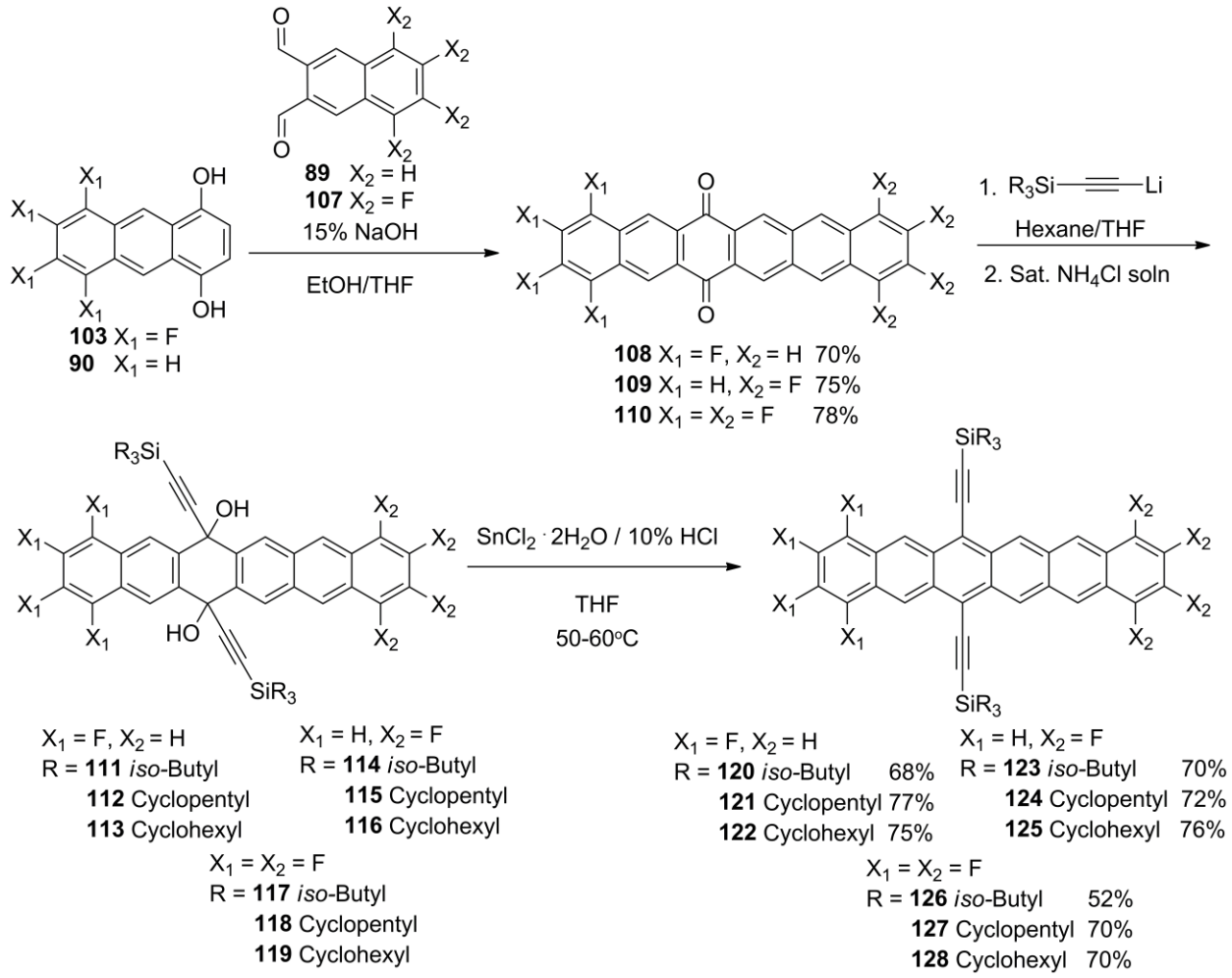

Scheme 3.3 Synthesis of partially fluorinated hexacenes

Partially fluorinated hexacenes were synthesized according to scheme 3.3. Treatement of the quinone with lithiated acetylenes gave the intermediate diol which was purified by silica gel chromatography. The diol was then converted into hexacene by treating with a saturated solution

of tin (II) chloride in 10% HCl at 50-60˚C in THF. Unlike the synthesis of non-fluorinated hexacenes, the partially fluorinated derivatives precipitate out as crystalline solid as the reaction progresses. The solids were further purified by recrystallization and subjected to single crystal x-ray diffraction.

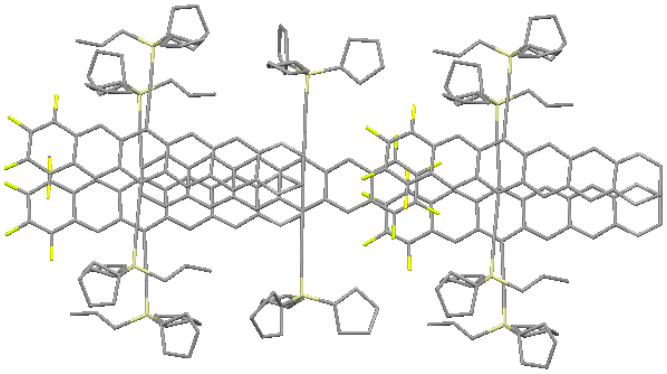

121

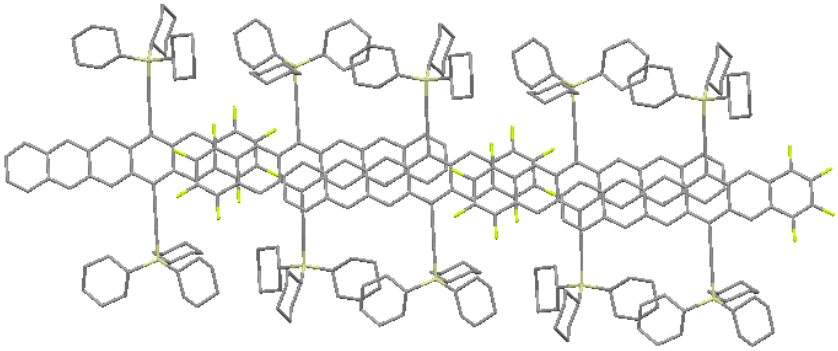

122

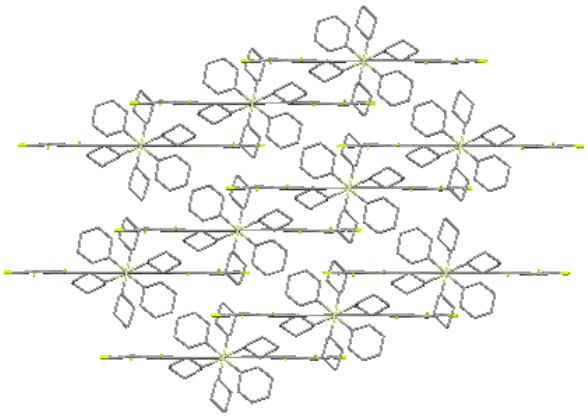

128

Figure 3.9 Crystal packing of partially fluorinated hexacenes

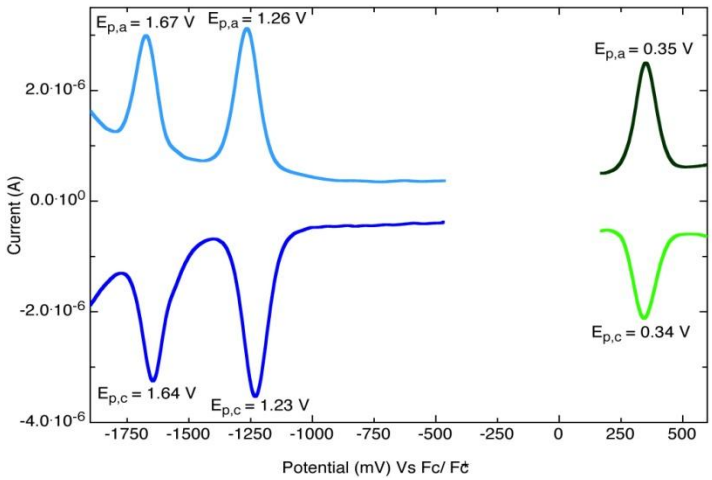

Figure 3.10 DPV of 6,13-TCPS F_4 hexacene

Table 3.2 Energy levels and solution half lives of partially fluorinated hexacene

Hexacene	Oxidation Potential (mV)	Reduction Potential (mV)	HOMO (eV)	LUMO (eV)	E_{gap} (eV)	Solution Half Life $t_{1/2}$ (min)
6,15-TIBS F_4 (120)	338	-1190	-5.14	-3.61	1.53	120
6,15-TCPS F_4 (121)	346	-1249	-5.15	-3.55	1.60	55
6,15-TCHS F_4 (122)	367	-1237	-5.17	-3.56	1.61	63
7,14-TIBS F_4 (123)	368	-1194	-5.18	-3.61	1.57	150
7,14-TCPS F_4 (124)	348	-1224	-5.15	-3.58	1.57	88
7,14-TCHS F_4 (125)	358	-1157	-5.16	-3.64	1.50	83
TIBS F_8 (126)	547	-980	-5.35	-3.81	1.54	176
TCPS F_8(127)	534	-1084	-5.33	-3.72	1.61	126
TCHS F_8 (128)	504	-1084	-5.30	-3.72	1.58	138

Differential pulse voltammetry was performed on all the hexacene derivatives to determine the oxidation and reduction potentials of these molecules (ferrocene used as internal standard – Table 3.2). Addition of electron withdrawing fluorine to the hexacene chromophore

lowers the LUMO energy levels of the molecules similar to that seen in partially fluorinated pentacene. Lowering of LUMO energy levels is more pronounced in F_8 hexacenes than F_4 hexacenes. However partially fluorination also increases the oxidation potential which might have significant effect on the hole transport properties.

In order to compare the relative solution stabilities between the differrent partially fluorinated hexacene derivatives UV-vis solution stability studies were done under the same condition used for non-fluorinated hexacene. Similar to non-fluorinated hexacene, disappearance of the long-wavelength hexacene absorptions is coupled with the appearance of a strong absorption at 430 nm, characteristic of an anthracene chromophore, and weak absorbance at ~540 nm, characteristic of tetracene (Figure 3.11).

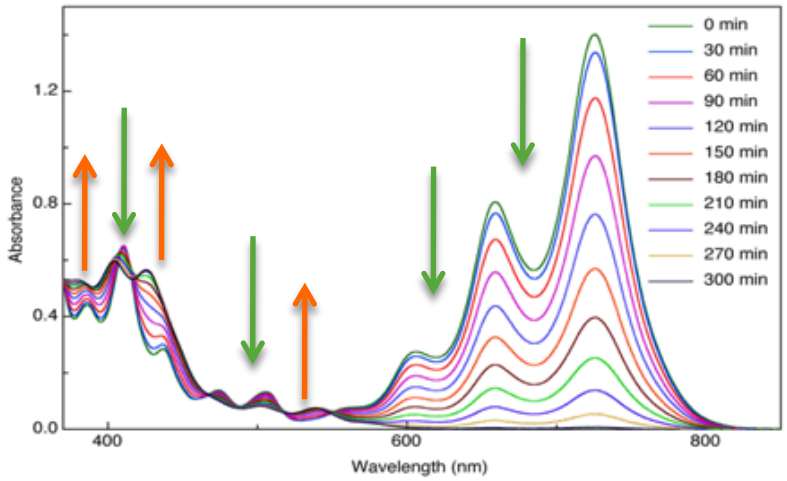

Figure 3.11 UV-vis stability study of TCPS F_8 hexacene

All the partially flurorinated hexacene derivatives exhibited improved solution stabilities compared to nonfluorinated hexacenes (Table 3.2). Between the two F_4 hexacene isomers the 7,14-trialkysilyethynyl F_4 hexacenes exhibited higher solution stability than 6,13-trialkysilyethynyl F_4 hexacenes. This difference in reactivity between the two isomers is due to the effect of the electron withdrawing fluorine on the most reactive carbon atoms of the hexacene chromophore. Fluorine substitution closer to those reactive inner rings lowers the electron

density at those reactive positions. Fluorination of both end rings of hexacene chromophore lead to a three fold increase in solution stability compared to non-fluorinated trialkylsilylethynyl hexacenes (Figure 3.12). It is also worthy to note that the TIBS derivative has a higher solution half life than TCPS and TCHS derivatives, similar to that of TIBS hexacene.

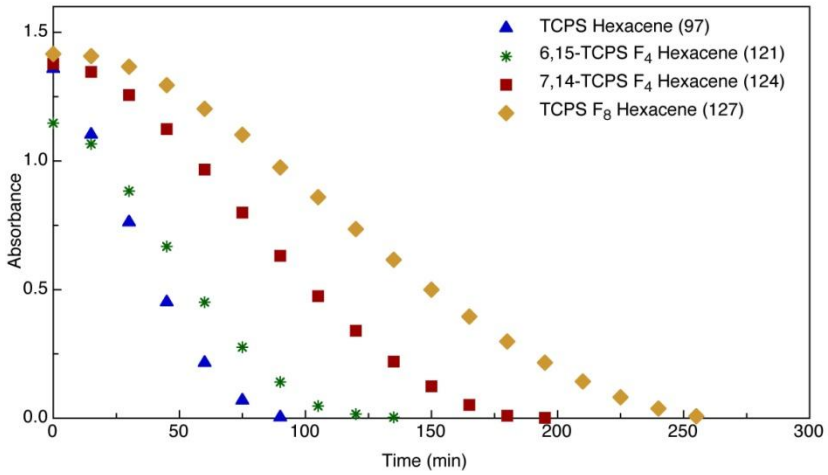

Figure 3.12 Comparison of solution stability between partially fluorinated hexacene

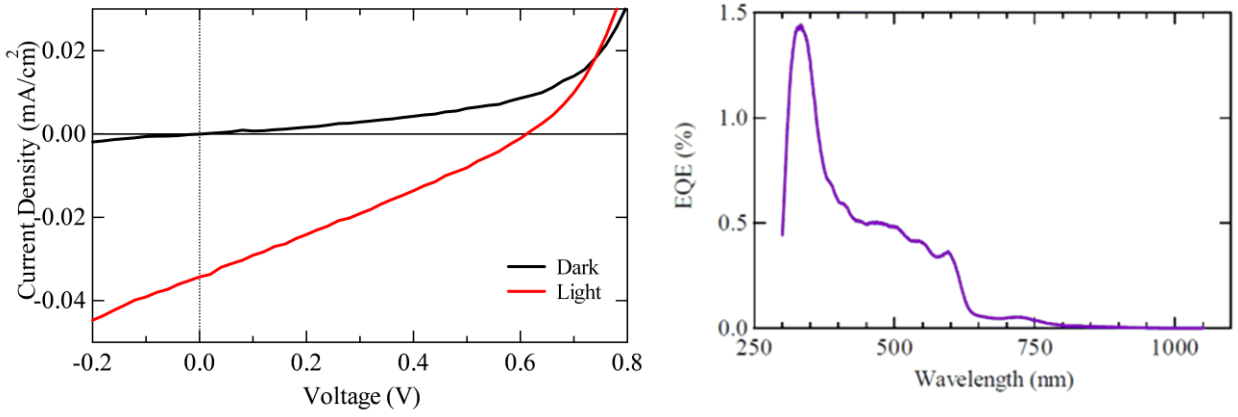

Figure 3.13 J-V curve (a) and EQE curve (b) of P3HT:TCPS F_8 hexacene solar cell (Devices fabricated by Yee-Fun Lim, Cornell University)

The improved stability of partially fluorinated hexacenes has enabled their use in devices. Since F_8 hexacene exhibited the highest stability I decided to test both TCPS (**127**) and TCHS F_8 hexacene (**128**) as acceptors in P3HT-based solar cells. The device studies were performed by Yee-Fun Lim at Cornell University. Solar cells were fabricated on pre-patterned ITO coated

glass substrate spin coated with PEDOT:PSS. The PEDOT:PSS layer was baked on a hot-plate at 170 $^{\circ}$C for 4 minutes to remove residual solvent. P3HT (**33**) and F_8 Hexacene were dissolved in toluene at a ratio of 1:1 by weight to give a total concentration of 20 mg/ml. Dichlorobenzene (30 % by volume) was added just before spin-coating on top of the PEDOT:PSS layer at 1000 rpm for 60 seconds. Finally, 4 Å of CsF and 400 Å of Al were thermally evaporated under high vacuum (~10^{-6} Torr) to form the cathode for the devices. The devices fabricated had an active area of 3 mm^2. While devices made using TCHS F_8 hexacene (**128**) formed poor films resulting in shorted devices, TCPS F_8 hexacene (**127**) gave working devices with V_{oc}=0.54 V, J_{sc}=0.03 mA/cm^2, FF=0.28, PCE=0.0052% (Figure 3.13). Even though efficiency was very low these cells exhibited surprising stability; the drop in efficiency was only about 5-10% even after exposure to 100 mW/cm^2 solar simulator light in air for 10 minutes. The results clearly indicate the improved stability of the partially fluorinated hexacene derivatives. It is also worthy to note that this the first solar cell performance reported for a hexacene derivative.

While fluorination did improve the stability of hexacene I was also interested in studying the effect of chlorination on the solution stability. Tricyclopentylsilylethynyl tetrachloro(Cl_4) hexacene (**134**) was synthesized according to scheme 3.4. The 5,6,7,8-tetrachloronaphthalene-2,3-dicarbaldehyde (**131**) was synthesized by a route similar to that of the fluoro analog. Cava reaction between 2,3-bis(bromomethyl)-3,4,5,6-tetrachlorobenzene (**75**) and dimethylacetylene dicarboxylate (DMAD) (**104**) gave the dimethyl ester (**129**). DIBALH reduction of the dimethyl ester (**129**) followed by Swern oxidation of the resulting dimethanol (**130**) gave the dialdehyde (**128**). Aldol condensation of dialdehyde (**131**) with 1,4-dihydroxyanthracene (**90**) gave the 1,2,3,4-tetrachlorohexacene-7,14-dione (**132**) which was treated with lithiated acetylene to give

the intermediate diol. Conversion to final hexacene (**134**) was achieved in good yield by treatment with $SnCl_2 \cdot 2H_2O$ in 10% HCl.

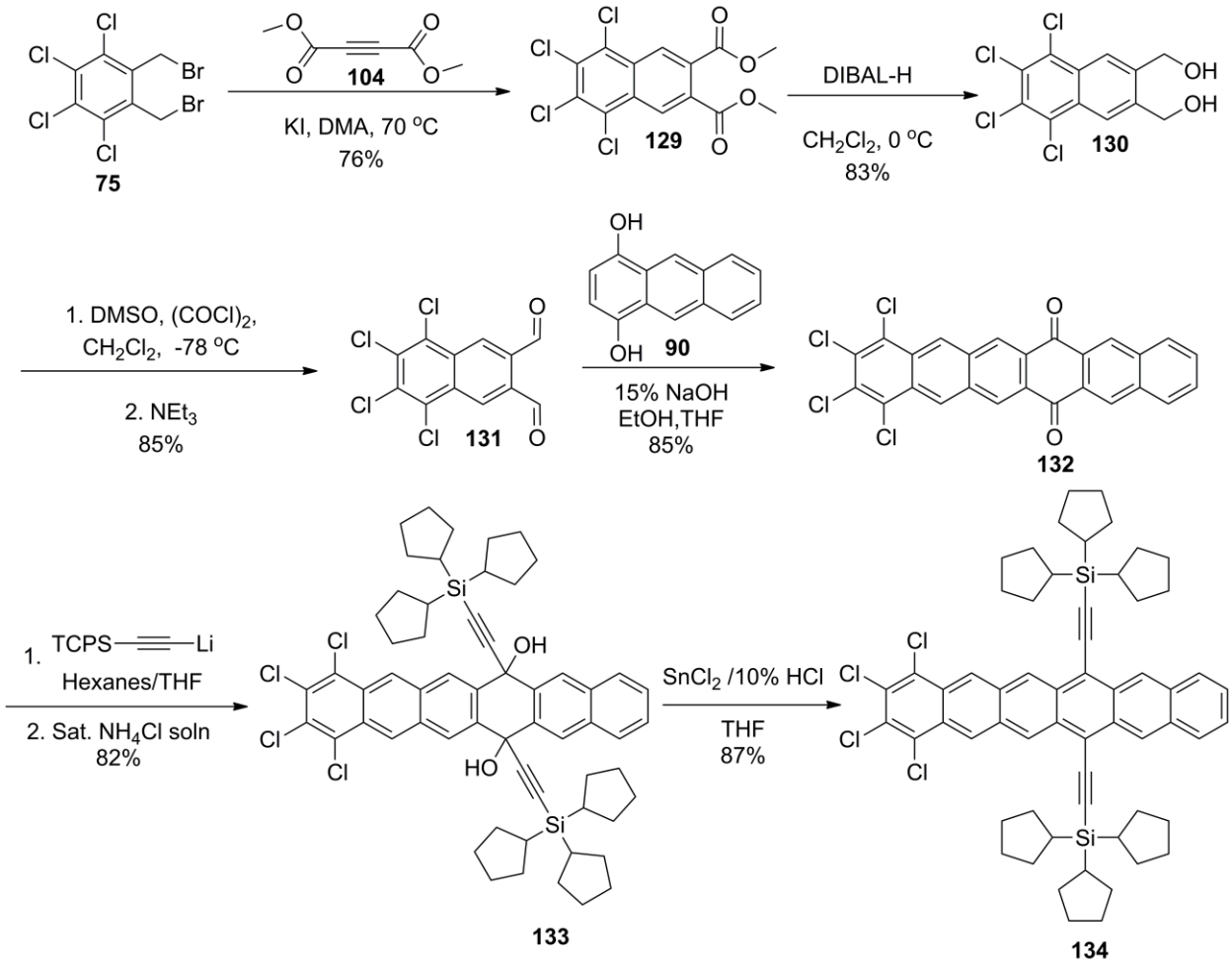

Scheme 3.4 Synthesis of 7,14-TCPS Cl_4 hexacene

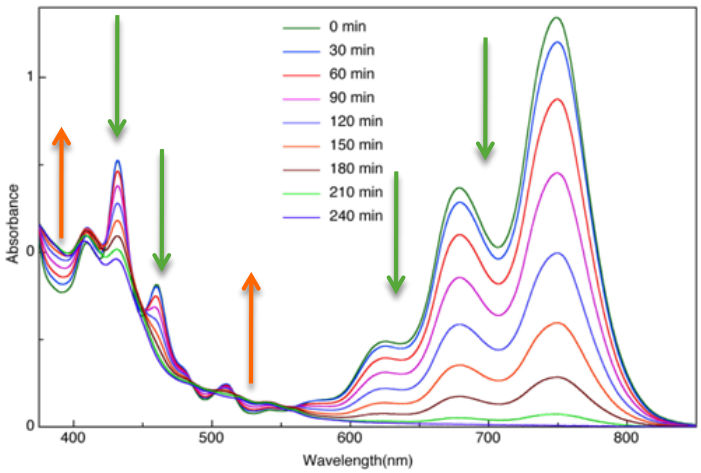

Figure 3.14 UV-vis stability study of 7,14-TCPS Cl_4 hexacene

In order to compare the solution stability of Cl_4 hexacene with that of the fluorine analog TCPS Cl_4 hexacene were subjected to a UV-vis stability study. TCPS Cl_4 hexacene (**134**) exhibited a moderate improvement in stability with a solution half life of 110 min (Figure 3.14) compared to 7,14-TCPS F_4 hexacene (**124**, $t_{1/2}$=88 min). The enhancement in solution stability is not only due to the electron withdrawing ability of chlorine atoms but likely also due to the steric nature of the chlorine substituent in slowing down the dimerization of hexacene chromophore. One of the drawbacks with chlorination is the poor solubility in common organic solvents compared to fluorinated hexacenes.

3.4 Conclusion

A series of new, more soluble trialkylsilylethynylated hexacenes were synthesized. However these molecules exhibited poor stability in solution preventing their use in devices. Dimerization of the hexacene chromophore was the most common decomposition pathway and photo-oxidation was only observed in materials where one of the alkyne substituents had been compromised. Enhancement of solution stability was achieved by partial fluorination of the hexacene chromophore. Among the fluorinated hexacene derivatives, F_8 hexacenes exhibited the highest stability enabling their use in solar cells. TCPS F_8 hexacene (**128**) was used as acceptor for P3HT (**33**) based solar cell exhibiting a PCE of 0.0052%. Chlorination of the hexacene chromophore resulted in improved stability however they exhibited poor soubility in common organic solvents.

3.5 Experimental details

All solvents were purchased from Pharmco Aaper except anhydrous tetrahydrofuran which was purchased from Aldrich. The solvents were degassed by purging N_2 gas through them for 30 min. n-Butyllithium (n-BuLi) was purchased from Aldrich. Chromatography was performed on

silica gel (60 Å, 40-63 μm) purchased from Silicycle Inc. Thin layer chromatography was performed using Silica Gel HL TLC plates (w/UV254) purchased from Sorbent Technologies. UV – Visible spectra were recorded using Shimadzu UV-visible Spectrophotometer model UV-2501PC. The spectra were recorded between the wavelength ranges of 350 – 850 nm using quartz cells with 1cm path length. 10^{-4} M solutions of hexacenes in degassed toluene (UV Grade, Pharmco Aaper) were made in the dark and an initial spectrum of the acene was obtained. The solution was then exposed to a bright full-spectrum light source and the spectra were acquired at regular intervals until the absorption bands at longest wavelength disappeared. A plot of absorbance maximum at longest wavelength *versus* time was used to calculate the solution half-life (time taken to reach half the initial absorbance) of each pentacene derivative. NMR spectra were recorded on Varian Inova 400MHz instrument. High resolution mass spectra were recorded in EI mode on JOEL JMS-700T MStation. Mass spectra were recorded in either EI mode on JOEL JMS-700T MStation or MALDI mode on Bruker Daltonics Autoflex MALDI-TOFMS. Electrochemical analysis was performed using BAS CV-50W voltammetric analyzer performed on 0.1M Bu_4NPF_6 solution in dichloromethane with ferrocene as internal standard. Naphthalene-2,3-dicarbaldehyde[164] and 1,4-dihdroxyanthracene[163] were prepared using previously reported literature methods.

6, 15 – Hexacenequinone (91)

To a 250 ml round bottom flask equipped with a stir bar was added 1 g (5.43 mmol) of naphthalene-2,3-dicarboxaldehyde (**90**) and 1.26 g (5.99 mmol) of 1,4-dihydroxyanthracene (8**9**). The mixture was then dissolved in 120 ml of hot ethanol. Drops of 15% aqueous NaOH solution were added to the stirring mixture until there was an observable precipitate formation and the thick slurry was allowed to stir for 30 minutes. 50 ml of methanol was added to the reaction

mixture and the precipitates were filtered through a Büchner funnel, washed with methanol followed by THF and finally with ether to give a yellow solid. Yield – 1.65 g, 85%. MS (MALDI) *m/z* = 358 (100%, M^+)

General procedure for the synthesis of 6,15 – Trialkylsilylethynylated Hexacenes

To a flame dried 100 ml flask cooled under nitrogen was added 5.58 mmol of acetylene, followed by 5 ml of hexanes. The reaction mixture was then placed in an ice bath. 2 ml of n-BuLi (4.88 mmol, 2.5 M solution in hexanes) was added dropwise and the reaction mixture stirred at 0 ºC for an hour. 13 ml of hexanes was added followed by 2 ml of anhydrous THF. 500 mg (1.4 mmol) of 6,15 – hexacenequinone (**91**) was then added and the reaction mixture allowed to stir overnight. The reaction mixture was quenched with saturated NH_4Cl solution and extracted into ether. The combined ether layers were washed with water and dried over anhydrous $MgSO_4$. The excess acetylene was recovered from the crude product by elution through a pad of silica gel initially with hexanes. The crude diol was obtained as a mixture of *syn* and *anti* isomers by slowly increasing the ratio of hexanes:DCM to 7:3. To a 50 ml round bottom flask were added 200 mg of crude diol, 20 ml of hexanes and 10 ml of THF. Nitrogen gas was bubbled through the solution for 15 min. A saturated solution of $SnCl_2 \bullet 2H_2O$ in 10% aqueous HCl was added and the reaction was followed by TLC by monitoring the disappearance of diol. The product mixture was then poured into a thick pad of silica gel and eluted with hexanes to give crude hexacene, which was further purified by chromatography on silica gel using 9:1 hexanes/ DCM. Recrystallization in hexanes/DCM gave crystalline hexacenes.

Note: The conversion of the intermediate diol to final hexacene was done in the dark. Solvents were degassed with nitrogen prior to use for recrystallization.

6,15-bis((triisobutylsilyl)ethynyl)hexacene (96) - 19 mg, Yield – 8%

^{1}H NMR (400 MHz, $CDCl_3$) δ 9.56 (s, 2H), 9.20 (s, 2H), 8.60 (s, 2H), 7.94 (dd, *J* = 6.6, 3.2 Hz, 2H), 7.91 (dd, *J* = 6.6, 3.2 Hz, 2H), 7.38 (dd, *J* = 6.7, 3.1 Hz, 2H), 7.34 (dd, *J* = 6.8, 3.1 Hz, 2H), 2.24 (sept, *J* = 6.8 Hz, 6H), 1.24 (d, *J* = 6.6 Hz, 36H), 1.01 (d, *J* = 7.0 Hz, 12H). ^{13}C NMR (100 MHz, $CDCl_3$) δ 132.69, 132.5, 131.19, 130.94, 130.42, 128.82, 128.77, 126.97, 126.77, 126.54, 126.32, 125.73, 118.39, 110.68, 105.16, 26.82, 25.7, 25.65 HRMS (EI) *m/z* (M^+) 772.4859 (Calcd. for $C_{54}H_{68}Si_2$ 772.4859) Decomposition temperature – 240 ºC

6,15-bis((tricyclopentylsilyl)ethynyl)hexacene (97) - 54 mg, Yield – 20%

^{1}H NMR (400 MHz, $CDCl_3$) δ 9.56 (s, 2H), 9.20 (s, 2H), 8.60 (s, 2H), 7.95 (dd, *J* = 6.6, 3.2 Hz, 2H), 7.91 (dd, *J* = 6.5, 3.2 Hz, 2H), 7.38 (dd, *J* = 6.7, 3.1 Hz, 2H), 7.34 (dd, *J* = 6.7, 3.1 Hz, 2H), 2.18 – 2.04 (m, 12H), 1.95 – 1.60 (m, 36H), 1.47 – 1.30 (m, 6H). ^{13}C NMR (100 MHz, $CDCl_3$) δ 132.71, 132.5, 131.15, 130.96, 130.4, 128.89, 128.78, 127.01, 126.63, 126.3, 126.01, 125.72, 118.4, 108.58, 104.26, 29.67, 27.35, 24.23 HRMS (EI) *m/z* (M^+) 844.4862 (Calcd. for $C_{60}H_{68}Si_2$ 844.4859) Decomposition temperature – 218 ºC

6,15-bis((tricyclohexylsilyl)ethynyl)hexacene (98) - 98 mg, Yield – 36%

^{1}H NMR (400 MHz, $CDCl_3$) δ 9.6 (s, 2H), 9.23 (s, 2H), 8.60 (s, 2H), 7.95 (dd, *J* = 6.8, 3.2 Hz, 2H), 7.92 (dd, *J* = 6.8, 3.2 Hz, 2H), 7.39 (dd, *J* = 6.8, 3.2 Hz, 2H), 7.35 (dd, *J* = 6.8, 3.2 Hz, 2H), 2.18 – 2.09 (m, 12H), 1.97 – 1.74 (m, 18H), 1.71 – 1.63 (m, 12H), 1.41 – 1.36 (m, 18H), 1.23 (tt, *J* = 12.8, 2.8 Hz, 6H). ^{13}C NMR (100 MHz, $CDCl_3$) δ 132.68, 132.49, 131.18, 130.93, 130.44, 128. 9, 128.78, 127.04, 126.96, 126.72, 126.33, 125.72, 118.41, 108.58, 105.42, 29.18, 28.69, 27.35, 23.73. MS (EI) *m/z* 928 (12%, M^+) Decomposition temperature – 290 ºC

Synthesis of 6,15 – bis(tris(trimetylsilyl)silylethynyl)hexacene (99)

To a flame dried 100 ml flask cooled under nitrogen was added 1.52 g (5.6 mmol) tris(trimethylsilyl)silylacetylene, followed by 3 ml of hexanes. The reaction mixture was then placed in an ice bath. 2 ml of n-BuLi (4.88 mmol, 2.5 M solution in hexanes) was added dropwise and the reaction mixture stirred at 0 ºC for an hour. 3 ml of anhydrous THF followed by 24 ml of hexanes was added. 500 mg (1.4 mmol) of 6, 15 – hexacenequinone (**91**) was then added to the reaction mixture and allowed to stir overnight. The reaction mixture was quenched with saturated NH_4Cl solution and extracted into ether. The combined ether layers were washed with water and dried over anhydrous $MgSO_4$. The solvent was removed under reduced pressure to give crude diol , which was dissolved in 43 ml of hexanes, 7 ml of THF. A saturated solution of $SnCl_2 \bullet 2H_2O$ in 10% aqueous HCl was added and the reaction was followed by TLC by monitoring the disappearance of diol. The reaction mixture was poured onto a thick pad of silica gel and eluted with hexanes to give crude hexacene, which was further purified by chromatography using 9:1 hexanes/ DCM. Recrystallization in hexanes gave 195 mg (16%) of crystalline TTMSS hexacene (**99**).

Note: The conversion of the intermediate diol to final hexacene was done in the dark. Solvents were degassed with nitrogen prior to use for recrystallization.

^{1}H NMR (400 MHz, $CDCl_3$) δ 9.54 (s, 2H), 9.19 (s, 1H), 8.57 (s, 2H), 7.93 (dd, *J* = 6.6, 3.2 Hz, 2H), 7.89 (dd, *J* = 6.5, 3.2 Hz, 2H), 7.36 (dd, *J* = 6.7, 3.1 Hz, 2H), 7.32 (dd, *J* = 6.7, 3.1 Hz, 2H), 0.47 (s, 54H). ^{13}C NMR (100 MHz, $CDCl_3$) δ 132.53, 132.36, 131.13, 130.88, 130.45, 128.84, 128.77, 126.91, 126.83, 126.65, 126.08, 125.56, 118.60, 107.02, 106.52, 1.00. MS (EI) *m/z* 868 (15%, M^+) Decomposition temperature – 282 ºC

Anthracene dimer (100)

Formed by allowing solutions of TIBS hexacene (**96**) to stand in air exposed to light.

^{1}H NMR (400 MHz, $CDCl_3$) δ 8.71 (s, 4H), 7.84 (dd, *J* = 6.5, 3.2 Hz, 4H), 7.56 (s, 4H), 7.45 (dd, *J* = 6.1, 3.3 Hz, 4H), 7.39 (dd, *J* = 6.5, 3.1 Hz, 4H), 7.26 (s, 4H), 7.13 (dd, *J* = 6.2, 3.2 Hz, 4H), 5.94 (s, 4H), 2.22 (sept, *J* = 6.8 Hz, 12H), 1.26 (dd, *J* = 6.6, 2.6 Hz, 18H), 1.06 (d, *J* = 6.9 Hz, 6H). ^{13}C NMR (101 MHz, $CDCl_3$) δ 142.55, 138.96, 132.53, 131.93, 129.95, 128.27, 127.48, 125.78, 125.59, 125.40, 118.91, 105.29, 104.21, 51.60, 27.01, 26.99, 25.72, 25.63. MS (LDI) *m/z* 772 (100%, M^+ - 772)

Off-set dimer (101)

Formed by allowing crystals of TIBS hexacene (**96**) to sit in air exposed to light.

^{1}H NMR (400 MHz, $CDCl_3$) δ 9.14 (s, 2H), 8.84 (s, 2H), 8.27 (s, 2H), 8.01 – 7.94 (m, 4H), 7.57 – 7.48 (m, 8H), 7.45 (dd, *J* = 6.7, 3.1 Hz, 2H), 7.23 – 7.16 (m, 4H), 6.75 (dd, *J* = 5.5, 3.2 Hz, 2H), 5.92 (d, *J* = 11.4 Hz, 2H), 5.10 (d, *J* = 11.4 Hz, 2H), 2.41 – 2.20 (m, 12H), 1.37 (d, *J* = 6.6 Hz, 36H), 1.32 (d, *J* = 6.6 Hz, 36H), 1.11 (d, *J* = 8 Hz, 12H), 1.06 (d, *J* = 8 Hz, 12H). ^{13}C NMR (100 MHz, $CDCl_3$) δ 143.71, 143.66, 143.61, 141.53, 141.47, 139.37, 139.31, 132.53, 132.08, 132.03, 130.32, 130.25, 129.82, 129.74, 129.27, 129.22, 128.25, 127.62, 127.55, 127.20, 126.90, 126.87, 126.78, 126.69, 126.45, 126.37, 126.03, 125.96, 125.59, 125.54, 125.26, 125.19, 125.10, 124.86, 123.99, 123.94, 118.79, 118.73, 118.68, 117.78, 117.73, 117.67, 107.73, 104.85, 104.56, 104.15, 77.55, 77.23, 76.91, 54.24, 52.97, 51.61, 28.86, 28.81, 27.66, 27.62, 27.57, 27.52, 26.86, 26.42, 26.38, 26.33, 25.70, 25.20, 25.16, 25.13, 25.09, 25.05, 25.01, 24.55. MS (LDI) *m/z* 772 (100%, M^+ - 772) Decomposition temperature – 270 ºC

TIBS Hexacene - Alkyne dimer endoperoxide (102)

Formed during chromatographic workup of TIBS hexacene (**96**).

^{1}H NMR (400 MHz, $CDCl_3$) δ 9.08 (s, 1H), 9.04 (s, 1H), 8.95 (s, 1H), 8.15 (d, *J* = Hz, 1H), 8.09 (d, *J* = Hz, 1H), 7.98 – 8.00 (m, 2H), 7.89 (d, *J* = Hz, 1H), 7.84 – 7.81 (m, 2H), 7.7 – 7.76 (m, 3H), 7.67 (s, 1H), 7.64 – 7.45 (m, 7H), 7.3 – 7.26 (m, 1H), 7.05 (d, *J* = Hz, 1H), 6.98 (s, 1H), 6.68 (s, 1H), 6.42 (s, 1H), 5.71 (s, 1H), 5.56 (s, 1H), 2.3 (sept, *J* = 6.8 Hz, 3H), 2.15 (sept, *J* = 6.8 Hz, 3H), 1.52 – 1.4 (m, 3H), 1.27 (dd, *J* = 10.4, 6.4 Hz, 21H), 1.18 (dd, *J* = 6.6, 3.2 Hz, 21H), 1.04 (d, *J* = 6.8 Hz, 6H), 0.92 (d, *J* = 6.8 Hz, 6H), 0.82 (dd, *J* = 14.8, 5.2 Hz, 3H), 0.72 (d, *J* = 6.4 Hz, 9H), 0.56 (d, *J* = 6.8 Hz, 9H), 0.49 (d, *J* = 6.4 Hz, 9H), 0.44 (d, *J* = 6.8 Hz, 9H), 0.05 – 0.00 (m, 3H) , -0.14 (dd, *J* = 14.8, 7.2 Hz, 3H). ^{13}C NMR (100 MHz, $CDCl_3$) δ 154.67, 148.9, 114.68, 143.10, 141.34, 140.97, 137.74, 135.58, 134.02, 133.98, 133.23, 132.61, 132.39, 132.30, 131.92, 130.57, 130.34, 130, 129.55, 129.42, 129.20, 128.73, 128.39, 128.34, 128.31, 128.23, 128.04, 127.88, 127.61, 126.71, 126.58, 126.49, 126.44, 126.37, 126.26, 126.17, 126.10, 125.84, 124.01, 122.84, 122.52, 116.10, 115.91, 115.47, 105.11, 104.76, 104.62, 103.24, 101.73, 101.51, 78.20, 77.43, 76.72, 57.72, 53.38, 31.17, 27.04, 26.98, 26.92, 26.74, 26.12, 26.03, 25.91, 25.78, 25.75, 25.63, 25.47, 24.87, 24.62, 24.40, 23.48. MS (LDI) *m/z* = 772 (100%, M^+-804)

5,6,7,8-tetrafluoro-1,4-dihydroxyanthracene (103)

To a nitrogen purged solution of 1:1 dioxane (15 ml) and water (15 ml) was added 1g (3.57 mmol) of 5,6,7,8-tetrafluoro-1,4-anthraquinone (**57**). 2.61g (14.99 mmol) of sodium dithionite ($Na_2S_2O_4$) was added and the reaction mixture was stirred overnight under nitrogen atmosphere. The reaction mixture was poured into nitrogen purged water and the precipitated solids were washed with nitrogen purged water and dried under vaccum to give 800 mg (80%) of greenish yellow solid.

^{1}H NMR (400 MHz, DMSO) δ 9.9 (s, 2H), 8.60 (s, 2H), 6.76(s, 2H). MS (EI 70eV) *m/z* = 282 (45%, M^+)

Dimethyl 5,6,7,8-tetrafluoronaphthalene-2,3-dicarboxylate (105)

To a 350 ml sealed tube equipped with a magnetic stir bar were added 15 g(44.65 mmol) of **53**, 12.69 g (89.3 mmol) of dimethyl acetylene dicarboxylate (**104**). 140 ml of degassed DMA was added followed by 16.56 g of KI. The reaction mixture was heated to 70˚C and allowed to stir for 24h. 22.5 g of sodium bisulfite was dissolved in 1400 ml of water in a 2000 ml Erlenmeyer flask. The hot reaction mixture was poured into the stirring sodium bisulfite solution and allowed to stir for 30 min. The precipitate was filtered, washed with plenty of water and air dried to give the crude product. Purification by silica gel chromatography using 1:1 hexanes/DCM gave the pure product in 69% (9.7 g) yield.

^{1}H NMR (400 MHz, $CDCl_3$) δ 8.38 (t, $J_{H\text{-}F}$ = 1.0 Hz, 2H), 3.96 (s, 6H). ^{19}F NMR (376 MHz, $CDCl_3$) δ -150.37 – -150.48 (m), -156.57 – -156.65 (m). MS (EI 70eV) *m/z* = 316 (33%, M^+)

2,3-dimethanol-5,6,7,8-tetrafluoronaphthalene (106)

11.56 g (36.56 mmol) of the dimethyl ester (**105**) was added to a flame dried, N_2 cooled 500 ml RB flask. 100 ml of DCM was added and the flask was cooled to 0˚C using ice water bath. 154 ml of 1M solution of DIBALH in hexanes was added drop wise and the reaction mixture was allowed to stir overnight. The reaction mixture was quenched by adding a saturated solution of NH_4Cl with cooling. The precipitated aluminum salts are filtered off and the filtrate is concentrated to give the diol dissolved solution. The precipitates were heated at reflux in 500 ml ethyl acetate for an hour and the precipitates were filtered off, washed with ethyl acetate and the filtrate was saved. The process was repeated couple of times and the filtrate were combined together and solvent was removed to give white solid (5.54 g, 58%).

^{1}H NMR (400 MHz, DMSO) δ 8.06 (s, 2H), 4.69 (s, 4H). ^{19}F NMR (376 MHz, $CDCl_3$) δ -153.48 – -153.57 (m), -163.42 – -163.52 (m). MS (EI 70eV) *m/z* = 242 (40%, M^+-18)

5,6,7,8-tetrafluoronaphthalene-2,3-dicarbaldehyde (107)

To a flame dried 500 ml round bottom flask equipped with a dropping funnel was added 60 ml of DCM follwed by 4.7 ml (53.23 mmol) of oxalyl chloride under nitrogen. The resulting solution was cooled to -78˚C using a dry ice bath. 7.6 ml (106.46 mmol) of DMSO dissolved in 15 ml of DCM was added dropwise to the stirring solution of oxalyl chloride in DCM. The solution was stirred for 15 minutes and 5.54 g (21.3 mmol) of diol dissolved in 10 ml of DMSO was added dropwise with stirrring. After addition is complete the reaction mixture was allowed to stir for 2h. 53 ml (378 mmol) of triethylamine was slowly added to the reaction mixture at -78˚C and was allowed to slowly warm up to room temperature overnight. The next day reaction mixture was poured into ice cold water, extracted into DCM (3x250 ml) and finally was washed with water (4x300 ml). The solvent was removed under reduced pressure to give crude dialdehyde which was further purified by silica gel chromatography using straight DCM to give pure dialdehyde as a light golden yellow solid (4.64 g, 85%).

^{1}H NMR (400 MHz, $CDCl_3$) δ 10.63 (s, 1H), 8.69 (s, 1H). ^{19}F NMR (376 MHz, $CDCl_3$) δ -148.21 – -148.29 (m), -153.76 – -153.84 (m). MS (EI 70eV) *m/z* = 256 (37%, M^+)

1,2,3,4-tetrafluorohexacene-6, 15 -dione (108)

To a 250 ml round bottom flask equipped with a stir bar were added 620 mg (2.2 mmol) of naphthalene-2,3-dicarbaldehyde (**90**) and 445 mg (2.4 mmol) of 5,6,7,8-tetrafluoro-1,4-dihydroxyanthracene (**103**). The mixture was then dissolved in minimal amount of 1:1 ethanol/THF. Drops of 15% aqueous NaOH solution was added to the stirring mixture until there was any observable precipitate formation and the thick slurry was allowed to stir for 30 minutes. 50 ml of methanol was added to the reaction mixture and the precipitates were filtered

through a Büchner funnel, washed with methanol followed by THF and finally with ether to give a yellow solid. Yield – 700 mg, 70%. MS (EI, 70 eV) *m/z* = 430 (100%, M^+)

General procedure for the synthesis of 6,15-Trialkylsilylethynylated-1,2,3,4-tetrafluorohexacenes

To a flame dried 100 ml flask cooled under nitrogen was added 4.65 mmol of acetylene, followed by 5 ml of hexanes. The reaction mixture was then placed in an ice bath. 1.7 ml of n-BuLi (4.18 mmol, 2.5 M solution in hexanes) was added dropwise and the reaction mixture stirred at 0 ºC for an hour. 13 ml of hexanes was added followed by 2 ml of anhydrous THF. 500 mg (1.16 mmol) of powdered 1,2,3,4-tetrafluorohexacene-6,15-dione (**108**) was then added and the reaction mixture was allowed to stir overnight. The reaction mixture was quenched with saturated NH_4Cl solution and extracted into ether. The combined ether layers were washed with water and dried over anhydrous $MgSO_4$. The excess acetylene was recovered from the crude product by elution through a pad of silica gel initially with hexanes. The crude diol was obtained as a mixture of *syn* and *anti* isomers by slowly increasing the ratio of hexanes:DCM to 7:3. To a 50 ml round bottom flask equipped with a magnetic stir bar were added 250 mg of crude diol, 20 ml of THF. Nitrogen gas was bubbled through the solution for 30 min. 2 ml of 10% aqueous HCl was added followed by 3 g of $SnCl_2 \bullet 2H_2O$ and the reaction mixture was placed in an oil bath maintained at 50˚C. The reaction was followed by TLC by monitoring the disappearance of diol. Fluorinated hexacene precipitates as crystalline solid during the course of the reaction. The precipitated solids were filtered and washed with 50 ml of 1:1 THF/acetone mixture followed by plenty of methanol. Finally the solids were washed with acetone followed by 15 ml of hexanes to give crystalline dark green powder.

6,15-bis(triisobutylsilylethynyl)-1,2,3,4-tetrafluorohexacene (120) - 163 mg (68%). The hexacene was further purified by recrystallization in hexanes/DCM. ^{1}H NMR (400 MHz, $CDCl_3$) δ 9.57 (s, 2H), 9.41 (s, 2H), 8.62 (s, 2H), 7.95 (dd, *J* = 6.7, 3.1 Hz, 2H), 7.36 (dd, *J* = 6.8, 3.0 Hz, 2H), 2.28 – 2.15 (m, 6H), 1.22 (d, *J* = 6.6 Hz, 36H), 1.00 (d, *J* = 7.0 Hz, 12H). ^{19}F NMR (376 MHz, $CDCl_3$) δ -153.25 – -153.35 (m), -161.32 – -161.41 (m). MS (LDI) *m/z* = 844.45 (100%, M^+)

6,15-bis(tricyclopentylsilylethynyl)-1,2,3,4-tetrafluorohexacene (121) - 186 mg (77%). The hexacene was further purified by recrystallization in hexanes/DCM. ^{1}H NMR (400 MHz, $CDCl_3$) δ 9.56 (s, 2H), 9.43 (s, 2H), 8.61 (s, 2H), 7.96 (dd, *J* = 6.6, 2.1 Hz, 2H), 7.39 – 7.34 (m, 2H), 2.18 – 2.01 (m, 12H), 1.91 – 1.72 (m, 24H), 1.73 – 1.59 (m, 12H), 1.45 – 1.30 (m, 6H). ^{19}F NMR (376 MHz, $CDCl_3$) δ -153.41 – -153.52 (m), -161.33 – -161.43 (m). MS (LDI) *m/z* = 916.45 (100%, M^+)

6,15-bis(tricyclohexylsilylethynyl)-1,2,3,4-tetrafluorohexacene (122) - 183 mg (75%). The hexacene was further purified by recrystallization in hexanes/DCM. ^{1}H NMR (400 MHz, $CDCl_3$) δ 9.62 (s, 2H), 9.47 (s, 2H), 8.62 (s, 2H), 7.95 (dd, *J* = 6.4, 2.8 Hz, 2H), 7.37 (dd, *J* = 6.5, 2.4 Hz, 2H), 2.12 (d, *J* = 12.8 Hz, 12H), 2.00 – 1.77 (m, 18H), 1.58 – 1.73 (m, 12H), 1.49 – 1.3 (m, 18H), 1.25 (t, *J* = 12.7 Hz, 6H). ^{19}F NMR (376 MHz, $CDCl_3$) δ -153.51 – -153.65 (m), -161.26 – -161.41 (m). MS (LDI) *m/z* = 1000.54 (100%, M^+)

Note: The conversion of the intermediate diol to final hexacene was done in the dark. Solvents were degassed with nitrogen prior to use for recrystallization.

1,2,3,4-tetrafluorohexacene-7, 14-dione (109)

To a 250 ml round bottom flask equipped with a stir bar were added 250 mg (0.98mmol) of 5,6,7,8-tetrafluoronaphthalene-2,3-dicarbaldehyde (**107**) and 226 mg (1.07 mmol) of 1,4-dihydroxyanthracene (**89**). The mixture was then dissolved in minimal amount of 1:1 ethanol/THF. Drops of 15% aqueous NaOH solution was added to the stirring mixture until there was any observable precipitate formation and the thick slurry was allowed to stir for 30 minutes. 50 ml of methanol was added to the reaction mixture and the precipitates were filtered through a Büchner funnel, washed with methanol followed by THF and finally with ether to give a yellow solid. Yield – 315 mg, 75%. MS (EI, 70 eV) *m/z* = 430 (100%, M^+)

General procedure for the synthesis of 7,14-Trialkylsilylethynylated-1,2,3,4-tetrafluorohexacenes

To a flame dried 100 ml flask cooled under nitrogen was added 4.65 mmol of acetylene, followed by 5 ml of hexanes. The reaction mixture was then placed in an ice bath. 1.7 ml of n-BuLi (4.18 mmol, 2.5 M solution in hexanes) was added dropwise and the reaction mixture stirred at 0 ºC for an hour. 13 ml of hexanes was added followed by 2 ml of anhydrous THF. 500 mg (1.16 mmol) of powdered 1,2,3,4-tetrafluorohexacene-7,14-dione (**109**) was then added to the reaction mixture. After 3h another 2 ml of anhydrous THF was added and allowed to stir overnight. The reaction mixture was quenched with saturated NH_4Cl solution and extracted into ether. The combined ether layers were washed with water and dried over anhydrous $MgSO_4$. The excess acetylene was recovered from the crude product by elution through a pad of silica gel initially with hexanes. The crude diol was obtained as a mixture of *syn* and *anti* isomers by slowly increasing the ratio of hexanes:DCM to 7:3. To a 50 ml round bottom flask equipped with

a magnetic stir bar were added 250 mg of crude diol, 20 ml of THF. Nitrogen gas was bubbled through the solution for 30 min. 2 ml of 10% aqueous HCl was added followed by 3 g of $SnCl_2 \bullet 2H_2O$ and the reaction mixture was placed in an oil bath maintained at 50˚C. The reaction was followed by TLC by monitoring the disappearance of diol. Fluorinated hexacene precipitates as crystalline solid during the course of the reaction. The precipitated solids were filtered and washed with 50 ml of 1:1 THF/acetone mixture followed by plenty of methanol. Finally the solids were washed with acetone followed by 15 ml of hexanes to give crystalline green powder.

7,14-bis(triisobutylsilylethynyl)-1,2,3,4-tetrafluorohexacene (123) - 168 mg (70%). The hexacene was further purified by recrystallization in hexanes/DCM. ^{1}H NMR (400 MHz, $CDCl_3$) δ 9.54 (s, 1H), 9.19 (s, 2H), 8.73 (s, 2H), 7.93 (dd, *J* = 6.6, 3.2 Hz, 2H), 7.41 (dd, *J* = 6.7, 3.0 Hz, 2H), 2.24 (dhept, *J* = 13.2, 6.5 Hz, 6H), 1.23 (d, *J* = 6.6 Hz, 36H), 1.02 (d, *J* = 6.9 Hz, 12H). ^{19}F NMR (376 MHz, $CDCl_3$) δ -153.93 – -154.06 (m), -162.02 – -162.11 (m). MS (LDI) *m/z* = 844.45 (100%, M^+)

7,14-bis(tricyclopentylsilylethynyl)-1,2,3,4-tetrafluorohexacene (124) - 173 mg (72%). The hexacene was further purified by recrystallization in hexanes/DCM. ^{1}H NMR (400 MHz, $CDCl_3$) δ 9.59 (s, 1H), 9.21 (s, 2H), 8.77 (s, 2H), 7.92 (dd, *J* = 6.5, 2.3 Hz, 2H), 7.41 (dd, *J* = 6.3, 2.4 Hz, 2H), 2.17 – 2.04 (m, 12H), 1.91 – 1.73 (m, 24H), 1.73 – 1.60 (m, 12H), 1.46 – 1.32 (m, 6H). ^{19}F NMR (376 MHz, $CDCl_3$) δ -153.88 – -154.00 (m), -162.05 – -162.13 (m). MS (LDI) *m/z* = 916.45 (100%, M^+)

7,14-bis(tricyclohexylsilylethynyl)-1,2,3,4-tetrafluorohexacene (125) - 183 mg (76%). The hexacene was further purified by recrystallization in hexanes/DCM. ^{1}H NMR (400 MHz, $CDCl_3$) δ 9.65 (s, 2H), 9.25 (s, 2H), 8.79 (s, 2H), 7.94 (dd, *J* = 6.6, 3.2 Hz, 2H), 7.42 (dd, *J* = 6.7, 3.0 Hz,

2H), 2.13 (d, *J* = 12.9 Hz, 12H), 1.96 – 1.79 (m, 18H), 1.72 – 1.58 (m, 12H), 1.48 – 1.31 (m, 18H), 1.25 (tt, *J* = 12.8, 2.8 Hz, 6H). ^{19}F NMR (376 MHz, $CDCl_3$) δ -153.93 – -154.06 (m), -162.04 – -162.13 (m). MS (LDI) *m/z* = 1000.54 (100%, M^+)

Note: The conversion of the intermediate diol to final hexacene was done in the dark. Solvents were degassed with nitrogen prior to use for recrystallization.

1,2,3,4,9,10,11,12-octafluorohexacene-6, 15-dione (110)

To a 250 ml round bottom flask equipped with a stir bar were added 227 mg (0.88 mmol) of 5,6,7,8-tetrafluoronaphthalene-2,3-dicarbaldehyde (**107**) and 250 mg (0.88 mmol) of 5,6,7,8-tetrafluoro-1,4-dihydroxyanthracene (**103**). The mixture was then dissolved in minimal amount of 1:1 ethanol/THF. Drops of 15% aqueous NaOH solution was added to the stirring mixture until there was any observable precipitate formation and the thick slurry was allowed to stir for 30 minutes. 50 ml of methanol was added to the reaction mixture and the precipitates were filtered through a Büchner funnel, washed with methanol followed by THF and finally with ether to give a light brown solid. Yield – 350 mg, 78%. MS (EI, 70 eV) *m/z* = 502 (100%, M^+)

General procedure for the synthesis of 6,15-Trialkylsilylethynylated-1,2,3,4,9,10,11,12-octafluorohexacenes

To a flame dried 100 ml flask cooled under nitrogen was added 7.96 mmol of acetylene, followed by 5 ml of hexanes. The reaction mixture was then placed in an ice bath. 2.9 ml of n-BuLi (7.25 mmol, 2.5 M solution in hexanes) was added dropwise and the reaction mixture stirred at 0 ºC for an hour. 13 ml of hexanes was added followed by 2 ml of anhydrous THF. 1 g (1.99 mmol) of pulverized 1,2,3,4,9,10,11,12-octafluorohexacene-6,15-dione (**110**) was then added to the reaction mixture. After 3 h another 2 ml of anhydrous THF was added and allowed

to stir overnight. The reaction mixture was quenched with saturated NH_4Cl solution and extracted into ether. The combined ether layers were washed with water and dried over anhydrous $MgSO_4$. The excess acetylene was recovered from the crude product by elution through a pad of silica gel initially with hexanes. The crude diol was obtained as a mixture of *syn* and *anti* isomers by slowly increasing the ratio of hexanes:DCM to 7:3. To a 50 ml round bottom flask equipped with a magnetic stir bar were added 250 mg of crude diol, 20 ml of THF. Nitrogen gas was bubbled through the solution for 30 min. 2 ml of 10% aqueous HCl was added followed by 3 g of $SnCl_2 \bullet 2H_2O$ and the reaction mixture was placed in an oil bath maintained at 50˚C. The reaction was followed by TLC by monitoring the disappearance of diol. Fluorinated hexacene precipitates as crystalline solid during the course of the reaction. The precipitated solids were filtered and washed with 50 ml of 1:1 THF/acetone mixture followed by plenty of methanol. Finally the solids were washed with acetone followed by 15 ml of hexanes to give crystalline green powder.

6,15-bis(triisobutylsilylethynyl)-1,2,3,4,9,10,11,12-octafluorohexacene (126) - 125 mg (52%). The hexacene was further purified by recrystallization in hexanes/DCM. ^{1}H NMR (400 MHz, $CDCl_3$) δ 9.56 (s, 2H), 9.41 (s, 2H), 8.75 (s, 2H), 2.28 – 2.16 (m, 6H), 1.22 (dd, J = 6.6, 1.3 Hz, 36H), 1.01 (dd, J = 7.0, 1.2 Hz, 12H). ^{19}F NMR (376 MHz, $CDCl_3$) δ -152.97 – -153.05 (m), -153.62 – -153.71 (m), -160.44 – -160.52 (m), -161.21 – -161.29 (m). MS (LDI) *m/z* = 916.41 (100%, M^+)

6,15-bis(tricyclopentylsilylethynyl)-1,2,3,4,9,10,12-octafluorohexacene (127) - 168 mg (69%). The hexacene was further purified by recrystallization in hexanes/toluene. ^{1}H NMR (400 MHz, $CDCl_3$) δ 9.55 (s, 2H), 9.43 (s, 2H), 8.74 (s, 2H), 2.16 – 2.04 (m, 12H), 1.87 – 1.73 (m, 24H), 1.73 – 1.60 (m, 12H), 1.45 – 1.33(m, 6H). ^{19}F NMR (376 MHz, $CDCl_3$) δ -153.14 – -153.22 (m),

-153.57 – -153.65 (m), -160.47 – -160.55 (m), -161.22 – -161.31 (m). MS (LDI) *m/z* = 988.41 (100%, M^+)

6,15-bis(tricyclohexylsilylethynyl)-1,2,3,4,9,10,11,12-octafluorohexacene (128) - 169 mg (70%). The hexacene was further purified by recrystallization in hexanes/toluene. ^{1}H NMR (400 MHz, $CDCl_3$) δ 9.66 (s, 2H), 9.48 (s, 2H), 2.10 (d, *J* = 12.6 Hz, 12H), 1.93 – 1.8 (m, 18H), 1.7 – 1.56 (m, 12H), 1.46 – 1.31 (m, 18H), 1.24 (tt, *J* = 12.8, 2.9 Hz, 6H). ^{19}F NMR (376 MHz, $CDCl_3$) δ -153.25 – -153.35 (m), -153.66 – -153.77 (m), -160.45 – -160.55 (m), -161.18 – -161.32 (m). MS (LDI) *m/z* = 1072.5 (100%, M^+)

Note: The conversion of the intermediate diol to final hexacene was done in the dark. Solvents were degassed with nitrogen prior to use for recrystallization.

Dimethyl 5,6,7,8-tetrachloronaphthalene-2,3-dicarboxylate (129)

To a 350 ml sealed tube equipped with a magnetic stir bar were added 15.1 g (37.58 mmol) of **75**, 10.7 g (89.3 mmol) of dimethyl acetylene dicarboxylate (**104**). 124 ml of degassed DMA was added followed by 16.56 g of KI. The reaction mixture was heated to 70˚C and allowed to stir for 24h. 19 g of sodium bisulfite was dissolved in 1240 ml of water in a 2000 ml Erlenmeyer flask. The hot reaction mixture was poured into the stirring sodium bisulfite solution and allowed to stir for 30 min. The precipitate was filtered, washed with plenty of water and air dried to give the crude product. Purification by silica gel chromatography using 1:1 hexanes/DCM gave the pure product in 76% yield (11 g).

^{1}H NMR (400 MHz, $CDCl_3$) δ 8.60 (s, 1H), 3.99 (s, 1H). ^{13}C NMR (100 MHz, $CDCl_3$) δ 167.09, 133.10, 132.55, 131.42, 130.48, 127.62, 53.30. MS (EI 70eV) *m/z* = 382 (33%, M^+), 380 (35%, M^+-2)

2,3-dimethanol-5,6,7,8-tetrachloronaphthalene(130)

14.4 g (37.7 mmol) of the dimethyl ester (**129**) was added to a flame dried, N_2 cooled 500 ml RB flask. 100 ml of DCM was added and the flask was cooled to 0˚C using ice water bath. 158 ml of 1M solution of DIBALH in hexanes was added drop wise and the reaction mixture was allowed stir overnight. The reaction mixture was quenched by adding a saturated solution of NH_4Cl with cooling. The precipitated aluminum salts were filtered off and the filtrate is concentrated to give the diol dissolved in solution. The precipitates were heated to reflux in 500 ml of ethyl acetate for an hour and the precipitates were filtered off, washed with ethyl acetate and the filtrate was saved. The process was repeated couple of times and the filtrate were combined together and solvent was removed to give white solid (10.2 g, 83%).

^{1}H NMR (400 MHz, DMSO) δ 8.20 (s, 2H), 5.58 (t, *J*=5.2 Hz, 2H), 4.7 (d, *J*=5.2 Hz, 4H). ^{13}C NMR (100 MHz, DMSO) δ 142.01, 129.18, 128.11, 127.73, 121.10, 59.63. MS (EI 70eV) *m/z* = 308 (33%, M^+-18)

5,6,7,8-tetrachloronaphthalene-2,3-dicarbaldehyde (131)

To a flame dried 250 ml round bottom flask equipped with a dropping funnel was added 25 ml of DCM followed by 2 ml (23 mmol) of oxalyl chloride under nitrogen. The resulting solution was cooled to -78˚C using a dry ice bath. 3.3 ml (46 mmol) of DMSO dissolved in 6.6 ml of DCM was added dropwise to the stirring solution of oxalyl chloride in DCM. The solution was stirred for 15 minutes and 2.5 g (7.67 mmol) of diol dissolved in 10 ml of DMSO was added dropwise with stirring. After addition is complete the reaction mixture was allowed to stir for 1h. 19 ml (136 mmol) of triethylamine was slowly added to the reaction mixture at -78˚C and was allowed to slowly warm up to room temperature overnight. The next day reaction mixture was poured into ice cold water, extracted into DCM (3x200 ml) and finally was washed with water (4x200

ml). The solvent was removed under reduced pressure to give crude dialdehyde which was further purified by silica gel chromatography using straight DCM to give pure dialdehyde as off-white solid (2.1 g, 85%).

^{1}H NMR (400 MHz, $CDCl_3$) δ 10.64 (s, 1H), 8.81 (s, 1H). ^{13}C NMR (100 MHz, $CDCl_3$) δ 191.46, 134.87, 134.57, 134.21, 132.06, 131.49. MS (EI 70eV) *m/z* = 322 (43%, M^+)

1,2,3,4-tetrachlorohexacene-7, 14-dione (132)

To a 250 ml round bottom flask equipped with a stir bar were added 1.5 g (0.98 mmol) of 5,6,7,8-tetrachloronaphthalene-2,3-dicarbaldehyde (**131**) and 1.08 g (1.07 mmol) of 1,4-dihydroxyanthracene (**89**). The mixture was then dissolved in minimal amount of 1:1 ethanol/THF. Drops of 15% aqueous NaOH solution was added to the stirring mixture until there was any observable precipitate formation and the thick slurry was allowed to stir for 30 minutes. 50 ml of methanol was added to the reaction mixture and the precipitates were filtered through a Büchner funnel, washed with methanol followed by THF and finally with ether to give a brownish yellow solid. Yield – 2.02 g, 87%. MS (EI, 70 eV) *m/z* = 496 (100%, M^+)

7,14-bis(tricyclopentylsilylethynyl)-1,2,3,4-tetrachlorohexacene (134)

To a flame dried 100 ml flask cooled under nitrogen was added 2.1 g (8.06 mmol) of tricyclopentylsilyl acetylene, followed by 5 ml of hexanes. The reaction mixture was then placed in an ice bath. 2.9 ml of n-BuLi (7.25 mmol, 2.5 M solution in hexanes) was added dropwise and the reaction mixture stirred at 0 ºC for an hour. 13 ml of hexanes was added followed by 2 ml of anhydrous THF. 1 g (2.01 mmol) of powdered 1,2,3,4-tetrachlorohexacene-7,14-dione (**132**) was then added to the reaction mixture. After an hour another 2 ml of anhydrous THF was added and allowed to stir overnight. The reaction mixture was quenched with saturated NH_4Cl solution and

extracted into ether. The combined ether layers were washed with water and dried over anhydrous $MgSO_4$. The excess acetylene was recovered from the crude product by elution through a pad of silica gel initially with hexanes. The crude diol was obtained as a mixture of *syn* and *anti* isomers by slowly increasing the ratio of hexanes:DCM to 7:3. To a 50 ml round bottom flask equipped with a magnetic stir bar were added 250 mg of crude diol, 20 ml of THF. Nitrogen gas was bubbled through the solution for 30 min. 2 ml of 10% aqueous HCl was added followed by 5 g of $SnCl_2 \bullet 2H_2O$ and the reaction mixture was placed in an oil bath maintained at 60˚C. The reaction was followed by TLC by monitoring the disappearance of diol. Chlorinated hexacene precipitates as a solid during the course of the reaction. The precipitated solids were filtered and washed with 50 ml of 1:1 THF/acetone mixture followed by plenty of methanol. Finally the solids were washed with acetone followed by 15 ml of hexanes to give green powder. (Poor solubility in solvents prevented NMR characterization)

MS (MALDI, DHB matrix) *m/z* = 982.33 (100%, M^+)

Note: The conversion of the intermediate diol to final hexacene was done in the dark. Solvents were degassed with nitrogen prior to use for recrystallization.

Chapter 4: Towards Stable Higher Acenes – Heptacene and Nonacene

4.1 Higher Acenes

The high mobility associated with pentacene has generated great interest in higher analogs of the acene family. While synthesis of larger acenes by conventional methods has been hampered due to its high reactivity in solution and solid state, several theoretical studies have been performed to understand its reactivity[156,157] and electronic properties. [158-162,169] Houk et al. predicted a triplet ground state for acenes larger than octacene using unrestricted B3LYP (UB3LYP) calculations.[169] In 2004, Bendikov et al. predicted that acenes larger than hexacene exist in the ground state as a singlet diradical.[158] Recent theoretical studies based on the density matrix renormalization group method have shown that higher acenes exist as an open shell singlet in the ground state.[159,169] The predicted radical nature of these molecules explains their high susceptibility to photooxidation and dimerization.

Synthesis of heptacene (**20**) was first reported by Clar in 1942,[153] and later by Bailey et al. in 1955.[150] However their claims have come under scrutiny due to poor reproducibility and lack of characterization of the final heptacene. The high reactivity of heptacene has made its synthesis essentially impossible by conventional methods. After nearly six decades Neckers et al. synthesized heptacene (**20**) by photobisdecarbonylation of diketone precursor (**19**) in PMMA matrix where the photooxidation of acenes can be retarded (Figure 1.10).[75] In 2005 Anthony et al. successfully extended their perifunctionalization approach to heptacene.[77] In order to stabilize these highly reactive materials, a significantly bulkier tris(trimethylsilyl)silylethynyl (TTMSS) substituent had to be used to prevent Diels-Alder reaction between the alkyne substituent of one molecule and the reactive heptacene chromophore of another.[79] The improved solubility of this

heptacene derivative enabled the slow growth of single crystals from solution which were characterized by single crystal X-ray diffraction. Unlike unfunctionalized heptacene, TTMS heptacene (**22**) was also characterized by both ^{1}H and ^{13}C NMR spectroscopy. TTMSS heptacene (**22**) decomposes rapidly in solution; however the crystalline solids were stable for a prolonged period of time on exposure to light and air. In a recent report, Wudl and co-workers have reported the synthesis of a stable tetraphenyl heptacene derivative (**23**) using a tri-*iso*-propylsilylethynyl substituent.[78] The phenyl groups are effective in preventing the aromatic cores from reacting with each other or with the alkyne, and as a result the smaller alkyne substituent could be used. These molecules exhibited no π-stacking between the heptacene cores in the solid state and decomposed by successive photooxidation of the heptacene chromophore. In 2009 Miller et al. reported the synthesis of *o*-dimethylphenyl heptacene (**135**) functionalized at the reactive C7 and C16 positions with thioaryl substituents (Figure 4.1(a)).[163] The authors claimed

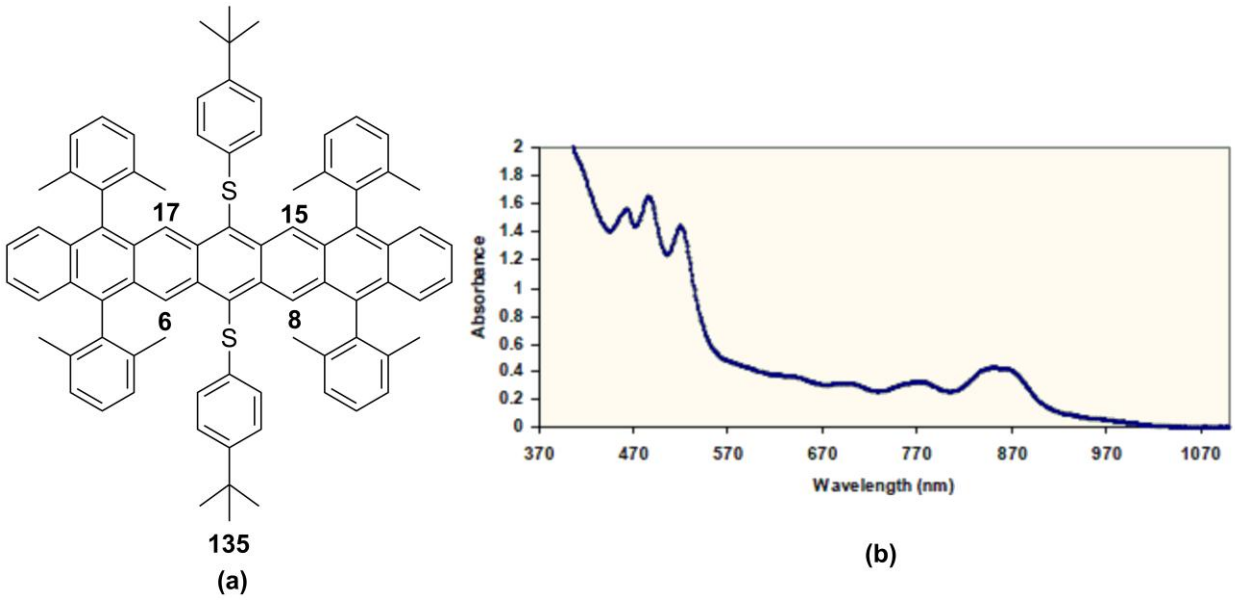

Figure 4.1 Thioaryl substituted heptacene (Miller et al. JACS 2009 ©)[163]

that the thioaryl substituents were used to increase the photooxidative stability of these acenes. However the UV-visble-NIR spectra of freshly prepared solution of heptacene (**135)** shows

absorption characteristic of heptacene along with absorptions at ~ 550 nm characteristic of a tetracene chromophore formed as a result of either photodimerization or photooxidation of the heptacene core (Figure 4.1(b)).

4.2 Partially Fluorinated Trialkylsilylethynyl Heptacene

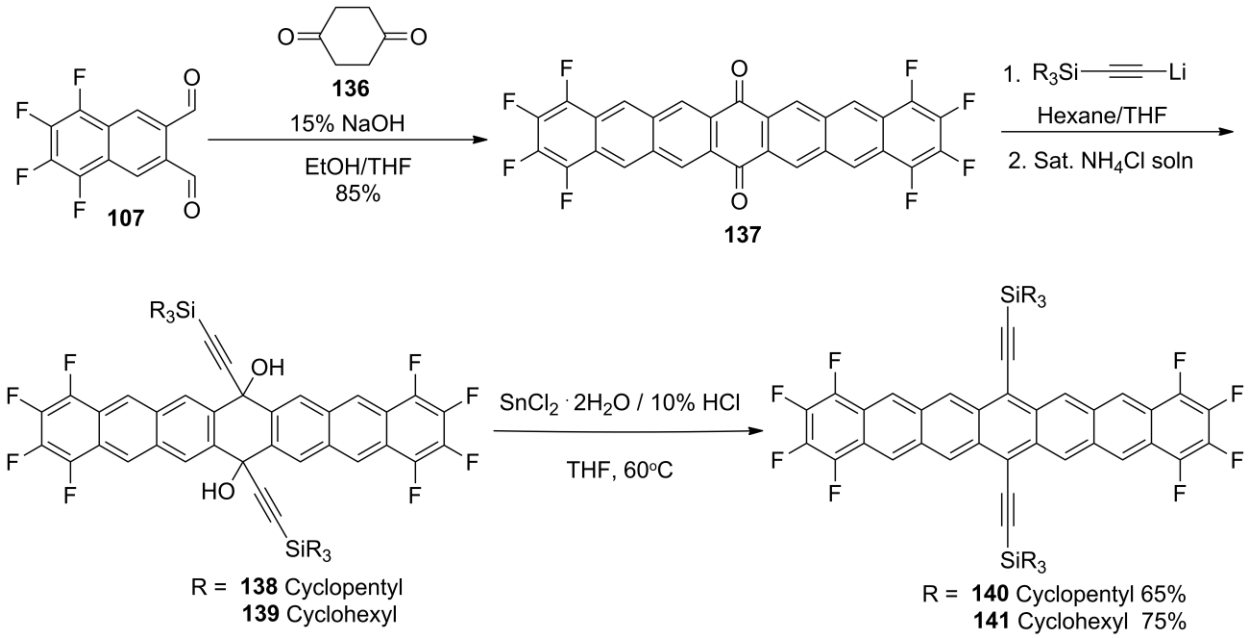

Scheme 4.1 Synthesis of trialkylsilylethynylated octafluoroheptacene

While progress has been made to stabilize these molecules, they are not yet stable enough for device application. Similar to my approach of improving the stability of hexacenes by partial fluorination I decided to enhance the stability of reactive heptacene by partial fluorination of the heptacene chromophore. Since F_8 hexacene gave the highest stability I decided to synthesize trialkylsilylethynyl substituted F_8 heptacene. Soluble trialkylsilylethynylated F_8 heptacenes were synthesized according to scheme 4.1. 1,2,3,4,10,11,12,13-heptacene-7,16-dione (**137**) was synthesized by Aldol condensation between cyclohexane-1,4-dione (**136**) and 5,6,7,8-tetrafluoronaphthalene-2,3-dicarbaldehyde (**107**). The quinone was converted into series of diethynyl diols by treatment with excess acetylide. Tricyclopentylsilylethynyl (TCPS) and

tricyclohexylsilylethynyl (TCHS) substituents were used to tune the solubility. Treatment of the resulting diols with a saturated solution of tin (II) chloride in 10% HCl gave desired heptacenes. Similar to F_4 & F_8 hexacenes the heptacene derivatives crashed out as crystalline solids. Attempts to recrystallize the heptacene failed due to poor solubility of TCPS (**140**) and TCHS F_8 heptacene (**141**).

In order to compare the relative solution stabilities between the different partially fluorinated heptacene derivatives UV-vis solution stability studies were done under the same conditions used for partially fluorinated hexacene. Disappearance of the long-wavelength heptacene absorptions is coupled with the appearance of a strong absorption at ~550 nm, characteristic of a tetracene chromophore (Figure 4.2). All partially fluorinated heptacene derivatives exhibited improved solution stabilities; with heptacene derivatives having bulky silyl substituents exhibiting the better solution stabilities (Table 4.1). In order to compare the stabilities of the new F_8 heptacene derivatives with the nonfluorinated heptacene, TCHS heptacene (**144**) was synthesized according to scheme 4.2 and subjected to UV-vis stability studies. TCHS F_8 heptacene (**141**) exhibited a threefold increase in solution stability in comparison to nonfluorinated TCHS heptacene (**144**) (Table 4.1). This is due to fact that fluorine substitution closer to the reactive inner rings lowers the electron density at the reactive C6, C8, C15 and C17 atoms of the heptacene chromophore thereby reducing their tendency to dimerize. Although fluorination of the heptacene chromophore resulted in improved stability, they exhibited poor solubility in common organic solvents preventing their study in thin film devices.

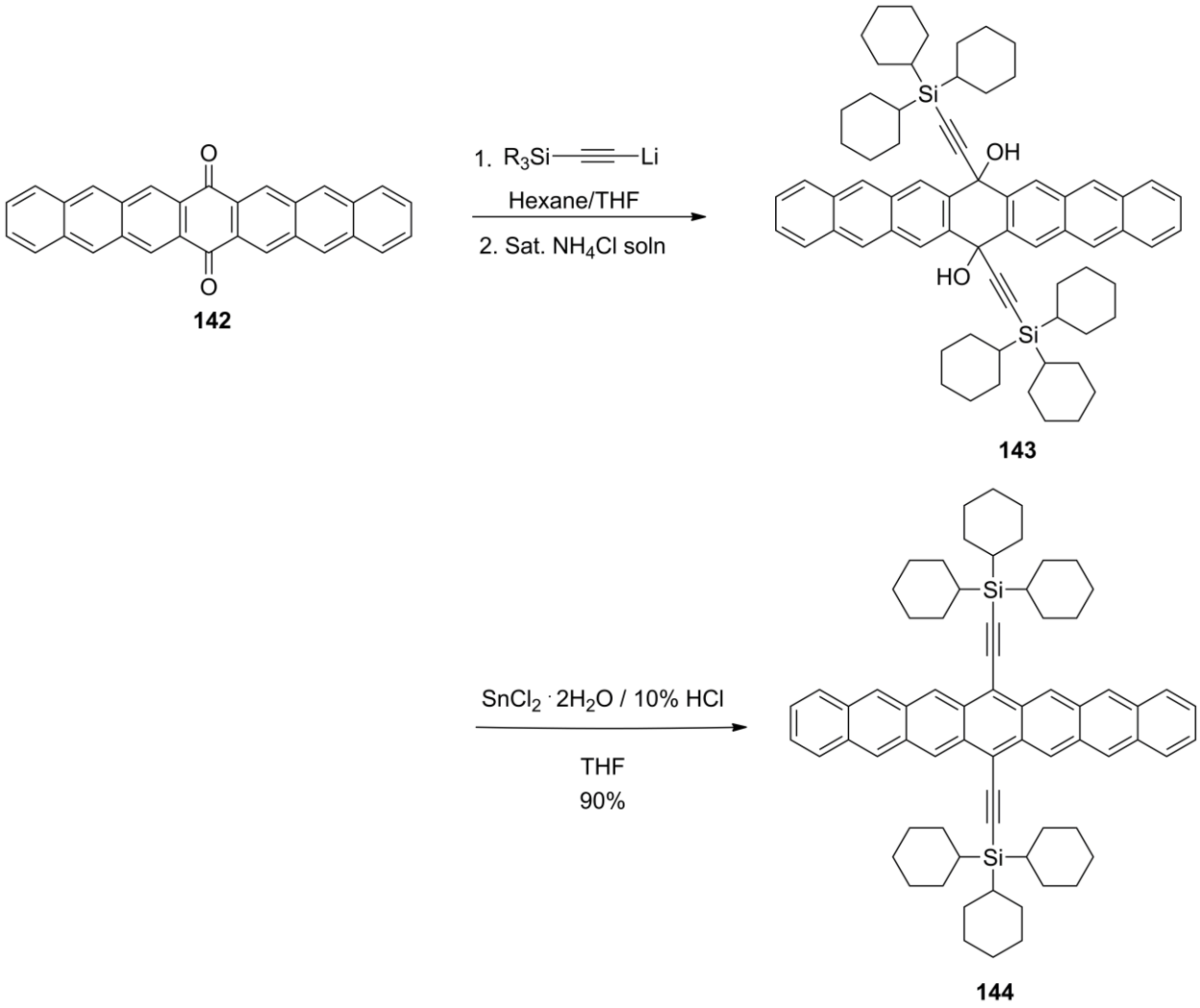

Scheme 4.2 Synthesis of TCHS Heptacene (146)

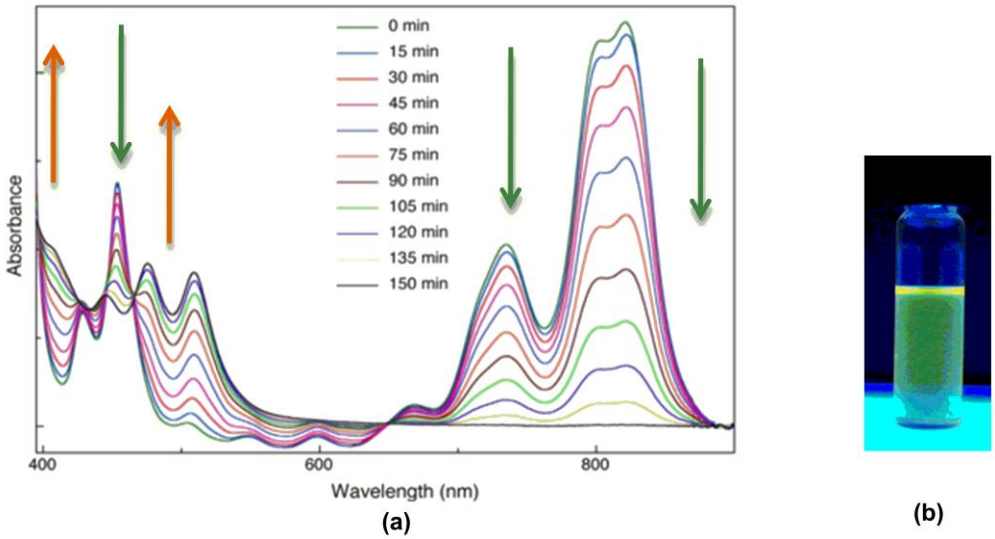

Figure 4.2 (a) UV-vis stability study of TCHS F_8 Heptacene (b) Decomposition product under short wave length UV light

Table 4.1 Solution half-life of new heptacene derivatives

Acene	$t_{1/2}$ (min)
TCPS F_8 Heptacene (140)	81
TCHS F_8 Heptacene (141)	88
TCHS Heptacene (144)	30

4.3 Nonacene

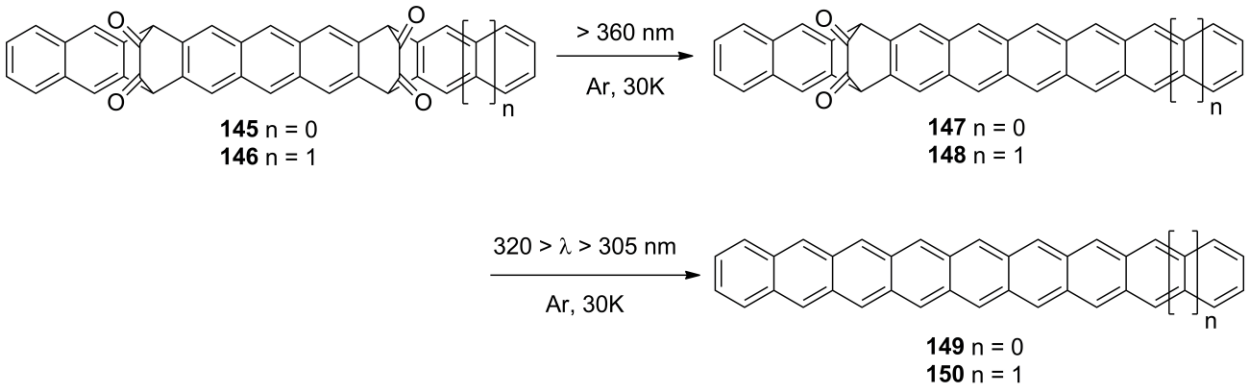

Figure 4.3 Synthesis of octacene and nonacene by photodecarbonylation (Bettinger et al. Angew. Chem. Int. Edn 2010)[76]

Acenes larger than heptacene have been unknown until 2010, when Bettinger et al. successfully extended the photodecarbonylation approach to octacene and nonacene (Figure 4.3).[76] In order to improve the solubility of the octacene and nonacene precursors the authors synthesized tetraketone precursors which were then converted into the final acene in solid argon matrix at 30K by stepwise photobisdecarbonylation. These higher acenes were stable enough for short period of time to be probed by UV-visible-NIR spectroscopy. In a recent report Miller et al. claimed to have synthesized the first stable nonacene derivative functionalized with both arylthio and aryl substituents (Figure 4.4(a)).[170] The nonacene derivative (**151**) was obtained as a black powder and exhibited a blood red fluorescence in solution. Similar to heptacenes and hexacenes

these reactive acenes were assumed to decompose by photooxidation into products with smaller acene chromophore.

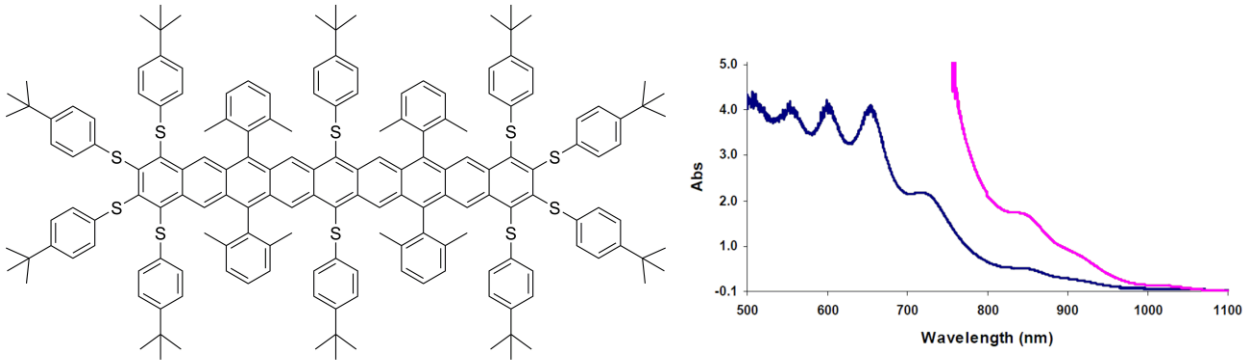

Figure 4.4 (a) Thioaryl functionalized nonacene (151) (b) Visible-NIR spectra of Nonacene (151) (Miller et al. JACS 2010 ©)[170]

In order to support their claim the authors characterized their nonacene derivative with both NMR and Visible-NIR spectroscopy along with mass spectral data. Based on my experience with trialylsilyethynylated hexacene, mass spectra of the dimers usually show the molecular ion peak of the monomers and are not a reliable tool to characterize higher acenes. Another important observation is that oxidation or dimerization of nonacene (**151**) should give a decomposition product with pentacene chromophore which usually exhibits a blood red fluorescence. Visible-NIR spectra of nonacene (**151**) show strong absorptions characteristic of pentacene chromophore along with weak absorptions in NIR region of the spectra characteristic of nonacene (Figure 4.4). These observations raise serious questions about the author's claims of stability and purity of the new nonacene derivative.

4.4 Partially Halogenated Nonacene

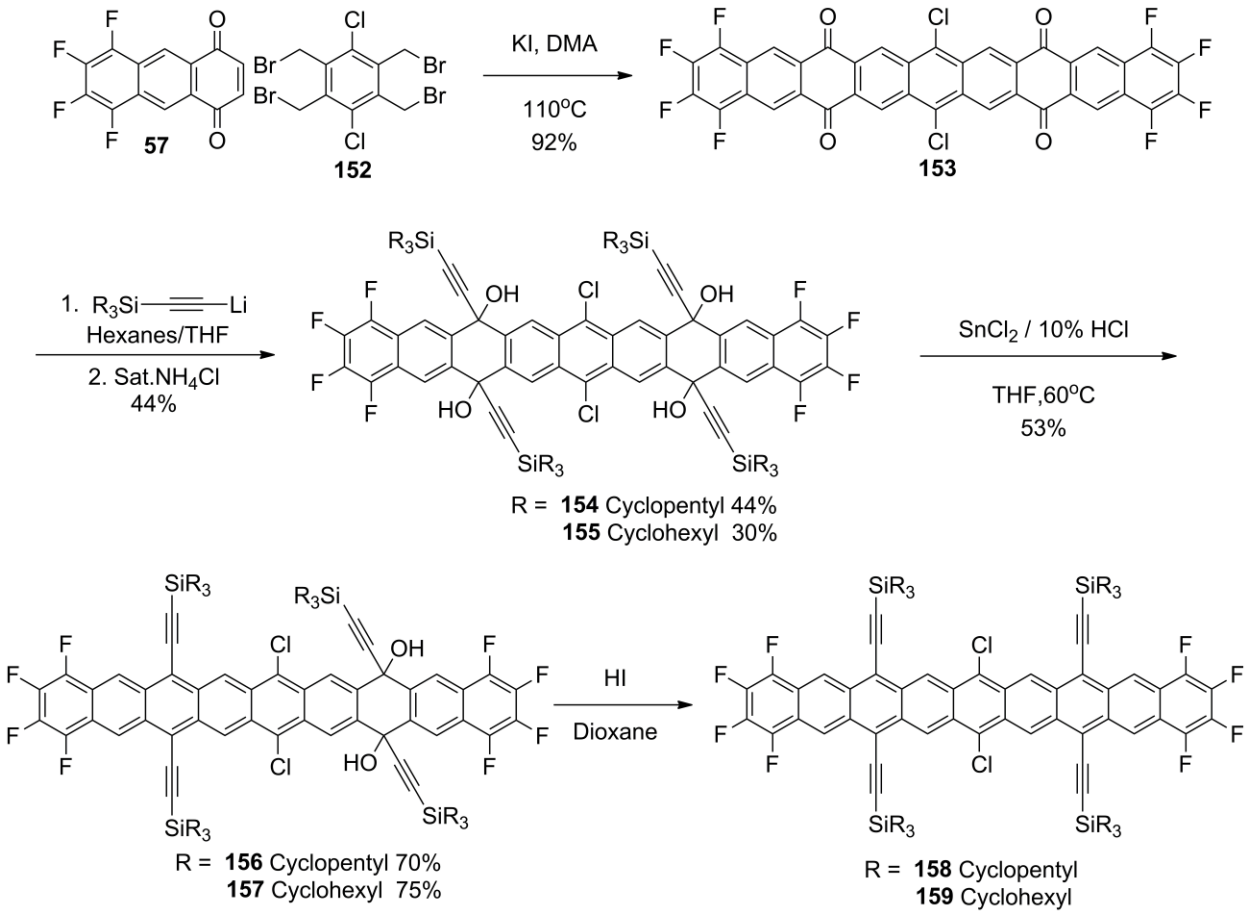

Scheme 4.3 Synthesis of partially halogenated nonacene

In order to study the reactivity of nonacene and to compare with the published visible-NIR spectra of "nonacene", I decided to apply my partial halogenation approach to stabilize nonacene. Partially halogenated nonacene derivatives were synthesized according to scheme 4.3. In order to improve the solubility of the nonacene I decided to synthesize the tetraethynylated nonacene derivative. Dichlorooctafluoro nonacenetetraone (**153**) was synthesized by Cava reaction between 1,2,4,5-tetrakis(bromomethyl)-3,6-dichlorobenzene (**152**) and 5,6,7,8-tetrafluoroanthracene-1,4-dione (**57**). The nonacene tetraone was treated with lithiated acetylenes to give the intermediate tetraol (**154 & 155**). Initial attempts to deoxygenate the tetraol with $SnCl_2 \bullet 2H_2O$ gave only the intermediate hexacene diol (**156 & 157**). A small aliquot of the

intermediate hexacene diol (**156 & 157**) in 1,4-dioxane was then treated with hydroiodic acid to give final nonacene (**158 & 159**). Attempts to isolate the final acene were unsuccessful, however quick visible-NIR spectra of the final product exhibited absorptions characteristic of a nonacene. Visible-NIR stability studies showed that these reactive acenes decompose rapidly to a light blue solution on exposure to a bright light source. The visible-NIR spectra of the decomposition product reveals absorption peaks characteristic of a pentacene chromophore and also exhibit blood red fluorescence under short wave length UV light. This clearly shows that the nonacene derivative (**151**) reported by Miller et al. was rapidly decomposing during isolation and calls into question the stability of the nonacene as claimed by the authors.

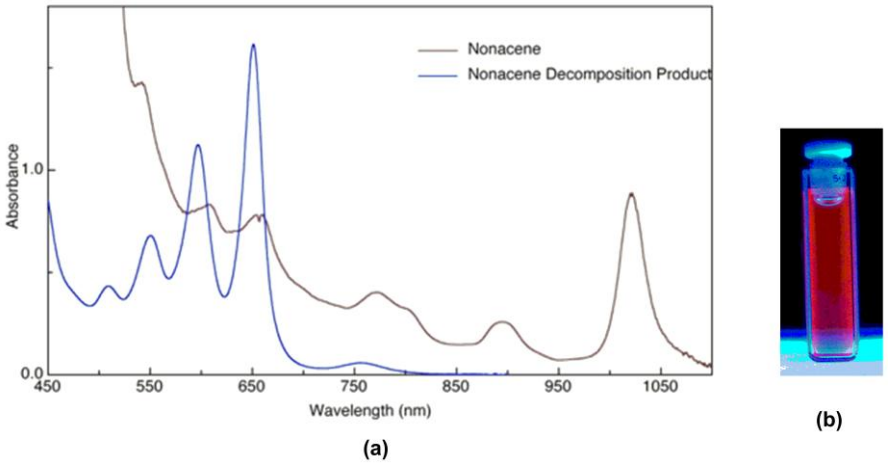

Figure 4.5 (a) Visible-NIR spectra of TCPS nonacene (158) and decomposition product (158) (b) Blood red fluorescence of nonacene decomposition product

4.5 Experimental details

All solvents were purchased from Pharmco Aaper except anhydrous tetrahydrofuran which was purchased from Aldrich. The solvents were degassed by purging N_2 gas through them for 30 min. n-Butyllithium (n-BuLi) was purchased from Aldrich. Chromatography was performed on silica gel (60 Å, 40-63 μm) purchased from Silicycle Inc. Thin layer chromatography was performed using Silica Gel HL TLC plates (w/UV254) purchased from Sorbent Technologies.

UV – Visible spectra were recorded using Shimadzu UV-visible Spectrophotometer model UV-2501PC. The spectra were recorded between the wavelength ranges of 400 – 900 nm for heptacene and 450 – 1100 nm for nonacene using quartz cells with 1cm path length. 10^{-4} M solutions of hexacenes in degassed toluene (UV Grade, Pharmco Aaper) were made in the dark and an initial spectrum of the acene was obtained. The solution was then exposed to a bright full-spectrum light source and the spectra were acquired at regular intervals until the absorption bands at longest wavelength disappeared. A plot of absorbance maximum at longest wavelength *versus* time was used to calculate the solution half-life (time taken to reach half the initial absorbance) of each pentacene derivative. NMR spectra were recorded on Varian Inova 400MHz instrument. Mass spectra were recorded in either EI mode on JOEL JMS-700T MStation or MALDI mode on Bruker Daltonics Autoflex MALDI-TOFMS. Electrochemical analysis was performed using BAS CV-50W voltammetric analyzer performed on 0.1M Bu_4NPF_6 solution in dichloromethane with ferrocene as internal standard. Heptacene-7,16-dione was synthesized according to reported literature methods.[171]

1,2,3,4,10,11,12,13-octafluoroheptacene-7,16-dione (137):

To a 250 ml round bottom flask equipped with a stir bar were added 250 mg (0.98 mmol) of 5,6,7,8-tetrafluoronaphthalene-2,3-dicarbaldehyde (**107**) and 250 mg (0.49 mmol) of cyclohexane-1,4-dione (**136**). The mixture was then dissolved in minimal amount of 1:1 ethanol/THF. Drops of 15% aqueous NaOH solution were added to the stirring mixture until there was an observable precipitate formation and the thick slurry was allowed to stir for 30 minutes. 50 ml of methanol was added to the reaction mixture and the precipitates were filtered through a Büchner funnel, washed with methanol followed by THF and finally with ether to give a light brown solid. Yield – 234 mg, 86%. MS (EI, 70 eV) *m/z* = 552 (100%, M^+)

General procedure for the synthesis of 7,16-Trialkylsilylethynylated-1,2,3,4,10,11,12,13-octafluoroheptacenes:

To a flame dried 100 ml flask cooled under nitrogen was added 3.62 mmol of acetylene, followed by 5 ml of hexanes. The reaction mixture was then placed in an ice bath. 1.3 ml of n-BuLi (3.26 mmol, 2.5 M solution in hexanes) was added dropwise and the reaction mixture stirred at 0 ºC for an hour. 13 ml of hexanes was added followed by 4 ml of anhydrous THF. 500 mg (0.90 mmol) of pulverized 1,2,3,4,9,10,11,12-octafluoroheptacene-7,16-dione (**137**) was then added to the reaction mixture and allowed to stir overnight. The reaction mixture was quenched with saturated NH_4Cl solution and extracted into ether. The combined ether layers were washed with water and dried over anhydrous $MgSO_4$. The excess acetylene was recovered from the crude product by elution through a pad of silica gel initially with hexanes. The crude diol was obtained as a mixture of *syn* and *anti* isomers by slowly increasing the ratio of hexanes:DCM to 7:3. To a 50 ml round bottom flask equipped with a magnetic stir bar were added 250 mg of crude diol, 20 ml of THF. Nitrogen gas was bubbled through the solution for 30 min. 2 ml of 10% aqueous HCl was added followed by 3 g of $SnCl_2 \bullet 2H_2O$ and the reaction mixture was placed in an oil bath maintained at 60˚C. The reaction was followed by TLC by monitoring the disappearance of diol. Fluorinated heptacene precipitates during the course of the reaction. The precipitated solids were filtered and washed with 50 ml of THF followed by plenty of methanol. Finally the solids were washed with acetone followed by 15 ml of hexanes to give green powder.

7,16-bis(tricyclopentylsilylethynyl)-1,2,3,4,10,11,12,13-octafluoroheptacene (140): 157 mg (65%). Poor solubility in solvents prevented NMR characterization.

7,16-bis(tricyclohexylsilylethynyl)-1,2,3,4,10,11,12,13-octafluoroheptacene (141): 183 mg (75%). Poor solubility in solvents prevented NMR characterization.

7,16 - tricyclohexylsilyethynyl Heptacene (144)

To a flame dried 100 ml flask cooled under nitrogen was added 2.23 g (7.34 mmol) of tricyclohexylsilylacetylene, followed by 5 ml of hexanes. The reaction mixture was then placed in an ice bath. 2.7 ml (6.75 mmol) of n-BuLi (2.5 M solution in hexanes) was added dropwise and the reaction mixture stirred at 0 ºC for an hour. 13 ml of hexanes was added followed by 4 ml of anhydrous THF. 750 mg (1.83 mmol) of 7,16 – heptacenequinone (**142**) was then added and the reaction mixture allowed to stir overnight. The reaction mixture was quenched with saturated NH_4Cl solution and extracted into ether. The combined ether layers were washed with water and dried over anhydrous $MgSO_4$. The excess acetylene was recovered from the crude product by elution through a pad of silica gel initially with hexanes. The crude diol (820 mg, 44%) was obtained by slowly increasing the ratio of hexanes:DCM to 7:3. To a 50 ml round bottom flask were added 200 mg of crude diol, 20 ml of THF. Nitrogen gas was bubbled through the solution for 30 min. 10 ml of 10% HCl was added followed by 10 g of $SnCl_2 \bullet 2H_2O$ and the reaction was followed by TLC by monitoring the disappearance of diol. The reaction is usually done within 5 minutes and the heptacene crashes out as an amorphous green solid. The solid was filtered and washed with methanol and finally with acetone to give the crude heptacene (175 mg, 90%).

1,2,3,4,12,13,14,15-octafluoro-8,19-dichlorononacene-6,10,17,21-tetraone (153)

To a 100ml RB flask equipped with a reflux condenser were added 1g of 1,2,4,5-tetrakis(bromomethyl)-3,6-dichlorobenzene (**152**), 1.35 g (18.6 mmol) of 5,6,78-

tetrafluoroanthracene-1,4-dione (**57**). 30 ml of degassed DMA was added and the reaction mixture was heated to 70˚C. 3.2 g of KI was added to the reaction mixture and the temperature was raised to 110˚C. The reaction mixture was allowed to stir for 24 h. During the course of the reaction yellow precipitate crashes out from solution. The hot reaction mixture was poured into 500 ml of water and allowed to stir for 30 min. The precipitate was filtered and washed with plenty of water, followed by acetone and finally with 100 ml THF. 1.34 g (92%) of the quinone was obtained as a dark brown solid. MS (LDI) *m/z* 750 (M^+, 100%)

General procedure for the synthesis of 6,10,17,21-Trialkylsilylethynylated-1,2,3,4,12,13,14,15-octafluoro-8,19-dichlorononacenes:

To a flame dried 100 ml flask cooled under nitrogen was added 5.32 mmol of acetylene, followed by 5 ml of hexanes. The reaction mixture was then placed in an ice bath. 1.92 ml of n-BuLi (4.79 mmol, 2.5 M solution in hexanes) was added dropwise and the reaction mixture stirred at 0 ºC for an hour. 13 ml of hexanes was added followed by 4 ml of anhydrous THF. 500 mg (0.66 mmol) of pulverized 1,2,3,4,12,13,14,15-octafluoro-8,19-dichlorononacene-6,10,17,21-tetraone (**153**) was then added to the reaction mixture and allowed to stir overnight. The reaction mixture was quenched with saturated NH_4Cl solution and extracted into ether. The combined ether layers were washed with water and dried over anhydrous $MgSO_4$. The excess acetylene was recovered from the crude product by elution through a pad of silica gel initially with hexanes. The crude diol was obtained as a mixture of *syn* and *anti* isomers by slowly increasing the ratio of hexanes:DCM to 7:3. 10 ml of hexanes was added to the crude tetraol and the yellow solids were filtered. The filtrate was concentrated and the process was repeated until all the tetraol was recovered. To a 50 ml round bottom flask equipped with a magnetic stir bar were added 250 mg of crude diol and 20 ml of THF. Nitrogen gas was bubbled through the solution

for 30 min. 2 ml of 10% aqueous HCl was added followed by 3 g of $SnCl_2 \bullet 2H_2O$ and the reaction mixture was placed in an oil bath maintained at 60˚C. The reaction was followed by TLC by monitoring the disappearance of tetraol. The intermediate hexacene diol precipitates during the course of the reaction. The precipitated solids were filtered and washed with 50ml of 1:1THF/acetone mixture followed by plenty of methanol. Finally the solids were washed with acetone followed by 15 ml of hexanes to give green powder. 5 mg of intermediate hexacene diol was dissolved in 4 ml of 1,4-dioxane and was treated with few drops of 57 wt% hydroiodic acid. A quick visible-NIR spectrum was collected to check for the presence of nonacene. Poor stability in solution prevented NMR characterization.

Chapter 5: Functionalized Anthradiselenophene for Thin Film Device Applications

5.1 Thiophene based organic semiconductors

The field of organic electronics has been dominated by both small molecule and polymer semiconductors. While polymers have the unique advantage of ease of processing, small molecules exhibit higher charge carrier mobility due to higher crystallinity of thin films. Both polymer and small molecule semiconductors based on thiophene chromophores have been widely studied.[172-174] Poly(3-hexylthiophene) (P3HT, **33**) which has been used extensively in organic solar cells and thin film transistors exhibits very low mobility (~ 10^{-3}- 10^{-6} cm^2/Vs) in devices due to their poor molecular ordering in thin films.[175,176] Improvement in device performance has been achieved by using more crystalline short chain oligothiophenes. Vapor deposited thin films of sexithiophene (α-6T, **160**) exhibited a hole mobility of 0.1 cm^2/Vs in a FET device.[177] Substitution of alkyl side chains to the oligothiophene core had significant effect on the device performance with short length alkyl substituents yielding higher mobility. α,α′-diethylsexithiophene (DiEt-α-6T, **161**) exhibited a high hole mobility of 1.1 cm^2/Vs in vapor deposited TFTs.[177] In order to further enhance the electronic properties fused oligothiophene semiconductors have been explored.[178-180] Compared to oligothiophenes, ring fusion of thiophene moieties results in a rigid planar chromophore with improved interactions in the solid state due to non-bonding S – S interactions.[178,181] Field effect transistors made from vapor deposited thin films of pentathienoacene (**162**) exhibited a modest hole mobility of 0.045 cm^2/Vs.[180]

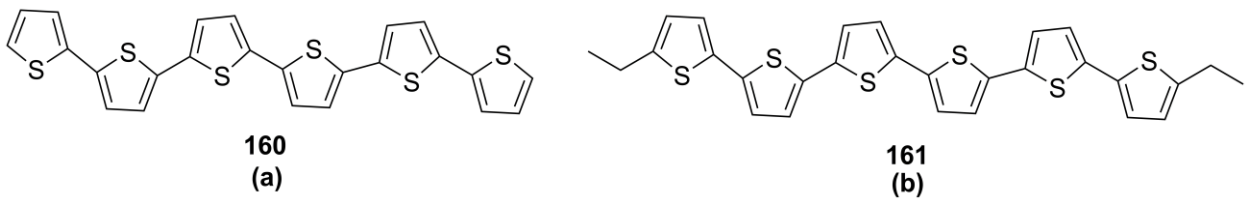

Figure 5.1 Sexithiophene (a) and diethyl sexithiophene (b)

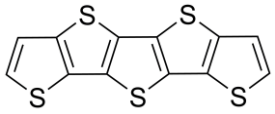

162

Figure 5.2 Pentathienoacene

In recent years acenedithiophenes have been explored because of their high crystallinity and ease of synthesis. Katz et al. reported the use of vapor deposited thin films of benzodithiophene dimers (**163**) in field effect transistors exhibiting a hole mobility of 0.04 cm^2/Vs.[182] In order to improve the charge carrier mobility in this class of molecules higher analogue anthradithiophenes (ADT) were explored by Katz and co-workers at Bell laboratories.[67]

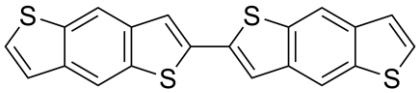

163

Figure 5.3 2,2'-bibenzo[1,2-b:4,5-b']dithiophene

These molecules exhibited better stability to molecular oxygen than pentacene, and the thiophene moieties allowed functionalization with alkyl substituents to improve the solubility of the heteroacene. Field effect transistors made from the dihexyl derivative (**16**, Figure 1.10) exhibited a hole mobility of 0.15 cm^2/Vs for vacuum deposited films, while solution processed films exhibited a lower mobility of 0.02 cm^2/Vs due to poor morphology of the as-cast thin films.[67] In order to improve the solubility and π-stacking in ADT Anthony et al. applied their *peri*-functionalization approach to these molecules. TES anthradithiophene (**17**, Figure 1.11) exhibits 2D π-stacking with a reduced close contact of 3.23 Å[68] between the molecules compared to TIPS pentacene (**15**, Figure 1.9) (3.36 Å).[65] Field effect transistors made from drop cast thin films of these molecules yielded mobility of 1 cm^2/Vs.[68]

While *peri*-fuctionalization of the anthradithiophene chromophore has improved the solubility and π-stacking of these molecules, the charge carrier mobility can be further enhanced by functionalizing the end thiophene rings. Anthony et al. have applied this approach to further enhance the device performance of anthradithiophenes.[69,183] Spin cast thin films of TES difluoroanthradithiophene (TES FADT, **18**) exhibited a high hole mobility of 1.5 cm^2/Vs compared to TES ADT.[69]

5.2 Selenophene based organic semiconductors

164 (a) **165** (b)

Figure 5.4 Tetrathiafulvalene (a) and Tetraselenafulvalene (b)

The electronic properties of ADT can also be modified by replacing sulfur atoms of the anthradithiophene chromophore with heavier chalcogens. This approach is common in the field of organic electronic materials, and has been used in the development of tetrathiafulvalene (TTF, **164**) based molecular conductors.[184] TTF molecules adopt 1D π-stacks, yielding highly anisotropic conductivity. These materials are known as quasi one-dimensional solids.

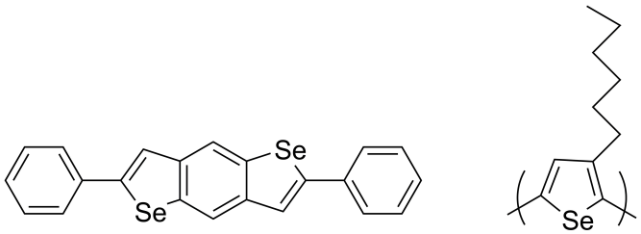

3 (a) **167** (b)

Figure 5.5 Benzodiselenophene (a) and Poly(3-hexylselenophene) (b)

By replacing sulfur atoms with heavier, more polarizable selenophene atoms it is possible to increase intermolecular chalcogen – chalcogen contacts leading to two dimensional interactions

in the solid state. The same approach has been used by Takimiya et al. to improve the hole mobility of benzodithiophenes. By replacing the sulfur atoms in 2,6-diphenylbenzodithiophenes (**166**) with heavier more polarizable selenium atoms the hole mobility increased from 0.08 cm^2/Vs to 0.17 cm^2/Vs.[185] The improvement in charge carrier mobility is due to the increased non-bonding Se – Se interactions in thin films. In 2007, Heeney et al. reported the synthesis of regioregular poly(3-hexylselenophene) (P3HS, **167**) and studied their optical and electrical properties in comparison with P3HT (**33**).[186] The authors reported that the selenium analogue exhibited smaller band gap and better photostability due to the lower lying LUMO energy level.

5.3 Trialkylsilylethynylated anthradisenophenes

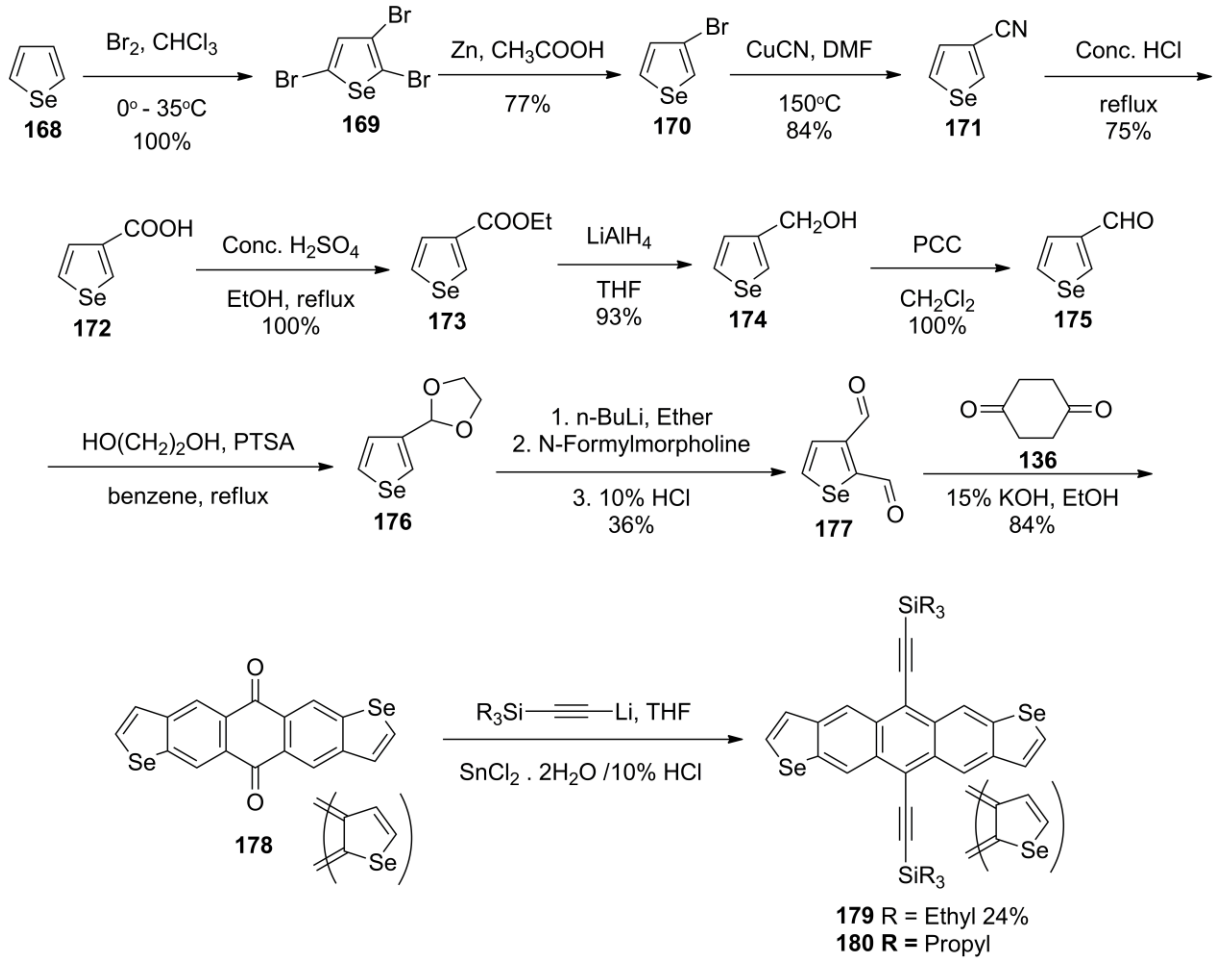

Scheme 5.1 Synthesis of trialkylsilylethynylated anthradiselenophenes

In order to further enhance the charge carrier mobility of ADT I decided to use the time tested approach of replacing the sulfur atoms with heavier selenium atoms. Trialkylsilylethynylated anthradisenophenes were synthesized according to scheme 5.1. Commercially available selenophene (**168**) was brominated in chloroform to give 2,3,5-tribromoselenophene (**169**) in quantitative yield. Zinc reduction of the tribromo derivative gave 3-bromoselenophene (**170**), which was then converted to 3-cyanoselenophene (**171**) using copper cyanide. Hydrolysis of cyano group using conc. HCl gave the corresponding acid (**172**). Fisher esterification of the acid followed by reduction of the resulting ethyl ester (**173**) gave the selenophene-3-methanol (**174**). Oxidation of the selenophene methanol using pyridinium chlorochromate (PCC) gave the selenophene-3-carbaldehyde (**175**) in quantitative yield. The monoaldehyde (**175**) was protected as an acetal, lithiated at the 2-position using n-butyllithium and was treated in-situ with N-formylmorpholine. Deprotection of the acetal using 10% HCl in tetrahydrofuran (THF) gave selenophene-2,3-dicarbaldehyde (**177**) in 36% yield. Aldol condensation of selenophene-2,3-dicarbaldehyde (**177**) with cyclohexane-1,4-dione (**136**) gave ADS quinone (**178**) as mixture of *syn* and *anti* isomers. Reaction with lithiated trialkylsilylacetyene gave the intermediate diol which was converted to the final acene by treatment with $SnCl_2 \bullet 2H_2O$ in 10% H_2SO_4.

The anthradiselenophenes were recrystallized from hexanes to give needle shaped crystals which were subjected to single crystal x-ray diffraction studies. Unlike TES ADT (**17**) which exhibits 2D π-stacking, TES ADS (**179**) packs in a 1D fashion with adjacent stacks having 'herringbone' interaction (Figure 5.6 (a)). The difference in the packing between TES ADS (**179**) (Figure 1.9) and TES ADT (**17**) is due to fact that the C – Se bond length (1.9 Å) is greater than C – S bond length (1.7 Å) and hence the length of the acene chromophore is larger in the former

case, requiring a larger solubilizing group to achieve two dimensional π-stacking. Also, the larger size of the selenium atoms resulted in increased spacing between the ADS chromophores compared to TES ADT. Using a larger triisopropylsilyl substituent improved the π-stacking between these molecules by preventing 'herringbone' interaction between adjacent stacks (Figure 5.6 (b)). The TIPS derivative (**180**) still exhibited 1D π-stacking with no significant reduction in close contacts (3.44 Å) between the acene chromophore compared to TES ADS (**179**) (3.45 Å). Crystal structures of both the derivatives indicate that there is no non-bonding Se – Se interaction between the ADS chromophores and as a result any attempt to improve the π-stacking in these molecules by using larger solubilizing groups will not likely improve the Se – Se contacts, which was the goal of this project.

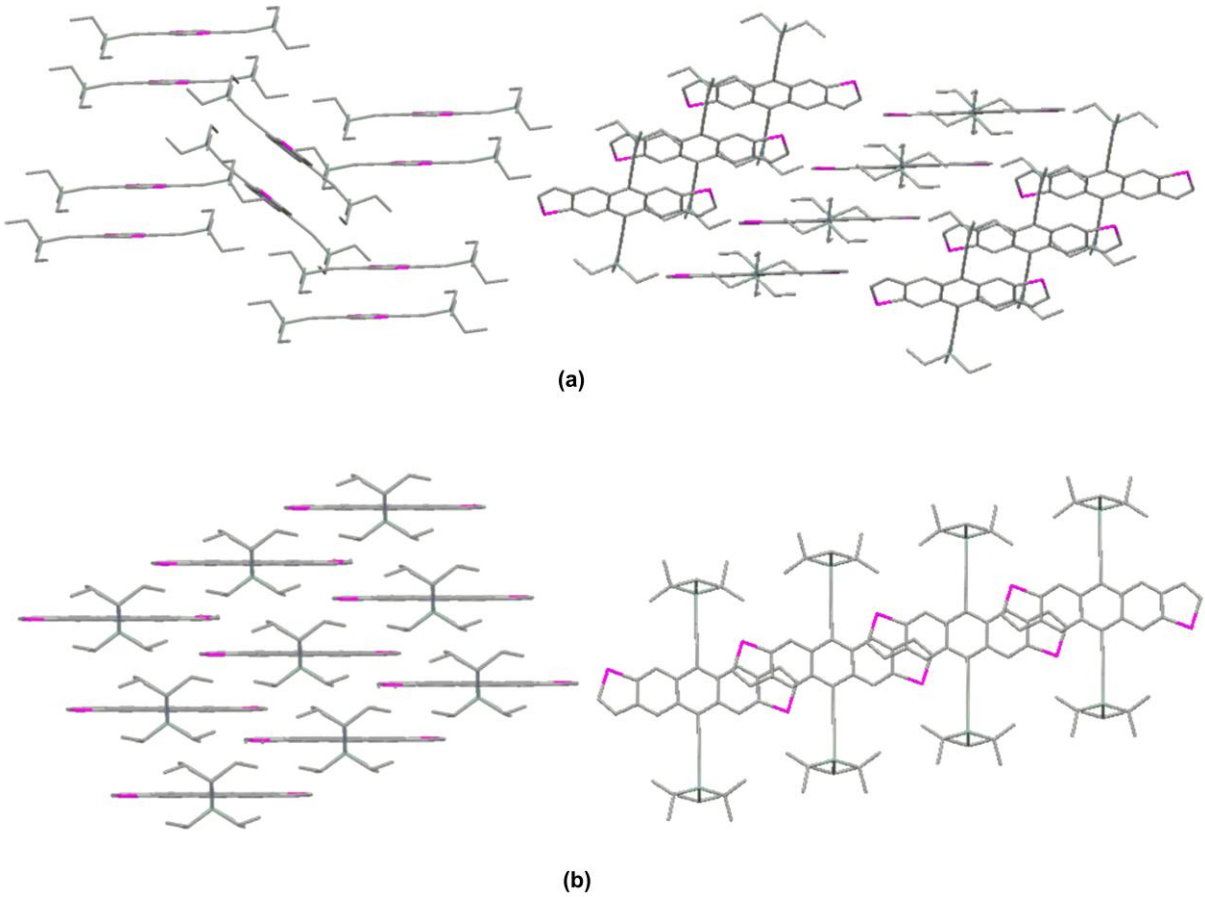

Figure 5.6 Crystal packing of TES ADS (a) and TIPS ADS (b)

Cyclic voltammetry was performed on the new anthradiselenophenes. Both TES (**179**) and TIPS ADS (**180**) exhibited higher oxidation potential than ADT indicating greater stabilization of the HOMO energy levels by selenium atoms than sulfur atoms.

Table 5.1 Crystal packing and device properties of anthradithiophenes and anthradiselenophenes

	TES ADT (17)	TIPS ADT (181)	TES ADS (179)	TIPS ADS (180)
π-stacking	**2D**	**1D**	**1D**	**1D**
Close contacts (Å)	**3.23**	**3.41**	**3.45**	**3.44**
Oxidation potential (mV)	**902**	**907**	**930**	**936**
μ (cm^2 / Vs)	**1**	**10^{-4}**	**3-6.5 x 10^{-5}**	**-**
$I_{on/off}$	**10^5-10^7**	**10^5-10^7**	**10^2-10^4**	**-**

In order to compare the electronic properties of the new ADS derivatives thin film transistor studies were performed by Jackson group at the Pennsylvania State University. Field effect transistors made from TES derivative (**179**) exhibited a very low mobility of 3-6.5 x 10^{-5} and an on/off ratio of 10^2-10^4. The above result is not surprising due to the poor π-stacking between the molecules in the solid state. Higher mobility can be attained if two dimensional π-stacking can be achieved between the molecules, perhaps by using unsymmetrical silyl groups.

5.4 Conclusion

In conclusion, new trialkylsilylethynylated anthradiselenophenes were synthesized for application in TFTs. Unlike TES ADT (**17**) which exhibits 2D π-stacking, TES ADS (**179**) packs in a 1D sandwich herringbone motif. The difference in packing motif between the two molecules

is due to the larger size of selenium atoms resulting in a larger acene chromophore than ADT. While using a larger TIPS substituent improved the π-stacking between the ADS chromophores, nevertheless both TIPS (**180**) and TES ADS (**179**) exhibited no Se – Se interactions in the solid state. Due to the poor π-stacking between the molecules TES ADS (**179**) exhibited poor mobility in solution processed TFTs.

5.5 Experimental details

All solvents were purchased from Pharmco Aaper except anhydrous tetrahydrofuran which was purchased from Aldrich. Selenophene and n-Butyllithium were purchased from Aldrich. Chromatography was performed on silica gel (60 Å, 40-63 μm) purchased from Sorbent Technologies. Thin layer chromatography was performed using Silica Gel HL TLC plates (w/UV254) purchased from Sorbent Technologies. UV-Vis absorbance spectra were recorded using Shimadzu UV-Vis Spectrophotometer model UV-2501PC. NMR spectra were recorded on Gemini 200MHz instrument. Mass spectra were recorded in either EI mode on JOEL JMS-700T MStation or MALDI mode on Bruker Daltonics Autoflex MALDI-TOFMS. Electrochemical analysis was performed using BAS CV-50W voltammetric analyzer performed on 0.1M Bu_4NPF_6 solution in dichloromethane with ferrocene as internal standard.

2,3,5-tribromoselenophene (169)

8.8 ml (171.7mmol) of bromine was added drop wise over a period of 30 min to a 500 ml round bottom flask containing 7.5 g (57.23mmol) of selenophene (**168**) dissolved in 200 ml of chloroform. The reaction mixture was stirred for an hour and then maintained at 35˚C for 12 h. The reaction mixture was washed with water followed by saturated sodium bicarbonate solution. The organic layer was finally washed with sodium thiosulfate solution, dried over anhydrous

$MgSO_4$ and concentrated to give light brown liquid (21 g, ~ 100%). MS (EI, 70 eV) *m/z* = 368 (100%, M^+). Experimental data matches well with data reported by Suginome et al.[187]

3-Bromoselenophene (170)

21 g (57.23 mmol) of **169** was dissolved in 300 ml of 80 % acetic acid taken in a 500 ml round bottom flask. 18.7 g (286 mmol) of activated zinc was slowly added and the reaction mixture was heated to reflux. The reaction was followed by GC/MS. 18.7 g of additional activated zinc was added to push the reaction to completion. After 3h the reaction mixture was poured through a thin pad of Celite to remove zinc powder and was washed with ether. The filtrate was washed with water (2 x 600 ml) and then with saturated sodium bicarbonate solution to remove acid. The organic layer was then washed with water, dried over $MgSO_4$ and concentrated to give 9.32 g (78%) of **170**. ^{1}H-NMR (200 MHz, $CDCl_3$) δ 8.26 (dd, *J* = 2.6, 1.4 Hz, 1H), 8.15 (dd, *J* = 3.2, 2.6 Hz, 1H), 7.32 (dd, *J* = 5.7,1.4 Hz, 1H). MS (EI, 70 eV) *m/z* = 210 (100%, M^+). Experimental data matches well with data reported by Hallberg et al.[188]

Selenophene-3-carbonitrile (171)

9.3 g (44.4mmol) of **170** was added to a 100 ml sealed tube followed by 40 ml of DMF. The resulting solution was degassed for 15 min and 12 g (133.19) of CuCN was added and the reaction vessel was securely sealed. The reaction mixture was heated to 155˚C and was maintained at this temperature for 48 h. The reaction mixture was added to 600 ml of 1:1 water: ammonium hydroxide and extracted with (3 x 250 ml) ether. The organic layer was then washed with water (4 x 500 ml), dried over anhydrous $MgSO_4$ and concentrated to give 5.85 g (84%) of **171**. ^{1}H-NMR (200 MHz, $CDCl_3$) δ 8.71 (dd, *J* = 2.6, 1.2 Hz, 1H), 8.12 (dd, *J* = 5.7, 2.6 Hz, 1H),

7.5 (dd, *J* = 5.7, 1.2 Hz, 1H). MS (LDI) *m/z* = Experimental data matches well with data reported by Franchetti et al.[189]

Selenophene-3-carboxylic acid (172)

5.85 g (37.48 mmol) of **171** was added to 300 ml of concentrated hydrochloric acid and heated to reflux for an hour. The reaction mixture was then allowed to cool to room temperature and extracted into DCM (2 x 200 ml). The organic layer was dried over $MgSO_4$ and concentrated to give 4.95 g (75%) of **172**. ^{1}H-NMR (200 MHz, $CDCl_3$) δ 10.4 (s, 1H), 9.06 (dd, *J* = 2.6, 1.2 Hz, 1H), 8.02 (dd, *J* = 5.4, 1.2 Hz, 1H), 7.9 (dd, *J* = 5.4, 2.6 Hz, 1H). Experimental data matches well with data reported by Franchetti et al.[189]

Ethyl selenophene-3-carboxylate (173)

60 ml of methanol was added to 4.95 g (28.28 mmol) of **172** in a 250 ml RB flask. 9 ml of conc. sulfuric acid was added to the reaction mixture slowly and the resulting solution was allowed to reflux for 36h. Next day the reaction mixture was cooled to room temperature, poured into 250 ml water and extracted with DCM (2 x 250 ml). The combined organic layer was dried over anhydrous $MgSO_4$ and concentrated to give the crude ester. Pure ester (5.74 g, ~100%) was obtained by column chromatography on silica gel using 3:1 hexane: ethyl acetate as eluent. ^{1}H-NMR (200 MHz, $CDCl_3$) δ 8.85 (dd, *J* = 2.6, 1.2 Hz, 1H), 7.91 (dd, *J* = 5.6, 2.6 Hz, 1H), 7.76 (dd, *J* = 5.6, 1.2 Hz, 1H), 4.26 (q, *J* = 7.2 Hz, 2H), 1.32 (t, *J* = 7.2 Hz, 3H). Experimental data matches well with data reported by Franchetti et al.[189]

Selenophene-3-methanol (174)

To a flame dried, nitrogen cooled 250 ml round bottom flask was added 5.74 g (28.28mmol) of **173** followed by 60 ml of anhydrous THF. The round bottom flask was placed in an ice bath and 77 ml (77 mmol) of 1 M solution of lithium aluminum hydride in THF was added drop wise. After the addition was complete the reaction mixture was warmed to room temperature and allowed to stir for 12 h. The reaction mixture was poured into 400 ml ether and was quenched by adding 3 ml of water, followed by 3 ml of 15% NaOH, finally with 9 ml of water. The ether layer was allowed to stir for 15 min, dried with anhydrous $MgSO_4$, concentrated to give 4.26 g (93%) of **174**. ^{1}H-NMR (200 MHz, $CDCl_3$) δ 8.22 (dd, *J* = 5.4, 2.6 Hz, 1H), 8.07 (dd, J = 2.6, 1.2 Hz, *1*H), 7.57 (dd, *J* = 5.6, 1.2 Hz, 1H), 4.82 (s, 2H). MS (EI, 70 eV) *m/z* = 162 (100%, M^+)

Selenophene-3-carbaldehyde (175)

To a 1000 ml round bottom flask containing 200 ml DCM was added 9.13 g PCC, 9.13 g of Celite followed by 9.13 g of molecular sieves. 4.26 g (26.45mmol) of **174** dissolved in 300 ml DCM was slowly added to the reaction mixture and the resulting solution was allowed to stir for 12h. The reaction mixture was poured on to a thick pad of silica gel and washed with DCM. Concentration of the organic layer gave 4.21 g (~100%) of **175**. ^{1}H-NMR (200 MHz, $CDCl_3$) δ 9.83 (s, 1H), 8.90 (dd, *J* = 2.6, 1.2 Hz, 1H), 7.99 (dd, *J* = 5.6, 2.6 Hz, 1H), 7.76 (dd, *J* = 5.6, 1.2 Hz, 1H). Experimental data matches well with data reported by Beelitz et al.[190]

Selenophene-2,3-dicarbaldehyde (177)

4.21 g (26.47mmol) of **23**, 2.1 g of ethylene glycol and 4 mg of *p*-toluenesulfonic acid monohydrate were added to 200 ml of benzene and allowed to reflux for 12 h. Water formed during the reaction was collected using a Dean-Stark trap. The reaction mixture was cooled to

room temperature, washed with 10% sodium bicarbonate solution followed by water and dried with anhydrous $MgSO_4$. Removal of solvent under reduced pressure gave 4.07 g (76%) of **176** which was used without further purification. **176** was dissolved in 40 ml of anhydrous THF and cooled to -78˚C. 10.5 ml of n-BuLi was added drop wise and the reaction mixture was stirred for 40 min. 4.7 ml of N-formylmorpholine was added drop wise to the reaction mixture and allowed to warm to room temperature overnight. The reaction mixture was added to water and extracted with DCM, dried over $MgSO_4$, concentrated to give the crude product. The acetal was deprotected by stirring in 250 ml of 10% HCl for 12 h. the mixture was extracted DCM, dried over $MgSO_4$ and concentrated to give the crude product. Column chromatography on silica gel using 9:1 hexane: ethyl acetate gave the dialdehyde **177** in 36% yield (1.82 g). ^{1}H-NMR (200 MHz, $CDCl_3$) δ 10.45 (s, 1H), 10.32 (s, 1H), 8.45 (d, *J* = 5.8 Hz, 1H), 7.92 (d, *J* = 5.4 Hz, 1H). Experimental data matches well with data reported by Paulmier et al.[191]

Anthra[2,3-b:6,7-b']diselenophene-5,11-dione and Anthra[2,3-b:7,6-b']diselenophene-5,11-dione (178)

To a 250 ml round bottom flask equipped with a stir bar were added 1.82 g (9.73mmol) of **177** and 520 mg (4.64mmol) of cyclohexane-1,4-dione (**136**). The mixture was then dissolved in minimal amount of ethanol. Drops of 15% aqueous NaOH solution was added to the stirring mixture until there was any observable precipitate formation and the thick slurry was allowed to stir for 30 minutes. 50 ml of methanol was added to the reaction mixture and the precipitates were filtered through a Büchner funnel, washed with methanol followed by ether to give 1.65 g of dark brown solid (84%). MS (MALDI) *m/z* = 414 (100%, M^+)

5, 11-Bis(triethylsilylethynyl)anthra[2,3-b:6,7-b']diselenophene and 5, 11-Bis(triethylsilylethynyl)anthra[2,3-b:7,6-b']diselenophene (179):

To a flame dried round bottom flask cooled under N_2 was added 20 ml of dry THF followed by 1.3 ml (1.02g, 7.24 mmol) of triethylsilylacetylene. 2.7 ml (6.76mmol, 2.5M solution) of n-BuLi was added dropwise and mixture was allowed to stir for an hour. 1 g (2.4mmol) of **178** was added and the reaction mixture was allowed to stir for 12 h. The reaction was quenched with wet THF and 1.65 g of $SnCl_2 \bullet 2H_2O$ dissolved in 10% H_2SO_4 was added and allowed to stir for an hour. The reaction mixture was then extracted with DCM, dried over $MgSO_4$ and concentrated to give the crude product. Pure **179** was obtained by column chromatography using hexanes. Recrystallization in hexanes gave 24% of **179**. ^{1}H NMR (400 MHz, $CDCl_3$) δ 9.18 (s, 1H), 9.10 (s, 1H), 8.02 (dd, *J* = 6.0, 1.6 Hz, 1H), 7.68 (dd, *J* = 6.0, 2.1 Hz, 1H), 1.26 (tt, *J* = 7.7, 2.5 Hz, 11H), 0.96 – 0.89 (m, 7H). ^{13}C NMR (101 MHz, $CDCl_3$) δ 142.71, 142.60, 139.78, 139.56, 130.56, 130.44, 130.29, 130.05, 130.03, 129.80, 127.94, 123.71, 123.64, 123.36, 123.26, 119.17, 117.53, 115.90, 107.34, 106.92, 106.51, 103.51, 103.46, 103.41, 8.04, 4.94. MS (EI, 70 eV) m/z 660 (62%, M^+).

5, 11-Bis(triisopropylsilylethynyl)anthra[2, 3-b:6, 7-b']diselenophene and 5, 11-Bis(triisopropylsilylethynyl)anthra[2, 3-b:7, 6-b']diselenophene (180)

To a flame dried round bottom flask cooled under N_2 was added 20 ml of dry THF followed by 0.82 ml (664 mg, 3.63 mmol) of triisopropylsilylacetylene. 1.4 ml (218 mg, 3.39 mmol) of n-BuLi was added drop wise and mixture was allowed to stir for an hour. 500 mg (1.2 mmol) of **178** was added and the reaction mixture was allowed to stir for 12 h. The reaction was quenched with wet THF and 1 g of $SnCl_2 \bullet 2H_2O$ dissolved in 10% H_2SO_4 was added and allowed to stir for

an hour. The reaction mixture was then extracted with DCM, dried over $MgSO_4$ and concentrated to give crude product. Pure **180** was obtained by column chromatography using hexanes. Recrystallization in acetone gave crystalline solid suitable for x-ray crystallographic studies. MS (EI, 70 eV) m/z 745 (8%, M^+).

Chapter 6: Conclusions and Outlook

6.1 Summary

The field of organic electronics has grown immensely over the past decade, from application in prototypes to commercially available devices. Recent research in this vastly growing field has been focused on improving the charge carrier mobility and stability in these devices. The goal of my research is to address these issues and develop acene semiconductors with better properties. Commercialization of organic semiconductors depends on their ability to be processed using existing well established printing methods such as ink jet printing, gravure printing and flexo printing. However the faster solvent evaporation rate associated with these techniques results in thin films with poor crystallinity. In order to enhance the crystallinity of spin cast thin films of TES ADT (**17**) Anthony et al. had functionalized the ADT core with fluorine substituents.[69] Spin cast thin films of TES FADT (**18**) exhibited a very high hole mobility of 1.5 cm^2/Vs. I have successfully applied the same approach to TIPS pentacene (**15**). TIPS difluoropentacenes exhibited significantly higher mobility than TIPS pentacene (**15**) on spin coating on to PFBT treated gold electrodes. The higher mobility of difluoropentacenes is attributed to its ability to form crystalline ordered films as evidenced from GIXD studies. The position of fluorine substitution had significant effect on both the mobility and stability of the pentacene. TIPS *cata*-difluoropentacene (TIPS CFP, **47**) exhibited a threefold increase in hole mobility (0.06 cm^2/Vs) than TIPS *peri*-difluoropentacene (TIPS PFP, **48**) (0.02 cm^2/Vs), while the latter exhibited higher stability in solution.

The success of difluoropentacene allowed me to further explore pentacene with different degrees of fluorination. Both trialkylsilylethynylated F_4 and F_8 pentacenes were synthesized and

their device performance in TFTs were explored. The size of the trialkylsilyl substituent had significant effect on the π-stacking and device performance of these molecules. Recently Bao et al. reported that chlorination of acene chromophore resulted in ambipolar semiconductors with high electron mobilities.[140] In order to enhance electron mobilities in pentacene I have synthesized trialkylsilylethynylated Cl_8 pentacenes for application in TFTs. However chlorination of the pentacene chromophore resulted in lower solubility in common organic solvents.

Trialkylsilylethynylated F_8 pentacenes were also used as acceptors in solar cells for both small molecule and polymer donors. Solar cells made from TCPS F_8 pentacene **(67)** acceptor and DPP donor **(83)** exhibited high V_{oc} with a PCE of 0.39%. Devices made from the same acene acceptor with P3HT (**33**) donor however gave a lower efficiency of 0.18% with a V_{oc} of 0.44V. The V_{oc} of P3HT based solar cells was increased by tuning the LUMO energy of pentacene acceptors. Higher V_{oc} was achieved using pentacene acceptors with single halogen substituent. TCPS 2-chloropentacene **(88)** exhibited PCE > 1% with a V_{oc} of 0.96V. However one of the drawbacks with pentacene solar cells is the low J_{sc} associated with these devices. The reason for this low J_{sc} might be due to the poor electron mobility and recombination of charge carriers in the bulk phase.

The high hole mobility associated with pentacene TFTs encouraged me to explore larger acene semiconductors. A series of trialkylsilylethynylated hexacene derivatives were synthesized to study their performance in TFTs. Solution stability studies on these new hexacene derivatives revealed that these molecules exhibited poor stability in solution preventing their use in thin film device application. Dimerization of the hexacene chromophore seemed to be the major decomposition pathway in both solution and solid state. Since partial fluorination of the

pentacene chromophore lead to improved stability I decided to partially fluorinate the hexacene chromophore to enhance its stability both in solution and solid state. A series of trialkylsilylethynylated partially fluorinated hexacene were synthesized and their solution stabilities were explored. Similar to pentacene the number and position of fluorine substituents on the hexacene chromophore had significant effect on the stability. Among the fluorinated hexacene derivatives, trialkylsilylethynylated F_8 hexacenes exhibited the highest stability enabling their use in solar cells. TCPS F_8 hexacene (**128**) was used as acceptor for P3HT (**33**) based solar cell exhibiting a PCE of 0.0052%. Chlorination of the hexacene chromophore resulted in improved stability however they exhibited poor solubility in common organic solvents similar to that seen in Cl_8 pentacene. While partial halogenation of the hexacene resulted in improved stability they exhibited low solubility in organic solvents. A more practical approach to enhance the stability of hexacene would be attaching halogen substituents closer to the reactive carbon atoms on the hexacene chromophore (Figure 6.1(a)).

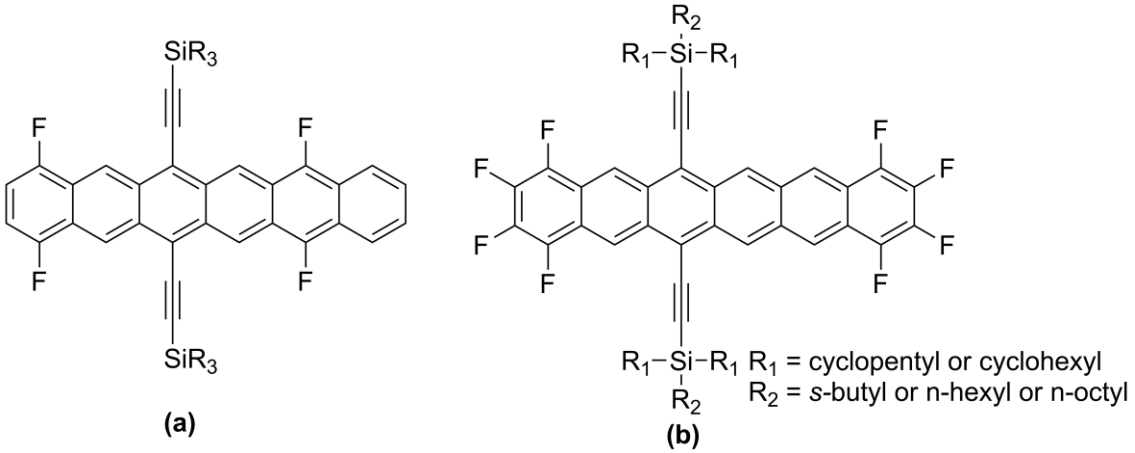

Figure 6.1 Stable and soluble partially fluorinated hexacene

Based on my success with improved stability of hexacene on partial fluorination I applied the same approach to heptacene and nonacene. Both TCPS (**127**) and TCHS F_8 heptacene (**128**) exhibited significantly higher stability than TCHS heptacene (**144**) however fluorination of

heptacene core resulted in poor solubility in solvents such as toluene and *o*-dichlorobenzene. Improvement in solubility can be achieved by functionalizing the heptacene chromophore with more trialkylsilylethynyl substituents (Figure 6.2 (a)). While my attempts to isolate a stable nonacene was unsuccessful nevertheless the presence of these reactive molecules in solution were confirmed by visible-NIR spectroscopy. Improvement in stability can be achieved by functionalizing the reactive carbon atoms of the central ring with sterically hindered substituents (Figure 6.2 (b)).

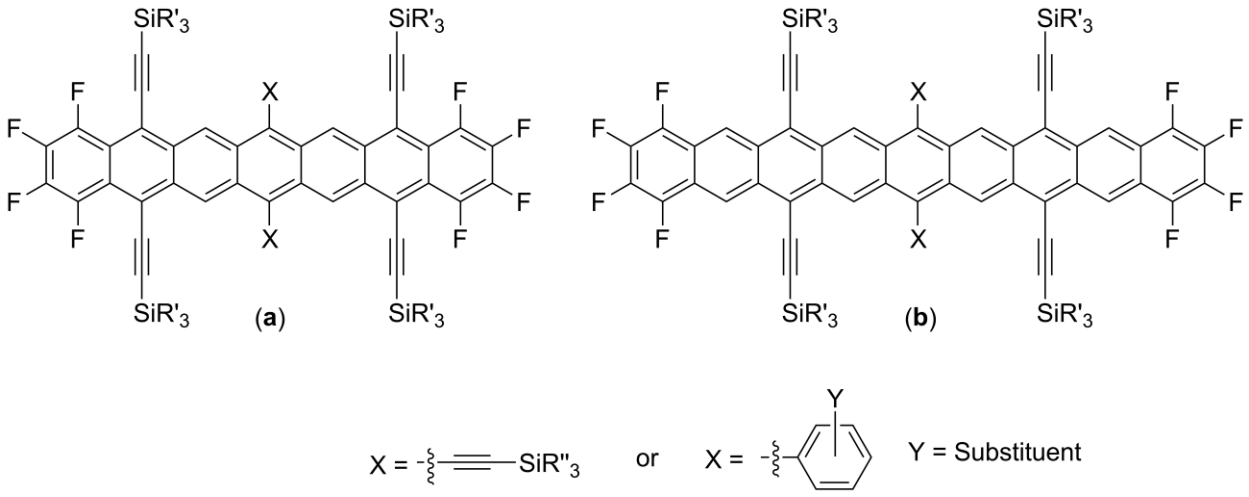

Figure 6.2 Future Heptacene and Nonacene targets

In order to improve the charge carrier mobility in TES ADT (**17**) I decided to replace the sulfur atoms with heavier more polarizable selenium atoms. The goal of this project was to improve the molecular ordering in the solid state by increasing non-bonding Se – Se interaction. However single crystal x-ray diffraction studies of TES (**179**) and TIPS ADS (**180**) revealed no such interaction between the ADS chromophore. The larger size of the selenium atoms resulted in a larger acene chromophore with increased spacing between the molecules preventing 2D π-stacking. While 2D π-stacking can be achieved by using suitable trialkylsilyl substituents nevertheless no Se – Se interaction can be achieved between the ADS chromophores.

6.2 Conclusion & Future Outlook

Solution stability studies on partially halogenated acenes clearly show that partial halogenation of acene chromophore seems to be a more practical approach to enhance stability of these reactive molecules. Halogenation especially fluorination has a significant effect on the π-stacking and morphology of solution cast thin films resulting in improved charge carrier mobility. However the partial halogenation of the acene chromophore leads to lower solubility in solvents which is a key requirement for solution processing. The solubility issue can be addressed by designing unsymmetrical trialkylsilylethynyl substituents which would enhance solubility without altering the solid state ordering (Figure 6.1(b)). For larger acenes a more practical approach to enhance stability and solubility would be functionalize the acene chromophore with more trialkylsilylethynyl substituents (Figure 6.2).

References

1. Cheng, Y. -J.; Yang, S. -H.; Hsu, C. -S. *Chem. Rev.* **2009**, *109*, 5868.
2. Shirota, Y.; Kageyama, H. Chem. Rev. **2007**, *107*, 953.
3. Katz, H. E.; Huang, J. Ann. Rev. Mater. Res. **2009**, *39*, 71.
4. Koch, N. *Chem. Phys. Chem*. **2007**, *8*, 1438.
5. Ong, B. S.; Wu, Y.; Li, Y.; Liu, P.; Pan, H. *Chem. Eur. J*., **2008**, *14*, 4766.
6. Anthony, J. E. *Angew. Chem., Int. Ed.* **2008**, *47*, 452.
7. Anthony, J. E. *Chem. Rev.* **2006**, *106*, 5028.
8. Bendikov, M.; Wudl, F.; Perepichka, D. F. *Chem. Rev.* **2004**, *104*, 4891.
9. Hioms,R. C.; Bettignies, R.; Leroy, J.; Bailly, S.; Firon, M.; Sentein, C.; Khoukh, A.; Preud'homme, H.; Dagron-Lartigau. C. *Adv. Funct. Mater.* **2006**, *16*, 2263.
10. Woo, C. H.; Holcombe, T. W.; Unruh, D. A.; Sellinger, A.; Frèchet, J. M. J. *Chem. Mater.* **2010**, *22*, 1673.
11. Abdou, M. S. A.; Lu, X.; Xie, Z. W.; Orfino, F.; Deen, M. J.; Holdcroft, S., *Chem. Mater.* **1995, 7,** 631
12. Klärner, G.; Lee, J. –I.; Lee, V. Y.; Chan, E.; Chen, J.-P.; Nelson, A.; Markiewicz, D.; Siemens, R.; Scott, J. C.; Miller. R. D., *Chem. Mater.* **1999,** *11*, 1800
13. Gundlach, D. J.; Royer, J. E.; Park, S. K.; Subramanian, S.; Jurchescu, O. D.; Hamadani, B. H.; Moad, A. J.; Kline, R. J.; Teague, L. C.; Kirillov, O.; Richter, C. A.; Kushmerick, J. G.; Richter, L. J.; Parkin, S. R.; Jackson, T. N.; Anthony, J. E. *Nature Mater.*, **2008,** *7*, 216.
14. T. Someya, T. Sekitani, S. Iba, Y. Kato, H. Kawaguchi, T. Sakurai, *Proc. Natl. Acad. Sci.* **2004**, *101*, 9966.

15. Steudel, S.; Myny, K.; Arkhipov, V.; Debel, C.; de Vusser, S.; Genoe, J.; Heremans, P. *Nat. Mater*. **2005**, ***4***, 597.

16. Huitema, H. E. A.; Gelinck, G. H.; van der Putten, J. B. P. H.; Kuijk, K. E.; Hart, C. M.; Cantatore, E.; Herwig, P. T.; van Breemen, A. J. J. M.; de Leeuw, D. M., *Nature*, **2001**, *414*, 599.

17. Klauk, H.; Hallik, M.; Zschieschang, U.; Schmid, G.; Radlik, W.; Werner, W. *J. Appl. Phys*. **2002**, *92*, 5259.

18. Chou, W. –Y.; Kuo, C. –W.; Cheng, H. –L.; Chen, Y. –R.; Yang, F. –Y.; Dun-Yin Shu, D. –Y.; Liao, C, -C.; Fu-Ching Tang, F. –C. *Jpn. J. Appl. Phys.*, **2006**, *45*, 7922.

19. Kelley, T. W.; Boardman, L. D.; Dunbar, T. D.; Muyres, D. V.; Pellerite, M. J.; Smith, T. P., *J. Phys. Chem. B,* **2003,** *107*, 5877.

20. Acton, O.; Ting, G. G. II.; Ma, H.; Hutchins, D.; Wang, Y.; Purushothaman, B.; Anthony, J. E.; Jen, A. K.-Y. *J. Mater. Chem*, **2009**, *19*, 7929**.**

21. Yun, Y.; Pearson, C.; Petty, M. C. *J. Appl. Phys*, **2009**, *105*, 034508/1

22. Puigdollers , J.; Voz, C.; Cheylan, S.; Orpella, A.; Vetter, M.; Alcubilla,R. *Thin. Solid. Films*, **2007**, 515, 7667.

23. Peng, X.; Horowitz, G.; Fichou, D.; Garnier, F., *Appl. Phys. Lett.*, **1990**, *57*, 2013.

24. Jang, Y.; Kim, D. H.; Park, Y. D.; Cho, J. H.; Hwang, M.; Cho, K. *Appl. Phys. Lett.*, **2006**, *88*, 072101.

25. L.-L. Chua, P.K.H. Ho, H. Sirringhaus, R.H. Friend, Appl. Phys. Lett.,**2004**, *84*, 3400.

26. Veres, J.; Ogier, S.; Lloyd, G.; de Leeuw, D., *Chem. Mater*., **2004**, *16*, 4543.

27. Walser, M. P.; Kalb, W. L.; Mathis, T.; Batlogg, B., *Appl. Phys. Lett*., **2009**, *95*, 233301.

28. Cheng, X.; Caironi, M.; Noh, Y. -Y.; Wang, J.; Newman, C.; Yan, H.; Facchetti, A.; Sirringhaus, H.,*Chem. Mater*., **2010**, *22*, 1559.

29. Pesavento, P. V.; Chesterfield, R. J.; Newman, C. R.; Frisbie, C. D., *J. Appl. Phys*., **2004**, *96*, 7312.

30. Yan, H.; Chen, Z.; Zheng, Y.; Newman, C.; Quinn, J. R.; Dötz, F.; Kastler, M.; Facchetti, A., *Nature*, **2009**, *457*, 679.

31. Lin, Y. Y.; Gundlach, D. J.; Nelson, S. F.; Jackson, T. N. *IEEE Electron Device Lett*. **1997**, *18*, 606.

32. Chen, Z. C.; Zheng, Y.; Yan, H.; Facchetti, A. *J. Am. Chem. Soc*. **2009**, *131*, 8.

33. Chang, J.-F.; Sun, B.; Breiby, D. W.; Nielsen, M. M.; Solling, T. I.; Giles, M.; McCulloch, I.; Sirringhaus, H. *Chem. Mater*. **2004**, *16*, 4772.

34. Yang. H.; Shin. T. J.; Ling. M. M.; Cho. K.; Ryu. C. Y.; Bao. Z., *J. Am. Chem. Soc*. **2005**, 127, 11542.

35. D. J. Gundlach, L. L. Jia, T. N. Jackson, *IEEE Electron Device Lett.* **2001**, *22*, 571.

36. K. Ihm, B. Kim, T.-H. Kang, K.-J. Kim, M. H. Joo, T. H. Kim, S. S. Yoon, S. Chung, *Appl. Phys. Lett.* **2006**, *89*, 033 504.

37. Youichi. S.; Toshiyasu. S; Masafumi. K.; Yuan. G.; Yasushi. F.; Youji. I.; Fumio. S.; Shizuo. T., *J. Am. Chem. Soc.*, **2004**, *126*, 8138.

38. de Leeuw, D. M.; Simenon, M. M. J.; Brown, A. R.; Einerhand, R. E. F. *Synth. Met.* **1997**, *87*, 53.

39. Jones, B. A.; Facchetti, A.; Wasielewski, M. R.; Marks, T. J. *J. Am. Chem. Soc.* **2007**, *129*, 15259.

40. Katz, H. E.; Johnson, J.; Lovinger, A. J.; Li, W. *J. Am. Chem. Soc.* **2000**, *122*, 7787.

41. Chen, H. A.; Ling, M. M.; Mo, X.; Shi, M. M.; Wang, M.; Bao, Z. *Chem. Mater.* **2007**, *19*, 816.

42. Chen, F. –C.; Liao, C. –H., *Appl. Phys. Lett*. **2008**, *93*, 103310.

43. Gsaenger, M.; Oh, J. H.; Koenemann, M.; Hoeffken, H. W.; Krause, A. -M.; Bao, Z.; Frank, W., *Angew. Chem. Int. Edn*., **2010**, *49*, 740.

44. Schmidt, R.; Ling, M. M.; Oh, J. H.; Winkler, M.; Konemann, M.; Bao, Z. N.; Wurthner, F. *Adv. Mater.* **2007**, *19*, 3692.

45. Jones, B. A.; Ahrens, M. J.; Yoon, M. H.; Facchetti, A.; Marks, T. J.; Wasielewski, M. R. *Angew. Chem., Int. Ed.* **2004**, *43*, 6363.

46. Yoon, M. H.; Facchetti, A.; Stern, C. E.; Marks, T. J. *J. Am. Chem. Soc.* **2006**, *128*, 5792.

47. Holmes, D.; Kumaraswamy, S.; Matzger, A. J.; Vollhardt, K. P. C., *Chem. Eur. J*, **1999**, *5*, 3399.

48. Fujikake, H.; Suzuki, T.; Isaka, F.; Sato, F., *Jpn. J. Appl. Phys*., **2004**, *43*, 536.

49. Reddy, A. R.; Bendikov. M. *Chem. Commun*. **2006**, 1179.

50. Berg, O.; Chronister, E. L.; Yamashita, T.; Scott, G. W.; Sweet, R. M.; Calabrese, J. *J. Phys. Chem. A.* **1999**, *103*, 2451.

51. Minakata, T.; Natsume, Y., *Synth. Met.*, **2005**, *153*, 1.

52. Brown, A. R.; Pomp, A.; de Leeuw, D. M.; Klaassen, D. B. M.; Havinga, E. E.; Herwig, P.; Mullen, K., *J. Appl. Phys.*, **1996**, *79*, 2136.

53. Herwig, P. T.; Mullen, K., *Adv. Mater.*, **1999**, *11*, 480.

54. Afzali, A.; Dimitrakopoulos, C. D.; Breen, T. L., *J. Am. Chem. Soc.***2002**, *124*, 8812.

55. Afzali, A.; Dimitrakopoulos, C. D.; Graham, T. O., *Adv. Mater.*, **2003**, *15*, 2066.

56. Weidkamp, K. P.; Afzali, A.; Tromp, R. M.; Hamers, R. J., *J. Am. Chem. Soc.*, **2004**, *126*, 12740.

57. Afzali, A.; Kagan, C. R.; Traub, G. P., *Synth. Met.*, **2005**, *155*, 490.

58. Meng, H.; Bendikov, M.; Mitchell, G.; Helgeson, R.; Wudl, F.; Bao, Z.; Siegrist, T.; Kloc, C.; Chen, C. –H., *Adv. Mater*. **2003**, *15*, 1090.

59. Chan, S. H.; Lee, H. K.; Wang, Y. M.; Fu, N. Y.; Chen, X. M.; Cai, Z. W.; Wong, H. N. C., *Chem. Commun*., **2005**, 66.

60. Allen, C. F. H.; Bell, A., *J. Am. Chem. Soc.* **1942**, *64*, 1253.

61. Anthony, J. E.; Eaton, D. L.; Parkin, S. R. *Org. Lett.* **2002**, *4*, 15.

62. Miao, S.; Smith, M. D.; Bunz, U. H. F. *Org. Lett.* **2006**, *8*, 757.

63. Tang, M. L.; Reichardt, A. D.; Siegrist, T.; Mannsfeld, S. C. B.; Bao, Z. *Chem. Mater.* **2008**, *20*, 4669.

64. Tang, M. L.; Oh, J. H.; Reichardt, A. D.; Bao. Z. *J. Am. Chem. Soc.* **2009**,131, 3733.

65. Anthony, J. E.; Eaton, D. L.; Parkin, S. R. *J. Am. Chem. Soc*. **2001**,*123*, 9842

66. Park, S. K.; Mourey, D. A.; Anthony, J. E.; Jackson, T. N. *Appl. Phys. Lett.*, **2007**,*91*, 063514

67. Laquindanum, J. G.; Katz, H. E.; Lovinger, A. J., *J. Am. Chem .Soc*.**1998**, *120*, 664.

68. Payne, M. M.; Parkin, S. R.; Anthony, J. E.; Kuo, C. C.; Jackson, T. N., *J .Am. Chem. Soc*. **2005**, 127, 4986.

69. Subramanian, S.; Park, S.K.; Parkin, S.R.; Podzorov, V.; Jackson, T.N.; Anthony, J.E. *J. Am. Chem. Soc*. **2008,** *130***,** 2706.

70. Deng, W. -Q.; Goddard III, W. A. *J. Phys. Chem. B.* **2004**, *108*, 8614.

71. Cheng, Y. C.; Silbey, R. J.; da Silva Filho, D.A.; Calbert, J. P.; Cornil, J.; Brédas, J. L. *J. Chem. Phys*. **2003**, *118*, 3764.

72. Brocks, G.; van den Brink, J.; Morpurgo, A. F. *Phys. Rev. Lett.* **2004**, *93*, 146405.

73. Clar, E. *Chem. Ber*. **1939**, *72B*, 2137. (b) Marschalk, C. *Bull. Soc. Chim.* **1939**, *6*, 1112.

74. Mondal, R.; Adhikari, R. M.; Shah, B. K.; Neckers, D. C. *Org. Lett.* **2007**, *9*, 2505.

75. Mondal, R.; Shah, B. K.; Neckers, D. C. *J. Am. Chem. Soc.* **2006**, *128*, 9612.

76. Tonshoff, C.; Bettinger, H. F., *Angew. Chem., Int. Ed.* **2010**, *49*, 4125.

77. Payne, M. M.; Parkin, S. R.; Anthony, J. E. *J. Am. Chem. Soc.* **2005**, *127*, 8028.

78. Chun, D.; Cheng, Y.; Wudl, F. *Angew. Chem., Int. Ed.* **2008**, *47*, 8380.

79. Payne, M. M.; Odom, S. A.; Parkin, S. R.; Anthony, J. E. *Org. Lett.* **2004**, *6*, 3325.

80. Zhao, J.; Wang, A.; Green, M. A.; Ferrazza, F. *Appl. Phys. Lett*. **1998**, *73*, 1991.

81. Ghosh, K. A.; Feng, T., *J. Appl. Phys.*, **1973**, *44*, 2781.

82. Morel, D. L.; Gosh, A. K.; Feng, T.; Stogryn, E. L.; Purwin, P. E.; Shaw, R. F.; Fishman. C., *Appl. Phys. Lett.*, **1978**, *32***,** 495.

83. Kearns, R.; Calvin. M., *J. Chem. Phys.*, **1958**, *29*, 950.

84. Tang, C. W. *Appl. Phys. Lett*. **1986**, *48*, 183.

85. Xue, J.; Uchida, S.; Rand, B. P.; Forrest, S. R. *Appl. Phys. Lett*. **2004**, *84*, 3013.

86. Yu, G.; Heeger, A. J., *J. Appl. Phys.*, **1995**, *78*, 4510.

87. Halls, J. J. M.; Walsh, C. A.; Greenham, N. C., *Nature.*, **1995**, *376*, 498.

88. Kietzke, T.; Horhold, H. –H.; Neher, D., *Chem. Mater.*, **2005**, *17*, 6532.

89. Yu, G.; Gao, J.; Hummelen, J. C.; Wudl, F.; Heeger, A. J. *Science* **1995**, *270*, 1789.

90. Shaheen, S. E.; Brabec, C. J.; Sariciftci, N. S.; Padinger, F.; Fromherz, T.; Hummelen, J. C. *Appl. Phys. Lett*. **2001**, *78*, 841.

91. Ma, W.; Yang, C.; Gong, X.; Lee, K.; Heeger, A. J.; *Adv. Funct. Mater.*, **2005**, *15*, 1617.

92. Reyes-Reyes, M.; Kim, K.; Carroll, D. L., *Appl. Phys. Lett.*, **2005,** *87*, 083506.

93. Kim, Y.; Cook, S.; Tuladhar, S. M.; Choulis, S. A.; Nelson, J.; Durrant, J. R.; Bradley, D. D. C.; Giles, M.; Mcculloch, I.; Ha, C.; Ree, M., *Nat. Mater.*, **2006**, *5*, 197.

94. Hioms, R. C.; Bettignies, R.; Leroy, J.; Bailly, S.; Firon, M.; Sentein, C.; Khoukh, A.; Preud'homme, H.; Dagron-Lartigau, C., *Adv. Funct. Mater.*, **2006**, *16*, 2263.

95. Kim, K.; Liu, J.; Namboothiry, M. A. G.; Carroll, D. L., *Appl. Phys. Lett.*, **2007,** *90*, 163511.

96. M. C. Scharber, M. C.; D. Muhlbacher, M. Koppe, P. Denk, C. Waldauf, A. J. Heeger and C. J. Brabec, Adv. Mater., **2006**,*18*, 789.

97. Peet, J.; Kim, J. Y.; Coates, N. E.; Ma, W. L.; Moses, D.; Heeger, A. J.; Bazan, G. C. *Nat. Mater*. **2007**, *6*, 497.

98. Price, S. C.; Stuart, A. C.; You, W., *Macromolecules.*, **2010**, *43*, 4609.

99. Hou, J.; Chen, H. -Y.; Zhang, S.; Chen, R. I.; Yang, Y.; Wu, Y.; Li, G., *J. Am. Chem. Soc.*, **2009**, *131*, 15586

100. Qin, R.; Li, W.; Li, C.; Du, C.; Veit, C.; Schleiermacher, H. -F.; Andersson, M.; Bo, Z.; Liu, .; Inganas, O.; Wuerfel, U.; Zhang, F., *J. Am. Chem. Soc.*, **2009**, *131*, 14612.

101. Chen,H. Y.; Hou, J. H.; Zhang, S. Q.; Liang, Y. Y.; Yang,G. W.; Yang, Y.; Yu, L. P.; Wu, Y.; G. Li, *Nat. Photonics*, **2009**, *3*, 649.

102. Liang, Y.; Xu, Z.; Xia, J.; Tsai, S. –T.; Wu, Y.; Li, G.; Ray, C.; Yu, L., *Adv. Mater.*, **2010**, *22*, E135.

103. S. Yoo, B. Domercq, B. Kippelen, *Appl. Phys. Lett*. **2004**, *85*, 5427.

104. Pandey. A.K.; Nunzi, J. –M, *Appl. Phys. Lett*, **2006**, *89*, 213506.

105. Yang. J.; Nguyen. T. –Q, Organic Electron, 2007, 8, 566.

106. Salzmann, I.; Duhm, S.; Opitz, R.; Johnson, R. L.; Rabe, J. P.; Koch, N., *J. Appl. Phys.*, **2008**, *104*, 114518.

107. Miller, G. P.; Briggs, J.; Mack, J.; Lord, P. A.; Olmstead, M. M.; Balch, A. L., *Org. Lett*., **2003**, *5*, 4199.

108. Lloyd, M. T.; Mayer, A. C.; Tayi, A. S.; Bowen, A. M.; Kasen, T. G.; Herman, D. J.; Mourey, D. A.; Anthony, J. E.; Malliaras, G. G. *Org. Electron*. **2006**, *7*, 243.

109. Gorodetsky, A. A.; Cox, M.; Tremblay, N. J.; Kymissis, I.; Nuckolls, C., *Chem. Mater*., **2009**, *21*, 4090.

110. Creegan, K. M.; Robbins, J. L.; Robbins, K. W.; Millar, J. M.; Sherwood, R. D.; Tindall, P. J.; Cox, D. M., *J. Am. Chem. Soc.* **1992**, *114*, 1103.

111. http://sesres.com/PCBM.asp Last accessed on June 14, 2010.

112. Shin, W. S.; Jeong, H. –H.; Kim, M. –K.; Jin, S. –H.; M. –R.; Lee. J. –K.; Lee. J. W.; Gal, Y. –S., *J. Mater. Chem.*, **2006**, *16*, 384.

113. Li, J.; Dierschke, F.; Wu, J.; Grimsdale, A. C.; Mullen, K., *J. Mater. Chem.*, **2006**, *16*, 96.

114. Camaioni, N.; Ridolfi, G.; Fattori,V.; Favaretto, L.; Barbarella, G., *J. Mater. Chem.*, **2005**, *15*, 2220.

115. Shin, R. Y. C.; Kietzke, T.; Sudhakar, S.; Dodabalapur, A.; Chen, Z. –K.; Sellinger, A., *Chem. Mater.*, **2007**, *19*,1892.

116. Kietzke, T.; Shin, R. Y. C.; Egbe, D. A. M.; Chen, Z. K.; Sellinger, A., *Macromolecules*, **2007**, *40*, 4424.

117. Woo, C. H.; Holcombe, T. W.; Unruh, D. A.; Sellinger, A.; Frechet, J. M. J., *Chem. Mater*., **2010**, *22*, 1673.

118. Swartz, C.R.; Parkin, S.T.; Bullock, J.E.; Anthony, J.E.; Mayer, A.C.; Malliaras,G.G. *Org Lett*. **2005**, *7*, 3163.

119. Lim, Y. –F.; Shu, Y.; Parkin, S. R.; Anthony, J. E.; Malliaras, G. G., *J. Mater. Chem*., **2009**, *19*, 3049.

120. Bao, Z.; Dodabalapur, A.; Lovinger, A. J. *Appl. Phys. Lett*. **1996**, *69*, 4108.

121. Headrick, R. L.; Wo, S.; Sansoz, F.; Anthony, J. E. *Appl. Phys. Lett*. **2008**, *92*, 063302.

122. Sirringhaus, H.; Brown, P. J.; Friend, H. R.; Nielsen, M. M.; Bechgaard, K.; Langeveld-Voss, B. M. W.; Spiering, A. J. H.; Janssen, R. A. J.; Meijer, E. W.; Herwig, P.; De Leeuw, D. M. *Nature*. **1999**, *401*, 685.

123. Kindera, L.; Kanickia, J.; Petroff. P. *Synth. Met.* **2004**, *146,* 181.

124. Miyazaki, E.; Kaku, A.; Mori, H.; Iwatani, M.; Takimiya, K. *J. Mater. Chem*. **2009**, *19*, 5913.

125. Bao, Q.; Li, J.; Li, C. M.; Dong, Z. L.; Lu, Z.; Qin, F.; Gong, C.; Guo, J. *J. Phys. Chem. B*. **2008**, *112*, 12270.

126. Wang, B.; Watt, S.; Hong, M.; Domercq, B.; Sun, R.; Kippelen, B.; Collard, D. M. *Macromolecules*, **2008**, *41*, 5156.

127. Mascaro, D. J.; Thompson, M. E.; Smith, H. I.; Bulovic, V. *Organic Electronics*. **2005**, *6*, 211.

128. Gundlach, D. J.; Jackson, T. N.; Schlom, D. G.; Nelson, S. F. *Appl. Phys. Lett*. **1999**, *74*, 3302.

129. De Luca, G.; Liscio, A.; Maccagnani, P.; Nolde, F.; Palermo, V.; Müllen, K.; Samorì, P. *Adv. Funct. Mater*. **2007**, *17*, 3791.

130. Dickey, K. C.; Anthony, J. E.; Loo, Y. -L. *Adv. Mater*. **2006**, *18*, 1721.

131. Lee, W. H.; Kim, D. H.; Cho, J. H.; Jang, Y.; Lim, J. A.; Kwak, D.; Cho, K. *Appl. Phys. Lett*. **2007**, *91*, 092105.

132. Adam, D.; Schuhmacher, P.; Simmerer, J.; Haussling, L.; Siemensmeyer, K.; Etzbach, K. H.; Ringsdorf, H.; Haarer, D. *Nature*. **1994**, *371*, 141.

133. Garnier, F.; Hajlaoui, R.; El Kassmi, A.; Horowitz, G.; Laigre, L.; Porzio, W.; Armanini, M.; Provasoli, F. *Chem. Mater*. **1998**, *10*, 3334.

134. Lee, W. H.; Lim, J. A.; Kim, D. H.; Cho, J. H.; Jang, Y.; Kim, Y. H.; Han, J. I.; Cho, K. Adv. Funct. Mater. 2008, 18, 560.

135. Gundlach, D. J.; Royer, J. E.; Park, S. K.; Subramanian, S.; Jurchescu, O. D.; Hamadani, B. H.; Moad, A. J.; Kline, R. J.; Teague, L. C.; Kirillov, O.; Richter, C. A.; Kushmerick, J. G.; Richter, L. J.; Parkin, S. R.; Jackson, T. N.; Anthony, J. E. *Nature Mater.,* **2008,** *7*, 216.

136. Russell, D. M.; Newsome, C. J.; Li, S. P.; Kugler, T.; Ishida. M.; Shimoda. T. *Appl. Phys. Lett*. **2005**, *87*, 222109.

137. Lee, S. S.; Kim, C. S.; Gomez, E. D.; Purushothaman, B.; Toney, M. F.; Wang, C.; Hexemer, A.; Anthony, J. E.; Loo, Y. -L. *Adv. Mater*. **2009**, *21*, 3605.

138. Coppo, P.; Yeates, S. G. *Adv. Mater*. **2005**, *17*, 3001.

139. Swartz, C.R.; Parkin, S.T.; Bullock, J.E.; Anthony, J.E.; Mayer, A.C.; Malliaras, G.G. *Org. Lett*. **2005**, *7*, 3163

140. Tang, M. L.; Oh, J. H.; Reichardt, A. D.; Bao. Z. *J. Am. Chem. Soc.* **2009**,*131*, 3733.

141. Curtis, M. D.; Cao, J.; Kampf, J. W. *J. Am. Chem. Soc*. **2004**, *126*, 4318.

142. Mas-Torrent, M.; Hadley, P.; Bromley, S. T.; Ribas, X.; Tarre´s, J.; Mas, M.; Molins, E.; Veciana, J.; Rovira, C. *J. Am. Chem. Soc.* **2004**, *126*, 8546.

143. Troisi, A.; Orlandi, G.; Anthony, J. E. *Chem. Mater*. **2005**, *17*, 5024.

144. Minari, T.; Seto, M.; Nemoto, T.; Isoda, S.; Tsukagoshi, K.; Aoyagi, Y. *Appl. Phys. Lett*. **2007**, *91*, 123501.

145. Chen, J.; Subramanian, S.; Parkin, S. R.; Siegler, M.; Gallup, K.; Haughn, C.; Martin, D. C.; Anthony, J. E. *J. Mater. Chem*. **2008**, *18*, 1961.

146. Abthagir, P. S.; Ha, Y. -G.; You, E. -A.; Jeong, S. -H.; Seo, H. -S.; Choi, J. -H. *J. Phys. Chem. B.* **2005**, *109*, 23918.

147. Chu, C. -W.; Shao, Y.; Shrotriya, V.; Yang, Y. *Appl. Phys. Lett.* **2005**, *86*, 243506.

148. Kamura, Y.; Inokuchi, H.; Maruyama, Y. *Chemistry Letters*. **1974**, *3*, 301.

149. Clar, E. *Chem. Ber*. **1942**, *75B*, 1283.

150. Bailey, W. J.; Liao, C. -W. *J. Am. Chem. Soc*. **1955**, *77*, 992.

151. Lang, K. F.; Zander, M. *Chem. Ber*. **1963**, *96*, 707.

152. Stacey, B. E.; Satchell, M. P. *J. Chem. Soc. C* **1971**, *3*, 468.

153. Clar, E. *Chem. Ber.* **1942**, *75B*, 1330.

154. Marschalk, C. *Bull. Soc. Chim*. **1943**, *10*, 511.

155. Campbell. R. B, Robertson. J. M, Trotter. J, *Acta Cryst*. **1962**, *15*, 289.

156. Schleyer, P.v. R.; Manoharan, M.; Jiao, H.; Stahl, F. *Org. Lett*. **2001**, *3*, 3643.

157. Reddy, A. R.; Fridman, -M. G.; Bendikov, M. *J. Org. Chem*. **2007**, *72*, 51.

158. Bendikov, M.; Houk, K. N.; Duong, H. M.; Starkey, K.; Carter, E. A.; Wudl, F. *J. Am. Chem. Soc*. **2004**, *126*, 7416.

159. Jiang, D.; Dai, S. *J. Phys. Chem. A* .**2008**, *112*, 332.

160. Deng, W. -Q.; Goddard III, W. A. *J. Phys. Chem. B.* **2004**, *108*, 8614.

161. Cheng, Y. C.; Silbey, R. J.; da Silva Filho, D.A.; Calbert, J. P.; Cornil, J.; Brédas, J. L. *J. Chem. Phys*. **2003**, *118*, 3764.

162. Brocks, G.; van den Brink, J.; Morpurgo, A. F. *Phys. Rev. Lett.* **2004**, *93*, 146405.

163. Kaur, I.; Stein, N. N.; Kopreski, R. P.; Miller, G. P. *J. Am. Chem. Soc.* **2009**, *131*, 3424.

164. Chen, Z.; Amara, J. P.; Thomas, III, S. W.; Swager, T. M. *Macromolecules*. **2006**, *39*, 3202.

165. Carlson, R. G.; Srinivasachar, K.; Givens, R. S.; Matuszewski, B. K. *J. Org. Chem.* **1986**, *51*, 3978.

166. Payne, M. M.; Odom, S. A.; Parkin, S. R.; Anthony, J. E. *Org. Lett.* **2004**, *6*, 3325.

167. Ishikawa, M.; Sugisawa, H.; Yamamoto, K.; Kumada, M. *J. Organometal. Chem.* **1979**, *179*, 377.

168. Qu, Z.; Zhang, D.; Liu, C.; Jiang, Y. *J. Phys. Chem. A*, **2009**, *113*, 7909.

169. Houk, K. N.; Lee, P. S.; Nendel, M. *J. Org. Chem.* **2001**, *66*, 5517.

170. Kaur, I.; Jazdzyk, M.; Stein, N. N.; Prusevich, P.; Miller, G. P. *J. Am. Chem. Soc.* **2010**, *132*, 1261.

171. Ried, W.; Anthofer, F. *Angew. Chem*. **1954**, *66*, 604.

172. Ong, B. S.; Wu, Y.; Li, Y.; Liu, P.; Pan, H. *Chem. Eur. J*. **2008**, *14*, 4766.

173. Perepichka, I. F.; Perepichka, D. F.; Meng, H.; Wudl, F. *Adv. Mater*. **2005**, *17*, 2281.

174. Chen, J.; Cao, Y. *Acc. Chem. Res*. **2009**, *42*, 1709.

175. Kline, R. J.; McGehee, M. D.; Kdnikova, E. N.; Liu, J.; Frechet, J. M. J. *Adv. Mater*. **2003**, *15*, 1519.

176. Zen, A.; Pflaum, J.; Hirschmann, S.; Zhang, W.; Jaiser, F.; Asawapirom, U.; Rabe, J. P.; Scherf. U.; Neher, D. *Adv. Funct. Mater*. **2004**, *14*, 757.

177. Halik, M.; Klauk, H.; Zschieschang, U.; Schmid, G.; Ponomarenko, S.; Kirchmeyer, S.; Weber, W. *Adv. Mater.* **2003**, *15*, 917.

178. Sato, N.; Mazaki, Y.; Kobayashi, K.; Kobayashi, T. *J. Chem. Soc. Perkin Trans 2*. **1992**, *5*, 765.

179. Zhang X.; Cote A. P.; Matzger A. J. *J. Am. Chem. Soc*. **2005**, *127*, 10502.

180. Xiao, K.; Liu, Y.; Qi, T.; Zhang, W.; Wang, F.; Gao, J.; Qiu, W.; Ma, Y.; Cui, G.; Chen, S.; Zhan, X.; Yu, G.; Qin, J.; Hu, W.; Zhu, D. *J. Am. Chem. Soc*. **2005**, *127*, 13281.

181. Zhang, X.; Johnson, J. P.; Kampf, J. W.; Matzger, A. J. *Chem. Mater*. **2006**, *18*, 3470.

182. Laquindanum, J. G.; Katz, H. E.; Lovinger, A. J.; Dodabalapur, A. *Adv. Mater*. **1997**, *9*, 36.

183. Anthony, J. E.; Subramanian, S.; Parkin, S. R.; Park, S. K.; Jackson, T. N. *J. Mater. Chem*. **2009**, *19*, 7984.

184. Engler, E. M.; Patel, V. V. *J. Am. Chem. Soc*. **1974**, *96*, 7376.

185. Takimiya, K.; Kunugi, Y.; Konda, Y.; Niihara, N.; Otsubo, T. *J. Am. Chem. Soc*. **2004**, *126*, 5084.

186. Heeney, M.; Zhang, W.; Crouch, D. J.; Chabinyc, M. L.; Gordeyev, S.; Hamilton, R.; Higgins, S. J.; McCulloch, I.; Skabara, P. J.; Sparrowe, D.; Tierney, S. *Chem. Comm*. **2007**, *47*, 5061.

187. Suginome, H.; Umezawa, S. *Bull. Chem. Soc. Jpn.* **1936**, *11*, 157.

188. Hallberg, A.; Liljefors, S.; Pedaja, P. *Synth. Comm.* **1981**, *11*, 25.

189. Franchetti, P.; Cappellacci, L.; Abu Sheikha, G.; Jayaram, H. N.; Gurudutt, V. V.; Sint, T.; Schneider, B. P.; Jones, W. D.; Goldstein, B. M.; Perra, G.; De Montis, A.; Loi, A. G.; La Colla, P.; Grifantini, M. *J. Med. Chem.* **1997**, *40*, 1731.

190. Beelitz, K.; Praefcke, K.; Gronowitz, S. *J. Organomet. Chem.* **1980**, *194*, 167.

191. Paulmier, C.; Morel, J.; Pastour, P.; Semard, D. *Bulletin de la Societe Chimique de France.* **1969**, *7*, 2511.

Vita

Balaji Purushothaman was born on 24th August 1980 in Chennai, India. He received his Masters degree in polymers in 2002 from University of Madras, Chennai, India. After graduation he worked as a Formulation Chemist for a textile ink manufacturer in Chennai and in January 2004, he was employed as a Lab supervisor/Chemist for a phenolic resin manufacturer in Chennai. In 2004, he was admitted to the Doctoral program in chemistry at University of Kentucky and in spring 2005, he joined the Anthony Aromatic Research Group. His research work is directed towards the synthesis of heteroacenes and partially halogenated acenes for use in OTFT's and solar cells.

Publications:

1. ***Purushothaman, Balaji***; Parkin, Sean R.; Anthony, John E. ***Synthesis and Stability of Soluble Hexacenes***, Organic Letters, 2010, 12, 2060.
2. Acton, Orb; Ting, Guy G., II; Ma, Hong; Hutchins, Daniel; Wang, Ying; ***Purushothaman, Balaji***; Anthony, John E.; Jen, Alex K.-Y**. π-ρ-Phosphonic acid organic monolayer-amorphous sol-gel hafnium oxide hybrid dielectric for low-voltage organic transistors on plastic**, Journal of Materials Chemistry, 2009, 19, 7929.
3. Lee, Stephanie S.; Kim, Chang Su; Gomez, Enrique D.; ***Purushothaman, Balaji***; Toney, Michael F.; Wang, Cheng; Hexemer, Alexander; Anthony, John. E.; Loo, Yueh-Lin. ***Controlling Nucleation and Crystallization in Solution-Processed Organic Semiconductors for Thin-Film Transistors***, Advanced Materials, 2009, 21, 3605.
4. Jurchescu, Oana D.; Feric, Marina; Hamadani, Behrang H.; Mourey, Devin A.; Subramanian, Sankar; ***Purushothaman, Balaji***; Anthony, John E.; Jackson, Thomas N.; Gundlach, David J. ***High performance organic thin-film transistors made simple through molecular design and processing***, ECS Transactions, 2008,16, 283.
5. Lobanova Griffith, Olga; Gruhn, Nadine E.; Anthony, John E.; ***Purushothaman, Balaji***; Lichtenberger, Dennis L, ***Electron Transfer Parameters of Triisopropylsilylethynyl-Substituted Oligoacenes.*** Journal of Physical Chemistry C, 2008, 112, 20518.
6. Palilis, Leonidas C.; Lane, Paul A.; Kushto, Gary P.; ***Purushothaman, Balaji***; Anthony, John E.; Kafafi, Zakya H. ***Organic photovoltaic cells with high open circuit voltages based on pentacene derivatives***, Organic Electronics, 2008, 9, 747.
7. Anthony, John E.; ***Purushothaman, Balaji***. ***Crystal design for organic semiconductors: The effects of substitution on crystal packing***, Proceedings of SPIE, 2007, 6658 (Organic Field-Effect Transistors VI), 66580L/1.